S ANGELES PUBLIC LIBRARY
MAR 2 8 1960
SCIENCE & TECHNOLOGY

ARS JOURNAL
A PUBLICATION OF THE AMERICAN ROCKET SOCIETY
VOLUME 30 NUMBER 3 MARCH 1960

BIND

SURVEY ARTICLE

Recent Advances in Chemical Kinetics of Homogeneous Reactions in Dissociated Air . . . Walter G. Zinman 233

CONTRIBUTED ARTICLES

Spectroscopic Studies of Reverse Jet Flame Stabilization . . . A. E. Fuhs 238
Contour Nozzles . . . Ellis M. Landsbaum 244
Relativistic Theory of Rocket Flight With Advanced Propulsion Systems . . . John Huth 250
Ascent From Inner Circular to Outer Co-Planar Elliptic Orbits . . . L. Rider 254
Structural Damage and Other Effects of Solar Plasmas . . . L. Reiffel 258

TECHNICAL NOTES

Surface Recombination in the Frozen Compressible Flow of a Dissociated Diatomic Gas Past a Catalytic Flat Plate . . . Paul M. Chung and Aamar D. Anderson 262
Vapor-Liquid Equilibria of Ozone–Oxygen Systems . . . Charles K. Hersh, Robert I. Brabets, Gerald M. Platz, Raymond J. Swehla and Donald P. Kirch 264
Measurements of the Heat Transfer Coefficients for Hydrogen Flowing in a Heated Tube . . . J. M. Fowler and C. F. Warner 266
A Method for Heat Rejection From Space Powerplants . . . Roger C. Weatherston and William E. Smith 268
Nonisentropic Nozzle Flow . . . William T. Snyder 179
A Magnetogasdynamic Analogy . . . M. D. Cowley 271
Analog Computer Technique for Plotting Frequency Response . . . John L. Webster and David N. Schultz 273
Some Characteristics of the Planar Satellite Orbit . . . Josef S. Pistiner 275
Symmetry of the Earth's Figure . . . J. L. Brenner, R. Fulton and N. Sherman 278
Thermal Decomposition of Liquid Phase n-Propyl Nitrate and Its Compatibility With Various Metals and Other Additives . . . Adolph B. Amster and Joseph B. Levy 280
Refraction Correction Techniques in Earth Satellite Optical Tracking for Precision Prediction . . . Albert D. Wassel 282
Iterative Solution of the N-Body Problem for Real Time . . . L. M. Rauch 284
Mass Considerations in Ring Supported Solar Sails . . . W. E. Jahsman 287
Prandtl-Meyer Expansion in Equilibrium Air . . . Heinz Kennet 289
Convection in a Fluid at Supercritical Pressures . . . J. D. Griffith and R. H. Sabersky 289

DEPARTMENTS

New Patents . . . 291
Book Reviews . . . 292
Technical Literature Digest . . . 296

TICKET TO ACHIEVEMENT

To the creative engineer, there is nothing more stimulating than to work in a creative environment. Space engineering programs now in process at Martin-Denver demand unusual creativity and may be your ticket to the personal and professional achievements which you are seeking. Make your desires and qualifications known to N. M. Pagan, Director of Technical and Scientific Staffing, The Martin Company, (Dept. 4) P. O. Box 179, Denver 1, Colorado.

MARTIN
DENVER DIVISION

Martin-designed Circular Space Computers are available FREE to interested persons by writing to the same address.

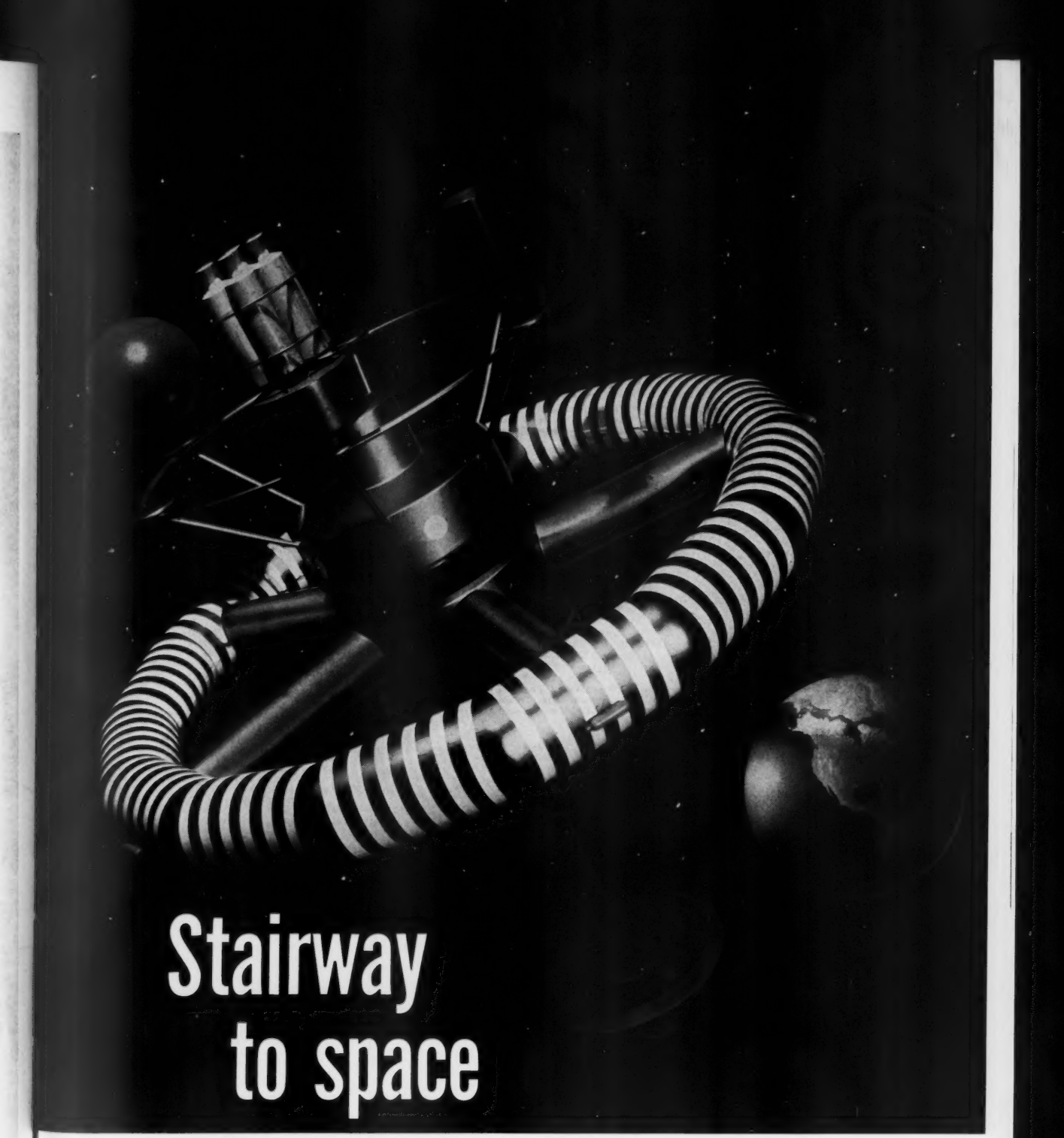

Stairway to space

Sometime in the 60's, America may have a manned station in space—and it could look a lot like this scale model by Lockheed.

We have much to learn before it can be built. Research is our stairway to space—basic research that seeks to discover the new rather than develop the known. We cannot predict what such research will discover, or when—but we delay it or curtail it at our peril.

Today, at Lockheed's Missiles and Space Division, more than 5,000 scientists and engineers are engaged in one of U.S. industry's broadest research and development programs. One group is conducting private industry's largest, most diversified program of fundamental research in space physics. Already they have made massive contributions to America's space technology—particularly in the Discoverer, MIDAS, and Samos satellite programs of the U.S. Air Force.

LOCKHEED MISSILES & SPACE DIVISION

Sunnyvale, California

ARS JOURNAL

A PUBLICATION OF THE AMERICAN ROCKET SOCIETY

EDITOR — Martin Summerfield

ASSOCIATE TECHNICAL EDITOR — Irvin Glassman

MANAGING EDITOR — Barbara Nowak

ART EDITOR — John Culin

CONTRIBUTOR — George F. McLaughlin

ASSOCIATE EDITORS

J. George Adashko, *Russian Supplement;* **Ali Bulent Cambel,** *Northwestern University, Book Reviews;* **Charles J. Mundo Jr.,** *Raytheon Manufacturing Co., Guidance;* **Bernard H. Paiewonsky,** *Aeronautical Research Associates of Princeton, Flight Mechanics;* **M. H. Smith,** *Princeton University, Technical Literature Digest*

ASSISTANT EDITORS

Julie Hight, Estelle Metz, Carol Rubenstein

ADVERTISING AND PROMOTION MANAGER

William Chenoweth

ADVERTISING PRODUCTION MANAGER

Walter Brunke

ADVERTISING REPRESENTATIVES

New York
D. C. Emery and Associates
400 Madison Ave., New York, N. Y.
Telephone: Plaza 9-7460

Los Angeles
James C. Galloway and Co.
6535 Wilshire Blvd., Los Angeles, Calif.
Telephone: Olive 3-3223

Chicago
Jim Summers and Associates
35 E. Wacker Dr., Chicago, Ill.
Telephone: Andover 3-1154

Detroit
R. F. Pickrell and Vincent Purcell
318 Stephenson Bldg., Detroit, Mich.
Telephone: Trinity 1-0790

Boston
Robert G. Melendy
17 Maugus Ave., Wellesley Hills, Mass.
Telephone: Cedar 5-6503

Pittsburgh
John W. Foster
239 4th Ave., Pittsburgh, Pa.
Telephone: Atlantic 1-2977

American Rocket Society

500 Fifth Avenue, New York 36, N. Y.

Founded 1930

OFFICERS

President	**Howard S. Seifert**
Vice-President	**Harold W. Ritchey**
Executive Secretary	**James J. Harford**
Treasurer	**Robert M. Lawrence**
Secretary and Asst. Treasurer	**A. C. Slade**
General Counsel	**Andrew G. Haley**
Director of Publications	**Irwin Hersey**

BOARD OF DIRECTORS

Terms expiring on dates indicated

Ali B. Cambel	1962	**William H. Pickering**	1961
Richard B. Canright	1962	**Simon Ramo**	1960
James R. Dempsey	1961	**William L. Rogers**	1960
Herbert Friedman	1962	**David G. Simons**	1961
Robert A. Gross	1962	**John L. Sloop**	1961
Samuel K. Hoffman	1960	**Martin Summerfield**	1962
A. K. Oppenheim	1961	**Wernher von Braun**	1960
		Maurice J. Zucrow	1960

TECHNICAL COMMITTEE CHAIRMEN

Lawrence S. Brown, Instrumentation and Control

Ali B. Cambel, Magnetohydrodynamics

William H. Dorrance, Hypersonics

James S. Farrior, Guidance and Navigation

Herbert Friedman, Physics of the Atmosphere and Space

George Gerard, Structures and Materials

Martin Goldsmith, Liquid Rockets

Andrew H. Haley, Space Law and Sociology

Samuel Herrick, Astrodynamics

Maxwell W. Hunter, Missiles and Space Vehicles

Herbert L. Karsch, Systems Operations and Support

David B. Langmuir, Ion and Plasma Propulsion

Max A. Lowy, Communications

Irving Michelson, Education

Peter L. Nichols Jr., Propellants and Combustion

Eugene Perchonok, Ramjets

Richard A. Schmidt, Test Facilities and Support Equipment

John I. Shafer, Solid Rockets

C. J. Wang, Nuclear Propulsion

Stanley C. White, Human Factors and Bioastronautics

George F. Wislicenus, Underwater Propulsion

Abe M. Zarem, Power Systems

Scope of ARS JOURNAL

This Journal is devoted to the advancement of astronautics through the dissemination of original papers disclosing new scientific knowledge and basic applications of such knowledge. The sciences of astronautics are understood here to embrace selected aspects of jet and rocket propulsion, spaceflight mechanics, high speed aerodynamics, flight guidance, space communications, atmospheric and outer space physics, materials and structures, human engineering, overall system analysis, and possibly certain other scientific areas. The selection of papers to be printed will be governed by the pertinence of the topic to the field of astronautics, by the current or probable future significance of the research, and by the importance of distributing the information to the members of the Society and to the profession at large.

Information for Authors

Manuscripts must be as brief as the proper presentation of the ideas will allow. Exclusion of dispensable material and conciseness of expression will influence the Editors' acceptance of a manuscript. In terms of standard-size double-spaced typed pages, a typical maximum length is 22 pages of text (including equations), 1 page of references, 1 page of abstract and 12 illustrations. Fewer illustrations permit more text, and vice versa. Greater length will be acceptable only in exceptional cases.

Short manuscripts, not more than one quarter of the maximum length stated for full articles, may qualify for publication as Technical Notes or Technical Comments. They may be devoted to new developments requiring prompt disclosure or to comments on previously published papers. Such manuscripts are published within a few months of the date of receipt.

Sponsored manuscripts are published occasionally as an ARS service to the industry. A manuscript that does not qualify for publication, according to the above-stated requirements as to subject, scope or length, but which nevertheless deserves widespread distribution among jet propulsion engineers, may be printed as an extra part of the Journal or as a special supplement, if the author or his sponsor will reimburse the Society for actual publication costs. Estimates are available on request. Acknowledgment of such financial sponsorship appears as a footnote on the first page of the article. Publication is prompt since such papers are not in the ordinary backlog.

Manuscripts must be double spaced on one side of paper only with wide margins to allow for instructions to printer. Include a 100 to 200 word abstract. State the authors' positions and affiliations in a footnote on the first page. Equations and symbols may be handwritten or typewritten; clarity for the printer is essential. Greek letters and unusual symbols should be identified in the margin. If handwritten, distinguish between capital and lower case letters, and indicate subscripts and superscripts. References are to be grouped at the end of the manuscript and are to be given as follows. For journal articles: Authors first, then title, journal, volume, year, page numbers; for books: Authors first, then title, publisher, city, edition and page or chapter numbers. Line drawings must be clear and sharp to make clear engravings. Use black ink on white paper or tracing cloth. Lettering should be large enough to be legible after reduction. Photographs should be glossy prints, not matte or semi-matte. Each illustration must have a legend; legends should be listed in order on a separate sheet.

Manuscripts must be accompanied by written assurance as to security clearance in the event the subject matter lies in a classified area or if the paper originates under government sponsorship. Full responsibility rests with the author.

Preprints of papers presented at ARS meetings are automatically considered for publication.

Submit manuscripts in duplicate (original plus first carbon, with two sets of illustrations) to the Managing Editor, ARS JOURNAL, 500 Fifth Avenue, New York 36, N.Y.

ARS JOURNAL is published monthly by the American Rocket Society, Inc. and the American Interplanetary Society at 20th & Northampton Sts., Easton, Pa., U. S. A. Editorial offices: 500 Fifth Ave., New York 36, N. Y. Price: $12.50 per year, $2.00 per single copy. Second-class mail privileges authorized at Easton, Pa. This publication is authorized to be mailed at the special rates of postage prescribed by Section 132.122. Notice of change of address should be sent to the Secretary, ARS, at least 30 days prior to publication. Opinions expressed herein are the authors' and do not necessarily reflect the views of the Editors or of the Society.

© Copyright 1960 by the American Rocket Society, Inc.

SCIENTISTS AND ENGINEERS: There are two sides to the STL coin...

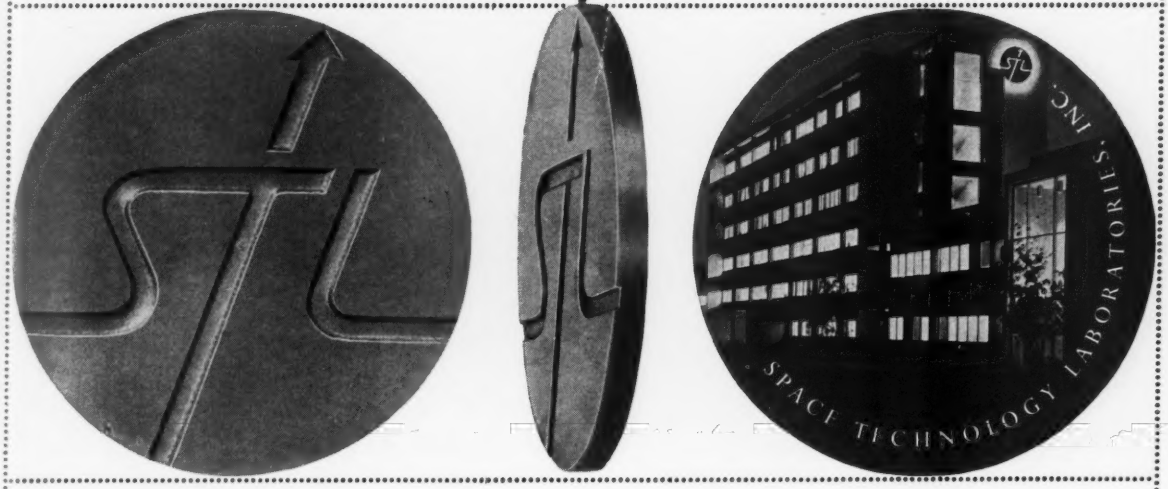

What STL does:

Space Technology Laboratories is making significant contributions in theoretical analysis, research, development and technical management of advanced ballistic missile and space systems. STL conducts advanced space flight experiments under the executive management of the Air Force on behalf of such agencies as ARPA and NASA. In addition STL's leadership in military applications of space technology is illustrated by its successful accomplishments as the contractor responsible for over-all systems engineering and technical direction of the Atlas, Titan, Thor, and Minuteman portions of the Air Force Ballistic Missile Program.

What STL offers:

For scientists and engineers with outstanding capabilities, STL offers unusual growth opportunities in many areas of technical activity, including:

Electronic and Electromechanical Systems
Vehicle Engineering and Development
Propulsion and Guidance Systems
Computer Technology
Systems Engineering and Technical Direction
Telecommunications
Airborne Systems
Ground Support Equipment

The Technical Staff of STL is the largest professional group in the nation devoted exclusively to research, development, and systems engineering in the field of ballistic missiles, space projects, and related advanced technology. If you want to apply your skills and talents, in these advanced areas working with leaders in your field, investigate positions at STL now. Please send your resume today to *Mr. Richard A. Holliday.*

Space Technology Laboratories, Inc., P.O. Box 95004
Los Angeles 45, California

STL

SPACE TECHNOLOGY LABORATORIES, INC.

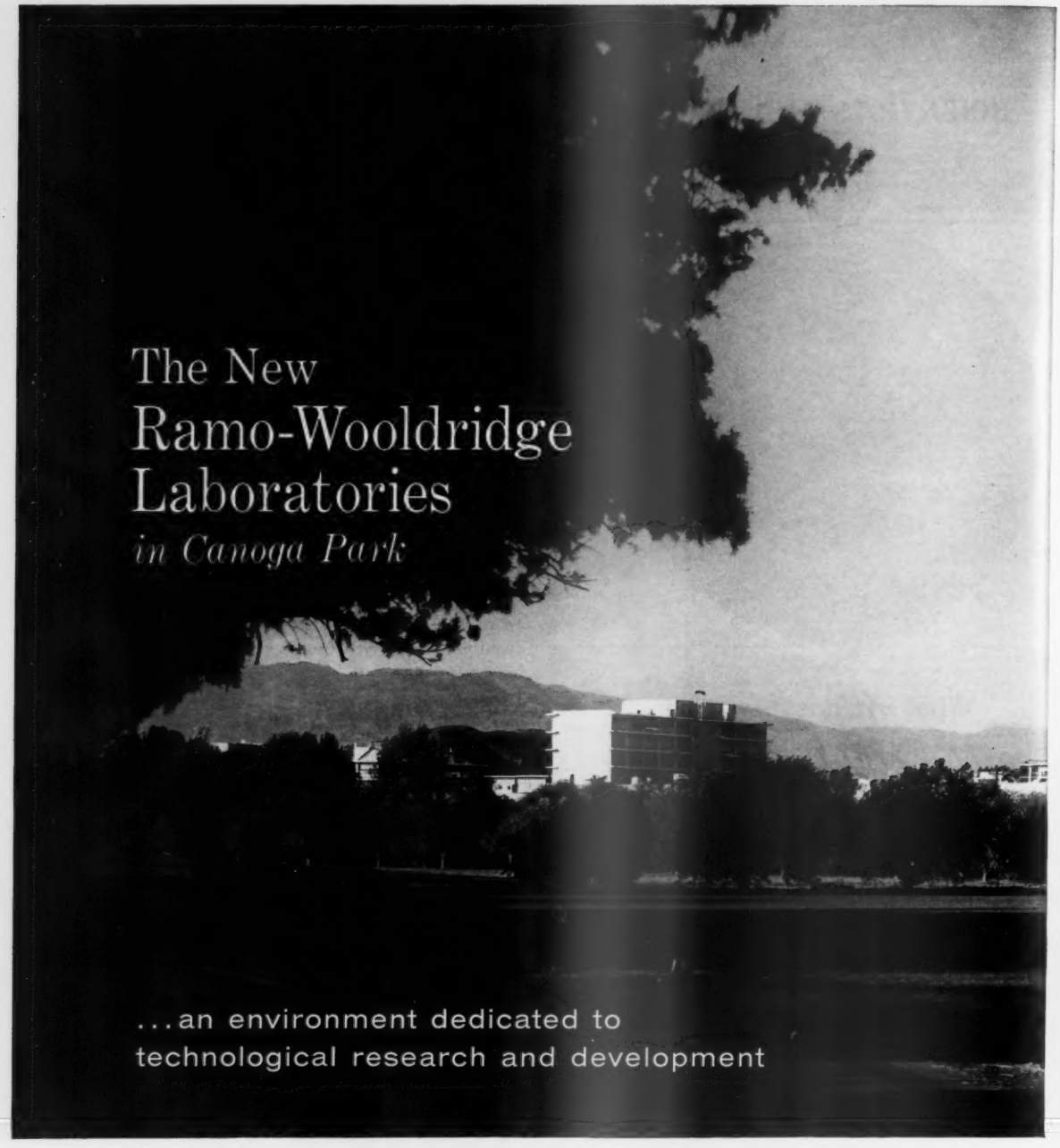

The new Ramo-Wooldridge Laboratories in Canoga Park, California, will provide an excellent environment for scientists and engineers engaged in technological research and development. Because of the high degree of scientific and engineering effort involved in Ramo-Wooldridge programs, technically trained people are assigned a more dominant role in the management of the organization than is customary.

The ninety-acre landscaped site, with modern buildings grouped around a central mall, contributes to the academic environment necessary for creative work. The new Laboratories will be the West Coast headquarters of Thompson Ramo Wooldridge Inc. as well as house the Ramo-Wooldridge division of TRW.

The Ramo-Wooldridge Laboratories are engaged in the broad fields of electronic systems technology, computers, and data processing. Outstanding opportunities exist for scientists and engineers.

For specific information on current openings write to Mr. D. L. Pyke.

THE RAMO-WOOLDRIDGE LABORATORIES

8433 FALLBROOK AVENUE, CANOGA PARK, CALIFORNIA

Recent Advances in Chemical Kinetics of Homogeneous Reactions in Dissociated Air[1]

WALTER G. ZINMAN

Republic Aviation Corp.
Farmingdale, N. Y.

The author is Principal Research and Development Engineer for Republic Aviation Corp. in the Materials Development Laboratory. He received his B.Ch.E. from Rensselaer Polytechnic Institute in 1951, and his Ph.D. in physical chemistry from Harvard in 1955. His doctoral thesis on gaseous detonations was prepared under the direction of Professor G. B. Kistiakowsky. Dr. Zinman then spent two years in the Army and three years at the Missile and Space Vehicle Department of General Electric Co. where he studied the reaction between carbon and dissociated gases. He has recently joined Republic Aviation Corp. where he plans to continue this work, and initiate related projects.

AS A MISSILE re-enters the atmosphere, it is surrounded by a detached shock wave. The air immediately behind the shock front becomes so hot that it partially dissociates into atomic oxygen and nitrogen. This dissociated air then diffuses toward the skin of the missile through a relatively cool boundary layer. The kinetics of possible homogeneous reactions in the boundary layer together with the transport properties of the gas mixture determine whether this dissociated gas recombines in the gas phase before impinging on the missile skin. The dissociated gas may well react much more rapidly with the missile skin than does the corresponding undissociated gas. For this reason, the kinetics of certain gas phase reactions may strongly influence the heat transfer rate to the missile, its aerodynamic characteristics and the ablation rate of the missile skin. Rosner (1)[2] discussed this in detail and reviewed several theories which considered the influence of kinetic parameters on convection heat transfer. This review will supplement Rosner's survey paper by examining in some detail the kinetics of some of the reactions which are considered to be of importance. The influence of chemical kinetic parameters also should be considered in many other aerodynamic problems; for example, in the design of a rocket nozzle (2), or in the interpretation of experiments conducted in hypersonic low density wind tunnels.

The predominant mechanism for the combination of atoms at ambient density and temperature is a three-body reaction. Two atoms simultaneously collide with a third particle and recombine; the third particle carries away some of the energy liberated during this recombination process and thereby prevents the reverse dissociation from occurring immediately. At sufficiently low densities, these three-body collisions become so uncommon, compared with two-body collisions, that radiative recombination becomes a predominant mechanism in the gas phase. In this case, two atoms collide and sometimes emit part of the energy of recombination as a light quantum instead of again flying apart. In a gas containing only one element, these would be the only reactions of importance. In mixtures, bimolecular reactions (e.g., $N + O_2 \rightarrow NO + O$), in which the total number of particles is conserved, couple the concentrations of the different dissociated gases to each other and are, therefore, of importance. Each of these processes is discussed in detail.

Trotman-Dickenson (3) prepared an outstanding book reviewing the research work on gaseous kinetics done prior to July 1954. However, he did not discuss radiative recombination. Since that time the application of the shock tube to chemical kinetic studies has led to a new understanding of reactions at elevated temperatures. Several publications have also appeared recently on various reactions of dissociated nitrogen and oxygen. For these reasons, a more current review appears highly desirable. This review is not intended to be exhaustive, but covers the work published prior to October 1959, which the author considers most pertinent in a boundary layer containing dissociated air.

Since the terminology of chemical kinetics has been defined in several texts (4–9), it will not be covered in this paper.

Three-Body Recombination

For most simple atom recombination reactions, k_r is of the order of 10^{14}–10^{15} cm^6 per gm-mol^2 sec (2.6×10^{16} to 2.6×10^{17} ft^6 per lb-mol^2 sec) at room temperature. For the recombination of a given pair of atoms, k_r depends on the choice of a third body. However, for most common third bodies, k_r is in the range indicated at room temperature as will be illustrated. The exceptions to this rule are not likely to be encountered in problems of technical interest.

As the temperature increases, k_r decreases slowly. The difference between k_r at room temperature and k_r at 1000 K is generally less than one order of magnitude. This is best illustrated by studies of iodine atom recombination and is corroborated by analogous work on bromine atom recombination (10,11), which is not discussed further in this paper. For oxygen atoms, it will be shown that sufficient work has been done to indicate that the magnitude of the recombination coefficient is about the same at 3500 K as at room temperature. The recombination of atomic nitrogen has been studied only at room temperature. However, it appears to be possible to predict the effect of raising the temperature by means of an analogy with iodine recombination. The effect of changes of k_r with temperature is illustrated also by some observations on flames (12). This work illustrates some applications of the

Received Jan. 11, 1960.

[1] This research is based on work performed under the auspices of the U. S. Air Force, Ballistic Missiles Division, Contract no. AF 04(647)-269 at General Electric Co., Missile and Space Vehicle Dept.

[2] Numbers in parentheses indicate References at end of paper.

concepts developed herein and is, therefore, reviewed at the end of this paper.

Several experimental determinations have been made of k_r for simple atoms. At room temperature, k_r can be measured directly by using flash photolysis, e.g., (13) or discharge tubes, e.g., (14). At very high temperatures, k_r is determined indirectly by means of a shock tube, e.g., (15).

With the shock tube, k_d is determined directly from the initial temperature and pressure, shock velocity, and measured density or concentration profile; k_r is then determined by dividing k_d by an appropriate equilibrium constant. Because k_d and the equilibrium constant are both much more sensitive to temperature than k_r, it has not been possible to determine experimentally the functional dependence of any given k_r on temperature.

Two theories have been proposed which predict that the recombination coefficient will decrease with temperature, and which are in qualitative agreement with experiment. One theory (10) is that when two atoms recombine, some of the energy of recombination will be dissipated through the internal degrees of freedom of the newly formed molecule and the third body. This theory predicts that the recombination coefficient will be inversely proportional to a half-integral power of the absolute temperature. A second theory (15–17) is that an atom forms an intermediate compound with the third body. When this compound collides with a second atom, it reacts to yield a molecule and the original third body. This theory predicts that the recombination coefficient will have a low negative energy of activation and will be exponentially dependent on temperature. A more general theory (18) is that the rate limiting step in recombination changes with temperatures. At low temperature the reaction rate is determined by the collision frequency and, therefore, increases with the square root of the absolute temperature; on the other hand, at very high temperatures, the rate limiting step will be one of those previously listed so that the recombination coefficient will tend to decrease with temperature. This theory is plausible; however, it has not been verified experimentally.

Iodine Atom Recombination

The recombination of iodine atoms has been studied extensively because of its experimental convenience. The low dissociation energy of molecular iodine makes it feasible to dissociate iodine by either photolysing it with visible light or by subjecting it to relatively weak shock waves, and the spectrum of molecular iodine permits one to monitor its concentration by absorption of the visible light. The results of this work give insight into reactions of greater technical interest.

At 298 K for iodine atoms with argon as a third body, k_r is $(2.9 \pm 0.3) \times 10^{15}$ cm^6 per gm-mol^2 sec (13). k_r is shown to have the same order of magnitude for most atoms with argon as the third body. At this relatively low temperature, iodine is at least 250 times more effective than argon as a third body. (I.e., the rate constant with iodine as a third body is more than 250 times greater than with argon as a third body.)

This reaction has been studied also at elevated temperatures in a shock tube (15). The results are tabulated in Table 1. At 1300 K, it was found that iodine was less than 35 times as effective a third body as nitrogen.

Two very important general results which have been found to be applicable to all atom recombination reactions are illustrated by this work:

1 The recombination coefficient with argon as a third body decreases very slowly with temperature. The difference between the recombination coefficient at 1300 K and that at 297 K is less than one order of magnitude.

2 From Table 1 and from the effect of temperature on the efficiency of iodine as a third body, it can be seen that the differences between the efficiencies of various third bodies tend to vanish at elevated temperatures, as suggested in (15). Because of this, molecular oxygen, molecular nitrogen and argon probably can be considered equivalent third bodies at elevated temperature. To within one order of magnitude, atomic oxygen and atomic nitrogen are probably equivalent to the respective undissociated molecules as third bodies. Although the theoretical explanation for these results has not been established, all of the current plausible theories discussed previously predict that the recombination coefficient becomes less dependent on the absolute temperature as the temperature is elevated (10,15–17). Thus, the recombination coefficient for atoms probably can be considered independent of temperatures above 1000 K for the third bodies encountered in a normal atmosphere.

In Table 1 as regards N_2 it has been assumed as it was also by Britton et al. (15) that the reaction of interest occurred so rapidly that the nitrogen remained vibrationally unrelaxed during this time. At 1300 K, the relaxation time for iodine dissociation under the conditions of Britton's experiments is 75 microsec. By contrast, Blackman's results (19) indicate that at the temperature and pressure at which this experiment was conducted, pure nitrogen has a vibrational relaxation time of 1700 microsec. The possibility must be considered that vibrational relaxation is much more probable when a nitrogen molecule collides with an iodine atom or molecule than when it collides with another nitrogen molecule. Since the atomic weight of iodine is greater than the molecular weight of nitrogen, the parameter (χ) will be even smaller for the above collision than for a collision between two nitrogen atoms. Therefore, according to the theory of Landau and Teller (20), it is even less likely that the vibrational energy of an excited nitrogen molecule will be dissipated as translational energy when it collides with an iodine particle than when it collides with another nitrogen molecule.

A vibrational quantum in molecular iodine (21) has 214.6 cm^{-1} of energy whereas that in nitrogen has 3394 cm^{-1}. Because of this large difference, resonance transfer of vibrational energy between nitrogen and iodine is improbable. Therefore, the assumption of Britton et al. seems plausible.

Oxygen Atom Recombination

At room temperature, the recombination of oxygen atoms might be studied under two extreme conditions. Either the ratio of oxygen atoms to oxygen molecules is much greater than 1, or much less than 1. In the former case, the following mechanism of recombination will predominate

$$O + O + M \rightarrow O_2 + M$$

Golden and Myerson (22) have studied the recombination of atomic oxygen under this condition by using an electric discharge to dissociate oxygen in a static system and then following the recombination with flash spectroscopy starting milliseconds after their discharge is extinguished. Their preliminary results indicate that k_r for the reaction described is 3×10^{14} cm^6 per gm-mol^2 sec at room temperature with oxygen as a third body. This constant is not unusually large for

Table 1 Recombination coefficients for iodine atoms with different third bodies

Third body	k_r, cm^6/gm-mol sec	T, K	k_r gas per k_r argon at temp. T	k_r gas per k_r argon at room temp.
A	2.9×10^{15}	298	...	...
A	4.5×10^{14}	1300	1	1
He	1.8×10^{14}	1400	0.36	...
N_2	4.4×10^{14}	1300	1.0	1.25
O_2	5.3×10^{14}	1275	1.2	1.8
I_2	...	1100	less than 35	250–600

Table 2 Rate constants for oxygen atom recombination by formation of ozone

	Reaction	Rate constant
1	$O_3 + O_2 \rightarrow O_2 + O_2 + O$	$(4.61 \pm 0.25) \times 10^{15} e^{-24{,}000/RT}$ cc/gm-mol sec
2	$O_3 + O_2 + O \rightarrow O_3 + O_3$	$(6.00 \pm 0.33) \times 10^{13} \times e^{+600/RT}$ cm^6/gm-mol^2 sec
3	$O + O_3 \rightarrow 2O_2$	$(2.96 \pm 0.21) \times 10^{13} \times e^{-6000/RT}$ cc/gm-mol sec

recombination. It indicates that the reaction $O + O_2 \rightarrow O_3$ followed by $O_3 + O \rightarrow 2O_2$ is unimportant under their experimental conditions.

By contrast, if the ratio of molecular oxygen to atomic oxygen is much greater than 1, collisions of the type $O + O_2 + M \rightarrow O_3 + M$ will be much more common than collisions of the type $O + O + M \rightarrow O_2 + M$. Under this condition, the mechanism for recombination will be

$$O + O_2 + M \underset{k_1}{\overset{k_2}{\rightleftharpoons}} O_3 + M$$

$$O_3 + O \xrightarrow{k_3} O_2 + O_2$$

These reactions can be studied through the thermal decomposition of ozone. Benson and Axworthy (23) made such a study; their results are given in Tables 2 and 3.

Schiff (24) and his co-workers have recently studied the recombination of oxygen atoms under these conditions. They began their measurements at least $\frac{1}{2}$ sec after the oxygen had been dissociated by a discharge; under their experimental conditions, the O_2 to O ratio was at least 20 to 1. Their results were in accord with the described mechanism and with the rate constants of Benson and Axworthy.

At elevated temperatures, this mechanism will become less important both because O_3 becomes more unstable and because O will probably be present in larger concentration. Matthews (25) has recently found that k_r for oxygen atoms, with molecular oxygen as a third body, is $(8.4 \pm 3) \times 10^{14}$ cm^6 per gm-mol^2 sec at 3500 K. This is an outstanding piece of work which illustrates how effectively a shock tube can be used in kinetic work. Because oxygen in contrast to iodine does not have a convenient absorption spectra in the visible, it was necessary to obtain the profile of the oxygen atom concentration from the density profile. This profile was determined from the profile of the index of refraction which was measured by interferometry. Matthews was able to show that the experimental density profile agreed with the calculated profile at seven points.

This work is corroborated by an earlier study of Chesick and Kistiakowsky (26) who measured the density profile of two shocked 75 per cent oxygen–25 per cent xenon mixtures by x-ray absorption. Within the experimental error their rate constants agree with those of Matthews, provided that the reasonable but very tacit assumption of Chesick and Kistiakowsky is accepted, i.e., that xenon cannot be much more effective than oxygen as a third body. This agreement is especially impressive because the technique of Chesick and Kistiakowsky does not require knowledge of the index of refraction of a partially dissociated gas at elevated temperature.

Byron (27) has recently published a shock tube study of oxygen dissociation similar to, but less precise than, that of Matthews. Byron's resolving time was 1 microsec, whereas Matthews' resolving time was 0.25 microsec. Instead of using the complete density profile, Byron determines the rate constants from the initial slope of the density profile immediately behind the shock front, and from the time ($t_{1/2}$) it took for the density to reach the average between the initial value immediately behind the shock and its ultimate limiting value at a point far enough behind the shock for thermodynamic equilibrium to be achieved. From the initial slope of the density profile, Byron determines k_r with molecular oxygen as a third body. This k_r lies at the lower limit found by Matthews. Then from $t_{1/2}$, the effect of atomic oxygen is found. Byron reports that atomic oxygen is 10 times more effective than molecular oxygen as a third body between 2000 and 5000 K. However, at equilibrium, Byron calculates that under his most favorable condition, 11 per cent of oxygen was dissociated. At $t_{1/2}$, there is only about 5 per cent dissociation at most. Therefore, collisions involving molecular oxygen occur 10 times as frequently as those involving atomic oxygen. The author feels that Byron's error in the rate constants is larger than Matthews', and that it is completely reasonable to assume that Byron's value of k_r with molecular oxygen as a third body should be doubled, bringing it into agreement with Matthews' result. Then the same $t_{1/2}$ would be found by assuming that molecular and atomic oxygen were about equal as third bodies.

Nitrogen Atom Recombination

A recent study (14) shows that k_r for nitrogen atoms with molecular nitrogen as a third body is $(5.7 \pm 0.8) \times 10^{15}$ cm^6 per gm-mol^2 sec between 195 and 450 K; with argon as a third body, this coefficient is $(2.8 \pm 0.3) \times 10^{15}$ cc^2 per mol^2 sec at 297 K. This is in fair agreement with an earlier piece of work (28) which is less precise as will be shown.

In both studies, nitrogen atoms were generated in a flow system by an electric discharge, and the concentration of atoms was then determined as a function of distance. Knowing the flow velocity, the rate constant could then be determined.

In the more recent study, the N atoms could be titrated with nitric oxide (28,29) at five points in the apparatus. This titration was followed by a mass spectrometer. By contrast, in the earlier work, the nitrogen atoms were titrated at only one point and the end point was determined visibly. The author has found in his own work that the end point determined in this way is very subjective. The intensity of the resultant afterglow was then used to measure the atom concentration. In the more recent work, total pressures between 1 and 10 mm Hg were used. It was shown directly that at higher pressures the nitrogen atoms disappeared by a third-order reaction, and therefore heterogeneous recombination at the wall of the apparatus was negligible; at lower pressures, a first-order reaction due to recombination at the wall had to be considered. By contrast, the earlier workers used pressures between 0.1 and 1 mm Hg and just assumed that wall recombination could be neglected.

No direct study has been made on the recombination of nitrogen atoms at elevated temperatures. However, note that the value of the recombination coefficient of nitrogen atoms at 297 K with argon as a third body is the same as the corresponding recombination coefficient for iodine atoms. It is

Table 3 Efficiencies of different third bodies relative to ozone in reactions 1 and 2 in Table 2

	Relative efficiency
O_3	1
O_2	0.44
N_2	0.41
CO_2	1.06
He	0.34

believed, therefore, that the values of the recombination coefficient for nitrogen atom recombination at elevated temperature are probably equal to the corresponding recombination coefficients for iodine atoms. However, the author feels that it is desirable to confirm this experimentally.

Radiative Recombination

It has been pointed out, using a theoretical argument, that radiative recombination will occur in less than one out of one million collisions between atoms in the most favorable case (30). Since the collision rate is about $10^{14.7}$ cc per gm-mol sec (31), the rate constant for radiative recombination has an upper limit of about 10^9 cc per gm-mol sec. It can be seen by appropriate substitutions that radiative recombination might become important when the particle density is less than one thousandth of its value at sea level.

However, various restraints which can be derived, at least in theory, by application of quantum mechanics generally will lower the radiative recombination coefficient by many orders of magnitude. For example, the radiative recombination of oxygen atoms and carbon monoxide to form carbon dioxide must occur through a transition not favored by selection rules derived through quantum mechanics (32). The rate constant for this reaction is 1.6×10^5 cc per gm-mol sec (33).

At present, it has not been shown that this mode of recombination is of sufficient technical importance to an aerodynamicist to warrant a more detailed review.

Bimolecular Reactions

Many bimolecular reactions are so rapid compared to the three-body recombination reactions discussed previously, that certain equilibria may be achieved even in a nonequilibrium system (34,35). For example, in a container of air in which the temperature is changing very rapidly, the equilibrium relation $(P_{N_2})(P_O)^2(P_N)^{-2}(P_{O_2})^{-1} = K_1(T)$ may be obeyed even though the equilibrium relations $(P_O)^2\,(P_{O_2})^{-1} = K_2(T)$ and $(P_N)^2(P_{N_2})^{-1} = K_3(T)$ are not satisfied. This illustration is discussed in more detail.

Consider a mixture of nitrogen atoms and oxygen atoms in equilibrium at high temperature (T_1). Assume that the temperature is rapidly reduced to a lower temperature (T_2) so that the degree of dissociation at equilibrium is now negligible. The problem is to find out how fast the atoms will recombine. A priori, one way of doing this is to assume that recombination takes place through the following reactions

$$N + O + M \rightarrow NO + M \qquad [1]$$

$$O + O + M \rightarrow O_2 + M \qquad [2]$$

$$N + N + M \rightarrow N_2 + M \qquad [3]$$

It is then necessary to solve three kinetic equations simultaneously. The previously illustrated treatment ignores the following two shuffling reactions

$$O_2 + N \rightarrow NO + O \qquad [4]$$

$$NO + N \rightarrow N_2 + O \qquad [5]$$

Under many conditions which can be determined from rate constants next described, reactions [4 and 5] will be so rapid compared with reactions [1, 2 and 3] and with the rate at which the temperature is changing, that the following equilibrium relations will be obeyed in the recombining mixture

$$\frac{(P_{NO})(P_O)}{(P_{O_2})(P_N)} = K_4(T_2) \qquad [6]$$

$$\frac{(P_{N_2})(P_O)}{(P_{NO})(P_N)} = K_5(T_2) \qquad [7]$$

If the first three reactions occur at about the same rate (as indicated, this is probably a reasonable assumption), then all the atoms can be lumped together and recombination can be considered to occur by the following mechanism

$$A + A + M \rightarrow A_2 + M$$

Relations [6 and 7] replace two kinetic equations. Of course, by multiplying Equations [6 and 7], it is found that the relation

$$K_1 = (K_4)(K_5) = (P_O)^2(P_{N_2})(P_{O_2})^{-1}(P_N)^{-2}$$

is also satisfied. This was previously indicated.

To determine which bimolecular reactions are rapid enough to achieve equilibrium, the appropriate rate constants must be known or reliably estimated. A rate constant can be written in the form $k = ae^{-E/RT}$ (36) (the Arrhenius equation).

For most reactions of the type $a + bc \rightarrow ab + c$, the pre-exponential factor is generally between 10^{12} and 10^{14} cc per gm-mol sec. However, because of quantum mechanical considerations reactions between materials of low molecular weight, in which electron spin (angular momentum) is not conserved, have much lower pre-exponential factors (37).

If the reaction is exothermic, the activation energy is generally less than 10,000 cal per gm mol and can be approximated by the Hirschfelder rule (38) which states that the activation energy is about 5.5 per cent of the energy of the bond between b and c. (To obtain the rate constant for the endothermic reaction in the opposite direction, divide the previously mentioned rate constant by the equilibrium constant.)

Several comparisons between experimental activation energies and activation energies calculated from Hirschfelder rules are given in Table 4. Most of the dissociation energies necessary to calculate the activation energies and heats of reaction in Table 4 were taken from Gaydon (43). For the reactions NOCl + Cl and O + NO_2, the data were taken from the Bureau of Standards Table (44). Several other comparisons between experimental results and results computed from Hirschfelder rules are given in (45).

Table 4 Calculated and experimental activation energies for several reactions

Reference	Activation energy, Kcal/gm-mol: Calculated values	Experimental values	Source
NO + N	8.3	very small	(29)
O_2 + N	6.5	6.2	(29)
H + H_2	6.2	7.5 ± 1.0	(39)
Cl + H_2	6.2	5.5	(40)
NOCl + Cl	2.0	1.1	(41)
O + NO_2	3.9	very small	(42)
O + O_3	1.25	6	(23)

A close examination of the table shows that some very exothermic reactions actually have lower activation energies than predicted by Hirschfelder rules. This is expected from theoretical considerations discussed in the literature (46). Some specific reactions are discussed in greater detail:

$$N + NO \rightarrow N_2 + O$$

Because this reaction is extremely rapid, only a lower limit of 5×10^{13} cc per gm-mol sec (47) can be set on its rate constant at room temperature.

$$O_2 + N \rightarrow NO + O$$

This reaction has also been studied experimentally (29). It was found that k equals $2 \times 10^{12} \exp(-6200/RT)$ cc per gm-mol sec between 394 and 515 K.

Reactions of the type $A_2 + B_2 \rightarrow 2AB$ are generally very

slow compared with other shuffling reactions. This is illustrated by the reaction below

$$N_2 + O_2 \rightarrow 2NO$$

This reaction is so slow that its rate constant has never been determined. An effort (48) to do this by measuring the rate of formation of NO in air between 2000 and 3000 K showed that oxygen atoms formed by the thermal dissociation of molecular oxygen reacted with molecular nitrogen so rapidly to yield NO and atomic nitrogen (i.e., $O + N_2 \rightarrow NO + N$), that the effect of the described reaction could not be observed. Therefore, the reaction rate can be considered virtually zero in all aerodynamic problems. This conclusion has been verified by direct studies (49,50) of the reverse reaction whose activation energy was found to be between 63 and 64 kcal per gm mole. By addition of the heat of the previously described reaction to the activation energy of the reverse reaction, the energy of activation of this reaction is found to be between 106 and 107 kcal per mole. This is extremely high.

Application

Some of the ideas expressed in this paper were originally suggested by Sugden and his colleagues who have utilized them in their work on flames. He has burned fuel rich mixtures of hydrogen, oxygen and nitrogen (12), and found that the gas rapidly reacts exothermally to yield a product containing an excess of H and OH radicals which slowly recombine as the gas streams from the burner. In this mixture, the following reactions are responsible for recombination

$$H + H + M \rightarrow H_2 + M$$

$$H + OH + M \rightarrow H_2O + M$$

The reaction

$$OH + OH + M \rightarrow H_2O_2 + M$$

is unimportant because H_2O_2 is unstable at the temperatures used (1600–2400 K).

Because of two-body reactions, the concentrations of H and OH are coupled and the following equilibrium is maintained

$$H + H_2O \rightleftarrows OH + H_2$$

This principle was utilized to measure the concentration of H in the flame. Flame gas containing less than 1 ppm of NaCl was used. This was not sufficient to perturb the flame. However, the sodium atom concentration would be measured from the intensity of its resonance line. This concentration was coupled to the hydrogen atom concentration because the equilibrium $Na + HCl \rightleftarrows NaCl + H$ was established in the flame.

At 1650 K, the following rate constants were found

$$H + OH + H_2O \rightarrow H_2O + H_2O$$

$$k_2 = 5.4 \times 10^{17} \text{ cm}^6/\text{gm-mol}^2 \text{ sec}$$

$$H + H + H_2O \rightarrow H_2 + H_2O$$

$$k_3 = 2.2 \times 10^{16} \text{ cm}^6/\text{gm-mol}^2 \text{ sec}$$

These rates slowly decreased with temperature.

Sugden (12) felt that this work showed that H_2O was 10 times as efficient as H_2 or N_2 in promoting the recombination of H and OH and that he could, therefore, neglect the effect of three-body collisions with H_2 or N_2 as third bodies in the burnt gas. He supported this argument by showing that the products $(k_2)(H_2O)$ and $(k_3)(H_2O)$ were independent of the composition of the burnt gas. The burnt gases used contained from 18 to 36 mole per cent H_2O. The remainder was various mixtures of nitrogen and hydrogen. Assuming that hydrogen and nitrogen had the same efficiency as water in promoting these recombinations, (k_2) (H_2O) would change by a factor of 2 over the composition range used. Unfortunately, the authors do not show that they can detect this difference, which is commonly the experimental error in kinetic work. Therefore, all that can be said is that H_2O is at least as efficient as H_2 and N_2 in promoting the illustrated recombination reactions. The rate constants given may, therefore, be as much as five times too large because the effect of N_2 and H_2 was neglected.

Summary

The kinetics of the homogeneous reactions involving mixtures of diatomic gases and their dissociation products are important in many aerodynamic problems. There are two general types of reactions of importance, atom recombination ($A + A + M \rightarrow A_2 + M$) and its reverse reaction (dissociation), and two-body reactions ($A + BC \rightarrow AB + C$).

For many atom recombination reactions of technical importance, k_r is about 10^{15} cm^6 per gm-mol^2 sec at room temperature and decreases slowly as the temperature is increased. Its value at elevated temperature generally differs by less than one order of magnitude from its value at room temperature.

For many two-body reactions as illustrated, $k = 10^{13}e^{-E/RT}$ cc per gm-mol sec where E is less than 10 kcal per gm mol for an exothermic reaction. These two-body reactions couple the concentrations of different dissociated gases to each other so that it is frequently possible to assume that thermodynamic equilibria of the type $A_2 + 2B \rightleftarrows 2A + B_2$ are achieved even though the equilibria $2A \rightleftarrows A_2$ and $2B \rightleftarrows B_2$ are not reached. An application of this to a study of flames is given.

Acknowledgment

I would like to acknowledge helpful discussions with several members of the Aerosciences Laboratory, in particular, Drs. Bortner, Scala and Myerson. I would also like to thank Dr. Korman of Republic Aviation Corp. for allowing me time and assistance to revise this paper. Finally, I would like to thank Messrs. Hyatt, Gravina and Eldridge of the Republic Aviation Corp. for reviewing this paper.

Nomenclature

E = activation energy
K = equilibrium constant
P = pressure
R = universal gas constant (cal/gm-mol K)
T = absolute temperature
a = pre-exponential factor
e = base of natural logarithms
k = rate constant
k_r = termolecular recombination rate constant
k_d = dissociation rate constant
χ = ratio of the time for a molecule to make one vibration to the time two molecules remain in contact during a collision
A = sum of all atomic species in a gas
A_2 = sum of all diatomic species in a gas
M = third body in a recombination reaction
N = atomic nitrogen
N_2 = molecular nitrogen
NO = nitric oxide
O = atomic oxygen
O_2 = molecular oxygen

References

1 Rosner, D. E., "Recent Advances in Convective Heat Transfer with Dissociation and Atom Recombination," JET PROPULSION, vol. 28, no. 7, July 1958, p. 445–451.

2 Hirschfelder, J. O., Curtiss, C. F. and Bird, R. B., "Molecular Theory of Gases and Liquids," J. Wiley and Sons, Inc., N. Y., 1954, p. 824.

3 Trotman-Dickenson, A. F., "Gas Kinetics," Butterworths Scientific Publications, London, 1955.

4 Frost, A. A. and Pearson, R. G., "Kinetics, a Study of Homogeneous Chemical Reactions," John Wiley and Sons, Inc., N. Y., 1953.

5 Moore, W. J., "Physical Chemistry," Prentice-Hall, Inc., N. J., 1955, 2nd edition, chap. 17.

6 Daniels, F. and Alberty, R. A., "Physical Chemistry," John Wiley and Sons, Inc., N. Y., 1955, chap. 13.
7 Prutton, C. F. and Maron, S. H., "Fundamental Principles of Physical Chemistry," The Macmillan Co., N. Y., 1951, 3rd edition, chap. 19.
8 Glasstone, S., "Textbook of Physical Chemistry," Van Nostrand Co., Inc., N. J., 1946, 2nd edition, chap. 13.
9 Glasstone, S., "The Elements of Physical Chemistry," Van Nostrand Co., Inc., N. J., 1946, chap. 18.
10 Palmer, H. L. and Hornig, D. F., "Rate of Dissociation of Bromine in Shock Waves," *J. Chem. Phys.*, vol. 26, 1957, p. 98.
11 Givens, W. G. and Willard, J. E., "Effect of Temperature and Br_2/Ar Ratio on the Rate of Recombination of Br Atoms Produced by Flash Photolysis of Gaseous Bromine," *J. Amer. Chem. Soc.*, vol. 81, 1959, p. 4773.
12 Bulewicz, E. M. and Sugden, T. M., "The Recombination of Hydrogen Atoms and Hydroxyl Radicals in Hydrogen Flame Gases," Trans. Faraday Society, vol. 54, 1958, p. 1855.
13 Bunker, D. L. and Davidson, N., "A Further Study of the Flash Photolysis of Iodine," *J. Amer. Chem. Soc.*, vol. 80, 1958, p. 5085.
14 Herron, J. T., Franklin, J. L., Bradt, P. and Dibeler, V. H., "Kinetics of Nitrogen Atom Recombination," *J. Chem. Phys.*, vol. 30, 1959, p. 879.
15 Britton, D., Davidson, N., Gehman, W. and Schott, G., "Shock Waves in Chemical Kinetics: Further Studies on the Rate of Dissociation of Molecular Iodine," *J. Chem. Phys.*, vol. 25, 1956, p. 804.
16 Bunker, D. L. and Davidson, N., "On the Interpretation of Halogen Atom Recombination Rates," *J. Amer. Chem. Soc.*, vol. 80, 1958, p. 5091.
17 Strong, R. L., Chien, J. C. W., Graf, P. E. and Willard, J. E., "Studies of Iodine Atom and Bromine Atom Recombination Following Flash Photolysis of Gaseous I_2 and Br_2," *J. Chem. Phys.*, vol. 26, 1957, p. 1287.
18 Keck, J. C., "Statistical Theory of Chemical Reaction Rates," *J. Chem. Phys.*, vol. 29, 1958, p. 410.
19 Blackman, V., "Vibrational Relaxation in Oxygen and Nitrogen," *J. Fluid Mech.*, vol. 1, 1956, p. 61.
20 Landau, L. and Teller, E., "Zur Theorie der Schalldispersion," *Physikalische Zeitschrift der Sowjetunion*," vol. 10, 1936, p. 34.
21 Herzberg, G., "Spectra of Diatomic Molecules," Van Nostrand Co., Inc., N. Y., 1950.
22 Golden, J. A. and Myerson, A., "Recombination of Atomic Oxygen by Means of the Flash Spectroscopy of Molecular Oxygen in the Vacuum Ultraviolet," *J. Chem. Phys.*, vol. 28, 1958, p. 978.
23 Benson, S. W. and Axworthy, A. E., "Mechanism of the Gas Phase, Thermal Decomposition of Ozone," *J. Chem. Phys.*, vol. 26, 1957, p. 1718.
24 Elias, L., Ogryzlo, E. A. and Schiff, H. I., "The Study of Electrically Discharged O_2 by Means of the Isothermal Calorimetric Detector," *Canadian J. Chem.*, vol. 37, 1959, p. 1680.
25 Matthews, D. L., "Interferometric Measurement in the Shock Tube of the Dissociation Rate of Oxygen," *Phys. Fluids*, vol. 2, 1959, p. 170.
26 Chesick, J. P. and Kistiakowsky, G. B., "Gaseous Detonation X, a Study of Reaction Zones," *J. Chem. Phys.*, vol. 28, 1958, p. 956.
27 Byron, S. R., "Measurement of the Rate of Dissociation of Oxygen," *J. Chem. Phys.*, vol. 30, 1959, p. 1380.
28 Harteck, P., Reeves, R. R. and Mannella, G., "Rate of Recombination of Nitrogen Atoms," *J. Chem. Phys.*, vol. 29, 1958, p. 608.
29 Kistiakowsky, G. B. and Volpi, G. G., "Reactions of Nitrogen Atoms I, Oxygen and Oxides of Nitrogen," *J. Chem. Phys.*, vol. 27, 1957, p. 1141.
30 Noyes, W. A. and Leighton, P. A., "The Photochemistry of Gases," Reinhold Publishing Corp., N. Y., 1941, p. 178.
31 Trotman-Dickenson, A. F., "Gas Kinetics," Butterworths Scientific Publications, London, 1955, p. 23.
32 Gaydon, A. G., "The Spectroscopy of Flames," John Wiley and Sons, Inc., N. Y., 1957, p. 104.
33 Kaskan, W. E., "The Source of the Continuum in Carbon Monoxide-Hydrogen-Air Flames," *Combustion and Flame*, vol. 3, 1959, p. 39.
34 Bulewicz, F. M., James, C. G. and Sugden, T. M., "Photometric Investigations of Alkali Metals in Hydrogen Flame Gases II. The Study of Excess Concentrations of Hydrogen Atoms in Burnt Gas Mixtures," Proc. Roy. Soc., vol. 235, section A, 1956, p. 89.
35 Kaskan, W. E., "Excess Free Radical Concentrations and Disappearance of Carbon Monoxide in Flame Gases from Some Lean Mixtures," *Combustion and Flame*, vol. 3, 1959, p. 49.
36 Trotman-Dickenson, A. F., "Gas Kinetics," Butterworths Scientific Publications, London, 1955, p. 6.
37 Laidler, K. J., "The Chemical Kinetics of Excited States," Clarendon Press, Oxford, 1955, p. 32.
38 Hirschfelder, J. O., "Semi-Empirical Calculations of Activation Energies," *J. Chem. Phys.*, vol. 9, 1941, p. 645.
39 Trotman-Dickenson, A. F., "Gas Kinetics," Butterworths Scientific Publications, London, 1955, p. 173.
40 Ashmore, P. G. and Chanmugen, J., "Reactions of the System Hydrogen, Chlorine, Nitric Oxide and Nitrosyl Chloride," Trans. Faraday Society, vol. 49, 1953, p. 254.
41 Burns, W. G. and Dainton, F. S., "The Rate Constants of the Reactions of Nitrosyl Chloride with Chlorine Atoms and COCl Radicals," Trans. Faraday Society, vol. 48, 1952, p. 52.
42 Kaufman, F., "The Air Afterglow and Its Use in the Study of Some Reactions of Atomic Oxygen," Proc. Roy. Soc., vol. 247, section A, 1958, p. 123.
43 Gaydon, A. G., "Dissociation Energies," Chapman Hall Ltd., London, 1953.
44 Rossini, F. D., Wagman, D. D., Evans, W. H., Levine, L. and Jaffe, S., "Selected Values of Chemical Thermodynamic Properties," Nat. Bur. Standards Circular 500, U. S. Government Printing Office, 1952.
45 Frost, A. A. and Pearson, R. G., "Kinetics, a Study of Homogeneous Chemical Reactions," John Wiley and Sons, Inc., N. Y., 1953, p. 102.
46 Trotman-Dickenson, A. F., "Gas Kinetics," Butterworths Scientific Publications, London, 1955, p. 229.
47 Kistiakowsky, G. B. and Volpi, G. G., "Reactions of Nitrogen Atoms II H_2, CO, NH_3, NO and NO_2," *J. Chem. Phys.*, vol. 28, 1958, p. 665.
48 Glick, H. S., Klein, J. J. and Squire, W., "Single Pulse Shock Tube Studies of the Kinetics of the Reactions $N_2 + O_2 \rightleftarrows 2NO$ between 2000–3000°K," *J. Chem. Phys.*, vol. 27, 1957, p. 850.
49 Yuan, E. L., Slaughter, J. L., Koerner, W. E. and Daniels, F., "Kinetics of the Decomposition of Nitric Oxide in the Range 700–1800°C," *J. Phys. Chem.*, vol. 63, 1959, p. 952.
50 Kaufman, F. and Kelso, J. R., "Thermal Decomposition of Nitric Oxide," *J. Chem. Phys.*, vol. 23, 1955, p. 1702.

Spectroscopic Studies of Reverse Jet Flame Stabilization[1]

A. E. FUHS[2]

California Institute of Technology
Pasadena, Calif.

Conditions in the critical zone have a strong influence on the stability of a flame which is held stationary by a small jet directed counter to the main stream. Using the spectral intensity ratio method, the local equivalence ratio in the critical zone was measured. The results suggest that there is *one* stability curve (blowoff velocity as a function of the equivalence ratio in the critical zone) regardless of jet composition. The equivalence ratio in a reverse jet stabilized flame was determined locally as a function of duct radius. Jet composition affects the observed equivalence ratio radially as far as the duct walls although only weakly beyond about one third of the duct radius.

IN ORDER to stabilize a flame in a high velocity stream of combustibles, it is necessary to provide a continuous ignition source. The recirculation zone associated with an obstacle placed in the flow is a low velocity region of hot, burned gases which ignite the reactants continuously. The obstacle may be a bluff body, an array of bluff bodies, a recess in the duct wall or a small jet opposing the main flow. A flame stabilized by a reverse jet has been studied using the spectral

Received Feb. 12, 1959.
[1] Supported by the Office of Ordnance Research, U. S. Army, under Contract DA-04-495-Ord-446.

[2] Formerly Lecturer in Jet Propulsion. Presently Member of the Technical Staff, Space Technology Laboratories, Inc. Member ARS. The author conducted this investigation at the suggestion of Dr. S. S. Penner and wishes to thank Dr. Penner for many helpful discussions.

intensity ratio method which presumably gives the local equivalence ratio. The restrictions on the application of this method will be discussed.

Reverse jet flame stabilization introduces several new variables and hence new design possibilities. Among the new variables are jet momentum, composition, temperature and mass flow rate. Since the jet has a pronounced effect on flame stability, the jet variables may be optimized to fit the widely varying operating conditions in ramjets and afterburners.

Experimental Evidence Indicating the Existence of a Critical Zone (1-6)[3]

Calculations show that the reverse jet contributes only about 0.01 of the mass flow of the main stream. Yet changing the jet composition from pure air to an air-fuel mixture produces a large effect in the stability curves (blowoff velocity as a function of equivalence ratio).

In order to account for the pronounced change in the stability curves, it seems reasonable to assume that there is a critical zone which determines flame holding properties. The jet flow, although only a very small fraction of the main stream flow, must contribute a large fraction to the flow entering the "critical zone." Numerous investigators (3,6) have proposed a model in which the critical zone is a region of turbulent mixing located directly behind the nose of the flame. Agoston, Noon and Witherly (11) agree with the critical zone concept but feel that it is a torroidal recirculation region with the jet as the axis.

Optimum flame stability occurs for a stoichiometric jet and main stream. When the main stream is not stoichiometric, Noon (5) found that the equivalence ratio in the critical zone φ_z at the maximum blowoff velocity V^*_{bo} is unity, regardless of jet temperature. Penner and Williams (6) have extended the concept by stating that at V^*_{bo}, φ_z is a constant characteristic of the fuel-air system.

Experimental results will be shown which suggest that actually there is *one* stability curve relating V_{bo} to φ_z for a given fuel and duct geometry.

Spectral Intensity Ratio Method

The ratio of the apparent peak intensities of two rotational lines belonging to different emitters, such as CH and C_2 can be correlated with the local equivalence ratio. To apply the spectral intensity ratio (SIR) method for determining local equivalence ratios, it is necessary to measure SIR as a function of φ using a known fuel-air input to a laminar flame. In order to apply the calibration curve with some degree of confidence, the manner in which changes in operating conditions affect SIR should be examined.

If the emission from optically thin gases is observed with a spectroscope having a slit width large compared to the line width, then it can be shown that SIR is proportional to the ratio of the population of emitters in the excited states.

In a flame the excitation is not necessarily thermal but may be the result of chemical reactions which produce molecules in excited states (chemiluminescence). In particular, the radiation from C_2 and CH must be associated with the combustion reactions. The SIR is assumed to be a function only of the local equivalence ratio. This same assumption has been made without proof also by several other investigators.

John and Summerfield (7) have measured the effect of turbulence on the radiation intensity from propane-air flames. Turbulence may reduce the specific intensity (radiation intensity divided by fuel flow rate) as much as 35 per cent for fuel-lean mixtures. Since the relative changes of C_2 and CH intensity for a turbulent flame enclosed in a duct are nearly equal, turbulence does not alter the correlation of SIR with φ.

A test for the application of the calibration curve obtained from a laminar flame to the reverse jet flame may be made by using a stoichiometric main stream. The results of these tests are shown in Fig. 1. Each point shown is the result of several different SIR measurements. The average is shown as a circle and the range of values are indicated by the lines. An inference from these data is that SIR does not necessarily yield correct absolute values for the reverse jet flame. However, relative values of φ are probably given correctly, because changes in jet composition produce the expected changes in the measured values of φ. Fortunately, the interpretation of the data does not depend in an important way on the absolute value of φ.

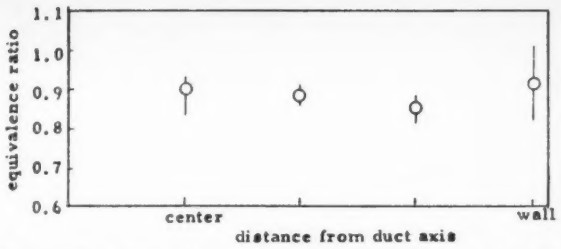

Fig. 1 The observed equivalence ratio as a function of radial distance from the duct axis for a stoichiometric main stream and stoichiometric jet. Duct: 1¼-in. standard pipe. Jet velocity: 480 fps. Main stream velocity: 42 fps

Radiation measurements were made by Clark and Bittker (8) to determine the extent to which radiant intensity could be used to measure flame velocities. There is a relation between surface area and radiation intensity for laminar flames burning at fixed equivalence ratio; the radiation per unit area of a laminar flame depends only on the equivalence ratio. Using the preceding conclusion, John, Wilson and Summerfield (9) correlated spectral intensity ratio with the equivalence ratio of a laminar flame stabilized by a bluff body in a duct. To obtain the correlation, interference filters with a band width of about 100 Å were used. One filter was centered to pass the emission from CH produced by the transition $^2\Delta \rightarrow {}^2\Pi(0, 0)$ and the other filter transmitted the emission from C_2 associated with the transition $^3\Pi \rightarrow {}^3\Pi$ (1, 1). Using the correlation of SIR with φ, John, Wilson and Summerfield (9) investigated preferential diffusion in flame stabilization. Later Wilson, John and Summerfield (10) studied the effect of boundary layer flow on flameholding by using the SIR method.

Experimental Determination of Local Equivalence Ratio in a Reverse Jet Stabilized Flame

In this section the apparatus and procedure for obtaining the calibration curve and the local equivalence ratio are described.

Experimental Determination of Spectral Intensity Ratios as a Function of Equivalence Ratio

A laminar flame from a welding torch served as the calibration flame. An image of the inner cone was formed on the slit of a diffraction grating spectroscope. Masking the slit prevented radiation from the tip and the base of the inner cone from entering the spectroscope. Spectral intensity ratios determined from any part of the straight portion of the inner cone were the same for identical fuel-air input to the flame. (See Table 1.) The lines given in Table 1 were selected because they are well isolated, and because, for a given equivalence ratio, the spectral intensity ratios based on these lines were reproducible to an accuracy of about 5 per cent.

[3] Numbers in parentheses indicate References at end of paper.

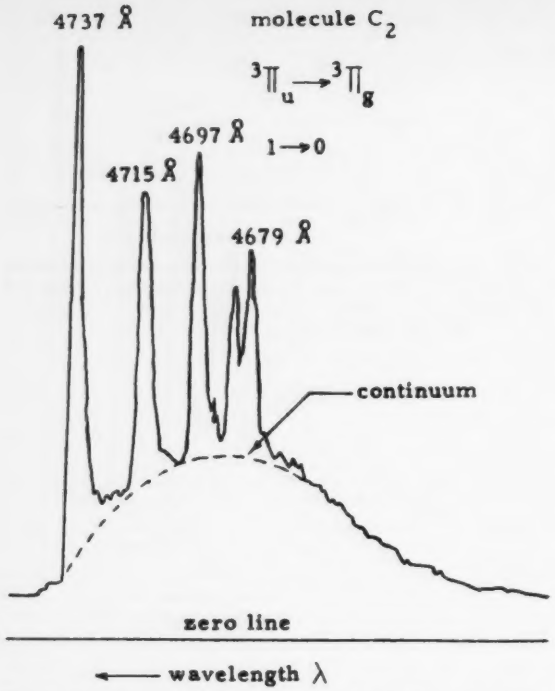

Fig. 2 Apparent emission intensity as a function of wave length

Table 1 Rotational lines selected for the computation of intensity ratios

Wave length, Å	Transitions	Emitter
4252	$^2\Delta \rightarrow {}^2\Pi(0, 0)$	CH
4312	$^2\Delta \rightarrow {}^2\Pi(0, 0)$	CH
4324	$^2\Delta \rightarrow {}^2\Pi(0, 0)$	CH
4737	$^3\Pi \rightarrow {}^3\Pi(1, 0)$	C_2
5129	$^3\Pi \rightarrow {}^3\Pi(1, 1)$	C_2
5165	$^3\Pi \rightarrow {}^3\Pi(0, 0)$	C_2
5635	$^3\Pi \rightarrow {}^3\Pi(0, 1)$	C_2
6191	$^3\Pi \rightarrow {}^3\Pi(0, 2)$	C_2

In the experimental studies steady-state conditions were established at a fixed equivalence ratio. A wave length interval including the line was then scanned. A typical recording of apparent intensity as a function of wave length is shown in Fig. 2. These data refer to the electronic transition $^3\Pi_u$ to $^3\Pi_g$ and the vibrational transition $1 \rightarrow 0$ of the radical C_2. The height of the peak was measured above the continuum. (See Fig. 2.)

Typical results of the calibration from the laminar flames are shown in Figs. 3 and 4. It is important to recognize that the calibration curves can be applied only to measurements of SIR made by the same instrument. The spectroscope in this case was a Jarrell Ash diffraction grating spectroscope using an RCA 1P28 photomultiplier tube for detection. The spectroscope has an f number of 6.5 and a linear dispersion of 18 Å/mm.

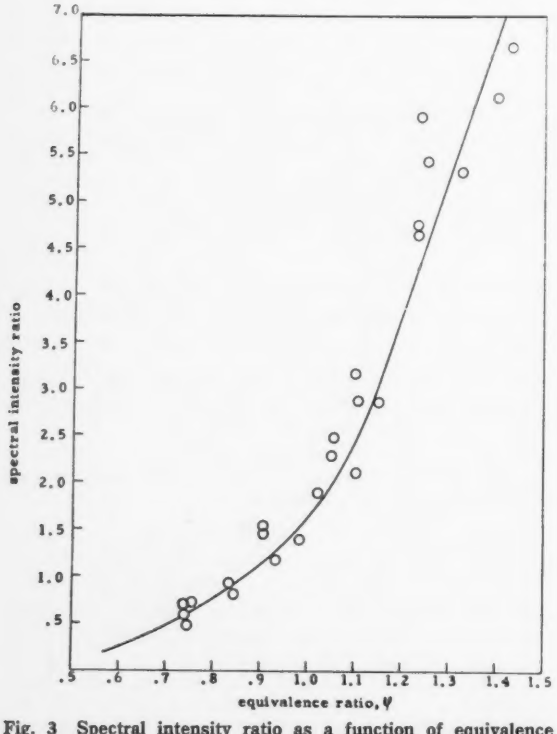

Fig. 3 Spectral intensity ratio as a function of equivalence ratio for the line with center at 4737 Å to the line with center at 4324 Å

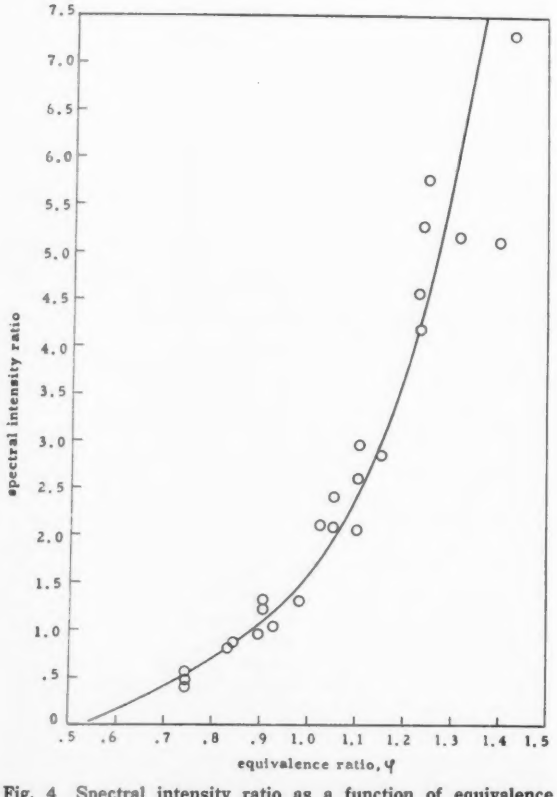

Fig. 4 Spectral intensity ratio as a function of equivalence ratio for the line with center at 4737 Å to the line with center at 4252 Å

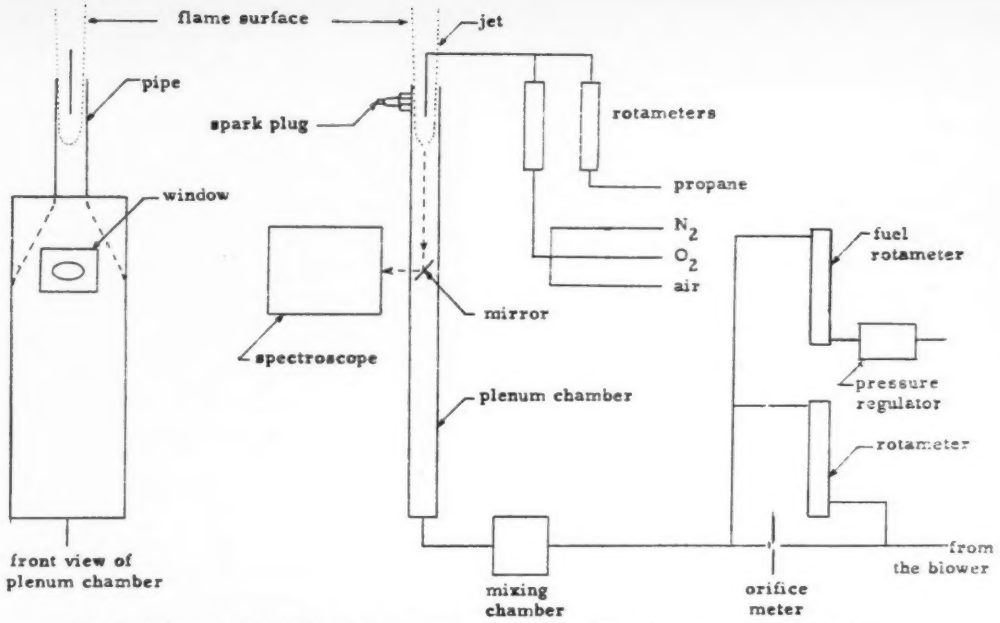

Fig. 5 Schematic illustration of the apparatus used for studies of a reverse jet stabilized flame

Description of the Apparatus and Procedure Used for Obtaining Local Equivalence Ratios

In order to view the flame, particularly the critical zone, and to measure emission intensity from limited portions of the flame, it was necessary to use a mirror system as shown in Fig. 5. A mirror was located on an adjustable mount within the plenum chamber so that the flame was viewed along the axis of the duct.

Commercial grade propane (95 per cent propane with higher hydrocarbons as impurities) was used as fuel. Facilities were provided for a jet of air, oxygen, nitrogen or fuel-air mixtures. Ignition was accomplished by means of an automobile spark plug. Two duct sizes were used: 1¼-in. diameter and 2-in. diameter standard pipe. Mixing of the fuel and air in the main stream was assured with a mixing chamber which had a porous metal (Poroloy) sheet across the flow. The diameter of the steel tubing used for the jet was $\frac{1}{16}$ in.

Steady-state operating conditions were established in the duct. By adjusting the mirror and masking off a portion of the spectroscope slit height, the radiation from a small portion of flame surface was selected for study. The size of the segment of the flame surface was an area about $\frac{1}{8}$ in. long by several hundred microns wide. The radiation entering the slit was scanned with the spectroscope; a large enough wave length interval on either side of the line was taken so as to determine the magnitude of the continuum radiation.

Experimental Results

Two types of experiments were conducted. The equivalence ratio in the critical zone at blowoff was determined, and the local equivalence ratio as a function of radial position was measured.

Equivalence Ratio in the Critical Zone at Blowoff

With an air jet, the observed equivalence ratio in the critical zone φ_s is less than the main stream equivalence ratio φ_{ms}. For the rich blowoff limit, φ_s is considerably smaller than the main stream equivalence ratio. (See Fig. 6.)

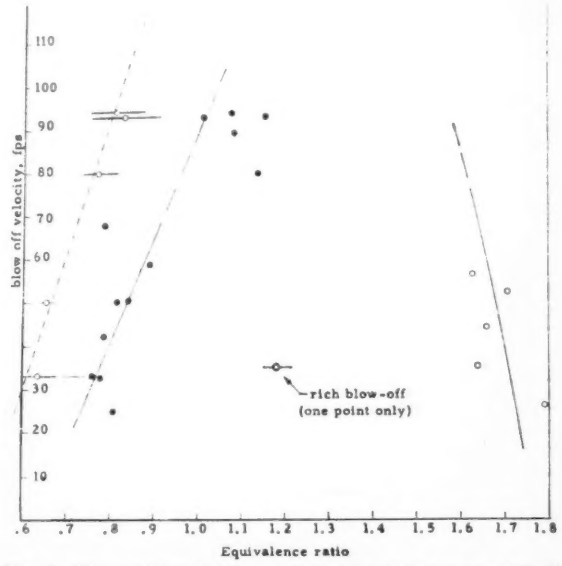

Fig. 6 Observed equivalence ratio in the critical zone at blowoff for an air jet. Open points are the observed equivalence ratio in the critical zone; the solid points are main stream values. Duct size: 1¼-in. standard pipe. Jet velocity: 480 fps

Addition of fuel to the jet shifts the blowoff curves toward the lean side. Substitution of pure oxygen for air in the jet shifts the blowoff curves toward richer mixtures. This agrees with the results which other investigators have reported (1–5). When the jet is a stoichiometric fuel-air mixture, then φ_s is larger than φ_{ms} for lean fuel-air mixtures in the approach streams. This result is illustrated in Fig. 7 by the points represented as squares. As with an air jet, the pure oxygen jet gives φ_s less than φ_{ms}. No data were obtained for an oxy-

gen jet or an air-fuel jet at the rich blowoff limit. When the main stream is rich and the jet is pure oxygen, the flame temperatures are very high, making it impossible to achieve a steady-state temperature without damage to the equipment.

The conclusion was previously stated that in the critical zone the local equivalence ratio at V^*_{bo} was the same for any jet composition. An extension of this idea is the statement that at blowoff, for any jet composition, there is *one* stability curve provided V_{bo} is plotted as a function of φ_z. In Fig. 7 the values of V_{bo} have been plotted as a function of φ_{ms} and φ_z. All points for φ_z fall nearly on the broken line curve. This is consistent with the idea of *one* stability curve $V_{bo} = V_{bo}(\varphi_z)$ regardless of jet composition. This statement merits additional discussion. As an example, consider $V_{bo} = 50$ fps. In Fig. 7 for an air-fuel jet blowoff occurs at a main stream equivalence ratio of 0.58, for any air jet φ_{ms} is 0.78, and for an oxygen jet φ_{ms} is 0.82. But for all three jet compositions, the local equivalence ratio in the critical zone φ_z is approximately 0.67. The flame geometry in the region of critical zone depends primarily on the ratio of jet velocity to main stream velocity. This is a fixed ratio for the data presented in Fig. 7. Under these flow conditions the minimum equivalence ratio at which the critical zone can maintain a flame is $\varphi_z = 0.67$.

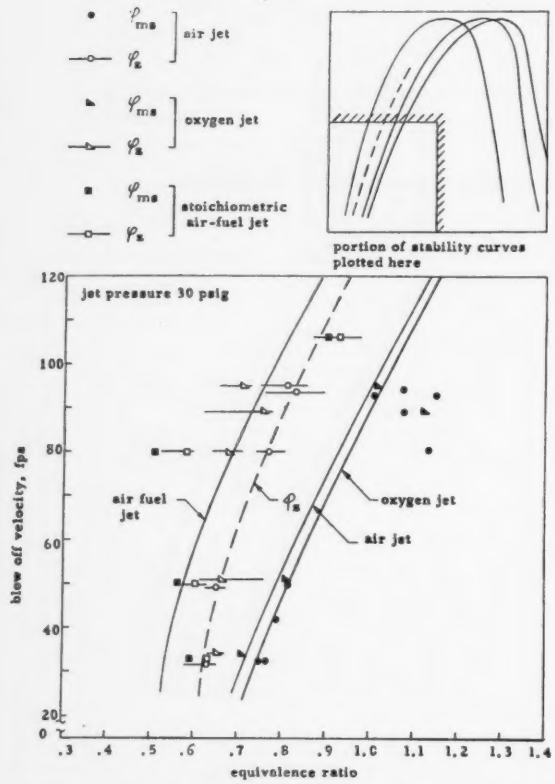

Fig. 7 Blowoff velocity as a function of main stream and critical zone equivalence ratios. Duct size: 1¼-in. standard pipe. Jet velocity: 480 fps

Local Equivalence Ratio as a Function of Radius

The equivalence ratio was measured as a function of radius. These data yield a comparison of the equivalence ratio in the critical zone with the equivalence ratio in other regions of the flame. When the jet stabilized flame is viewed parallel to the duct axis, the depth of luminous gas increases with increasing radius. (See Fig. 5.) Experiments were performed to establish the equivalence ratio gradient for a stabilized flame and also the φ_{obs}-gradient (spectroscopically determined values) for a pilot flame.

Stabilized flame

In Fig. 8 curves of the observed equivalence ratio as a function of radial distance from the duct axis are presented. For a rich main stream φ_{obs} remains constant to a radius $R/3$. Here R is the duct radius. At larger radii it decreases. The air jet and the oxygen jet give results which are practically indistinguishable. When fuel is added to the jet, φ_{obs} is higher by about 5 per cent near the center of the duct; near the duct walls, φ_{obs} merges with the other curves. The fact that φ_{obs} for the air-fuel jet is constant from the axis to $R/3$ may be explained if the assumption is made that the jet tip, and hence the critical zone, precesses about the duct axis. The precession of jet tip has been observed by Agoston, Noon and Witherly (11).

In Fig. 9, $\varphi_{obs}(r)$ has been plotted for a lean main stream. As in the case of the rich main stream, the observed equivalence ratio decreases slightly near the walls.

Pilot flame

It was not possible to maintain a flame when the jet consisted of pure fuel and the main stream of air only; however, it was possible to burn a "pilot flame" by having a fuel-air jet with equivalence ratio $\varphi_j = 2.8$ and $\varphi_{ms} = 0$. The observed equivalence ratios φ_{obs} for the pilot flame are plotted in Fig. 10. The luminous portion of the pilot flame did not fill the duct.

When there was no fuel in the main stream, the flame burned with uniform equivalence ratio. Addition of fuel to the main stream ($\varphi_{ms} = 0.26$ and $\varphi_{ms} = 0.47$) resulted in larger apparent equivalence ratios for the center of the flame. Addition of more fuel to the main stream causes an upward shift of the curve. Near the center of the duct, the flame burns locally at leaner mixtures.

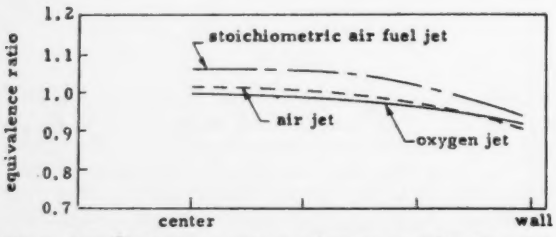

Fig. 8 Local equivalence ratio as a function of radius for a rich main stream ($\varphi = 1.16$) and various jet compositions. Jet velocity: 480 fps. Main stream velocity: 42 fps

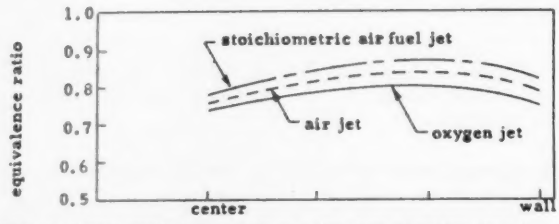

Fig. 9 Local equivalence ratio as a function of radius for a lean main stream ($\varphi = 0.92$) and various jet compositions. Jet velocity: 480 fps. Main stream velocity: 42 fps

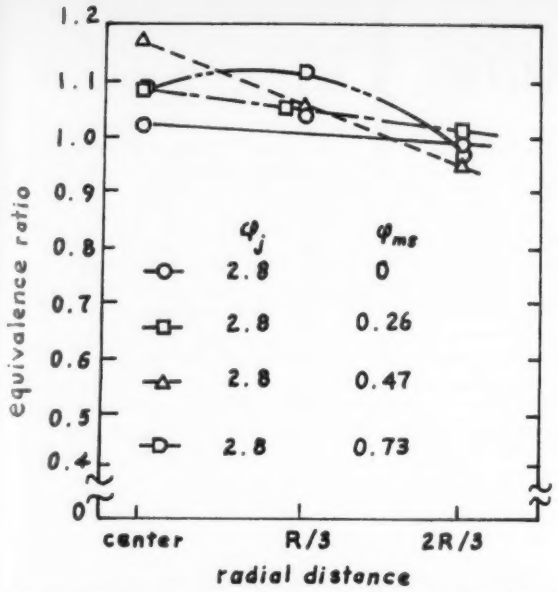

Fig. 10 Local equivalence ratio in a pilot flame as a function of φ_{ms} and radial distance. Jet velocity: 480 fps. Main stream velocity: 32 fps

Table 2 Observed equivalence ratio for an open flame stabilized by a reverse jet

Velocity at outlet of nozzle, fps	Jet pressure, psig	Fluid in jet[a]	Average jet velocity, fps	Input equivalence ratio	Equivalence ratio in critical zone
42	14	Air	330	2.12	1.02
39	12	Air	306	2.19	1.08
38	12	Air	306	2.12	1.01
40	14	Air	330	2.29	1.05
40	14	Air	330	2.29	1.06
40	9	Air	264	2.49	1.05
53	10	Air	278	1.57	0.76
53	10	N_2	286	1.56	0.79
53	10	O_2	254	1.57	0.79
40	10	O_2	254	2.18	1.06
40	10	N_2	286	2.17	1.05
40	10	Air	278	2.18	1.04
45	10	Air	278	1.68	0.83

[a] The inside diameter of the tubing used for the jet was $\frac{1}{16}$ in.

Equivalence Ratio for an Open Flame Stabilized by a Reverse Jet

For the series of experiments involving an open flame, the main stream, which was an air-fuel mixture, emerged as a jet from a nozzle with an opening of 2 in. by $\frac{1}{2}$ in. The flame-holding jet was located 16 in. vertically above the main stream nozzle. The open flame was stabilized between the outlets of the nozzle and the jet at a position which was determined by the jet pressure. It should be emphasized that the physical processes occurring in an open flame may differ from a flame stabilized in a duct. A new variable, the amount of entrained air, is introduced. Since there is no wall to provide constraint, the flame spreads laterally. The jet composition does not have a detectable influence on the combustion occurring at the tip of the flame. For an open flame the concept of a critical zone appears to lose its significance.

Air from the surroundings was entrained by the main stream and by the jet, diluting the combustibles. In order to maintain a flame, the nozzle flow had to be considerably richer than stoichiometric. The results are summarized in Table 2.

Conclusions

The spectral intensity ratio method for determining equivalence ratio must use a calibration curve which is preferably obtained under operating conditions similar to those of the test flame. When applied to flames burning under conditions unlike those of the calibration flame, the absolute value for φ may be in error; however, relative values of φ are probably given correctly.

The equivalence ratio is nearly independent of radial distance for lean flames. For rich flames the equivalence ratio decreases near the duct wall. Jet composition not only influences φ near the axis of the duct but also affects the equivalence ratio at larger radii.

The importance of the critical zone is illustrated by the experimental result that there appears to be a single stability curve relating the blowoff velocity V_{bo} to φ_s, regardless of jet composition.

References

1 Schaffer, A. and Cambel, A. B., "Continued Investigations of the Opposing Jet Flameholder," JET PROPULSION, vol. 26, 1956, pp. 576–578.

2 Schaffer, A. and Cambel, A. B., "The Effect of an Opposing Jet on Flame Stability," JET PROPULSION, vol. 25, 1955, pp. 284–287.

3 Cambel, A. B., "A Review of Flame Stabilization of Gaseous Jets," Combustion and Propulsion: 3rd AGARD Colloquium, Pergamon Press, 1959.

4 Eustis, R. H. and Mraz, C. L., "Investigations of Jet Flameholders," WADC Technical Note 56-316, April 1956.

5 Noon, A. W., "Investigations of Jet Flameholders, Part II," WADC Technical Note 56-316, April 1957.

6 Penner, S. S. and Williams, F., "Recent Studies on Flame Stabilization of Premixed Turbulent Gases," *Appl. Mech. Rev.*, vol. 10, June 1957, 229–237.

7 John, R. R. and Summerfield, M., "Effect of Turbulence on Flame Radiation," JET PROPULSION, vol. 27, 1957, pp. 169–175, 178–179.

8 Clark, T. D. and Bittker, D. A., "A Study of the Radiation from Laminar and Turbulent Open Propane-Air Flames as a Function of Flame Area, Equivalence Ratio, and Fuel Flow Rate," NACA Research Memorandum E54F29, Aug. 24, 1954.

9 John, R. R., Wilson, E. S. and Summerfield, M., "Studies of the Mechanism of Flame Stabilization by Spectral Intensity Method," JET PROPULSION, vol. 25, 1955, p. 535.

10 Wilson, E. S., John, R. R. and Summerfield, M., "Spectroscopic Studies of the Effect of Boundary Layer Flow on Flameholding," JET PROPULSION, vol. 27, 1957, pp. 892–894.

11 Agoston, G. A., Noon, A. W. and Witherly, T. D., "Experimental Study of a Reversed Jet Flameholder," *Combustion and Flame*, vol. 2, 1958, pp. 333–347.

Contour Nozzles[1]

ELLIS M. LANDSBAUM[2]

Jet Propulsion Laboratory,
California Institute of Technology
Pasadena, Calif.

A number of contour nozzles for an ideal gas with $\gamma = 1.22$ are presented. The variation of gamma is considered. The design is based upon the assumption of a radial flow section in the initial divergent section which is turned to uniform axially directed flow at the exit. For each specified exit Mach number, about 95 per cent of the maximum expansion angles were used. The contours obtained were cut back in order to yield nozzles of various exit areas. The surface area of the divergent section, thrust coefficient and length of these cutback nozzles are compared with those properties of 15-deg half-angle conical nozzles with the same exit area. Simple heat flux calculations for some of the designs are also presented. These designs result in moderate savings in length, surface area and heat flux over a 15-deg nozzle with the same thrust coefficient. Greater savings are possible at the expense of reducing the thrust coefficient.

IN THE past decade, as the result of a great deal of work, significant advances were made in all phases of rocketry. However, relatively little attention was given to the problem of nozzle configuration. This is easily understood, as there were many problems of greater significance which required attention. The conical nozzle, which had proved satisfactory in most respects, was used almost exclusively. The conical nozzles with a 15-deg half-angle (hereafter referred to as a 15-deg nozzle) has become almost a standard as it is a good compromise on the basis of weight, length and divergence loss.

The literature sporadically has had suggestions on the possibilities of configurations other than conical for rocket nozzles. The Prandtl-Buseman design, also known as a contour or bell, has usually been suggested. However, most of the work in this field has been concerned with wind tunnels. In order to obtain uniform straight flow in the test section, these nozzles are designed with rather low expansion angles which result in long nozzles impractical for use in rockets. Clippinger (1)[3] did design a number of axisymmetric nozzles for air, $\gamma = 1.4$, using initial expansion angles up to the allowable maximum. Unfortunately, these results are not applicable to the rocket nozzle problem, and designs based on the rocket exhaust gases must be made. There has been some experimental work with one of Clippinger's designs (2).

Whereas the problem of nozzle configuration has been considered, little design information has been presented. Recently, indicating a renewed interest in the subject, optimization of nozzle configuration has again been considered (3–5) and a few designs were presented (4,5). It may be presumed that this renewed interest is the result of the separate problems of continuously trying to increase performance, and the large nozzles of large thrust engines. As it is becoming more difficult to increase performance by making major improvements, more attention must be given to minor details, such as nozzle configuration.

Large thrust engines present a slightly different problem. As an example, the size of a rocket engine delivering 1,000,000 lb of thrust from one nozzle is considered. A chamber pressure of 300 psia and an exhaust gas of $\gamma = 1.22$ are assumed. If the engine is to deliver this thrust at sea level, optimum expansion in a 15-deg conical nozzle requires that the divergent section be 91.5 in., or almost 8 ft, long. If the engine is to operate in a vacuum, an area ratio of 20 requires a nozzle length of 306 in., or 25.5 ft. Obviously, shorter nozzles would be of interest. The other pertinent dimensions are listed in Table 1. The use of multiple nozzles is immediately suggested; however, these nozzles present new problems, and any thorough study must consider other configurations.

This paper considers length, weight and thrust coefficient for a consistent set of contour nozzles for a gas with $\gamma = 1.22$. These axisymmetric nozzles were designed on the same basis as wind tunnel nozzles; however, much larger expansion angles were used. The resulting contours were then cut off, resulting in nozzles which were practical for use in rockets. Some of the designs result in savings in length and weight over a 15-deg nozzle of the same thrust coefficient. Because a weight calculation requires a detailed design, the surface area of the expansion cone was used as a weight parameter. Heat flux calculations were made for several contour designs and are compared with conical nozzles of the same area ratio or thrust coefficient. Three contours with the same exit Mach number and different value of γ are also presented.

Contours

The determination of the contours presented herein is based upon the assumptions which have been previously used in the calculation of wind tunnel nozzles. The procedure, originally presented by Foelsch (6), assumes that downstream of the throat there exists a radial flow region resulting from a source flow. This flow is then turned in order to give uniform axial flow at the exit. Although most wind tunnel nozzles are

Table 1 1,000,000-lb thrust engine

Parameter	I	II
P_a, psia	15	0
P_e, psia	15	1.5
A_t, in.^{2}	2380	1850
ϵ	3.5	20
C_F	1.4	1.8
l, in.	91.5	306

$P_c = 300$ psia; $\gamma = 1.22$

Presented at the ARS 13th Annual Meeting, New York, N. Y., Nov. 17–21, 1958.

[1] This paper presents the results of one phase of research carried out at the Jet Propulsion Laboratory, California Institute of Technology, under Contract no. DA-04-495-Ord 18, sponsored by the Department of the Army, Ordnance Corps.

[2] Research Group Supervisor, Solid Propellant Rockets Section. Member ARS.

[3] Numbers in parentheses indicate References at end of paper.

Table 2 Contour nozzle design data

γ	M_e	$\nu(M)$, deg	θ_m, deg	θ_t, deg	L_t	R_t	S_t	$(C_{Fv})_t$ Calculated	$(C_{Fv})_t$ Theoretical[a]
1.22	3	61.872	15.468	14.70	1.627	1.356	3.85	1.4247	1.4248
1.22	4	85.372	21.343	21.00	1.975	1.612	5.24	1.4765	1.4781
1.22	4.6	96.38	24.095	22.90	2.416	1.850	7.03	1.5170	1.5194
1.22	5	102.724	25.681	24.40	2.586	1.978	7.90	1.5309	1.5337
1.22	6	115.808	28.952	27.50	3.018	2.295	10.38	1.5545	1.5601
1.22	7	125.408	31.352	29.80	3.344	2.610	12.75	1.5692	1.5790
1.22	8	133.800	33.450	31.75	3.579	2.884	14.87	1.5742	1.5895
1.22	9	140.164	35.041	33.30	3.950	3.141	17.83	1.5739	1.5963
1.24	4.6	92.93	23.233	22.10	2.353	1.797	6.71	1.5071	1.5090
1.26	4.6	89.75	22.438	21.30	2.314	1.755	6.49	1.4985	1.5009

[a] See discussion under "Design Considerations."

two-dimensional, there have been some axisymmetric designs based on this method (7,8).

Remarkably, there has been little experimental verification of this assumption in the literature. Apparently, the attainment of uniform flow was deemed proof of the assumption; whereas, nonuniform flows were discovered to be the result of other problems. Foster and Cowles (9) used an actual rocket motor and made pressure measurements on the centerline and wall to within 2 in. of a 1.5-in. throat. Oliver and Nagamatsu (10) measured the distribution across a section of a two-dimensional hypersonic wind tunnel. Both investigations showed good agreement with the radial flow assumption.

Secondary proof might be gained from the agreement between calculated and measured values of the thrust coefficient. There have been several experiments in which the variation of thrust coefficient with divergence angle has been measured. The agreement with the theoretical values of Tsien (11) is good in some instances (11,12) and only fair in others (13,14).

The radial flow assumption, although it may not be exact, appears to be reasonable. The assumption of a distribution at, or near, the throat (1,3–5) does not appear to be any better. The necessity of further experimental evidence is obvious. The calculations based on the radial flow assumption are presented in the following section.

Calculation of Contours

The flow regions of a typical contour nozzle are pictured in Fig. 1. The contour in Region I, the entrance section, is arbitrarily drawn. Region II is the radial flow region. Its boundaries are the characteristic lines AB and BC. The flow is turned in Region III in order to give axially directed flow. The flow field is calculated by the method of characteristics in this region, the contour being essentially identical with the streamline through point B the inflection point. The flow is uniform and axial in Region IV. The nozzles, discussed herein, were obtained by cutting off the aft end of the rather long nozzles obtained in the calculation, and therefore they do not have uniform axial flow at the exit.

The flow field along BC was determined by the method previously outlined by Foelsch (6). Starting with the flow along BC and knowing that the flow along CD is uniform and axial, the flow in Region III is determined by the characteristics method. The details of the calculation have been examined many times (1,7,8) and are not discussed here. A thorough discussion of the design techniques used here is currently under preparation.[4] Certain aspects of the problem are of interest and are mentioned briefly.

[4] The programming and computation of the contours was done by Ying-Nien Yu of the Sandberg-Serrell Corporation, Pasadena, Calif. "A Summary of Design Techniques for Axisymmetric Hypersonic Wind Tunnels" by Ying-Nien Yu is to be published.

The problem was originally programmed on an IBM 704 for the calculation of axisymmetric nozzles for wind tunnel use. The program works off the centerline Mach number distribution, a procedure previously suggested for two-dimensional nozzles (15). The change in Mach number at C is rather abrupt. Therefore, the nozzle is lengthened by 2 per cent and a more gradual change made at C. A check of the $M_{4.6}$ contour, eliminating this added section, showed a negligible change in nozzle length over the region of interest.

Since there was some concern about the functioning of the program with maximum expansion angles, angles about 95 per cent of maximum were used. The data are presented in Table 2. Subsequent analysis showed that these fears were unnecessary, and the calculation of some contours at maximum expansion angles are planned. The results of the present data are given in the following section.

Design Considerations

The design of a nozzle configuration must consider factors other than length. In general, length is probably the least important parameter. Among the other factors to be considered are weight, thrust coefficient and heat flux.

Since a 15-deg nozzle has only about a 1.7 per cent divergence loss, the possible increase in thrust coefficient is small. However, it would usually be desirable to keep the same thrust coefficient while making improvements in the other factors. A shorter length will not necessarily result in a lower weight-expansion section. However, as previously pointed out (3), a shorter length will probably result in a reduction of the weight of the attachment section and, in the case of swivel nozzles, the actuating mechanism. The heat flux may be smaller with a lower area; however, it must be investigated in

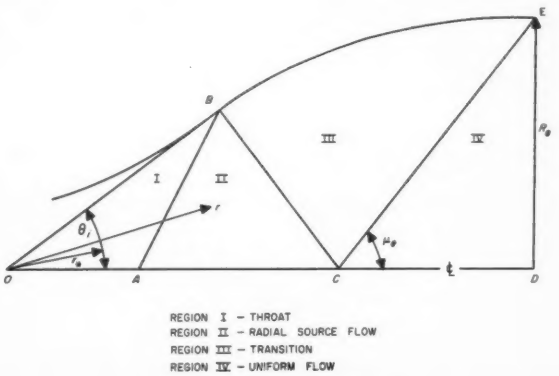

Fig. 1 Contour nozzle flow regions

order to be sure that the heat-transfer coefficient has not increased.

Contours and Length Comparison

The results of the calculation gave the contour downstream of the inflection point (B, Fig. 1). The contour between throat and inflection point was not computed, but drawn arbitrarily. This section has a radius of curvature equal to the throat diameter and tangent to the radial flow line extending to the inflection point. Recent work (13) indicates that this entry radius will probably be most efficient commensurate with weight considerations. Smaller radii have been used at this laboratory. The distance from throat to inflection point is then

$$L_i = [K + (R_i - 1 - K) \cos \theta_i]/\sin \theta_i \qquad [1]$$

where K is the ratio of entry radius to throat radius and is 2 for these nozzles. The values of L_i used are given in Table 2. The resulting contours are plotted in Fig. 2, in which the contour of a 15-deg nozzle is also plotted for comparison. The contours are designated by the full contour exit Mach number. The wall angles as a function of radius are plotted in Fig. 3.

The foregoing method of obtaining the initial contour may give a somewhat longer section than is necessary. In this respect, this design is conservative. A shorter nozzle will be obtained by assuming that the change in Mach number with length is constant from the throat to point A (Fig. 1) and equal to (dM/dL) at A. The method of characteristics may then be used to compute the contour in Region I (Fig. 1) (7,8) or the general method of this paper may be used (6). Although wind tunnels use an arbitrary entrance section, their long radius of curvature results in a long entrance section, necessary to fit their special requirements for a flexible throat (16).

A contour for a particular ϵ is then obtained by cutting off the aft end in order to obtain the desired area ratio. In order to facilitate the length comparison, the ratios of the lengths of these nozzles to that of a 15-deg nozzle of the same exit area are plotted in Fig. 4. Obvious savings in length are possible; however, weight, thrust coefficient and heat transfer must also be considered.

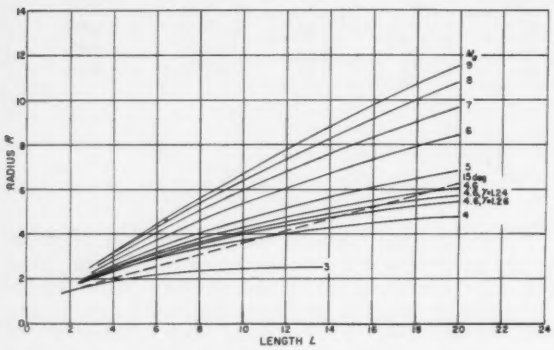

Fig. 2 Contours of nozzles, $\gamma = 1.22$, varying M_e

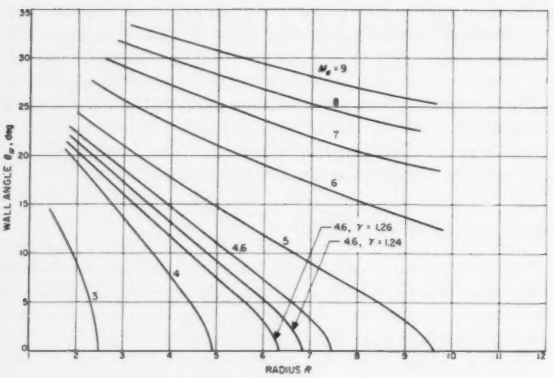

Fig. 3 Flow angles along wall, $\gamma = 1.22$, varying M_e

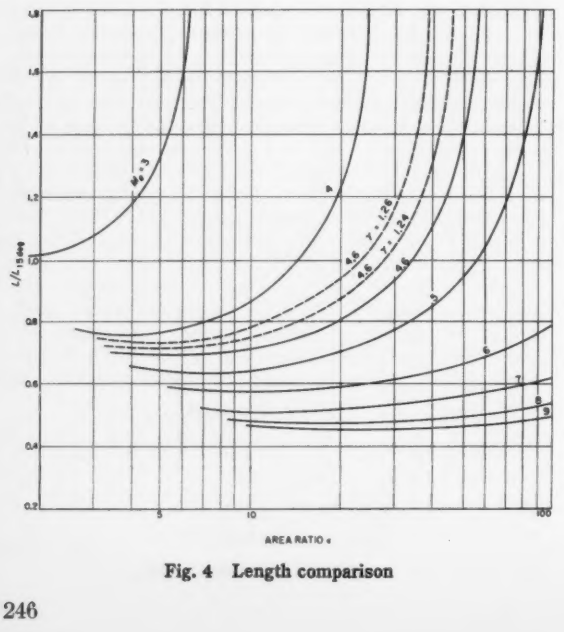

Fig. 4 Length comparison

Surface Area of Expansion Section

A comparison of nozzle weights is difficult without a detailed design. As previously mentioned, some weight savings will result from merely a shorter length, since the weight of the attachment section and, in the instance of swivel nozzles, the actuating mechanism will be reduced. The weight of a cooled nozzle constructed of tubing should be closely related to the surface area of the nozzle. For an uncooled nozzle, a true comparison requires more details. However, the surface area of the divergent section will bear some relation to weight for either type of nozzle. This surface area is presented in Fig. 5. The values up to the inflection point are listed in Table 2. A comparison with a 15-deg

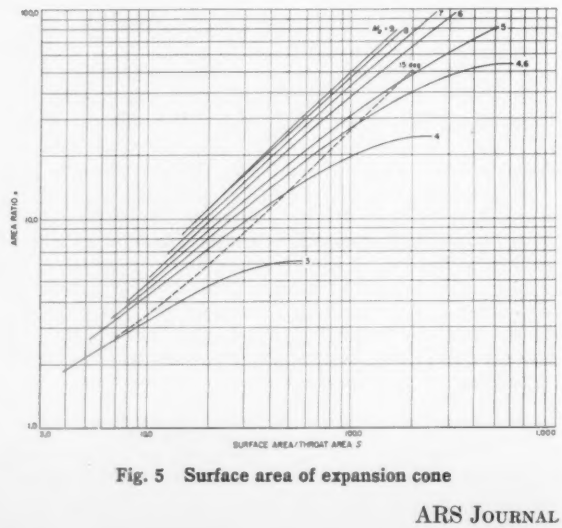

Fig. 5 Surface area of expansion cone

nozzle is made in Fig. 6. The surface area of a conical nozzle is

$$S = 2K\,[(1 + K)\,\omega - K \sin \omega] + (\epsilon - \epsilon_i)/\sin \omega \qquad [2]$$

Here ω is the expansion angle, and ϵ_i is the area ratio at the tangency point and is related to the other variables by

$$\epsilon_i = [1 + K(1 - \cos \omega)]^2 \qquad [3]$$

The first term in Equation [2] is the area to the tangency point, and the second term is the area of the conical section. It appears that large reductions in nozzle weight are possible, but this will be at the expense of decreasing the thrust coefficient.

Thrust Coefficients

The vacuum thrust coefficients obtained are plotted against ϵ in Figs. 7 and 8. The values for the 15-deg nozzle are 0.983 = [(1 + cos 15 deg)/2] of the theoretical one-dimensional vacuum thrust coefficients.

The vacuum thrust coefficients were calculated by subtracting the pressure integral along the wall from the value at the nozzle exit

$$C_{F_v}(\epsilon) = C_{F_v}(\epsilon_e) - \int_{\epsilon}^{e} \frac{P d\epsilon}{P_c} \qquad [4]$$

The vacuum thrust coefficient at the exit of the nozzles, where uniform axial flow exists, can be related to the exit Mach number

$$C_{F_v}(\epsilon_e) = \frac{\gamma M_e^2 + 1}{\left(1 + \dfrac{\gamma - 1}{2} M_e^2\right)^{\frac{\gamma}{\gamma-1}}} \epsilon_e = \left(\frac{2}{\gamma + 1}\right)^{\frac{\gamma+1}{2(\gamma-1)}} \times \frac{\gamma M_e^2 + 1}{M_e \left(1 + \dfrac{\gamma - 1}{2} M_e^2\right)^{1/2}} \qquad [5]$$

The data included the Mach number distribution along the wall, and a simple numerical integration was carried out in order to obtain C_{F_v}.

The thrust coefficient at any point can also be determined by integrating the flow conditions occurring along the plane of constant L. The required equation is

$$C_{F_v} = \int_0^{\epsilon_w} \frac{(\gamma M^2 \cos^2 \theta + 1)\, d\epsilon}{\{1 + [(\gamma - 1)/2]\, M^2\}^{\gamma/(\gamma-1)}} \qquad [6]$$

This requires a rather tedious interpolation of the points in the Mach net which may be eliminated as follows. The net force across any two control surfaces meeting at the nozzle wall will be zero. The integration can then be made along one of the lines in the net for which the data are available. The required equation is

$$C_{F_v} = 2 \int \frac{\gamma M^2 \cos \theta\, R\, (\cos \theta dR \pm \sin \theta dL) + RdR}{\{1 + [(\gamma - 1)/2]\, M^2\}^{\gamma/(\gamma-1)}} \qquad [7]$$

in which the correct sign and appropriate limits are taken.

The flow-net data were used to calculate several vacuum-thrust coefficients for each of the nozzles for purposes of comparison with the wall calculation. Significant differences were not expected. The net calculations gave higher results than the wall calculation, increasing from 0.1 per cent for the M_3 nozzle to about 4 per cent for the M_9 nozzle. A small part of the difference was the result of the net spacing and, thus, the simple trapezoidal numerical integration used gives slightly higher results. In some instances values higher than theoretical were obtained. To date, these differences have not yet been resolved.

The thrust coefficient at the inflection point calculated using Equation [4] may be compared with the theoretical value expected from radial flow considerations. This comparison is made in Table 2. Initially, the agreement is exceedingly good, the difference increasing as the initial angle increases. The calculated values are lower than the theoretical values. The theoretical values were obtained from Seifert and Crum (17), with the necessary correction for divergence loss being made (18).

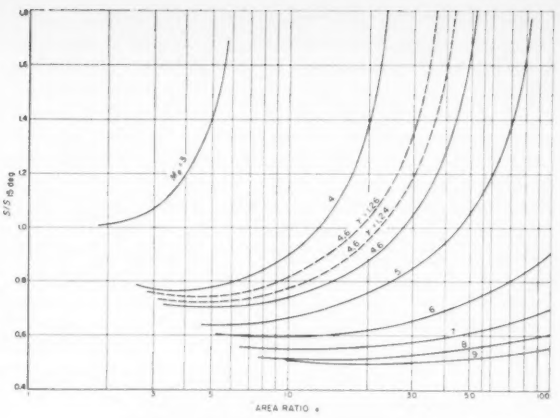

Fig. 6 Surface area comparison

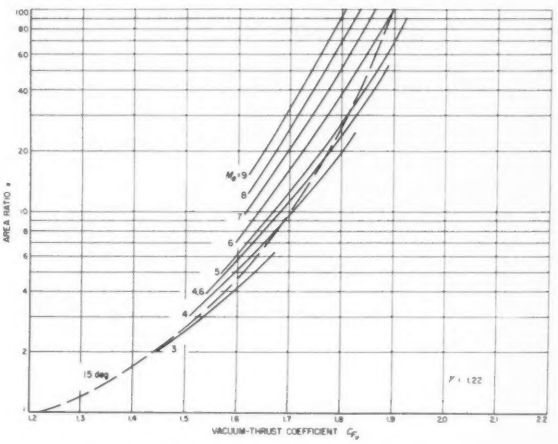

Fig. 7 Thrust coefficients, $\gamma = 1.22$, varying M_e

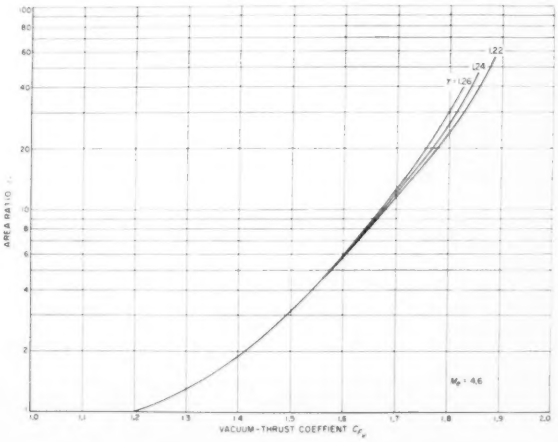

Fig. 8 Thrust coefficients, $M_{4.6}$, varying γ

It is believed that these differences are the result of the net spacing. Future calculations will use a smaller net. Fortunately, the differences in those contours of interest are negligible.

The thrust coefficient plot, Fig. 7, indicates that, for each area ratio, there will be a design from this consistent set which has the same thrust coefficient as a 15-deg nozzle. Reference to Figs. 4 and 5 shows that these nozzles will have shorter lengths and lower surface areas than their respective conical nozzles. The $M_{4.6}$ nozzle was designed after the others, as it appeared likely that it would cross the 15-deg thrust coefficient line at an area ratio of 20, a design currently of interest at this laboratory; it very nearly does fit this condition.

Of greater interest would be a plot of surface area and length against thrust coefficient for each design in order to determine the minimum values of these parameters for each thrust coefficient. The minimums are rather flat, and the graphs are too crowded to be of practical use. For each thrust coefficient of interest, the surface area or length must be plotted against contour number (M_e) to give the optimum contour. This has been done in Fig. 9. The minimums are rather flat and the $M_e = 5$ contour gives approximately minimum surface-area for expansion-area ratios from 6 to 28.

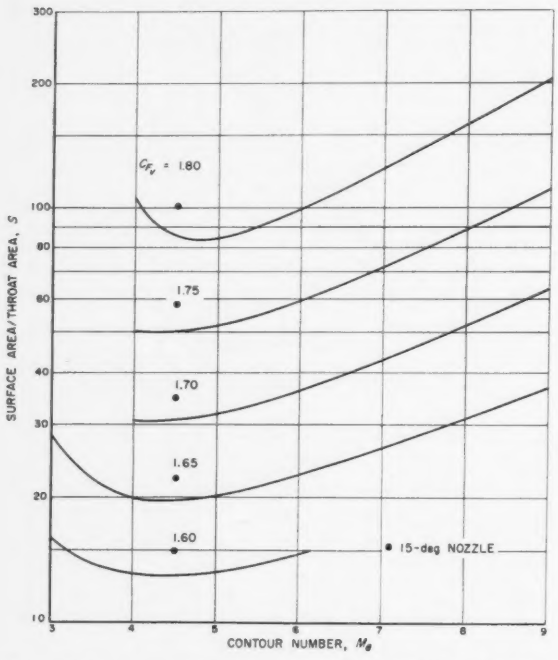

Fig. 9 Surface area comparison for constant thrust coefficient

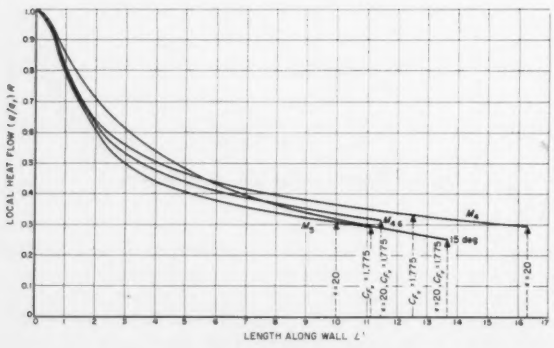

Fig. 10 Heat flux along wall

Further analysis shows that, although the contour obtained from the crossing point on the thrust coefficient plot is near minimum, further reduction in surface area is obtained with a contour of slightly greater exit area, shorter length and a larger divergence loss. This is only for vacuum thrust; if there is any back pressure the process must be repeated for those conditions.

Heat Flux

In order to obtain an idea of the extent of variation of heat flux in the divergent section, calculations were made for several contour and conical nozzles at either a constant ϵ of 20 or a constant $C_{F_v} = 1.775$. The simplified equations of Bartz (19) were used to calculate the heat transfer coefficient.[5] A constant wall temperature was assumed. Calculations were made for the M_4, $M_{4.6}$ and M_5 contours and 13-, 15- and 17-deg conical nozzles. The results are presented in Table 3 and Figs. 10 and 11.

The local heat flux as a function of the length along the nozzle wall L' is given in Fig. 10. Initially, the heat flux decreases as the expansion angle increases. Later, the curves for some of the contour nozzles cross that of the 15-deg nozzle. Although the total flux may be lower for some contours, the local flux at the exit cone may be higher than a 15-deg nozzle for some designs. This might affect the design of an uncooled nozzle.

The total heat flux was obtained from an integration of the curves in Fig. 10. For the contour nozzles

$$\frac{Q}{q_t A_t} = 2 \int \frac{qR dL'}{q_t} \qquad [8]$$

The total heat flux to the conical nozzles was calculated at this laboratory[6]

$$\frac{Q}{q_t A_t} = 0.8 + \frac{\ln \epsilon}{\sin \omega} \qquad [9]$$

Inspection of Table 3 reveals that, in general, the contour nozzles will have lower Q than the conical nozzles. The surface areas and lengths will also be lower. The Q for the contour nozzles is plotted in Fig. 11. The $M_e = 5$ nozzle has 17 per cent lower total heat flux than the 15-deg nozzle of the same thrust coefficient. The surface area is only 12 per cent less, indicating a reduction also in the average heat transfer coefficient.

Effect of γ

The effect of γ was considered. An $M_{4.6}$ nozzle was designed with $\gamma = 1.24$ and 1.26. The contours and other associated data are presented in the graphs and figures previously mentioned. This is not the best way of studying the effect of γ. Studying the variation of γ in a fixed contour

Table 3 Total heat flux

	$C_{F_v} = 1.775$		$\epsilon = 20$	
Nozzle	ϵ	$Q/q_t A_t$	C_{F_v}	$Q/q_t A_t$
M_4	16.4	12.4	1.801	14.7
$M_{4.6}$	20.0	11.1	1.775	11.1
M_5	22.8	10.3	1.759	9.6
13 deg	18.8	13.8	1.782	14.1
15 deg	20.3	12.4	1.774	12.3
17 deg	22.4	11.4	1.765	11.1

[5] Donald R. Bartz, this laboratory, performed the heat transfer calculations.

[6] Private communication from Donald R. Bartz, Aug. 1958.

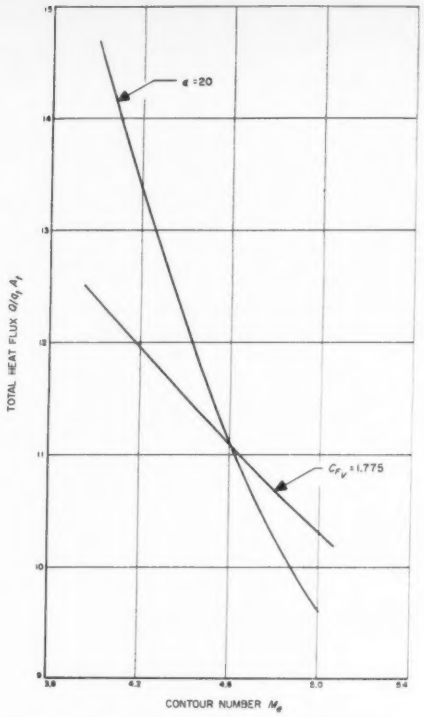

Fig. 11 Total heat flux for different contours

would give more useful results. However, this problem had not been programmed on the computer.

Varying γ while keeping the exit area and initial expansion angle constant will probably affect the contour only slightly. There is one limitation: The initial expansion angles cannot be too close to the theoretical maximum. However, if approximately $\theta_i \leq 0.95\,\theta_m$, then the initial design conditions can be met, at least over the range of γ and ϵ of interest. The effect on thrust coefficient is unknown, but will probably only be that resulting from the change in γ.

Comparison of Contour With Other Designs

The only contour designs in the literature with which those of this paper can be compared are those presented by Rao (4). In this reference, there are two contours for $\gamma = 1.23$, $\epsilon = 19.36$ and $\epsilon = 4.973$. There is insufficient information in this paper to enable a comparison with the smaller nozzle; however, the $M_{4.6}$ data can be interpolated between $\gamma = 1.22$ and 1.24 in order to make a comparison with the larger nozzle. These data are presented in Table 4.

Table 4 Nozzle comparison, $\gamma = 1.23$

Parameter	JPL data[a] I	JPL data[a] II	Rao data (4)
ϵ	19.4	15.3	19.36
C_{F_v}	1.7676	1.737	1.7676
L	10.75	8.7	8.19
S	64.5	48.1	48.1

[a] Interpolation of $M_{4.6}$ contour.

If the nozzles are compared at the same thrust coefficient, the design presented by Rao has a shorter length and smaller surface area. If a nozzle of comparable surface area is selected, it has a lower exit area and thrust coefficient and slightly longer length. The length difference is the result of the shorter radius of curvature ($K = 0.45$) used by Rao. The difference in thrust coefficients is 1.75 per cent. The thrust coefficient in Rao's design may easily be that much lower in actual use because of the small radius of curvature used at the throat (13). Based on the actual vacuum thrust coefficient to be expected, it is believed that both methods of design will result in essentially the same savings in weight and length.

Conclusions

The information presented in this paper has been abstracted from a Jet Propulsion Laboratory Memorandum (20). Additional points discussed in the memorandum are the pressure ratio and Mach number distribution along the wall. The pressure ratios are larger than the theoretical one-dimensional pressure ratios allowing a slightly larger expansion ratio for a particular atmospheric pressure. The variation of Mach number with ϵ is approximately the same for all the contours. The memorandum also contains, in tabular form, all the design information discussed herein.

This paper has presented a number of bell-shaped nozzle contours designed on reasonable assumptions about the initial flow conditions in the nozzle. Some of the designs result in savings in length, weight and heat flux over a 15-deg nozzle with the same thrust coefficient. It is believed that the design is conservative and that these nozzles will exhibit the performance indicated.

Nomenclature

A = area
C_F = thrust coefficient
K = radius of curvature at throat/R_t
L = length along centerline/R_t
L' = length along wall/R_t
M = Mach number
P = pressure
Q = total heat flux, Btu/(time)
q = local heat flux, Btu/(area)(time)
R = radius (from centerline)/R_t
S = surface area of expansion section/A_t
γ = specific heat ratio
ϵ = expansion area ratio
θ = flow angle with centerline
$\nu(M)$ = Prandtl-Meyer angle
ω = expansion angle of conical nozzle

Subscripts

c = chamber
e = exit
i = inflection point
m = maximum
t = throat
v = vacuum
w = wall

References

1 Clippinger, R. F., "Supersonic Axially Symmetric Nozzles," Ballistics Research Laboratory Rep. no. 794, Aberdeen Proving Grounds, Aberdeen, Md., Dec. 1951.

2 Krull, H. G. and Beale, W. T., "Internal Performance Characteristics of Short Convergent-Divergent Exhaust Nozzles Designed by the Method of Characteristics," NACA Research Memorandum E56D27a, Washington, D. C., July 24, 1956.

3 Dillaway, R. B., "A Philosophy for Improved Rocket Nozzle Design," Jet Propulsion, vol. 27, no. 10, 1957, pp. 1088–1093.

4 Rao, G. V. R., "Exhaust Nozzle Contour for Optimum Thrust," Jet Propulsion, vol. 28, no. 6, 1958, pp. 377–382.

5 Guderly, G. and Hantsch, E., "Beste Formen für achsensymmetrische Überschallschubdüsen," *Zeits. für Flugwissenschaften*, Brauschneig, Sept. 1955.

6 Foelsch, K., "The Analytical Design of an Axially Symmetric Laval Nozzle for a Parallel and Uniform Jet," *J. Aeron. Sci.*, vol. 16, no. 3, 1949, pp. 161–166, 188.

7 Beckwith, I. E., Ridyard, H. W. and Cromer, N., "The Aerodynamic

Design of High Mach Number Nozzles Utilizing Axisymmetric Flow with Application to a Nozzle of Square Test Section," NACA Tech. Note 2711, Washington, D. C., June 1952.

8 Enkenhus, K. R. and Tucker, N. B., "Design and Testing of an Axisymmetric Nozzle for Mach Number Seven," UTIA Tech. Note no. 4, Univ. Toronto, Toronto, Canada, Jan. 1955.

9 Foster, C. R. and Cowles, F. B., "Experimental Determination of the Static-Pressure Distribution in an Overexpanded Rocket-Motor Exhaust Nozzle," Progress Rep. no. 4–125, Jet Propulsion Laboratory, Pasadena, Calif., March 21, 1950.

10 Oliver, R. E. and Nagamatsu, H. T., "Investigation of Flow in the Throat Region for a Hypersonic Nozzle," Memorandum no. 24, Hypersonic Wind Tunnel, Guggenheim Aeronaut. Lab., California Inst. of Technol., Pasadena, Calif., Jan. 1955.

11 Tsien, H. (Editor), "Jet Propulsion," Air Tech. Service Command, Washington, D. C., 1946, p. 140.

12 Foster, C. R. and Cowles, F. B., "Experimental Study of the Divergence-Angle Effect in Rocket-Motor Exhaust Nozzles," Progress Rep. no. 20–134, Jet Propulsion Laboratory, Pasadena, Calif., Jan. 16, 1951.

13 Fraser, R. P., Rowe, P. N. and Coulter, M. D., "Efficiency of Supersonic Nozzles for Rockets and Some Unusual Designs," Proc. Inst. Mech. Engrs. (London), vol. 171, no. 16, 1957, pp. 553–580.

14 Rowe, P. N., "The Effect of Divergence Angle on the Thrust of a Supersonic Nozzle," Jrl. no. 36, Imperial College of Science, South Kensington, Eng., Sept. 1957.

15 Squires, P. K., et al., "A Method for Designing Supersonic Nozzles Using the Centerline Mach Number Distribution," NavOrd Rep. 3995, Navy Dept., Bureau of Ordnance, Washington, D. C., Oct. 10, 1956.

16 Riise, H. N., "Flexible-Plate Nozzle Design for Two-Dimensional Supersonic Wind Tunnels," Rep. no. 20–74, Jet Propulsion Laboratory, Pasadena, Calif., June 9, 1954.

17 Seifert, H. S. and Crum, J., "Thrust Coefficient and Expansion Ratio Tables," Ramo-Wooldridge Corp., Los Angeles, Calif., Feb. 1956.

18 Landsbaum, E. M., "Thrust of a Conical Nozzle," ARS Journal, vol. 29, no. 3, 1959, pp. 212–213.

19 Bartz, D. R., "A Simple Equation for Rapid Estimation of Rocket Nozzle Convective Heat Transfer Coefficients," Jet Propulsion, vol. 27, no. 1, 1957, pp. 49–51.

20 Landsbaum, E. M., "Contour Nozzles," Mem. no. 20–169, Jet Propulsion Laboratory, Pasadena, Calif., Sept. 15, 1958.

Relativistic Theory of Rocket Flight With Advanced Propulsion Systems

JOHN HUTH[1]

The Rand Corp.
Santa Monica, Calif.

This paper presents a general relativistic theory of rocket propulsion, applicable to either adiabatic or diabatic jets, and to several methods for handling fuel residual. Emphasis is given to the performance limitations imposed by both fuel energetics and power supply weight. The discussion is limited to constant-thrust vehicles.

CHEMICAL rockets, although capable of producing high thrust-to-weight ratios, are essentially mass limited. That is, no standard chemical reaction (as opposed to a free radical reaction) is sufficiently energetic to yield specific impulses of over a few hundred seconds. As a result, the ratio of initial to burnout rest mass becomes very large. To surmount this limitation, advanced propulsion systems attempt to utilize more energetic sources of energy. These are listed in Table 1, with matter annihilation as a point of reference. Nuclear fission is the most energetic source which we currently know how to utilize on a large scale.

Generally speaking, however, it is not possible to use the more energetic sources in as direct a manner as chemical propellants in a rocket. In the latter case, the products of the chemical reaction are themselves exhausted directly. In the former, reaction energy is usually transferred from a separate energy source (such as a reactor) to the jet. Although this adds some flexibility, the greater bulk involved severely limits the acceleration capabilities of such systems. This paper develops a general approach to a wide variety of propulsion systems, clearly indicating the performance limitations imposed by both fuel energetics and specific power.

Powerplant Performance

In developing a general theory of rocket propulsion, it is convenient to first separate fuel energetics from considerations of powerplant weight. For this purpose let us imagine a rocket engine fixed on a test stand. (The test stand itself will be assumed fixed in an inertial coordinate system.) Define:

m_f = total fuel consumption per unit time

In a heterogeneous reactor, for example, m_f would represent the fresh fuel element mass divided by the length of time between shutdowns for recharging.

ϵ = fraction of m_f converted to energy

In accordance with Table 1 ϵ could never exceed about 10^{-3} in a fission reactor.

m_j = mass of inert[2] working fluid ejected per unit time in the jet

Table 1 Primary energy sources

Type	Energy release, erg/gm	Fraction of annihilation energy[a]
Chemical (hydrogen-oxygen)	1.33×10^{11}	1.48×10^{-10}
Free radical ($H + H \rightarrow H_2$)	2.2×10^{12}	2.45×10^{-9}
Nuclear fission, with complete "burnup"[b]	7.1×10^{17}	7.9×10^{-4}
Nuclear fusion	3.6×10^{18}	4.0×10^{-3}
Matter annihilation	9.0×10^{20}	1.0

[a] Clearly, this is also the fraction of the fuel mass converted to energy.

[b] Only 1 per cent burnup is not uncommon in current reactors.

Received Jan. 30, 1959.

[1] Head, Novel Devices Group, Aeronautics Dept. Member ARS.

[2] Inert is here used in the sense that the working fluid does not enter into the energy producing reaction.

In a nuclear rocket, m_i would thus represent the mass flow of hydrogen, ammonia or other working fluid through the nozzle.

η = fraction of unconverted fuel mass (residue) ejected with the working fluid, at the jet velocity

Thus η would include any fission products or unconverted uranium caught up in the stream of working fluid. For an ordinary chemical rocket, $\eta = 1$, since the jet is made up entirely of reaction products.

v = jet velocity relative to the test stand
c = light velocity
α = m_i/m_f
w = fraction of the power developed which is wasted, does not add to the thrust
g = acceleration of gravity

Now allowing relativistic jet velocities, conservation of mass and energy can be written as (1)[3]

$$m_f c^2 + m_i c^2 = \frac{m_f c^2}{\sqrt{1-(v/c)^2}} + \frac{(1-\epsilon)\eta m_f c^2}{\sqrt{1-(v/c)^2}} + (1-\epsilon)(1-\eta)m_f c^2 + w\epsilon m_f c^2 \quad [1a]$$

This can be solved generally to yield

$$\left(\frac{v}{c}\right)^2 = 1 - \left[\frac{\alpha + (1-\epsilon)\eta}{(1+\alpha) - (1-\epsilon)(1-\eta) - w\epsilon}\right]^2 \quad [1b]$$

with the resulting specific impulse[4]

$$I = \frac{v}{g}\left[\frac{\alpha + \epsilon_1 + \eta(1-\epsilon)}{1+\alpha}\right]^2 \qquad \epsilon_1 = \epsilon(1-w) \quad [1c]$$

We now wish to consider three special cases. For the first, $\alpha = w = 0$ and $\eta = 1$. There is no separate working fluid; instead, the reaction product is used in the jet. An ideal chemical rocket would be characterized by this choice of parameters. From Equations [1]

$$(v/c) = \sqrt{2\epsilon - \epsilon^2} \quad [2]$$

This formula has been previously given by Sänger (2). The specific impulse appears as

$$I = (c/g)\sqrt{2\epsilon - \epsilon^2} \quad [3]$$

Therefore the maximum attainable specific impulse using pure hydrogen and oxygen would be about 500 sec. An ideal rocket of this sort will be referred to as adiabatic, since there is neither a separate powerplant (such as a reactor) to add energy to the jet stream, nor radiation losses.

The second case will fit either a heat exchanger nuclear rocket or an ionic propulsion device. For this case a separate working fluid is used, so that $\eta = 0$. Now the jet itself is nonadiabatic even though $w = 0$. We shall refer to propulsion units with separate working fluids as "diabatic" rockets. Again from Equations [1]

$$\left(\frac{v}{c}\right) = \frac{1}{(\alpha+\epsilon_1)}\sqrt{2\alpha\epsilon_1 + \epsilon_1^2}$$

$$I = \frac{c}{g}\frac{\sqrt{2\alpha\epsilon_1 + \epsilon_1^2}}{(1+\alpha)} \quad [4]$$

where the specific impulse takes into account consumption of fuel as well as working fluid. It should be noted that as $\alpha \to \infty$, $I \to v/g$. However, for relativistic jet velocities, this simplified form in which we neglect fuel consumption is quite different. For example, if we take $\epsilon_1 = 10^{-4}$ and $v/c = 1/2$ then I is approximately equal to $(c/2g) \times 10^{-3}$.

[3] Numbers in parentheses indicate References at end of paper.
[4] The specific impulse as here defined takes into account consumption of fuel as well as working fluid. In the discussion, we will justify our preference for this definition.

The quantity α may be varied to maximize I. The particular value of $\alpha_{opt} = 1 - \epsilon_1$ (which for $\epsilon_1 \ll 1$ means equal consumption of fuel and working fluid), and

$$\left(\frac{v}{c}\right)_{opt} = \sqrt{2\epsilon_1 - \epsilon_1^2}$$

$$I_{opt} = \frac{c}{g}\frac{\sqrt{2\epsilon_1 - \epsilon_1^2}}{(2-\epsilon_1)} \quad [5]$$

These formulas illustrate clearly the limitations imposed by fuel energetics. If we try to increase (v/c) indefinitely, I will actually decrease due to increased fuel consumption. For a heat exchanger nuclear rocket ϵ_1 is about 10^{-4} or less. Therefore $(v/c)_{opt}$ is approximately equal to 10^{-2}, and I_{opt} is approximately equal to 10^3 sec.

The third case is the photon rocket. Applicable formulas can be obtained from Equations [4] by merely allowing $\alpha \to 0$. Then $(v/c) \to 1$ and

$$I_{photon} = \frac{c}{g}\epsilon(1-w) = \frac{c}{g}\epsilon_1 \quad [6]$$

For $\epsilon_1 = 10^{-4}$, the photon rocket would yield an I_{photon} only about 10^{-2} of I_{opt} (Eq. [5]). The photon rocket will give optimum performance only for $\epsilon_1 = 1$ (100 per cent efficient mass annihilation).

In passing, one might comment that this general approach can also be applied to solar powered vehicles, for example, solar heating of a gaseous working fluid such as hydrogen. It is only necessary to replace $m_f c^2$ by the collected solar power, and ϵ_1 by the fraction of this power which appears in the jet. The factor η of course would equal zero.

In this section we have illustrated the test stand limitations imposed by fuel energetics. Next let us turn to the performance of a rocket vehicle in gravity-free space. This will bring into focus the additional limitations imposed by powerplant weight as well as some other interesting points.

Straight Line Burnout Velocities in Gravity-Free Space

For a diabatic photon rocket, Sänger (2) gives the formula

$$\frac{U}{c} = \frac{1 - \nu^2\epsilon_1}{1 + \nu^2\epsilon_1} \quad [7]$$

where

U = burnout velocity in relation to an inertial coordinate system at rest relative to the initial position of the rocket
ν = ratio of final to initial ship rest masses in the same coordinate system
ϵ = the fraction of fuel mass converted to energy

On the other hand Tsien (3) derives a form

$$\frac{U}{c} = \frac{1 - \nu^{2v/c}}{1 + \nu^{2v/c}} \quad [8]$$

which can apply to either an adiabatic or a diabatic rocket. However, for a diabatic rocket, setting $v = c$ does not determine ϵ (see Eq. [4]). Therefore, Equations [7 and 8] do not agree except for the special case of $\epsilon_1 = 1$.

To resolve this apparent discrepancy and elucidate the problem, we shall derive a general result, including both Tsien's and Sänger's as special cases. Let us define the following symbols:

u_0 = instantaneous ship velocity, relative to a coordinate system at rest with respect to the initial position of the rocket
m_0 = instantaneous ship rest mass in the same coordinate system
u_1 = rocket exhaust velocity relative to the same coordinate system

dm_1 = rest mass of the mass ejected from the rocket during a small time interval in the same coordinate system

dm = rest mass of the mass of unconverted fuel (residue) produced per unit time

f = fraction of dm dumped overboard at zero velocity (in the $\vec{U}$ direction) relative to the ship during the same time interval

$f + \eta \leqq 1$

Then from these definitions

$$dm_0 = -dm_1 - \frac{\epsilon dm}{(1-\epsilon)} - f dm$$

$$dm_1 = \frac{\alpha}{(1-\epsilon)} dm + \eta dm \qquad \ldots\ldots [9]$$

Therefore

$$dm = \frac{-(1-\epsilon)}{\alpha + \epsilon + f(1-\epsilon) + \eta(1-\epsilon)} dm_0$$

$$dm_1 = -\frac{\alpha + \eta(1-\epsilon)}{\alpha + \epsilon + f(1-\epsilon) + \eta(1-\epsilon)} dm_0$$

Conservation of mass and energy[5] requires

$$d\left(\frac{m_0 c^2}{\sqrt{1-(u_0/c)^2}}\right) = -\frac{c^2 dm_1}{\sqrt{1-(u_1/c)^2}} - \frac{fc^2 dm}{\sqrt{1-(u_0/c)^2}} - \frac{c^2 w \epsilon dm}{(1-\epsilon)\sqrt{1-(u_0/c)^2}} \qquad [10]$$

whereas conservation of momentum requires[6]

$$d\left(\frac{m_0 u_0}{\sqrt{1-(u_0/c)^2}}\right) = -\frac{u_1 dm_1}{\sqrt{1-(u_1/c)^2}} - \frac{fu_0 dm}{\sqrt{1-(u_0/c)^2}} - \frac{w\epsilon u_0 dm}{(1-\epsilon)\sqrt{1-(u_0/c)^2}} \qquad [11]$$

In addition we have the relativistic formula

$$u_1 = \frac{v - u_0}{1 - (u_0 v/c^2)} \qquad [12]$$

where v represents the exhaust velocity relative to the ship.[7] The formulas derived previously for v/c can now be applied, so that for a diabatic jet Equation [4] would yield

$$\left(\frac{v}{c}\right) = \frac{1}{(\alpha + \epsilon_1)} \sqrt{2\alpha\epsilon_1 + \epsilon_1^2}$$

(We are, of course, assuming a constant thrust throughout this discussion.) Equation [9] can first be substituted into Equations [10 and 11] to eliminate m_1 and m. The factor $\sqrt{1-(u_1/c)^2}$ can easily be eliminated between the resulting two equations, and (u_1/c) itself by application of Equation [12]. The final formulation appears as

$$-\frac{dm_0}{m_0} = \left[\left(\frac{\alpha + \epsilon + f(1-\epsilon) + \eta(1-\epsilon)}{\alpha + \epsilon_1 + \eta(1-\epsilon)}\right)\left(\frac{c}{v}\right)\right] \times \left[\frac{1}{1-(u_0/c)^2} d\left(\frac{u_0}{c}\right)\right] = \frac{\theta}{1-(u_0/c)^2} d\left(\frac{u_0}{c}\right) \qquad [13]$$

Integration yields

$$\frac{U}{c} = \frac{1 - \nu^{2/\theta}}{1 + \nu^{2/\theta}}$$

where for

$\eta = 1, \quad f = 0, \quad w = 0; \quad \theta = c/v$ adiabatic rocket

$$\eta = 0 \begin{cases} f = 0 \quad w = 0 & \theta = \dfrac{c}{v} \text{ Tsien} \\ f = 1 & \theta = \dfrac{c}{gI} \text{ Sänger} \end{cases} \text{ diabatic rocket}$$

$\ldots\ldots [14]$

Here I is the specific impulse, including fuel consumption, as previously defined. For the particular case of a diabatic photon rocket, $I = (c/g)\epsilon_1$ and Equations [14] reduce to Sänger's result.

From the table of special cases, it is clear that the difference (with $w = 0$) between Tsien's and Sänger's results for diabatic rockets lies in the treatment of fuel residual. Tsien keeps it aboard, whereas Sänger has it discharged (at zero velocity relative to the ship) as formed. The latter course is to be desired, but may not always be possible.

Discussion

When fuel residual is discharged along the way, ν may be written as

$$\nu = \frac{kc^2\epsilon_1 m_f + P}{(kc^2\epsilon_1 m_f + P) + (m_f + m_j)t_b g} \qquad [15]$$

where

P = payload (Earth weight)[8]

k = powerplant weight per unit of useful power output

t_b = time interval during which constant thrust is applied

Under some circumstances, such as delivery of a powerplant, $(kc^2\epsilon_1 m_f)$ might correctly be included in the payload. In any event, if one can take an unlimited time to attain a prescribed velocity increment, the powerplant weight can be made vanishingly small. Under these conditions, $\nu = P/G$, where G is the gross initial weight. The specific impulse I should then be maximized to achieve a maximum ν. This explains our preference for a definition of specific impulse including fuel consumption; it represents a quantity which at least under these limiting conditions should be made as large as possible. If one were to take instead the usual definition $I = v/g$, then I would appear in the exponent of Tsien's case. However, the specific impulse with this definition should not be maximized, since one must also consider the fuel residual carried through to burnout.

Let us now turn finally to the problem of attaining a prescribed velocity increment in a given finite time interval. Taking again the special case of a diabatic rocket with continuous discharge of spent fuel, the appropriate formulas drawn from the previous text appear as

$$\nu = \left[\frac{1 - U/c}{1 + U/c}\right]^{(1+\alpha)/2\sqrt{2\alpha\epsilon_1 + \epsilon_1^2}}$$

$$\left(\frac{P}{kc^2\epsilon_1 m_f}\right) = \left(\frac{\nu}{1-\nu}\right)\left(\frac{t_b g}{kc^2\epsilon_1}\right)(1+\alpha) - 1$$

$$\left(\frac{P}{G}\right) = \frac{\nu[P/(kc^2\epsilon_1 m_f)]}{1 + (P/kc^2\epsilon_1 m_f)} \qquad \ldots\ldots [16]$$

From Equations [16], with ϵ_1, t_b, g, c, k and U/c given, α will determine (P/G). There will be one value of α which will maximize (P/G). These values have been computed numerically for a range of the variable t_b, and the appropriate results are presented in Figs. 1 and 2.

[5] In the coordinate system at rest with respect to the initial position of the rocket, and in gravity-free space.

[6] Actually only one of Equations [10 and 11] need be used. However it seems simpler to carry out the derivation as indicated.

[7] v is now measured in an inertial system instantaneously moving with the ship.

[8] To be more consistent, one could of course express the right-hand side of Equation [15] entirely in terms of masses.

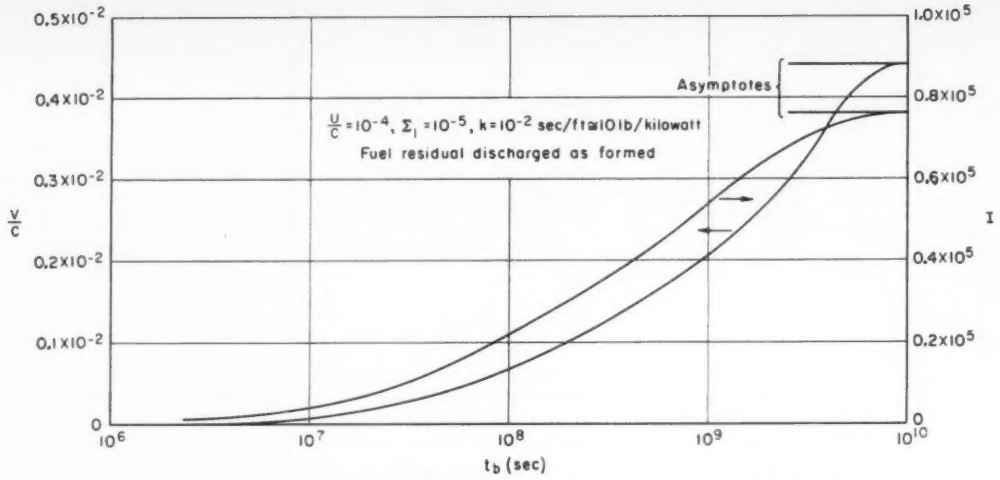

Fig. 1 Optimum specific impulse and exhaust velocities as functions of mission duration

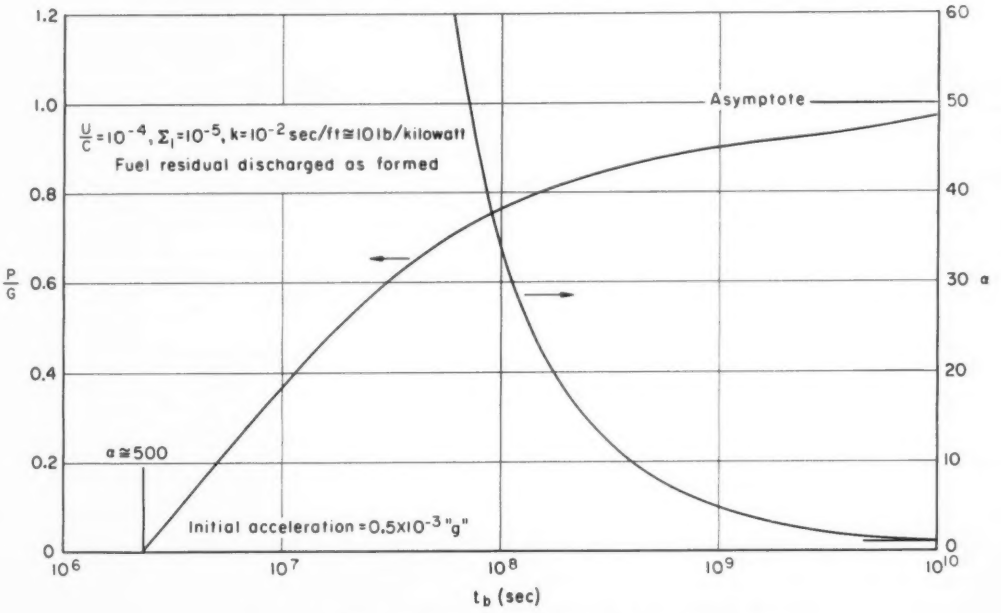

Fig. 2 Optimum value of P/G and α vs. mission duration

As $t_b \to \infty$, α approaches $1 - \epsilon_1$ corresponding to maximizing the specific impulse (Eq. [5]). The role played by ϵ_1 is then dominant. For lower values of t_b, the effect of powerplant weight becomes increasingly important. When α becomes large, I approaches v/g, and the results begin to behave as if the fuel were massless. An approximate analysis made on the basis of a massless fuel and nonrelativistic velocities[9] has been given by Langmuir (4). Specific powerplant weight is then the controlling factor. The results are cut off when t_b becomes so small that $P/G = 0$. The required velocity increment could not be attained, with the prescribed parameters, in any shorter time interval. When $P = 0$, $kc^2\epsilon_1$ is about $\alpha t_b g$; i.e., powerplant weight equals propellant weight.

Conclusions

We have given an analysis sufficiently general to cover:

1 Fuel mass limitations.
2 Specific power limitations.
3 Relativistic velocities.
4 Various methods for handling fuel residual.

One specific example has been carried through, illustrating the shift in importance from fuel energetics to powerplant weight as the allowable mission time shrinks.

Long flight times and high efficiency lightweight energy conversion equipment both tend toward increasing the relative role played by fuel mass. A photon rocket cannot be the optimum choice unless we have a complete mass annihilation energy source and massless conversion equipment.

[9] In our numerical example, U/c is also much less than 1. However Equations [16] would hold even if this were not true.

References

1 Heitler, F., "The Quantum Theory of Radiation," Oxford University Press, London, 1954, 3rd ed., pp. 14–15.

2 Sänger, E., "Zur Theorie der Photonenraketen," Space Flight Problems, Proc. 4th International Astronautical Congress, Laubscher and Co., Biel-Bienne, Switzerland, 1953, pp. 32–40.

3 Tsien, H., "Rockets and Other Thermal Jets Using Nuclear Energy," vol. 2, "The Science and Engineering of Nuclear Power," Addison-Wesley Press, Inc., Cambridge, Mass., 1949, pp. 177–196.

4 Langmuir, P. B., "Power Limited Flight in Field Free Space," UCLA Space Technology Course Notes, Jan. 17, 1958.

Ascent From Inner Circular to Outer Co-Planar Elliptic Orbits

L. RIDER[1]

Convair-Astronautics
San Diego, Calif.

The general energy requirement measured in terms of a characteristic velocity for the ascent from an initial circular parking orbit to any outer co-planar elliptic orbit by a two-instantaneous-impulse, cotangential transfer is determined as a function of the location of the second impulse on the final orbit. Of the infinity of such transfers to any particular final orbit, it is demonstrated generally that injection into the final orbit apogee is the most economical whereas injection at final orbit perigee the least economical. For the special case of final orbit perigee located on the initial parking orbit, the most economical transfer requires a single impulse applied at perigee.

EARLY investigations of co-planar transfer trajectories between co-planar orbits using instantaneous velocity increments were conducted by Lawden (1–3)[2] and indicated that:

1 Approximation methods are required for the general optimal solution.

2 The optimal number of impulse velocity changes is generally not known.

3 For a two-impulse transfer there exists a graphical method for choosing a particular trajectory (2).

4 For a two-impulse transfer between circular orbits, the optimal method is Hohmann's tangential ellipse (3).

5 For transfer between orbits of similar size and shape, the best tangential ellipse (two-impulse) gives a good approximation to the optimal solution.

The success of a cotangential type of transfer in providing an optimal or near optimal transfer between certain types of co-planar orbits with respect to characteristic velocity requirement has motivated the present investigation of two-impulse cotangential transfers between nonintersecting circular and elliptic co-planar orbits. Between circular and elliptic co-planar orbits there are, in general, an infinite number of possible cotangential transfer ellipses. In the present analysis all such transfers are examined as a function of the location of the injection into (or departure from) an outer elliptic orbit. It is found generally that injection (or departure) at outer elliptic orbit apogee is the most economical and injection (or departure) at perigee the least economical. The most economical transfer to an outer elliptic orbit of particular energy (or period) is found to occur when the eccentricity of the orbit is such that perigee is located on the circular orbit. Minor modifications of the analysis can be made indicating reversal of the choice of apogee and perigee injection or departure for the case of transfer between inner elliptic and outer circular co-planar orbits. The present analysis makes use of the simplified two-body assumptions.

Subsequent to the original submission of the present paper, personal communication with Silber brought to the author's attention the existence of two reports (6,7) not available in the open literature but related to the present paper. In the first report (6) the authors have made the interesting discovery that for co-planar transfers between circular orbits whose radii are at a ratio larger than 11.94, there exist three-impulse, "bi-elliptic" transfers more economical than the Hohmann two-impulse transfer between such orbits. In the second report (7) the authors investigate the special cases of perigee and apogee transfer from an inner circular into an outer co-planar elliptic orbit and determine that apogee injection is the more economical.

More recently, Munick (8) has demonstrated that the two-impulse cotangential transfer from inner elliptic orbit perigee to an outer co-planar circular orbit is the optimal two-impulse transfer from perigee.

Received March 17, 1959.

[1] Senior Research Engineer, Preliminary Design Group. Member ARS.

[2] Numbers in parentheses indicate References at end of paper.

General Energy Requirement

Derivation

First impulse magnitude

By the conservation of angular momentum

$$c^2 = V^2 r^2 \cos^2 \beta = \text{constant} \qquad [1]$$

For the transfer ellipse, we have

$$V_T^2 = \mu^2 \left(\frac{2}{r} - \frac{1}{a_T} \right)$$

$$a_T = \frac{r_0}{2 - b_0} \qquad [2]$$

where

$$\mu^2 = r_0 V_{c0}^2 \qquad [3]$$

$$b_0 = (V_0/V_{c0})^2$$

at $r = r_0$. Therefore at P' in Fig. 1

$$c_T^2 = V_{c0}^2 r_0^2 b_0 = r^2 \mu^2 \left(\frac{2}{r} - \frac{2}{r_0} + \frac{b_0}{r_0} \right) \cos^2 \beta \qquad [4]$$

and generally

$$b_0 = \frac{2(r/r_0)(r/r_0 - 1) \cos^2 \beta}{(r/r_0)^2 \cos^2 \beta - 1} \qquad [5]$$

At the point of tangency F, let $r = r_F$, $\sigma = r_F/r_0$ and $\beta = \beta_F$. Now, since

$$b_0 = \left(\frac{V_0}{V_{c0}} \right)^2 = \left(\frac{V_{c0} + \Delta V_0}{V_{c0}} \right)^2 \qquad [6]$$

then

$$\frac{\Delta V_0}{V_{c0}} = \sqrt{\frac{2\sigma(\sigma - 1)\cos^2\beta_F}{\sigma^2\cos^2\beta_F - 1}} - 1 \qquad [7]$$

where β_F is to be determined.

Consider the characteristics of the final orbit at the point of tangency F

$$c^2 = V_F^2 r_F^2 \cos^2\beta_F$$

$$V_F^2 = \mu^2\left(\frac{2}{r_F} - \frac{1}{a}\right)$$

.....[8]

Substitution gives

$$\frac{c^2}{\mu^2} = r_F^2\left(\frac{2}{r_F} - \frac{1}{a}\right)\cos^2\beta_F \qquad [9]$$

However, the relation between the kinematics and geometry of an elliptic orbit is such that

$$c^2/\mu^2 = a(1 - \epsilon^2) \qquad [10]$$

therefore

$$\cos^2\beta_F = \frac{a(1-\epsilon^2)}{r_F^2\left(\frac{2}{r_F} - \frac{1}{a}\right)} = \frac{a(1-\epsilon^2)}{r_0\sigma^2\left(\frac{2}{\sigma} - \frac{r_0}{a}\right)} \qquad [11]$$

which provides the attitude at any point on the final orbit as a function of the final orbit characteristics and the point of interest $r = r_F$.

To satisfy the condition of tangency at F it is required that β_F in Equation [7] be equal to β_F in Equation [11]. Therefore, substituting Equation [11] in [7] we have

$$\frac{\Delta V_0}{V_{c0}} = \sqrt{\frac{2(\sigma - 1)(1-\epsilon^2)}{\sigma(1-\epsilon^2) - \frac{r_0}{a}\left(\frac{2}{\sigma} - \frac{r_0}{a}\right)\sigma}} - 1 \qquad [12]$$

Determination of second impulse magnitude

The second impulse magnitude ΔV_F will be that velocity added to the velocity in the transfer ellipse at F such that the total velocity equals that in the final orbit at F.

The velocity in the final orbit at F is given by

$$V_F = \mu\sqrt{\frac{2}{r_F} - \frac{1}{a}} \quad \text{or} \quad \frac{V_F}{V_{c0}} = \sqrt{\frac{2}{\sigma} - \frac{r_0}{a}} \qquad [13]$$

The velocity in the transfer ellipse at F is

$$V_T = \mu\sqrt{\frac{2}{r_F} - \frac{2 - b_0}{r_0}} \qquad [14]$$

Substituting Equations [5 and 11] results in

$$\frac{V_T}{V_{c0}} = \sqrt{\frac{\left[\frac{2(\sigma-1)}{\sigma}\right]\left(\frac{r_0}{a}\right)\left(\frac{2}{\sigma} - \frac{r_0}{a}\right)}{(1-\epsilon^2) - \left(\frac{r_0}{a}\right)\left(\frac{2}{\sigma} - \frac{r_0}{a}\right)}} \qquad [15]$$

Thus, second impulse magnitude is given by

$$\frac{\Delta V_F}{V_{c0}} = \frac{V_F}{V_{c0}} - \frac{V_T}{V_{c0}} = \sqrt{\frac{2}{\sigma} - \frac{r_0}{a}} - \sqrt{\frac{\left[\frac{2(\sigma-1)}{\sigma}\right]\left(\frac{r_0}{a}\right)\left(\frac{2}{\sigma} - \frac{r_0}{a}\right)}{(1-\epsilon^2) - \left(\frac{r_0}{a}\right)\left(\frac{2}{\sigma} - \frac{r_0}{a}\right)}} \qquad [16]$$

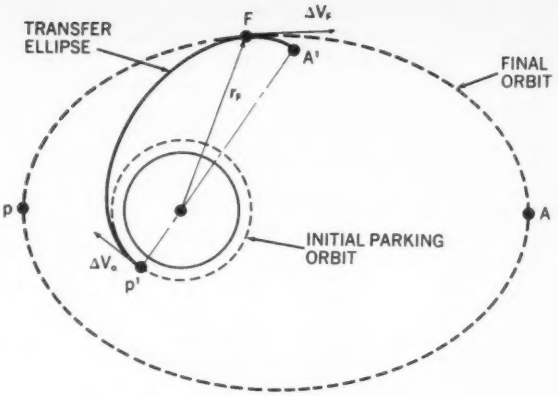

Fig. 1 General configuration

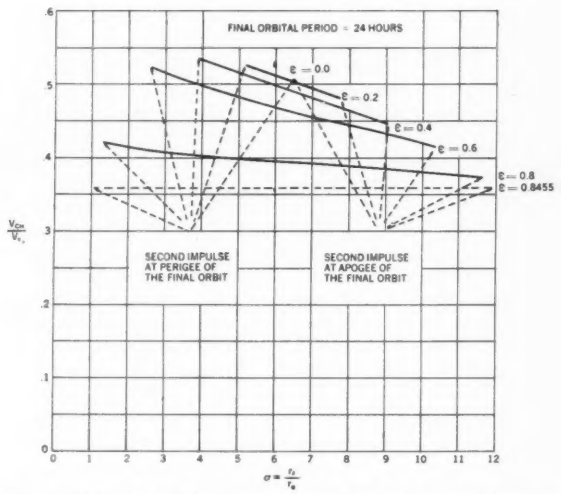
FINAL ORBITAL PERIOD = 24 HOURS
ε = 0.0
ε = 0.2
ε = 0.4
ε = 0.6
ε = 0.8
ε = 0.8455
SECOND IMPULSE AT PERIGEE OF THE FINAL ORBIT
SECOND IMPULSE AT APOGEE OF THE FINAL ORBIT
$\frac{V_{c0}}{V_{c_1}}$
$\sigma = \frac{r_F}{r_0}$

Fig. 2 Variation of characteristic velocity with second impulse location

Characteristic velocity

The total velocity requirement is given by

$$\frac{V_{CH}}{V_{c0}} = \frac{\Delta V_0}{V_{c0}} + \frac{\Delta V_F}{V_{c0}} = \sqrt{\frac{2(\sigma-1)/\sigma}{(1-\epsilon^2) - \left(\frac{r_0}{a}\right)\left(\frac{2}{\sigma} - \frac{r_0}{a}\right)}}\left[\sqrt{1-\epsilon^2} - \sqrt{\frac{r_0}{a}\left(\frac{2}{\sigma} - \frac{r_0}{a}\right)}\right] + \sqrt{\frac{2}{\sigma} - \frac{r_0}{a}} - 1 \qquad [17]$$

It is of interest to note that for a final orbit which is circular, i.e., $\epsilon = 0$ and

$$\frac{r_0}{a} = \frac{r_0}{r_F} = \frac{1}{\sigma}$$

expression [17] reduces to

$$\frac{V_{CH}}{V_{c0}} = \sqrt{\frac{2\sigma}{\sigma+1}}\left(1 - \frac{1}{\sigma}\right) + \frac{1}{\sqrt{\sigma}} - 1 \qquad [18]$$

which is exactly the optimal solution for the two-impulse transfer between circular orbits (Hohmann transfer).

The variation of characteristic velocity with second impulse location on the final orbit is shown in Fig. 2 for various eccentricities and final orbital period of 24 hr. From the

figure it can be seen that as much as a 24 per cent savings in characteristic velocity (depending upon eccentricity) may be achieved by apogee rather than perigee injection. (The initial circular orbital altitude is taken as 100 statute miles.)

Fig. 3 illustrates the variation of characteristic velocity with final orbital period for perigee and apogee injections into final orbit. In this figure σ in the range

$$1 \leq \sigma < a/r_0$$

refers to an injection at final orbit perigee, and

$$\frac{a}{r_0} < \sigma \leq \left(\frac{2a}{r_0} - 1\right)$$

refers to injection at final orbit apogee. For $\sigma = a/r_0$, V_{CH}/V_{c0} is the Hohmann characteristic velocity.

Behavior of the Function V_{CH}/V_{c0} Over the Possible Range of the Independent Variable

Fig. 2 illustrates that for a final orbital period of 24 hr, apogee injection is more economical than perigee injection. Since the curves were calculated at finite intervals, it is possible that at some intermediate value of the independent variable σ a minimum over the closed interval may occur; i.e., application of the second impulse at some point of the final orbit between apogee and perigee may be more economical than for second impulse at final orbit perigee.

Additionally, even if Fig. 2 represents the true variation of characteristic velocity with location of the second impulse on the final orbit, the character of the variation has been shown only for a final orbit period of 24 hr. It is true generally?

That the previous questions are pertinent and not of academic interest only is illustrated by the solution to the Hohmann problem which provides the minimum energy ascent from an initial circular orbit to an outer co-planar circular orbit. The results of the Hohmann analysis (5) indicate that the two-impulse incremental velocity requirement is greatest for a final orbit located at approximately 15.6 initial orbit radii from Earth center; i.e., the energy requirement to a final circular orbit located at any distance greater or less than 15.6 initial orbit radii is less than that required at 15.6 initial orbit radii.

The generality of minimum energy ascent occurring for second impulse at final orbit apogee for any particular final orbit will be demonstrated by showing:

1 The maximum and minimum values of V_{CH}/V_{c0} occur at the end points of the range of the independent variable σ for any final orbit configuration where

$$\frac{a}{r_0}(1 - \epsilon) \leq \sigma \leq \frac{a}{r_0}(1 + \epsilon) \qquad [19]$$

i.e., r_F ranges between values at perigee and at apogee.

2 Second impulse at final orbit apogee is always equally or more economical than second impulse at final orbit perigee.

Statement 1 is accomplished by demonstrating that no maximum or minimum of V_{CH}/V_{c0} exists except at the end points of the range of σ, for any final orbit configuration. Let

$$\begin{aligned} E &= 1 - \epsilon^2 \neq 0 \\ m &= \sqrt{2E} \\ A &= r_0/a \neq 0 \\ n &= \sqrt{2A} \\ B &= E + A^2 \end{aligned} \qquad [20]$$

and let

$$\begin{aligned} y^2 &= (\sigma - 1)/(B\sigma - 2A) \\ z^2 &= (2 - A\sigma)/\sigma \end{aligned} \qquad [21]$$

The equation for V_{CH}/V_{c0} then becomes

$$V_{CH}/V_{c0} = my - nyz + z - 1 \qquad [22]$$

and

$$\frac{d(V_{CH}/V_{c0})}{d\sigma} = \left(\frac{\dot{V}_{CH}}{V_{c0}}\right) = (m - nz)\dot{y} + (1 - ny)\dot{z} \qquad [23]$$

Since y^2 and z^2 are given functions of σ, we can eliminate σ and find

$$y^2 = \frac{2 - (z^2 + A)}{m^2 - n^2 z} \qquad [24]$$

Now, the problem of finding the σ values which correspond to maximum and minimum values of V_{CH}/V_{c0} where $y(\sigma)$ and $z(\sigma)$ can also be considered a problem of constrained maxima and minima. That is, it can be formulated as:

Find the extremal values of

$$\frac{V_{CH}}{V_{c0}} = my - nyz + z - 1$$

subject to the condition

$$\Phi = y^2(m^2 - n^2z^2) + z^2 + A - 2 = 0 \qquad [25]$$

The solution is supplied by the following equations (4)

$$\begin{aligned} \frac{\partial(V_{CH}/V_{c0})}{\partial y} + \lambda\frac{\partial\Phi}{\partial y} &= 0 \\ \frac{\partial(V_{CH}/V_{c0})}{\partial z} + \lambda\frac{\partial\Phi}{\partial z} &= 0 \end{aligned} \qquad [26]$$

where λ is the undetermined Lagrangian multiplier.

The Equations [25 and 26] are equivalent to

$$\begin{aligned} (m - nz) + 2\lambda y(m^2 - n^2z^2) &= 0 \\ (1 - ny) + 2\lambda z(1 - n^2y^2) &= 0 \\ \Phi = y^2(m^2 - n^2z^2) + z^2 + A - 2 &= 0 \end{aligned} \qquad [27]$$

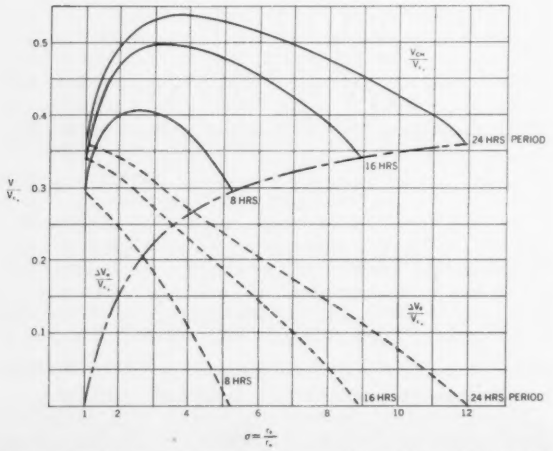

Fig. 3 Variation of characteristic velocity with orbital period

which provides the solution

$$\sigma = \frac{2A}{E + A^2 \pm \sqrt{E[E - A(2 - A)]}} \qquad [28]$$

the σ values giving extremal values of V_{CH}/V_{c0}.

There are two nondegenerate cases which can be interpreted by realizing that for final orbit perigee on or outside the initial parking orbit we must have $E \geq A(2 - A)$.

Now, for $E > A(2 - A)$

$$\frac{2A}{E + A^2 + \sqrt{E[E - A(2 - A)]}} <$$

$$\frac{2A}{E + A^2 - \sqrt{E[E - A(2 - A)]}} < \sigma_P = \frac{1 - \epsilon}{A} \qquad [29]$$

Algebraic reduction shows this statement to be true if

$$2\sigma_P{}^3 + (1 + \epsilon) > (3 + \epsilon)\sigma_P{}^2 \qquad [30]$$

Since we consider only those situations where $0 \leq \epsilon < 1$, the statement is satisfied. Consequently, for final orbit perigee outside the initial circular parking orbit, no maxima or minima of V_{CH}/V_{c0} occur over the open interval

$$\sigma_P = \frac{1 - \epsilon}{A} < \sigma < \frac{1 + \epsilon}{A} = \sigma_A$$

For the limiting case where final orbit perigee is located on the parking orbit, we substitute $E = A(2 - A)$, i.e.

$$1 - \epsilon^2 = \frac{r_0}{a}\left(2 - \frac{r_0}{a}\right)$$

in Equation [17] and find

$$\frac{V_{CH}}{V_{c0}} = \sqrt{2 - \frac{r_0}{a}} - 1 = \sqrt{1 + \epsilon} - 1 \qquad [31]$$

Thus for final orbit perigee on the initial parking orbit, the value of V_{CH}/V_{c0} is independent of σ, and all possible σ values between apogee and perigee are equally economical (in fact *the* most economical to a final orbit of particular period). However, in this particular case there are only two possible σ values—those corresponding to apogee and perigee of the final orbit. This follows since the only possible elliptic cotangential transfers between the parking orbit and final orbit coincide with these orbits and either first or second impulse is zero. Both possibilities reduce to a single impulsive transfer with impulse applied at the final orbit perigee.

To demonstrate Statement 2 that apogee injection is equally or more economical than perigee injection, we make use of the expression for characteristic velocity when second impulse is at final orbit apogee or perigee. The general expression reduces to

$$\frac{V_{CH}}{V_{c0}} = \left(1 - \frac{1}{\sigma}\right)\sqrt{\frac{2\sigma}{\sigma + 1}} + \sqrt{\frac{2 - A\sigma}{\sigma}} - 1 \qquad [32]$$

It is required to show that

$$\left(\frac{V_{CH}}{V_{c0}}\right)_{\sigma_P} \geq \left(\frac{V_{CH}}{V_{c0}}\right)_{\sigma_A}$$

That is, show that

$$\left(1 - \frac{1}{\sigma_P}\right)\sqrt{\frac{2\sigma_P}{\sigma_P + 1}} + \sqrt{\frac{2 - A\sigma_P}{\sigma_P}} - 1 \geq$$

$$\left(1 - \frac{1}{\sigma_A}\right)\sqrt{\frac{2\sigma_A}{\sigma_A + 1}} + \sqrt{\frac{2 - A\sigma_A}{\sigma_A}} - 1$$

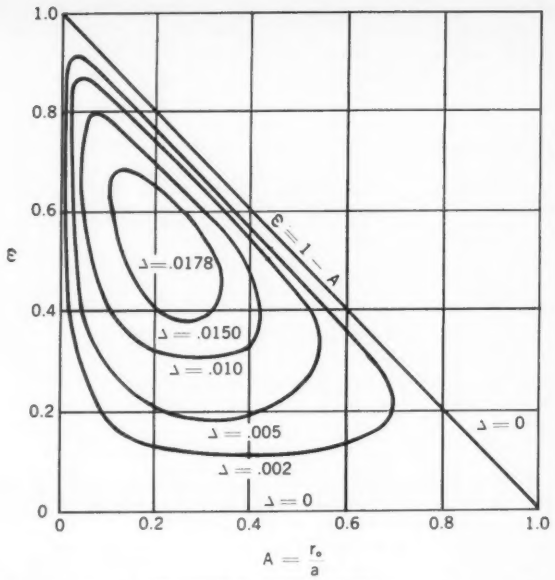

Fig. 4 $\Delta = \{\sqrt{(1 - \epsilon^2)[(1 + A)^2 - \epsilon^2]}[(1 - A)^2 - \epsilon^2]\} - \{(1 + A)(1 - A)^2 + [A^2(1 - A) - 2]\epsilon^2 + (1 + A)\epsilon^4\}$

where

$$\sigma_P = \frac{1 - \epsilon}{A}$$

$$\sigma_A = \frac{1 + \epsilon}{A}$$

Algebraic manipulation provides the following necessary and sufficient condition

$$\Delta = \{\sqrt{(1 - \epsilon^2)[(1 + A)^2 - \epsilon^2]}[(1 - A)^2 - \epsilon^2]\} - \{(1 + A)(1 - A)^2 + [A^2(1 - A) - 2]\epsilon^2 + (1 + A)\epsilon^4\} \geq 0 \qquad [33]$$

subject to the side condition that $\epsilon \leq 1 - A$ (i.e., that final orbit perigee is at a radial distance equal or greater than initial orbit radial distance).

Graphical analysis of the Δ function indicates that all possible combinations of ϵ and A consistent with the side condition provide values of $\Delta \geq 0$.

A contour representation of the three-dimensional surface defined by Equation [33] is shown in Fig. 4.

Nomenclature

r = radial distance from Earth center to point of interest
V = scalar velocity
V_c = circular velocity
a = semimajor axis of the final orbit
a_T = semimajor axis of the transfer orbit
ϵ = eccentricity of the final orbit
σ = r_F/r_0
ΔV = impulse magnitude
V_{CH} = characteristic velocity = $\Delta V_0 + \Delta V_F$
β = angle between tangent to the orbit and the local horizontal
b = $(V/V_c)^2$ square of ratio of velocity to local circular velocity

Subscripts

0 = conditions at the initial circular orbit

F = conditions at the point of tangency between transfer and final orbits
A = apogee of final orbit
P = perigee of final orbit
T = the transfer ellipse

References

1 Lawden, D. F., "The Determination of Minimal Orbits," *J. Brit. Interplanet. Soc.*, vol. 11, no. 5, Sept. 1952.

2 Lawden, D. F., "Orbital Transfer Via Tangential Ellipse," *J. Brit. Interplanet. Soc.*, vol. 11, no. 6, Nov. 1952.

3 Lawden, D. F., "Inter-Orbital Transfer of a Rocket," *J. Brit. Interplanet. Soc.*, Annual Rep., 1952.

4 Sokolnikoff, I. S., "Advanced Calculus," McGraw-Hill Book Co., Inc., N. Y., first ed., pp. 327–334.

5 Vargo, L. G., "Criteria for Orbital Entry," JET PROPULSION, vol. 28, no. 1, Jan. 1958, pp. 54–55.

6 Hoelker, R. F. and Silber, R., "The Bi-Elliptical Transfer Between Circular Coplanar Orbits," DA Technical Memo no. 2-59, Jan. 1959, Army Ballistic Missile Agency, Redstone Arsenal, Ala.

7 Silber, R. and Horner, J. M., "Two Problems of Impulse Minimization Between Coplanar Orbits," DA Technical Memo no. 23-59, Feb. 1959, Army Ballistic Missile Agency, Redstone Arsenal, Ala.

8 Munick, H., "An Optimum Transfer Path From an Elliptic Orbit to a Higher Energy Circular Orbit," ARS JOURNAL, vol. 29, no. 6, June 1959, pp. 449–451.

Structural Damage and Other Effects of Solar Plasmas

L. REIFFEL[1]

Armour Research Foundation
Chicago, Ill.

For orbits or trajectories that carry large area lightweight structures outside of protected regions of space defined by planetary magnetic fields, the damaging effects of solar plasma streams are shown to be potentially serious and may result in low durability or high payload penalties. Estimates given depend directly on plasma stream densities and velocities which are only very approximately known. However a reduction by one order of magnitude or more in widely held current estimates of the properties of the solar plasma would still imply a considerable effect on particular structural materials. Substances used as thin coatings on more massive structures would be similarly affected.

RECENTLY there has been increasing interest in the possibility of erecting structures of large area on or near the surface of the moon or planets or in interplanetary space. Large area structures are of potential utility as marker balloons, as passive components in communications systems, as sampling devices and as focusing collectors for power production from solar radiation. They have often been suggested as means for production of thrust from light pressure. Because of the great cost per pound of payload, all such devices are necessarily envisioned as extremely lightweight and extremely thin. The possibility of using very fragile structures derives, of course, from the very low forces of acceleration to which they are to be subjected during the performance of their mission.

It is of interest to examine limitations on the use of such structures imposed by certain aspects of the interplanetary environment. Although there are still many gaps in our knowledge of the environment of space, it is reasonably certain that, outside of limited regions protected by the presence of planetary magnetic fields, space is permeated by an ionized plasma whose effect on very thin structural members could be considerable. In some cases what would ordinarily be thought of as a surface effect from such a plasma might become, in actuality, a bulk volume effect to the detriment of important physical properties. Any such effects are additional to those produced by solar electromagnetic radiations, exposure to high vacuum, and other more frequently considered aspects of the environment of space. The ionized plasma presumed to be issuing from the sun, especially during periods of high solar activity, can also produce mechanical loadings far in excess of light pressure effects. We shall consider some of these effects of solar plasmas after a brief review of current ideas on the nature of corpuscular emission from the sun and the particle content of interplanetary space.

Received March 20, 1959.

[1] Director of Physics Research, Physics Division. Member ARS.

Quiescent Solar Plasma and Solar Streams

There exist a variety of observations which lead to the conclusion that interplanetary space out to somewhat beyond 1 astronomical unit (A.U.) (1 A.U. = 1.5×10^{13} cm = radius of Earth's orbit) of the sun is occupied by a tenuous highly ionized gas. Details as to the composition, temperature, and the possible presence of non-Maxwellian components are not completely certain, and such knowledge must presumably await the results of space probe experiments, some of which are now underway. Strong evidence for the presence of an outward streaming component from the sun has, however, been presented by Biermann (1,2)[2] in early papers and more recently (3). He shows that the accelerations and radial alignment observed in type I comet tails containing CO^+, N_2^+, etc., cannot be explained in terms of solar radiation (light) pressure. These accelerations ordinarily appear to be 100 to 200 times as large as solar gravity but may reach 1000 times solar gravity under very active conditions on the sun. A streaming solar hydrogen plasma would produce the observed accelerations because of electric fields set up by the greater

[2] Numbers in parentheses indicate References at end of paper.

stopping power of the cometary material for electrons relative to the protons. Neutral ionized streams having velocities of about 1000 km/sec and densities of the order of 10^3 to 10^4 particles/cm^3 at the orbit of Earth were suggested to account for these observations. Biermann points out that the highest accelerations can be related to interactions with individual solar corpuscular beams of still higher density presumably connected with discrete geomagnetic storms. On occasions of high solar activity, the suggested density of the streams (4) may reach 10^5 protons and electrons per cm^3 at 1 A.U., and velocities might be upwards of 2000 km/sec. Similar values may be obtained from observations on changes in solar radio noise (5).

For a quiet sun, Behr and Siedentopf (6) have examined the polarized component of the zodiacal light and find an electron density at 1 A.U. of 700 particles/cm^3. Electrical neutrality would then require an equal number density of protons. In a discussion of Biermann's early papers, Kiepenheuer (7) derives a lower limit for the particle density of about 6 particles/cm^3 assuming a velocity of 1000 km/sec for the solar plasma.

Recently, Kuiper has suggested (8) that a reasonable average density for quiet conditions might be about 600 protons/cm^3.

In a series of papers (9) Parker has summarized various geomagnetic effects which are assumed to be associated with discrete solar streams from an active sun. He goes on to suggest possible mechanisms for suprathermal particle generation as a possible source of auroral effects and considers cosmic ray modulation by solar plasmas as well as magnetic storm effects. From these considerations, densities for quietest conditions appear to be at least 10^2 ions/cm^3 with a minimum velocity of 500 km/sec. Under active conditions, densities of 10^5 ions/cm^3 and velocities of 1500 km/sec or more are obtained.

Russian workers (10) studying the dissipation of a high temperature nonstationary solar corona in the presence of a directed stream of matter also conclude that the density of particles in solar streams near the Earth is between 10^3 and 10^5 particles/cm^3. Summaries of observations together with some views on the nature of the solar plasma prior to the launching of the Russian space probe of Jan. 2, 1959, have also been given (11). Velocities of between 1000 and 3000 km/sec are suggested with stream concentrations ranging from 10 to 10^3 particles/cm^3. With the low density stream, a background gas at about 10^4 deg K is also considered to be present.

It should be emphasized that the properties of the solar plasma under discussion pertain to conditions away from the perturbing influence of planetary magnetic fields. Such fields will shield out or markedly change the influence of the solar plasma in nearby regions of space. In the case of the Earth, we may compute the approximate distance beyond which solar plasma effects to be discussed will be active. Roughly, the requirement (9) is that the plasma kinetic energy density exceed the magnetic energy density, and we may write this condition as

$$\frac{1}{2} nmv^2 = \frac{B^2}{8\pi}$$

In the equatorial plane of the Earth, assuming a pure dipole field, we have

$$B = B_0(r_0/r)^3$$

from which the minimum distance for onset of the effects is

$$r = r_0(B_0^2/4\pi nmv^2)^{1/6}$$

Assuming the Earth's surface field (horizontal component) as $B_0 = 0.4$ gauss, setting $r_0 = 6.4 \times 10^8$ cm as the terrestrial radius and taking the stream density n to be 10^3 particles/cm^3 with $v = 10^3$ km/sec and m appropriate for protons, we find $R = 2.9 r_0$. For this illustrative case, we would expect effects beyond 8000 miles from the Earth's surface in the plane of the geomagnetic Equator. This is to be taken only as an order of magnitude figure for a variety of reasons; particularly because of the perturbation of the Earth's dipole field by the plasma itself, because of the anisotropy of the pressures involved, and because of the probable presence of a radial solar magnetic field. It does appear that "stationary" satellites orbiting at 22,000 miles might be affected. Note that r varies slowly with n and v.

Mechanical Forces Due to Solar Plasma Streams

It is of interest to compare the force per unit area exerted on a material body by solar plasma streams with that produced by light pressure. The latter, in general, is given by the sum of momenta carried by incident solar radiation and the antiparallel component of reflected or absorbed and subsequently reradiated flux minus the parallel component of momentum from reradiated flux. If we assume a perfect reflector, no reradiation can occur, and the force per unit area at 1 A.U. reaches a maximum value of about 9×10^{-5} dynes/cm^2.

If we assume a solar plasma containing, say, 600 particles per cm^3 and traveling at an average velocity of 1000 km/sec, we obtain a force of 10^{-5} dynes/cm^2 if the beam is simply stopped in the material. For an active sun during a severe storm, with stream densities of 10^5 particles/cm^3 and velocities of, say, 2000 km/sec, we obtain 6.7×10^{-3} dynes/cm^2. Thus, for quiet conditions the plasma produces 0.11 times the maximum light pressure, but during a storm it may exert in "gusts" perhaps 75 times the solar radiation pressure on a perfect reflector at 1 A.U. from the sun.

The very difficult problem of locating and tracking a small instrument package in the vicinity of the moon, for example, has led to the very interesting suggestion that highly reflective balloons be periodically discharged from the package (12). According to this suggestion, dispersion of these balloons by light pressure would then produce an advancing line of objects of high visibility. If such a system were indeed employed, it would be of interest to attempt to observe additional accelerations above the light pressure value which could be ascribed to the solar plasma. Conceivably, some information on the fluctuations in momentum transfer due to changes in solar plasma velocities and densities could also be obtained from such observations. No telemetry of data would be required. Consideration should, however, be given to possible destruction of the balloons or their reflective coatings by the plasma. This will be discussed more fully in the next section, since these effects are also germane to questions of long-lived passive communications reflector satellites and the durability of balloon markers (13) for the lunar surface assuming the absence of a lunar magnetic field (14)[3] and to power generation equipment using thin films.

Before leaving the subject of the forces exerted by solar plasmas, mention may be made of an apparent revival of interest in the old idea of using light pressure for propulsion. Originally suggested in the literature of science fiction (15),[4] it has received attention in the serious press (16) and in this Journal (17). The practicality of these ideas has already been questioned on other grounds by Greenwood (18), and there is no need to repeat his criticisms here. To the list of problems may be added the thought that in the presence of a strong solar plasma stream, the forces on the shrouds of a "solar sail" will be orders of magnitude greater than the results

[3] Recent Russian observations on gaseous emission from the moon have been interpreted by D. H. Menzel as giving evidence that the solar plasma can indeed reach the lunar surface. There are a number of widely accepted reasons to expect a very small lunar magnetic field.

[4] The author is indebted to a number of his colleagues for general information on the history of this idea in science fiction, and to the Editor of *Astounding Science Fiction* for providing the most pertinent reference (15). In spite of the fictional nature of the magazine, this particular article is a detailed technical evaluation of light pressure propulsion.

given in (17), for example. In the latter paper the author, who opines that light pressure propulsion is practical, proposes the use of commercially available metallized plastic film of 0.1 mil thickness and suggests, as an improved design, that film of thickness 2×10^{-5} cm be used. Assuming such a structure could be built, if it were struck by a solar plasma stream, considerations to follow show that its function might be seriously impaired in a short time.

Sputtering by Solar Plasmas

When high velocity ions or atoms impinge on a solid surface, momentum transfer processes or in some cases chemical processes lead to the ejection or sputtering of atoms from the surface. For the case of physical sputtering of metals, the threshold energy V_0 for particles of atomic weight M impinging normal to a surface of atomic weight M_s is given by

$$V_0 = \left(\frac{1.6 \times 10^6 (M + M_s)\phi}{M^{1/2} M_s W}\right)^2 \text{ electron volts}$$

where

ϕ = heat of sublimation of the surface material, kcal/mol
W = bulk sound velocity for the material, cm/sec

This semi-empirical expression was obtained by Wehner (19)[5] and fits experimental observations obtained with thick samples at room temperature or above. Applying these results to the sputtering of very thin structures or coatings by the hydrogen-rich solar plasma stream can only give approximate results because of:

1 The possibility of chemical sputtering through metal hydride formation which would require much lower threshold energies.

2 Possible differences between thin film properties and bulk mechanical properties which can change the kinematics of momentum transfer—empirically, this might be accounted for by changes in ϕ and W.

3 Differences between ionized and neutral atom sputtering mechanisms (20, 21).

For protons on aluminum, the calculated threshold for perpendicular incidence, using $\phi = 75$ kcal/mol and $W = 5.1 \times 10^5$ cm/sec, is $V_0 = 560$ ev. The energy of solar protons may be readily computed and, for 1000 km/sec streams is ~5100 ev. Thus, even for considerably slower streams than suggested by some of the observations, sputtering thresholds at normal incidence are likely to be exceeded by large margins.

The yield of sputtered atoms per incident particle is a difficult question, and observations as well as theoretical predictions vary widely. Depending on the circumstances, yields ranging from 0.05 to well over 1.0 might be appropriate for our situation on the basis of the measurements reported by Weiss and by Wehner and the calculations of Whipple (22). Still higher yields would presumably be observed at other than normal incidence; Goldman and Simon (23) suggest a sec θ dependence in the theoretically simple case of high energy sputtering with the yield going with energy as ln V/V. It should be mentioned that the sputtering properties of some compounds, especially oxides, are not well understood. This gap in our knowledge is important both from the standpoint of understanding the relationship between sputtering and meteorite longevity, a subject to be discussed further elsewhere, and also in the present situation. Sputtering studies in the laboratory are frequently done by methods such that much, if not all, of the available experimental data really refer to oxide films. This is especially true in the case of aluminum. In space, atomically clean metallic surface films could result from a variety of processes involving both irradiation and chemical reactions. In view of the uncertainties involved, we shall assume a sputtering yield of unity and note that the destructive effects to be computed can be readily scaled to other values.

Consider now a reflective structure consisting of metallized plastic. In order to achieve high visible opacity, a metal thickness of the order of 300 Å will be required which, in the case of aluminum, would weigh about 10^{-5} gm/cm^2 and contain about 2×10^{17} atoms/cm^2. Supporting the metal coating would be a plastic film which, for marker balloons or focusing collectors, might be 0.1 to 0.25 mil thick and which would weigh between 25×10^{-5} gm/cm^2 and 60×10^{-5} gm/cm^2. Thus, metal thicknesses in excess of 10 times the assumed value (e.g., 3000 Å of aluminum) begin to cost heavily in payload for fixed structural area. For light pressure propulsion where plastic film thicknesses of 2×10^{-5} cm have been proposed (17), even the 300 Å coating adds one third to the mass per unit area.

Complete stripping of a coating by sputtering would occur in a time t given by

$$t = NLd/M\sigma\langle nv\rangle$$

where

N = Avogadro's number
L = coating thickness
σ = sputtering yield assumed independent of L but averaged over angle and weighted according to the incident velocity distribution
M = coating atomic weight
d = density
$\langle nv\rangle$ = the solar flux averaged over the exposure time

Optical properties will, of course, begin to change well before complete removal is effected. This expression does, however, ignore atoms removed from one part of the structure and deposited on another region, either because of the physical design of the structure or by virtue of image charge forces. Most sputtered particles are neutral. We also ignore atoms ejected in the forward direction through the structure. Mass losses or atomic displacements through an interface between materials from this latter mechanism could give quite interesting effects especially for very thin films.

The time required for solar protons to destroy a 300 Å coating, on the basis of an average yield of unity, a density of 600 particles/cm^3 and a velocity of 1000 km/sec would be less than one month of exposure. For densities and velocities corresponding to an intense storm ($v = 1500$ km/sec and $n = 10^6$/cm^3) the coating would be completely removed in about 10^4 sec. This time is within an order of magnitude of that required for an average beam from a single solar event to pass the Earth at a velocity of 1000 km/sec. A beam length in space of about 10^{11} cm is suggested by Kiepenheuer (24) to account for the time dependence of geomagnetic effects, whereas Unsold and Chapman (4) give a beam length of 1.2×10^{12} cm. Thus, depending on how literally one takes the assumptions, a *single* encounter with a beam ejected from an active sun could conceivably destroy the reflective coating. Scaling to other assumptions about proton densities, velocities and yields is direct and obvious.

We turn now to an aspect of the solar plasma usually ignored—the presence of elements heavier than hydrogen. Except for Unsold and Chapman's attention to possible Ca II content of a stream, a plasma consisting purely of protons and electrons is generally assumed. However, since the corpuscu-

[5] The author is indebted to Dr. Wehner for comments on the present state of knowledge on certain aspects of the sputtering process.

Note added in proof: Wehner has recently used spectroscopic methods to measure sputtering thresholds and no longer feels the expression used here is valid. All thresholds he has measured appear to lie near 50 ev so the effects under discussion here are not affected by this change. Recently, yield measurements both in the vicinity of threshold and in the kilovolt region have been made in a number of laboratories. Implications of these new data in the present context will be discussed in a separate paper.

lar beams appear to be merely segments of the solar corona blown out bodily, one should expect both helium and higher Z elements to be present. If one assumes that no fractionation occurs during the explosive acceleration, an assumption which might be more applicable to individual streams from an active sun than to quiet conditions, it would be reasonable to expect a plasma composition similar to that of the corona itself, by weight roughly 75 per cent hydrogen, 23 per cent helium and 2 per cent heavy elements (25). For the last we may take an average atomic weight of around 32 (26). In the plasma a population ratio, H:He:Heavy, of about 75:6:0.06 might then be expected. Charged heavy species would travel at the same velocity as the general proton stream because of initially high collision frequencies and polarization fields and would therefore possess correspondingly higher energies and momenta. From the viewpoint of any impulse delivered to a structure, the influence of all but the helium is negligible (and, in fact, is partially taken into account by the methods used to calculate stream properties from observations in the first place). From the viewpoint of sputtering, however, the presence of these components could lead to appreciable effects. In comparison to protons, momentum transfer from such particles to atoms of a surface is more efficient, differences between charged and neutral components not so marked, and a variety of chemical sputtering mechanisms possible. For example, the work of Weiss et al. (21) for silver shows a sputtering yield for He^+ higher than for H^+ by a factor of about 9 in the 10-kev region. This alone would make the sputtering by solar He^+ about equal to that by solar protons.

The heavy component in a 5-kev proton stream might have an average energy in the vicinity of 160 kev, whereas the sputtering threshold for such particles incident normally on an Al surface would drop to the order of 94 ev because of higher momentum transfer efficiency. It might be noted that if such particles were present even in the form of a cold stationary gas, perhaps the remnants of previous solar streams, and the structure under consideration were moving along with the Earth's orbital velocity (but outside the magnetic shielding limit, e.g., near the moon), the equivalent energy of the gas impinging on the surface would be about 180 ev—well above the sputtering threshold.

In passing it should be noted that considerations similar to the foregoing may be applicable to questions of longevity of thin coatings of prescribed properties applied, for instance, with the purpose of temperature regulation of extraterrestrial structures whether or not these are constructed of especially thin members.

Radiation Damage by Solar Plasmas

If the surface of the plastic film itself, rather than an overlying metal coating, were exposed to the solar plasma, radiation damage effects over and above those caused by solar ultraviolet and x-ray emission are to be expected. Hydrogen evolution leading to charring and carbonization at exposures of more than 10^{10} rad (1 rad = 100 erg/gm) should occur. If the reflecting film were behind the plastic, a marked drop in albedo would presumably precede final destruction by some sort of sputtering away of the carbon skeleton of the polymer.

Radiation damage produced by relatively slow, heavy particles of the kind present in solar plasmas has not been extensively studied. As a first approximation, we shall assume the dose to be delivered uniformly over the range of the incident particles. This is justified because multiple scattering and similar effects will smear any strong dependence on details of the primary energy loss mechanisms. Since hydrogen evolution results from molecular excitation and ionization, direct conversion from energy loss to chemically effective dosage should be permissible down to a limit below which elastic collisions predominate as a result of the incident particle velocity dropping below the pertinent orbital electron velocities. Seitz (27) suggests for this limit the point at which the incident particle velocity is that of an electron with about one eighth to one quarter of the required excitation energy E_i. If $E_i \sim 4$ ev, the proton energy required for excitation would be 1 to 2 kev. For the heavy element component, the lower limit would be around 30 to 60 kev. In both cases, the velocities associated with the solar plasma are well above the required limits. For a rough estimate we shall compute the range of the particles and then convert the energy loss sustained up to these limits to rads.

For solar protons, the range measurements of Cook et al. (28) may be used along with a range-energy relation of the form $R = kE^{1/2}$ to obtain a range of $\sim 10^{-5}$ gm/cm² for a velocity of 1000 km/sec. For a density of 600 particles/cm³ the dose would be about 5×10^5 rad/sec. Carbonization requires of the order of 10^{10} rad and hence would occur in about 2×10^4 sec. For a beam from an active sun, the time required would be about 100 sec or less than the exposure time provided by a single major event.

For the heavy elements discussed earlier, the range may be computed from the expression (29)

$$R = 6 \times 10^{-7} \frac{(Z_1^{2/3} + Z_2^{2/3})^{1/2}}{Z_1 Z_2} \left(\frac{A_1 + A_2}{A_2}\right) A_1 E \frac{\text{gm}}{\text{cm}^2}$$

where

Z_1, A_1, Z_2, A_2 = atomic number and weight of the absorber and stream particles, respectively

E = stream energy, kev

The range of this component in plastics is thus calculated to be 5 to 10×10^{-5} gm/cm² for velocities presumed appropriate to a quiet sun. For storm conditions, with velocities of 1500 km/sec or more, the range of the particles would exceed 25×10^{-5} gm/cm² allowing them to completely penetrate a 0.1-mil structure. The dose delivered to these thicknesses of material is of the order of 3500 rad/sec for the quiet sun, assuming 8×10^{-4} heavy particles per proton, and might rise to perhaps 5×10^5 rad/sec as a result of an intense beam. The corresponding time to deliver 10^{10} rad from the heavy component alone is about 40 days in the former case. The dosage from the heavy component is naturally small compared to the proton component but is effective over larger thicknesses. It does not require any sputtering away for total penetration of sufficiently thin sections.

Conclusion

The detrimental effect of solar plasmas on the performance of various thin lightweight structures which might be erected in space outside of magnetically protected regions has been shown to be potentially serious. The precise magnitude of the problem cannot be established with certainty, but assumptions which appear reasonable in the light of present knowledge lead either to low durability or to high payload penalties. For certain effects a reduction of plasma density by one or more orders of magnitude, as a result of more complete experimental data collected in the future, would still imply a considerable problem. It will be of interest to review these suggestions when such information becomes available for both quiet and active conditions on the sun.

References

1 Biermann, L., "Comets Tails and Solar Corpuscular Radiation," *Zeitschrift für Astrophysik*, vol. 29, no. 3, 1951, pp. 274–286.

2 Biermann, L., "The Tail of Halley's Comet in 1910," *Zeitschrift für Naturforschung*," vol. 7a, 1952, pp. 127–136.

3 Biermann, L., "Solar Corpuscular Radiation and the Interplanetary Gas," *Observatory*, vol. 77, 1957, pp. 109–110.

4 Unsold, A. and Chapman, S., "Optical and Radio Frequency Absorption by Solar Corpuscular Bursts," *Observatory*, vol. 69, 1949, pp. 219–221.

5 Hey, J. S., Parsons, S. J. and Phillips, J. W., "Some Characteristics of Solar Radio Emissions," *Monthly Notices of the Royal Astronomical Society*, vol. 108, no. 5, 1948, pp. 354–371.

6 Behr, A. and Siedentopf, H., "Untersuchungen uber zodiakallicht und gegenschein nach lichtlektrischen messungen auf dem Jungfraujoch," *Zeitschrift für Astrophysik*, vol. 32, no. 1, 1953, pp. 19–50.

7 Kiepenheuer, K. O., "The Sun," edited by G. P. Kuiper, University of Chicago Press, 1953, p. 440.
8 Kuiper, G. P., private communication, Dec. 1958.
9 Parker, E. N., "Interaction of the Solar Wind with the Geomagnetic Field," *Phys. Fluids*, vol. 1, 1958, pp. 171–187; and "Dynamics of the Interplanetary Gas and Magnetic Fields," *Astrophys. J.*, vol. 128, 1958, pp. 664–677; and "Cosmic Ray Modulation by Solar Wind," *Phys. Rev.*, vol. 110, 1958, p. 1445.
10 Vshekhsvaytskiy, S. K. et al., "Fizika Solnechnykh Korpuskulyarnukh Potokov i ikh Vozdeystviye na Verkhnyuyu Atmosferu Zemli" (Physics of Corpuscular Streams and Their Effect on the Upper Atmosphere of the Earth), 1957, pp. 51–57, 57–58 and 76–86. Quoted from *Referativnyi Zhurnal-Astronomiya i Geodesiya*, no. 7, July 1958, Abstract no. 4459 by Soviet Bloc IGY Information, Sept. 19, 1958, U. S. Dept. of Commerce PB 131632-32, p. 14.
11 Soviet Bloc IGY Information, U. S. Dept. of Commerce, PB 131632-51, Jan. 30, 1959, p. 15.
12 Johnson, M. H., Denver Astronautics Symposium, April 28, 1958.
13 Reiffel, L. and Kapany, N. S., Armour Research Foundation Rep. Project A-119, unpublished; *see also* Rand Memorandum RM-1900, ASTIA no. AD 133032, May 27, 1957.
14 Menzel, D. H., Harvard Observatory. Interpretation of recent Russian observations on gaseous emission, privately communicated to the writer Feb. 26, 1959.
15 Saunders, R., "Clipper Ships of Space," *Astounding Science Fiction*, vol. 47, 1951, p. 136.
16 Cotter, T. P., "Trade Wind in Space," *Time*, vol. 72, 1958, p. 35; *see also* Tsu, T. C., "WTR goes Critical in '59," *Industrial Laboratories*, vol. 9, 1958, p. 16.
17 Garwin, R. L., "Solar-Sailing—A Practical Method of Propulsion Within the Solar System," JET PROPULSION, vol. 28, March 1958, p. 188.
18 Greenwood, S. W., "Solar-Sailing—Practical Problems," JET PROPULSION, vol. 28, Nov. 1958, p. 765.
19 Wehner, G. K., "Advances in Electronics and Electron Physics," Academic Press, N. Y., vol. 7, 1955, p. 289.
20 Moore, W. J. et al., "Sputtering of Silver by Hydrogen Ions," *J. Chem. Phys.*, vol. 29, no. 1, 1958, pp. 3–7.
21 Weise, A. et al., "Sputtering of Silver by Neutral Beams of Hydrogen and Helium," *J. Chem. Phys.*, vol. 29, no. 1, 1958, pp. 7–8.
22 Whipple, F. L., "A Comet Model. III. The Zodiacal Light," *Astrophys. J.*, vol. 121, 1955, pp. 750–770; *see also* comments by Wood, J. A., "The Destructive Effect of Solar Corpuscular Radiation on Small Particles," *Astrophys. J.*, vol. 127, 1958, pp. 241–242.
23 Goldman, D. T. and Simon, A., "Theory of Sputtering by High Speed Ions," *Phys. Rev.*, vol. 111, no. 2, 1958, pp. 383–386; *see also* Henschke, E. B., "New Collison Theory of Cathode Sputtering of Metals at Low Ion Energies," *Phys. Rev.*, vol. 106, no. 4, 1957, pp. 737–753.
24 Kiepenheuer, K. O., *op. cit.*, p. 449.
25 Stromgren, B., "The Sun," edited by G. P. Kuiper, University of Chicago Press, 1953, p. 79.
26 Struve, O., "Stellar Evolution," Princeton University Press, 1950, pp. 62 ff.
27 Seitz, F., "On the Disordering of Solids by Action of Fast Massive Particles," *Faraday Society Discussions*, vol. 5, 1949, pp. 271–282; *see also* Seitz, F. and Koehler, J., "Displacement of Atoms During Irradiation," in "Solid State Physics," Academic Press, N. Y., vol. 7, 1958, p. 347.
28 Cook, C. J., Jones, E., Jr. and Jorgensen, T., Jr., "Range-Energy Relations of 10 to 250-Kev Protons and Helium Ions in Various Gases," *Phys. Rev.*, vol. 91, no. 6, 1953, pp. 1417–1422.
29 Schmitt, R. A. and Sharp, R. A., "Measurement of the Range of Recoil Atoms," *Phys. Rev. Letters*, vol. 1, no. 12, 1958, pp. 445–447.

Technical Notes

Surface Recombination in the Frozen Compressible Flow of a Dissociated Diatomic Gas Past a Catalytic Flat Plate[1]

PAUL M. CHUNG[2] and AEMER D. ANDERSON[3]

Ames Research Center, NASA, Moffett Field, Calif.

THE BOUNDARY layer concept was first applied to catalytic reaction problems by Chambré and Acrivos (1,2,3).[4] At the stagnation region, affine closed form solutions were obtained for catalytic surface recombination by Goulard (4) and by Chung (5). Solutions for regions other than the stagnation point are not so simple. In (1), two solutions, one exact and one approximate, were obtained for the incompressible flow of a reactant past a catalytic flat plate, assuming a first-order surface reaction. Both solutions are in series form. The exact solution has a small radius of convergence, making its applicability limited. Rosner (6) presented a rather comprehensive treatment of the incompressible case, including a solution for a first-order reaction on a flat plate.

This note concerns the compressible frozen flow of a dissociated diatomic gas past a flat plate upon which a first-order surface recombination occurs. The surface concentration distribution, which determines the amount of recombination of the atomic species, is to be determined.

The equation of state for such a dissociated gas is

$$p = (1 + mc_s)\rho\, RT/M \qquad [1]$$

The boundary layer equations are

$$\frac{\partial(\rho u)}{\partial x} + \frac{\partial(\rho v)}{\partial y} = 0 \qquad [2]$$

$$\rho u \frac{\partial u}{\partial x} + \rho v \frac{\partial u}{\partial y} = \frac{\partial}{\partial y}\left(\mu \frac{\partial u}{\partial y}\right) \qquad [3]$$

$$c_p \rho u \frac{\partial T}{\partial x} + c_p \rho v \frac{\partial T}{\partial y} = \frac{\partial}{\partial y}\left(k \frac{\partial T}{\partial y}\right) + \mu \left(\frac{\partial u}{\partial y}\right)^2 \qquad [4]$$

$$\rho u \frac{\partial c}{\partial x} + \rho v \frac{\partial c}{\partial y} = \frac{\partial}{\partial y}\left(\rho D \frac{\partial c}{\partial y}\right) \qquad [5]$$

The usual boundary conditions apply to Equations [2, 3 and 4]; however, the boundary condition at the wall for Equation [5] depends upon the chemical kinetics of the surface reaction and is

$$\rho_0 D_0 \left(\frac{\partial c}{\partial y}\right)_0 = k\rho_0 c_0 = k\left(\frac{m_0 c_s}{1 + m_0 c_s}\right)\frac{PM}{RT_0} \qquad [6]$$

Equations [1–5] can be solved by the von Kármán-Pohlhausen integral method described in (7). The ratio $\rho\mu/\rho^*\mu^*$, the Schmidt number, the pressure and the wall temperature are considered to be constant. This method is valid for Sc

Received Aug. 17, 1959.

[1] This note is part of a more complete study of chemically reacting boundary layers being carried out at the Ames Research Center.

[2] Aeronautical Research Scientist.

[3] Aeronautical Research Scientist.

[4] Numbers in parentheses indicate References at end of paper.

EDITOR'S NOTE: The Technical Notes and Technical Comments sections of ARS JOURNAL are open to short manuscripts describing new developments or offering comments on papers previously published. Such manuscripts are usually published without editorial review within a few months of the date of receipt. Requirements as to style are the same as for regular contributions (see masthead page).

of the order of magnitude of unity. The numerical calculations reported here are for $Sc = 0.72$.

With the previous assumptions, solution of the energy equation is not necessary to the solution of the concentration equation.

The momentum equation was solved in (7) using a sixth degree polynomial for the velocity profile. The results, which are used here, are

$$f = u/u_e = 2\eta - 5\eta^4 + 6\eta^5 - 2\eta^6 \qquad [7]$$

$$\lambda = \left(\frac{\delta_T}{L}\right)^2 \frac{Lu_e\rho^*}{C\mu^*} = A\xi \qquad [8]$$

where $A = 36{,}036/985$. When Equation [5] is integrated with respect to y, the resulting integro-differential equation is, after a change in variables

$$\lambda \frac{dF}{d\xi} + \frac{F}{2}\frac{d\lambda}{d\xi} = \frac{1}{Sc}\left(\frac{\partial m}{\partial \eta}\right)_0 \qquad [9]$$

where

$$F = \int_0^1 f(1 - m)d\eta \qquad [10]$$

A fifth degree polynomial is used here to approximate the concentration profile. The boundary conditions on this profile are:

At $\eta = 0$

$$\frac{\partial m}{\partial \eta} = \left(\frac{kLSc\rho^*}{\mu^*}\right)\frac{A^{1/2}}{C^{1/2}} Re^{-1/2}\xi^{1/2}\left(\frac{m_0}{1 + m_0c_e}\right) \qquad \frac{\partial^2 m}{\partial \eta^2} = 0$$

At $\eta = 1$

$$m = 1 \qquad \frac{\partial m}{\partial \eta} = 0 \qquad \frac{\partial^2 m}{\partial \eta^2} = 0$$

..... [11]

The reference state ( )* is chosen at the wall temperature with zero concentration, so that $\rho_0 = \rho^*/(1 + m_0c_e)$.

Upon evaluation of F, Equation [9] becomes

$$(\varphi + K_1\varphi^2\beta^2)(d\beta/d\varphi) + K_2\varphi\beta^2 - (K_2\varphi - K_3)\beta^2 - \beta = 0 \qquad [12]$$

where

$$K_1 = \frac{128}{495}\frac{A^{1/2}}{C^{1/2}}\frac{SckL\rho^*}{\mu^*} Re^{-1/2}$$
$$K_2 = (2 + 495/16ASc)K_1$$
$$K_3 = 1 + c_e$$
$$\varphi = \xi^{1/2}$$
$$\beta = 1/(1 + m_0c_e)$$

..... [13]

It can be seen at this point that solutions to Equation [12] will be in terms of three dimensionless parameters, K_1, Sc and K_3, with K_3 being the free stream compressibility. The parameter K_1 varies from about 10^{-3} for almost inert surfaces at low pressures to about 10^2 for highly catalytic surfaces at high pressures.

When the compressibility at the wall, $1 + m_0c_e$, is sufficiently near 1, Equation [12] simplifies to a first-order linear equation

$$\frac{dm_0}{d\xi} + \left[\frac{(1 + 495/32ASc)K_1\xi^{1/2} + 1/2}{(1 + K_1\xi^{1/2})\xi}\right] m_0 = \frac{1}{2}\frac{1}{(1 + K_1\xi^{1/2})\xi} \qquad [14]$$

This corresponds to the problem treated in (1 and 6) where compressibility was not taken into account.

The closed form solution to Equation [14] which satisfies the boundary condition that m_0 is finite at $\xi = 0$, is

$$m_0 = \frac{1 - (1 + K_1\xi^{1/2})^{-(1+495/16ASc)}}{(1 + 495/16ASc)K_1\xi^{1/2}} \qquad [15]$$

This solution is valid for all values of K_1. It shows that m_0 is 1 at $\xi = 0$. This was not an a priori assumption as it was in (1 and 6).

In terms of the parameter used in (1)

$$z = \frac{Re^{-1/2}}{0.339Sc^{1/3}}\frac{SckL\rho^*}{\mu^*}\xi^{1/2} \qquad [16]$$

the solution is

$$m_0 = \frac{1 - (1 + 0.530C^{1/2}Sc^{1/3}z)^{-(1+0.846/Sc)}}{(1 + 0.846/Sc)0.530C^{1/2}Sc^{1/3}z} \qquad [17]$$

The approximate solution given in (1) is

$$m_0 = 1 - 0.731z + 0.453z^2 - 0.252z^3 + \ldots \qquad [18]$$

The present solution, Equation [17], is compared to Equation [18] and other known solutions in Fig. 1 for $Sc = 0.72$ and $C = 1.0$. The present solution gives results almost identical with the exact solution, which is for $Sc = 0.72$, in the interval of convergence of the exact solution.

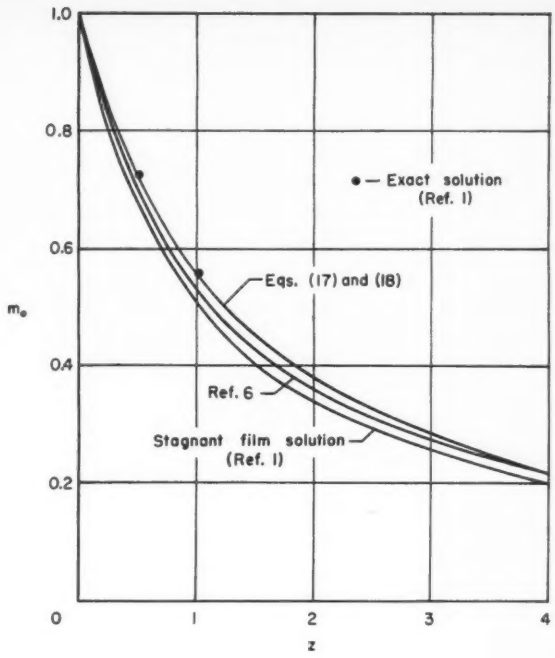

Fig. 1 Solutions for $m_0c_e = 0$

For finite m_0c_e, no closed form solution of Equation [12] can be obtained analytically. A solution based on a power series expansion about the point $\varphi = 0$ was found to converge rapidly for small values of K_1. If all but the first two terms are neglected, the solution is

$$m_0 = (2K_3^2 - K_2\varphi)/[2K_3^2 + (K_3 - 1)K_2\varphi] \qquad [19]$$

This solution agrees quite well with the exact solution for $K_1 \leq 0.2$.

Numerical solutions to Equation [12] were obtained using an IBM 704 digital computer for the conditions not covered

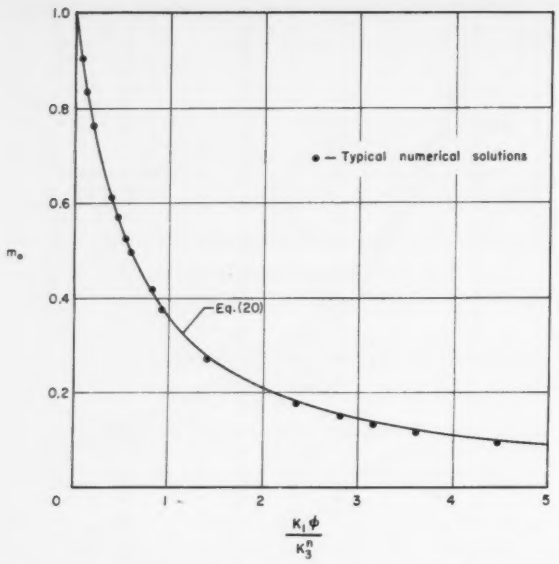

Fig. 2 Correlation of Equation [20] with numerical solutions

by Equations [15 and 19]. A study of these numerical solutions revealed that for each K_1 the solutions were congruent with Equation [15] when m_0 was plotted vs. φ/K_3^n, where $n = 0.23 + 0.77m_0$. The form of Equation [15] was then utilized to bring the solutions together for all values of K_1. The semi-empirical closed form solution thus obtained is

$$m_0 = \frac{1 - (1 + K_1\varphi/K_3^n)^{-(1+495/16ASc)}}{(1 + 495/16ASc)K_1\varphi/K_3^n} \qquad [20]$$

This correlation has been checked only for $Sc = 0.72$ and $K_1 \gtrsim 0.2$. It is shown in Fig. 2 with several numerical solutions for various values of K_1, K_3 and φ.

Nomenclature

A	=	constant, defined by Equation [8]
c	=	mass fraction of atomic species
c_p	=	specific heat at constant pressure
C	=	constant, $\rho\mu/\rho^*\mu^*$
D	=	binary diffusion coefficient
f	=	u/u_e
F	=	concentration integral, Equation [10]
k	=	specific catalytic reaction rate constant
K_1, K_2, K_3	=	parameters defined by Equations [13]
L	=	length of flat plate
m	=	c/c_e
M	=	molecular weight of undissociated diatomic gas
n	=	$0.23 + 0.77m_0$
p	=	pressure
R	=	universal gas constant
Re	=	Reynolds number, ρ^*u_eL/μ^*
Sc	=	Schmidt number, $\mu/\rho D$
T	=	absolute temperature
u	=	x component of velocity
v	=	y component of velocity
x	=	coordinate along plate
y	=	coordinate normal to plate
z	=	dimensionless variable, defined by Equation [16]
β	=	$1/(1 + m_0c_e)$
δ	=	boundary layer thickness
δ_T	=	$\int_0^\delta \frac{\rho}{\rho^*}\,dy$
η	=	$\int_0^y \frac{\rho}{\rho^*}\,dy \Big/ \int_0^\delta \frac{\rho}{\rho^*}\,dy$
λ	=	dimensionless variable, defined by Equation [8]
μ	=	dynamic viscosity
ξ	=	x/L
ρ	=	density
φ	=	$\xi^{1/2}$

Subscripts

e	=	edge of boundary layer
0	=	wall
$*$	=	reference state

References

1 Chambré, P. L. and Acrivos, A., "On Chemical Surface Reactions in Laminar Boundary Layer Flows," *J. Appl. Phys.*, vol. 27, no. 11, Nov. 1956, pp. 1322–1328.

2 Acrivos, A. and Chambré, P. L., "Laminar Boundary Layer Flows With Surface Reactions," *Ind. Engng. Chem.*, vol. 49, no. 6, 1957, pp. 1025–1029.

3 Chambré, P. L., "On Chemical Surface Reactions in Hydrodynamic Flows," *Appl. Sci. Res.*, sec. A, vol. 6, no. 2–3, 1956, pp. 97–113.

4 Goulard, R., "On Catalytic Recombination Rates in Hypersonic Stagnation Heat Transfer," JET PROPULSION, vol. 28, no. 11, Nov. 1958, pp. 737–745.

5 Chung, P. M., "Shielding Stagnation Surfaces of Finite Catalytic Activity by Air Injection in Hypersonic Flight," NASA TN D-27, 1959.

6 Rosner, D. E., "Chemically Frozen Boundary Layers With Catalytic Surface Reaction," *J. Aero/Space Sci.*, vol. 26, no. 5, May 1959, pp. 281–286.

7 Morduchow, M., "Analysis and Calculation by Integral Methods of Laminar Compressible Boundary Layer With Heat Transfer and With and Without Pressure Gradient," NACA Rep. 1245, 1955.

Vapor-Liquid Equilibria of Ozone-Oxygen Systems[1]

CHARLES K. HERSH,[2] ROBERT I. BRABETS,[3] GERALD M. PLATZ,[4] RAYMOND J. SWEHLA[5] and DONALD P. KIRSH[6]

Armour Research Foundation, Illinois Institute of Technology, Chicago, Ill.

Received Aug. 27, 1959.

[1] The authors are grateful to C. Brown and M. J. Klein for their helpful discussions and comments.

[2] Research Engineer, Propellant Research.

[3] Research Engineer, Propellant Research. Member ARS.

[4] Supervisor, Propellant Research. Present address: U.S. Industrial Chemical Co., Tuscola, Ill. Member ARS.

[5] Associate Engineer, Propellant Research. Present address: Joslyn Mfg. and Supply Co., Chicago, Ill. Member ARS.

[6] Assistant Engineer, Propellant Research.

THE VAPOR-LIQUID equilibria of ozone-oxygen systems at 78 to 93 K and at comparatively low total pressures have been the subjects of several recent publications (1–4).[7] In addition, the vapor pressures of the individual components in their pure state have been determined (5,6). The objectives of this investigation have been to verify the 1-atm vapor-liquid equilibria curve and to extend the data to a total pressure of 20 atm.

Experimental Procedure

The experimental procedure consisted of determining the vapor and the liquid curves separately and by different techniques. When a pressurized vapor of known concentration is slowly cooled, the temperature at which liquefaction first occurs can be determined from a study of the temperature-pressure graph. When the vapor volume in a closed system is kept small, the amount of liquid which must be vaporized

[7] Numbers in parentheses indicate References at end of paper.

to provide 20 atm of pressure will also be small. However, when a relatively large liquid volume is used, the change in liquid composition can be considered negligible. In both of these techniques, it is essential that the composition be accurately known.

Therefore, the test equipment was divided into two sections. The first section, which was constructed entirely of glass, was used for the collection, distillation and accurate measurement of the ozone and oxygen. High concentration ozone was separated from the effluent of a Welsbach ozonizer in a trap maintained at 90 K and 100 mm Hg absolute pressure. After a sufficient quantity had been collected, the ozone was concentrated to 100 per cent by vacuum pumping. The desired amount of ozone was distilled into the precalibrated measuring tube, where the volume was accurately measured by means of a cathetometer; then the ozone was distilled into the test chamber which was held at 77 K. Similarly, the oxygen was measured and transferred into the test chamber.

The test chamber, constructed of stainless steel and connected to the manifold by a ball and socket joint, consisted of a $\frac{1}{4}$-in. pipe tee, a short length of small ID tubing, a hypodermic tube leading to a strain-gage type of pressure pickup and a high pressure valve. All joints were sealed with silver solder. A copper-constantan thermocouple was soldered to the tee. A thin coating of Thermon,[8] a high thermal conductivity material, was applied to the unit to equalize the temperature. A 1-in. insulating blanket of glass wool surrounded the chamber to lower the rate of temperature change. Three chambers were constructed and used interchangeably to check the validity of the procedure. Each chamber had a different volume: 8.1, 12.0 and 14.0 cc, respectively.

During a run the chamber was supported at only one point so that it could be completely detached from the manifold by removing the double ball and socket bridge. Thus, agitation of the ozone-oxygen solution could be maintained by swinging the chamber in a small arc. A slow rise in temperature was obtained by removing the refrigerant Dewar and allowing the chamber to warm in a draft-free location. A slow and steady decrease in temperature was obtained by placing the chamber in the vapor portion of a partially filled Dewar and allowing the cold gas to flow over it.

The following procedure was used to obtain the vapor data:

1 A sufficient quantity of material of the desired concentration was completely vaporized in the chamber, and a uniform gas concentration was obtained by maintaining the gas at 240 K for 10–15 min. Since most of the gas was in the pipe tee and the connecting line, the concentration of the gas was assumed to be the same as that of the original liquid in the chamber.

2 The chamber was slowly cooled and the temperature and pressure were recorded at intervals.

3 Temperature vs. pressure points were plotted, and a change in the slope of the resultant curve indicated the point of initial condensation at which the known gas composition was in equilibrium with a liquid of unknown concentration.

Because of the similarity of the pressure-time lines in a vapor-liquid equilibrium diagram, a minimum number of experimental points at different temperatures, pressures and concentrations are required.

The vapor pressures of various ozone-oxygen solutions at various temperatures were measured in a different manner. For liquid data, a large quantity, usually about 2.5 cc, of an ozone-oxygen solution was prepared. The amount was large enough so that the small quantity vaporized did not appreciably change the liquid concentration. In all tests below 175 K, the vapor pressure data showed that essentially all of the vaporized gas was oxygen. The amount of oxygen necessary to produce 1–20 atm of pressure in each apparatus

[8] Thermon Manufacturing Co., Houston, Texas.

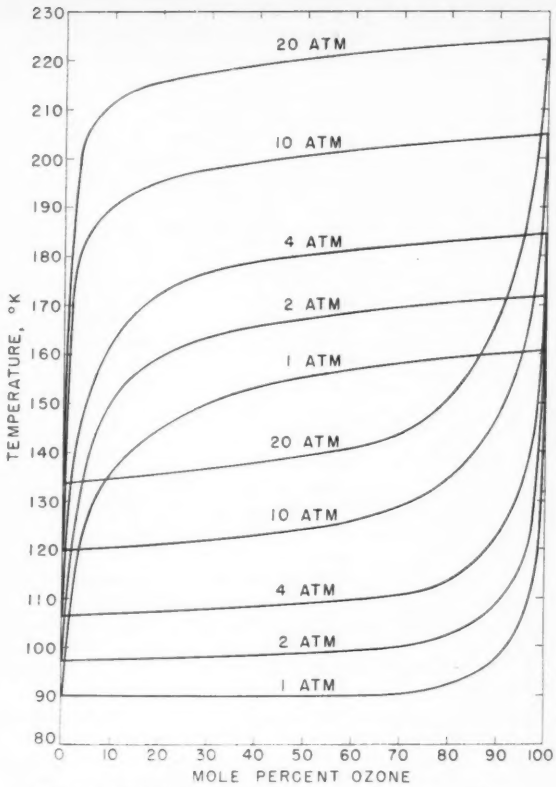

Fig. 1 Vapor-liquid equilibria of ozone-oxygen systems

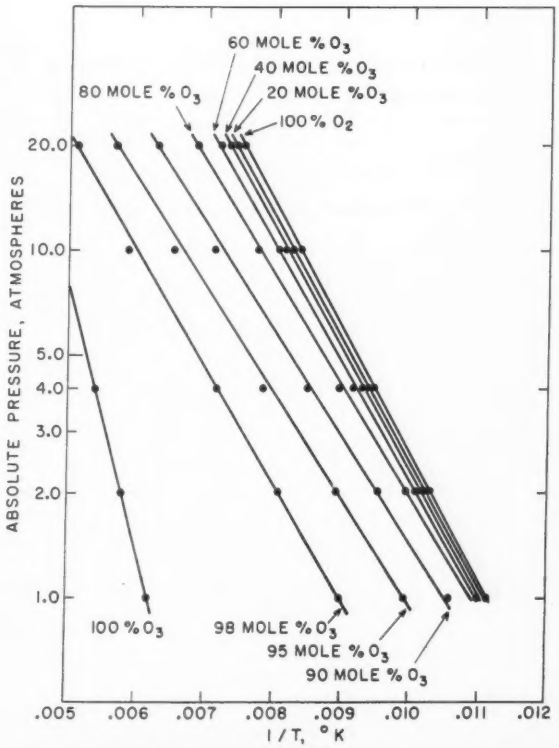

Fig. 2 Temperature-pressure relationships for ozone-oxygen systems

Table 1 Latent heat of vaporization and integral heat of solution of the ozone-oxygen system

Mole per cent ozone	Latent heat, kcal/mole	Integral heat of solution kcal/mole solution	Integral heat of solution kcal/mole ozone
100	3.630 (3.626)[a]	...	...
90	1.422	+2.01	+2.23
80	1.499	+1.73	+2.16
60	1.586	+1.24	+2.07
40	1.642	+0.79	+1.98
20	1.642	+0.39	+1.95
10	1.642	+0.19	+1.90
0	1.642 (1.636)[b]	...	...

[a] Reference (7).
[b] Reference (8).

was experimentally measured. Thus, the liquid concentration at any point could be calculated accurately. Data were obtained by slowly warming the test chamber and recording the temperature and pressure. The solution was agitated continually during the run to insure a uniform liquid composition. The accuracy of the procedure used to measure the temperature and pressure was established by a duplicate run on one sample. The data were reproducible to within 1 per cent or $\frac{1}{2}$ deg K.

Results

A total of 29 runs was considered sufficient to obtain the vapor-liquid equilibria relationship. These runs produced approximately 100 points, and each run was plotted individually. The data are presented graphically in Fig. 1 which is the typical plot of vapor-liquid equilibria for a two-component system. The consistency of the data is shown in Fig. 2 by the straight line produced from the plot of $\log_{10} P$ vs. $1/T$ K for various ozone concentrations (mole per cent). The calculated slopes of the constant composition lines from Fig. 2 are shown in Table 1. These slopes are proportional to the heat of vaporization of the solutions at constant composition. Thermodynamically, this latent heat is equal to the sum of the heats of vaporization of the pure components and the integral heat of solution. The integral heat computations were based on the assumptions that the vapor is ideal and that the sensible heat of the liquid and vapor is negligible compared to the latent heat.

The heat of solution at infinite dilution is estimated to be +1.90 kcal per mole of ozone (heat evolved). In Table 1, the values for the latent heats of pure ozone and pure oxygen in column 2 can be compared with the literature values of 3.626 kcal per mole for ozone (7) and 1.636 kcal per mole for oxygen (8). In both cases the error is less than 0.5 per cent.

References

1 Schumacher, H. J., "Solubility Diagram and the Temperature Composition Diagram at Atmospheric Pressure of the Liquid System Ozone-Oxygen," *J. Chem. Phys.*, vol. 21, 1953, p. 1610.
2 Schumacher, H. J., "The System Ozone-Oxygen and Its Behavior at Various Pressures and Temperatures," *Anales asoc. quim. Argentina*, vol. 41, 1953, pp. 198–264.
3 Brown, C., Berger, A. W. and Hersh, C. K., "Phase Diagram of Liquid Ozone-Oxygen System," *J. Chem. Phys.*, vol. 23, 1955, p. 1340.
4 Jenkins, A. C., DiPaolo, F. S. and Birdsall, C. M., "The System Ozone-Oxygen," *J. Chem. Phys.*, vol. 23, 1955, p. 2049.
5 Jenkins, A. C. and Birdsall, C. M., "Vapor Pressure and Critical Constants of Pure Ozone," *J. Chem. Phys.*, vol. 20, 1952, p. 1158.
6 Hilsenrath, J. et al., "Thermal Properties of Gases," Nat. Bur. Standards Circular 564, Nov. 1, 1955.
7 Thorp, C. E., "Bibliography of Ozone Technology," vol. 2, Swift, Chicago, Ill., 1955.
8 Furukawa, G. and McCoskey, R. E., NACA TN 2969 (1953), as reported in "Cryogenic Engineering," R. B. Scott, Van Nostrand Co., Princeton, 1959.

Measurements of the Heat Transfer Coefficients for Hydrogen Flowing in a Heated Tube[1]

J. M. FOWLER[2] and C. F. WARNER[3]

Jet Propulsion Center, Purdue University, Lafayette, Ind.

THIS note presents a portion of the results obtained during a recent investigation of forced convective heat transfer and the related frictional pressure drop for gaseous hydrogen flowing through a smooth electrically heated tube. During the experiments the ratio of the average absolute wall temperature to average absolute gas bulk temperature $\overline{T}_w/\overline{T}_b$ was varied from 1.17 to 2.47 for average gas bulk Reynolds numbers ranging from 3670 to 62,200. The gas pressure in the test section was varied from 40 to 100 psia. The experiments were conducted in an electrically heated test section of 0.306 in. ID having a length of 40 diam. The flow conditions at the entrance to the heated test section were characterized by a fully developed turbulent velocity profile and a uniform temperature profile.

Thermocouples attached to the exterior surface of the test section permitted the determination of values of the local heat flux input to the gas. In Fig. 1 is presented the variation in local heat flux along the axial length of the test section for three different gas flow rates. As can be seen from Fig. 1, the boundary condition for the gas at the tube wall was essentially that of constant heat flux. The slight variations in heat flux at the ends of the test section are attributed to heat transfer by conduction from the test section to the flanges welded to the ends of the tube for electrical connections. Heat balances for all of the experiments reported in this note were within the limits of ±5 per cent.

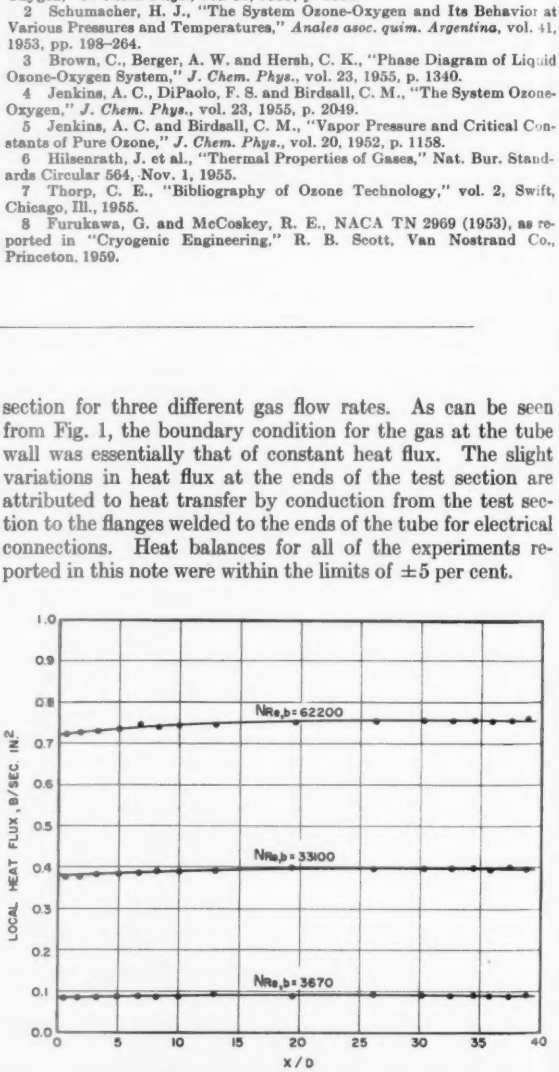

Fig. 1 Variation in local heat flux with dimensionless axial distance x/d for hydrogen; uniform initial temperature, fully developed velocity profile at entrance to test section

Received Aug. 27, 1959.
[1] This work was sponsored by the Office of Naval Research under Contract no. Nonr 1100(14). Reproduction in full or in part is permitted for any use of the U. S. Government.

[2] Graduate Assistant. Member ARS.
[3] Professor of Mechanical Engineering. Member ARS.

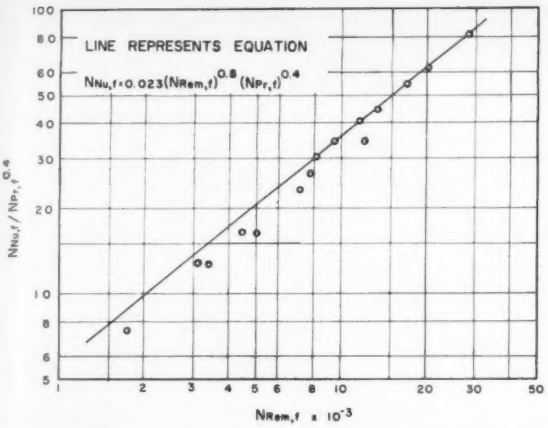

Fig. 2 Correlation of average heat transfer coefficients with constant heat flux; properties evaluated at film temperature $\bar{T}_f$

The average heat transfer coefficients were found to correlate well, as can be seen from Fig. 2, by an equation presented by Desmon and Sams (1),[4] $N_{Nu,f} = 0.023\ (N_{Rem,f})^{0.8}(N_{Pr,f})^{0.4}$ over the range of modified Reynolds numbers from 8000 to 30,000. Good agreement was also found by comparing the data for hydrogen with those of a recent and similar experiment performed with helium gas by Taylor and Kirchgessner (2). In Fig. 3 is presented the experimental data for hydrogen together with the line of the correlating equation recommended by Taylor and Kirchgessner. It should be pointed out that the correlation for L/d developed by Taylor and Kirchgessner was obtained for test section lengths having length to diam ratios of 60 and 92, whereas the test section employed in the experiments with hydrogen had a length to diam ratio of 40.

The one-half Fanning friction factors obtained from the experiments with hydrogen are shown in Fig. 4. The line suggested by von Kármán is presented in Fig. 4 for comparison. From Fig. 4 it can be seen that the data for isothermal flow are in good agreement with the von Kármán line; however, the data for diabatic heating are in poor agreement. It should be pointed out that in computing the friction factor, the calculated momentum pressure drop was subtracted from the measured pressure drop to obtain the frictional pressure drop.

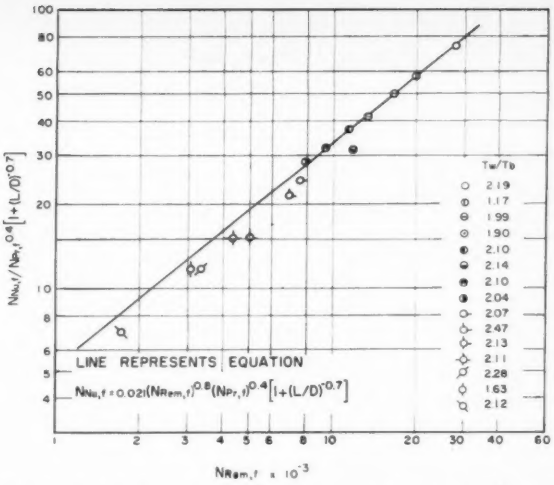

Fig. 3 Correlation of average heat transfer coefficients with constant heat flux; properties evaluated at film temperature $\bar{T}_f$

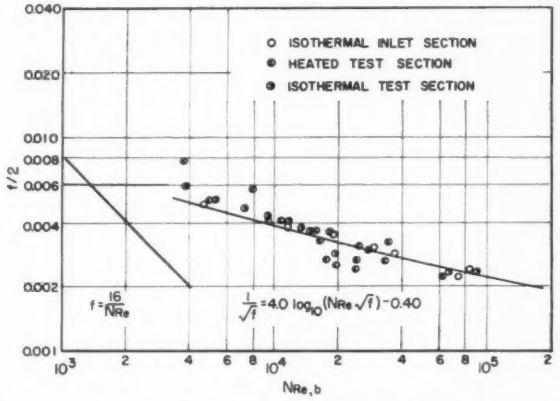

Fig. 4 Correlation of average half Fanning friction factor for hydrogen. The average gas density was employed in evaluating the Reynolds number and the viscosity was evaluated at the average bulk temperature

Nomenclature

f = Fanning friction factor
$\bar{T}_w$ = absolute average temperature of test section wall, R
$\bar{T}_b$ = absolute average bulk temperature of gas, R
T_f = absolute average film temperature $(\bar{T}_w + \bar{T}_b)/2$, R
N_{Re} = Reynolds number $VD\rho/\mu$
N_{Rem} = modified Reynolds number $V_b D\rho_f/\mu_f$
N_{Pr} = Prandtl number $C_p\mu/k$
N_{Nu} = Nusselt number hD/k

[4] Numbers in parentheses indicate References at end of paper.

Subscripts

b = bulk, indicates properties evaluated at the bulk temperature
f = film, indicates properties evaluated at film temperature

References

1 Desmon, L. G. and Sams, E. W., NACA Research Mem. E50H23, Nov. 1950.
2 Taylor, M. F. and Kirchgessner, T. A., "Measurements of Heat-Transfer and Friction Coefficients for Helium Flowing in a Tube at Surface Temperatures up to 5900 R," ARS preprint 850–59, 1959.

A Method for Heat Rejection From Space Powerplants[1]

ROGER C. WEATHERSTON[2] and WILLIAM E. SMITH[3]

Cornell Aeronautical Laboratory, Buffalo, N. Y.

FUNDAMENTAL to the design of closed-cycle powerplants providing high specific impulse for space propulsion motors is the means by which waste heat is dissipated. Heat can be rejected to a space environment only by radiation. The conventional radiator for high power levels is very massive; above the megawatt power level, in fact, its weight is about half of the weight of the powerplant. A different type of radiator, described here, should weigh considerably less than conventional radiators. In addition, its operation should be relatively unaffected by meteoritic impacts, a serious design consideration for the conventional radiator. This new radiator concept may permit significant reduction of the weights of other nuclear powerplant components as well, through modification of the thermodynamic cycle.

A conventional radiator relies on circulation of the powerplant working fluid or a secondary heat exchange fluid through a system of supply and return headers which serve as manifolds for many smaller tubes interposed among them (1,2).[4] The exterior surfaces of these smaller tubes constitute almost all of the heat exchange area of the radiator. The headers are made of material sufficiently thick to withstand all meteoroid impacts that will probably be encountered during the life of the device, from several months to years. The smaller tubes can have thinner walls than have the headers, and, in the event of penetration by a meteoroid, a damaged tube can be sealed off from the system to prevent loss of fluid. Despite the use of thin-walled tubing, the total weight of the smaller tubes is about one half of the entire radiator weight.

The heat exchanger proposed herein would typically consist of a rotating drum or other contact surface, which is heated either directly or indirectly by the waste heat of the powerplant, and a long thin flexible belt (Fig. 1).[5] The coolest portion of the belt contacts the hot drum, conducts heat from its surface, and stores the heat by virtue of the thermal capacity of the belt. Upon leaving the drum, the heated belt element travels through space until the heat lost by radiation is sufficient to re-establish its original temperature. The cooled belt element then returns to the drum, and the cycle is repeated. It is possible to contemplate a number of variations of the foregoing scheme. The purpose of this note is to bring out the advantages of capacity coolers for heat rejection in space. Therefore, the arrangement sketched in Fig. 1 should be considered as illustrative of a more general class of devices.

Referring to the configuration shown in Fig. 1, one may show that the rate per unit area at which the belt conducts heat from the rotating drum is much greater than the rate at which it radiates to space. Consequently, the contact area between belt and drum is much less than the radiation area. Thus, the ratio of these areas, as well as the belt speed, could easily be controlled in flight to accommodate a range of drum temperatures and radiative power levels. Further, the aspect ratio of the belt could easily be made large enough that both surfaces of the belt radiate to space, with very little mutual occlusion by the inner surfaces.

The belt system when compared to the tube-and-header

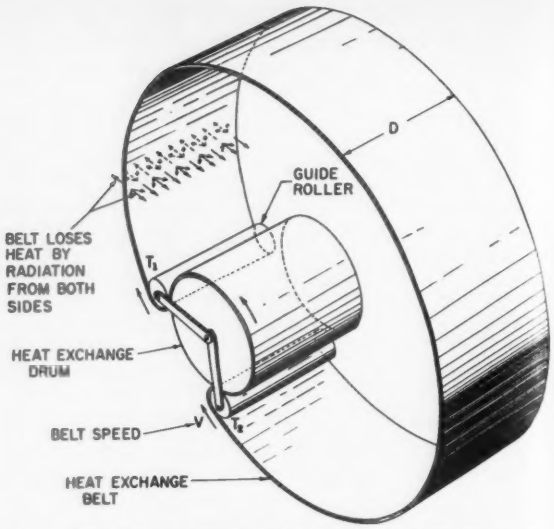

Fig. 1 Possible configuration of a capacity heat exchange system for a space radiator

system is characterized by its simplicity, a fact from which numerous advantages can be derived. The belt does not contain a cooling fluid; therefore, its penetration by meteoroids should not significantly impair its operation. Consequently, very thin and possibly woven material can be employed for the belt. Such a belt could easily withstand boost loads, as it could be either rolled completely round the drum and spliced in space or "accordioned" on opposite sides of the drum and simply unfolded in space.

The chief advantage of the belt system is, of course, its low weight as compared with a system comprising tubes, supply and return headers, and contained fluid. As an example of the saving in radiator weight expected for the proposed system, an approximate, though conservative, design is offered to accomplish the heat rejection task set forth in (1). Neglecting the weight of the small portion of belt in contact with the drum at any time, one can express the rate of heat lost from the belt in terms of the change of its heat content and the belt cycle time as

$$q = Wc(T_1 - T_2)V/L \qquad [1]$$

where

W = weight of the belt
c = belt heat capacity
$T_1 - T_2$ = temperature change belt experiences
V = speed with which the belt circulates
L = length of belt loop

The belt must radiate energy at the same rate q so that

$$q = 2DL\epsilon\sigma T^{-4} \qquad [2]$$

where

$2D$ = effective radiating perimeter of the belt cross section
ϵ = belt surface emissivity
σ = Stefan-Boltzmann constant

The mean belt temperature is defined by

$$\overline{T} = \left(\frac{1}{L}\int_0^L T^4 dl\right)^{1/4} \qquad [3]$$

T is the instantaneous temperature of an element of length,

Received Jan. 22, 1960.
[1] This study was supported as part of the Internal Research Program at the Cornell Aeronautical Laboratory, Inc.
[2] Principal Research Engineer.
[3] Associate Research Engineer.
[4] Numbers in parentheses indicate References at end of paper.
[5] In an alternative design, the contact surface may be eliminated and the waste heat transferred directly to the belt by convection.

dl. By elimination of L between Equations [1 and 2] the belt weight is obtained as

$$W = q^2/2DV\epsilon\sigma T^4c(T_1 - T_2) \quad [4]$$

Now it can be shown that

$$\bar{T} = T_1\left[\frac{3(1 - T_2/T_1)}{(T_2/T_1)^{-3} - 1}\right]^{1/4} \quad [5]$$

Equation [4] now becomes

$$W = \frac{q^2[(T_2/T_1)^{-3} - 1]}{6DV\epsilon\sigma T_1^5c(1 - T_2/T_1)^2} \quad [6]$$

Finally it can be shown that, irrespective of other considerations, the belt weight is minimized when $T_2/T_1 = 0.69$. The resulting equation for the minimum belt weight is

$$W_{min} = 3.55q^2/DV\epsilon\sigma T_1^5c \quad [7]$$

To illustrate the weight comparison between the belt heat exchanger and the conventional one, consider the heat rejection requirements for the 20,000-kw powerplant discussed (1). This example is chosen because it represents the composite design of a well-engineered space power supply whose radiator weight has been minimized on the basis of a conventional radiator design. The amount of heat to be dissipated from the radiator in (1) is 64,600 Btu/sec. The heat rejection temperature of the powerplant is 1800 R. If T_1 is 20 R less than the heat rejection temperature, i.e., 1780 R, and if ϵ is 0.90, the belt weight (lb) is calculated to be

$$W = 1.91 \times 10^6/DVc \quad [8]$$

where D is in ft, V is in fps, and c is in Btu/lb R. At the present time it is difficult to specify the practical limits for the parameters in Equation [8], but let D, V and c be conservatively chosen as 38 ft, 50 fps, and 0.10 Btu/lb R (steel). The belt would then weigh only about 10,000 lb, and its loop would be 430 ft long. The assumption of negligible mutual occlusion effects is borne out in this numerical example: Since the loop would be constrained to a circular shape or would be made into a Mobius strip, it is found that the effective radiating belt width D is within a few per cent of its actual width.

Since the contemplated vehicle acceleration is on the order of 10^{-4} g, there will be practically no load on the bearings of the rotating drum, and since there is no mechanism for attenuating the belt speed, the torque exchange between belt and drum would be nil. Hoop stresses and fatigue would become appreciable problems in belt and drum only when the belt speed reaches several hundred feet per second. With these considerations in mind, it may be practicable to use a belt speed of 100 fps. Furthermore, the average heat capacity of the belt could be elevated to at least 0.20 Btu/lb R, for example, by making a graphite matrix (c about 0.40 Btu/lb R) adhere on or between thin steel belt members. These changes would decrease the belt weight to 2500 lb.

It is contemplated that sodium vapor would be fed from the turbine, as in (1), to the rotating drum where the vapor would condense on the interior drum surface and be drained and pumped to the primary heat exchanger, again as in (1). It can be shown that a 3-ft diam, 38-ft long steel drum, 0.025-in. thick, is more than adequate to accomplish the transfer of heat to the belt. The drum with internal bracing, end plates and bearings is estimated to weigh 2000 lb. Baffles, injectors, wipers, drains and other plumbing within the drum are estimated to weigh 1000 lb. To withstand meteoroid impacts the drum would be shielded by a steel plate, 0.125-in. thick [the header thickness in (1)], which would weigh about 1500 lb. The weight of the guide rollers, which may be widely spaced disks, and auxiliary structure is taken as 1500 lb. This 6000-lb drum system is, of course, a preliminary design that appears to be capable of accomplishing the stipulated tasks. Thus, the combined system of belt and drum would weigh about 16,000 lb at 50 fps belt speed and 0.10 Btu/lb R heat capacity or 8500 lb at 100 fps and 0.20 Btu/lb R.[6] This system would replace the 42,750-lb radiator in (1).

Corresponding savings in weight could be illustrated for lower powered space vehicles. For example, it is estimated that the 4800-lb conventional radiator for the 1-megawatt space powerplant described in (2) could be replaced by a belt-drum system weighing 1400 lb.

The first radiator weight comparison cited previously is normalized upon the thermodynamic cycle given in (1). Such cycles, for which the conventional radiator dominates all other components in weight, are designed primarily to minimize the ratio of radiator area to net power output. Whereas the conventional radiator area is intimately related to its weight; this is not true for the belt-drum system. Therefore the cited cycle design criterion and concomitant temperatures increase the weight of the belt-drum system unduly. Furthermore, if the proposed belt radiator design proves to be practicable, and if significant weight savings should accrue, then the criteria for cycle design would not depend on minimizing the radiator weight. As a consequence, more efficient thermodynamic cycles and additional savings in powerplant weight may be contemplated.

It will be recalled that the weight of the belt-drum system in the foregoing example was based on T_1 being 1780 R, about the optimum rejection temperature for the radiator and powerplant in (1). It is found, however, that for a given net power from the turbine the belt weight in this example is minimized with respect to the heat rejection temperature when T_1 is 1600 R despite a concomitant increase in belt area. Equal belt weights can be attained, however, even when T_1 is reduced further, because belt materials of higher heat capacity may be employed. Possibly, because of high efficiency cycles associated with low heat rejection temperatures, one can afford to operate with moderate evaporator temperatures so as to alleviate materials problems throughout the nuclear powerplant.

The object of this paper has been to acquaint the reader with the concept of capacity type heat exchangers for heat rejection from space powerplants. No pretense is made here regarding the finality of design. The heat transfer to and from the drum surfaces certainly will require critical examination. Nonetheless what seems irrefutable is that the weight of the belt can be made almost an order of magnitude less than the weight of the tubes in conventional heat exchangers. It appears that the equipment associated with the belt can be made sufficiently light, relative to conventional radiator accessories, to maintain this advantage.

References

1 English, R. E., Slone, H. O., Bernatowicz, D. T., Davison, E. H. and Lieblein, S., "A 20,000-Kilowatt Nuclear Turboelectric Power Supply for Manned Space Vehicles," NASA Memo 2-20-59E, March 1959.

2 Schnetzer, E. and Corliss, W., "A One Megawatt Nuclear Power Package for Applications in Outer Space," General Electric Co., Flight Propulsion Laboratory, presented at the Detroit Meeting of the American Nuclear Society, Dec. 1958.

[6] Previous consideration given to minimizing the belt weight, i.e., choosing T_2/T_1 to be 0.69, does not optimize the ultimate belt-drum system. For example, an increase of T_2/T_1 would permit reduction of the belt width by 30 to 50 per cent, while increasing its thickness and weight. This increase of belt weight would be completely offset by the attendant decrease in length of the drum and guide rollers.

Nonisentropic Nozzle Flow

WILLIAM T. SNYDER[1]

North Carolina State College, Raleigh, N. C.

IT IS a well-known fact that for isentropic flow of a perfect gas in a converging-diverging nozzle, the velocity at the nozzle throat is the acoustic velocity. That is, the Mach number is unity at the throat. For nonisentropic flow in a nozzle, however, there is sometimes a misunderstanding concerning the location of the $M=1$ condition relative to the throat. Durham (1)[2] states that "the throat velocity will be sonic in the actual case as well as in the isentropic case." It is the purpose of this note to show that for nonisentropic flow the throat velocity is not sonic, and to discuss a physical mechanism which can account for this condition. Although the flow in a real nozzle is not one-dimensional, a one-dimensional analysis will be made with a nozzle efficiency being utilized to account for deviations from one-dimensionality. Because of the analytical simplicity of the one-dimensional analysis, this approach is frequently used in the design of nozzles for propulsion engines (2).

Theoretical Analysis

In addition to the assumption of one-dimensionality, the following assumptions will be introduced in the analysis: Steady flow, adiabatic flow, thermally and calorically perfect gas, and initial velocity zero.

It is convenient to represent the nozzle process in the h-s plane. Fig. 1 illustrates the end states for an isentropic and a nonisentropic expansion between the same pressure limits. The governing equations can be written as follows:

Energy

$$h_0 = h + (1/2)V^2 \qquad [1]$$

Continuity

$$\dot{m} = \rho A V \qquad [2]$$

State

$$p = \rho RT \qquad [3]$$

Isentropic specifying equation

$$p\rho^{-k} = \text{constant} \qquad [4]$$

The procedure for determining the Mach number at the throat is to obtain an expression for the mass velocity G as a function of M. At the throat, the mass velocity will be a maximum and thus setting the first derivative of G with respect to M equal to zero will determine M at the throat. The expression for the mass velocity as a function of M can be obtained as

$$G = \frac{\dot{m}}{A} = \rho V = \rho_0 \left(\frac{\rho}{\rho_0}\right) Ma = \rho_0 \left(\frac{\rho}{\rho_0}\right) M \sqrt{kRT_0 \left(\frac{T}{T_0}\right)}$$

or

$$G = \rho_0 a_0 M \left(\frac{p}{p_0}\right) \sqrt{\left(\frac{T_0}{T}\right)}$$

The quantities ρ_0, a_0 are properties of the reservoir and thus are constants for the system. Defining a new quantity G' as

$$G' = \frac{G}{\rho_0 a_0} = M \left(\frac{p}{p_0}\right) \sqrt{\frac{T_0}{T}} \qquad [5]$$

reduces the problem to that of setting the first derivative of G' with respect to M equal to zero. The ratios T_0/T and p/p_0 must now be determined as functions of M.

The following relationships between stagnation and static properties may be obtained from the governing equations and the properties of a perfect gas

$$\frac{T_s}{T_0} = \left(\frac{p_s}{p_0}\right)^{(k-1)/k} = \left(\frac{p}{p_0}\right)^{(k-1)/k} \qquad [6]$$

$$\frac{T_0}{T} = 1 + \frac{k-1}{2} M^2 \qquad [7]$$

The nozzle efficiency η between the reservoir and some section in the nozzle is defined as the ratio of actual to isentropic kinetic energy. Thus the expression for η becomes

$$\eta = \frac{(V^2)/2}{C_p(T_0 - T_s)} = \frac{(k-1)TM^2}{2T_0(1 - T_s/T_0)} \qquad [8]$$

Equations [6, 7 and 8] may be combined and solved for the pressure ratio with the result

$$\frac{p_s}{p_0} = \left[1 - \frac{1}{\eta} \frac{(1/2)(k-1)M^2}{1 + (1/2)(k-1)M^2}\right]^{k/(k-1)} \qquad [9]$$

Substituting Equations [7 and 9] into Equation [5] gives the desired expression for G'

$$G' = M\left[1 + \frac{1}{2}(k-1)M^2\right]^{1/2} \left[1 - \frac{1}{\eta} \frac{(1/2)(k-1)M^2}{1 + (1/2)(k-1)M^2}\right]^{k/(k-1)} \qquad [10]$$

Setting the first derivative of G' with respect to M equal to

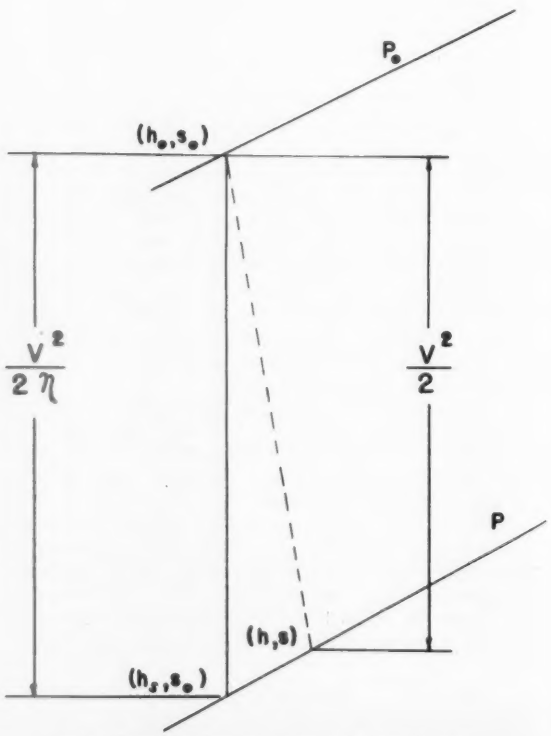

Fig. 1 Enthalpy-entropy diagram for nozzle process

Received Sept. 11, 1959.

[1] Assistant Professor of Mechanical Engineering.

[2] Numbers in parentheses indicate References at end of paper.

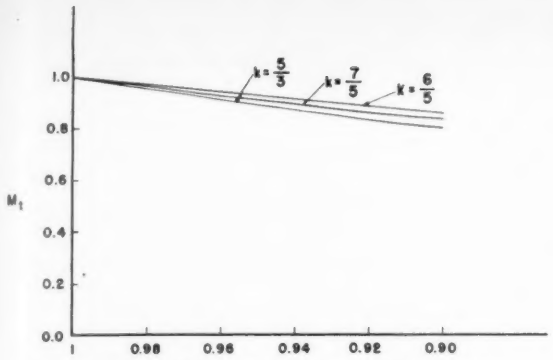

Fig. 2 Throat Mach number vs. nozzle efficiency

zero yields the following value for M at the throat

$$M_t^2 = \frac{4/(k-1)}{\left\{\left[\frac{1}{\eta}\left(\frac{3k-1}{k-1}\right)-3\right]^2+8\left(\frac{1}{\eta}-1\right)\right\}^{1/2}+\left\{\frac{1}{\eta}\left(\frac{3k-1}{k-1}\right)-3\right\}} \quad [11]$$

It is easily verified that for $\eta = 1$, Equation [11] yields $M_t = 1$. The equation is rather formidable and difficult to interpret quantitatively for $\eta < 1$. However, a qualitative interpretation may be obtained by converting the equation into an inequality. By observing that

$$\left\{\left[\frac{1}{\eta}\left(\frac{3k-1}{k-1}\right)-3\right]^2+8\left(\frac{1}{\eta}-1\right)\right\}^{1/2} > \left\{\frac{1}{\eta}\left(\frac{3k-1}{k-1}\right)-3\right\}$$

Equation [11] may be written

$$M_t^2 < \frac{4/(k-1)}{2\left[\frac{1}{\eta}\left(\frac{3k-1}{k-1}\right)-3\right]}$$

or

$$M_t^2 < \frac{2}{3k(1/\eta-1)+3(1-1/3\eta)} \quad [12]$$

The heat capacity ratio k is always greater than unity, and thus the limiting maximum value of the right-hand side of inequality, Equation [12], occurs for $k = 1$. Putting $k = 1$ gives

$$M_t^2 < \eta \quad [13]$$

The throat Mach number is therefore less than unity for a nonisentropic expansion. To show the dependence of M_t on η, Equation [11] is plotted in Fig. 2 for various values of k.

Physical Mechanism

The primary source of irreversibility in nozzle flow is the boundary layer which unavoidably develops. The boundary layer effects are confined to a relatively thin region in the vicinity of the solid boundary, and it is convenient to describe the boundary layer thickness in terms of the displacement thickness. The physical significance of the displacement thickness is the distance the solid boundary must be displaced in the direction of the fluid in order to create a nonviscous flow with the same mass flow rate as the real flow.

In terms of nozzle flow, if the actual nozzle were replaced by a hypothetical nozzle corresponding to the displacement boundary layer thickness, the flow in the hypothetical nozzle could be considered as isentropic. The sonic velocity would then occur at the throat of the hypothetical nozzle. Since the foregoing analysis shows that the velocity is subsonic at the throat of the physical nozzle, it may be concluded that the throat of the hypothetical nozzle occurs downstream of the throat of the physical nozzle. Because of the small, but finite, radial component of velocity in the boundary layer at the physical throat, there is probably a *vena contracta* effect which accounts for the occurrence of the hypothetical throat downstream from the physical throat.

Nomenclature

a = acoustic velocity
A = cross-sectional area
C_p = constant pressure heat capacity
G = mass velocity, mass flow per unit area
G' = $G/\rho_0 a_0$, dimensionless mass velocity
h = enthalpy
k = heat capacity ratio
$\dot{m}$ = total mass flow rate
M = Mach number
p = pressure
R = gas constant
T = absolute temperature
V = velocity
ρ = fluid density
η = nozzle efficiency

Subscripts

0 = stagnation conditions
t = throat conditions
s = isentropic process conditions

References

1 Durham, F. P., "Thrust Characteristics of Underexpanded Nozzles," JET PROPULSION, vol. 25, no. 12, Dec. 1955, pp. 696–700.
2 Zucrow, M. J., "Aircraft and Missile Propulsion," vol. 2, John Wiley and Sons, Inc., N. Y., 1958, p. 373.

A Magnetogasdynamic Analogy

M. D. COWLEY[1]

University of Cambridge, Cambridge, England

A new analogy with pure gasdynamics is given for the flow of a perfectly conducting gas. The velocity and magnetic fields are parallel.

A SMALL perturbation theory was outlined by Sears (1)[2] for the plane steady flow of a perfectly conducting gas with parallel undisturbed velocity and magnetic fields. The analysis was made originally by Resler, but it has not yet been published elsewhere.[3] A simpler but more general approach to this problem can be found by forming an analogy with pure gasdynamics.

We assume an ideal steady flow (viscosity, heat conduction, radiation and resistivity neglected) of a gas, where in MKS units

$$\boldsymbol{E} + \boldsymbol{v} \times \boldsymbol{B} = 0 \quad [1]$$

One form of axially symmetric flow, which is consistent with

Received Oct. 9, 1959.
[1] Research Student, Dept. of Engineering.
[2] Numbers in parentheses indicate References at end of paper.
[3] Since the writing of this note, the work has become available (4).

the usual equations of magnetogasdynamics, has

$$\boldsymbol{B} = (B_r, 0, B_z)$$

$$\boldsymbol{v} = (v_r, 0, v_z)$$

$$\boldsymbol{E} = (0, E_\theta, 0)$$

$$\boldsymbol{j} = (0, j_\theta, 0)$$

In a steady state, where $\partial \boldsymbol{B}/\partial t$ is zero everywhere, it follows from curl $\boldsymbol{E} = 0$, that $E_\theta = 0$, and $\boldsymbol{v}$ is parallel or antiparallel to $\boldsymbol{B}$. We can imagine a plane system, which approximates flow in an annulus whose width is much smaller than the radius.

The equation for the stagnation enthalpy $h_0 (= h + \frac{1}{2}v^2)$ can be written

$$\rho \boldsymbol{v} \cdot \nabla h_0 = \boldsymbol{j} \cdot \boldsymbol{E} = 0 \qquad [2]$$

so that h_0 is constant along streamlines.

With $\boldsymbol{v} \times \boldsymbol{B} = 0$, conservation of the magnetic and material flux along a streamtube requires that $B/\rho v$ is constant along the tube. Since there is no dissipation or heat flow, entropy s is another conserved quantity along streamtubes. We shall now assume that *throughout the flow*

$$\boldsymbol{B} = k\rho\boldsymbol{v} \qquad (k = \text{constant}) \qquad [3a]$$

$$s = \text{constant} \qquad [3b]$$

$$h_0 = \text{constant} \qquad [3c]$$

With equations of state, and assuming thermodynamic equilibrium, all variables are now functions of each other. The theory will be developed without reference to the actual form of the equations of state. With the conditions [3], the only equations which we require are

$$\text{div } \rho \boldsymbol{v} = 0 \qquad [4]$$

$$\text{curl } \boldsymbol{v} \times \boldsymbol{v} + \nabla \frac{1}{2} v^2 + \frac{\nabla p}{\rho} = \frac{\boldsymbol{j} \times \boldsymbol{B}}{\rho} = \frac{\text{curl } \boldsymbol{B} \times \boldsymbol{B}}{\mu\rho} \qquad [5]$$

From the conditions [3b and 3c], Equation [5] degenerates to

$$\text{curl } \boldsymbol{v} \times \boldsymbol{v} = \frac{\text{curl } \boldsymbol{B} \times \boldsymbol{B}}{\mu\rho}$$

Since curl $\boldsymbol{v}$ is perpendicular to $\boldsymbol{v}$ for the flows considered here, we obtain with the aid of condition [3a]

$$\text{curl } \boldsymbol{v} = \pm \frac{B}{\mu\rho v} \text{ curl } \boldsymbol{B} = k\boldsymbol{j} \qquad [6]$$

where the positive and negative signs refer to $\boldsymbol{B}$ parallel and antiparallel to $\boldsymbol{v}$, respectively. Thus the vorticity is proportional to the current density in the gas. From Equations [4 and 6] we may derive equations in terms of the velocity components, as Kogan (2) has done for a perfect gas. It is easily shown that the conditions [3] are sufficient to insure that all properties are uniform in a region of rectilinear flow; both Kogan (2) and Resler started with the assumption of uniform properties in such a region.

From Equation [6] a vector may be constructed which remains irrotational. With the condition [3a]

$$\text{curl } (\boldsymbol{v}(1 - B^2/\mu\rho v^2)) = 0 \qquad [7]$$

We define our irrotational vector by $\boldsymbol{v}^* = \boldsymbol{v}(1 - b^2/v^2)$, where b is the Alfvén wave speed $(B/\sqrt{\mu\rho})$. It should be noted that $\boldsymbol{v}^*$ is parallel to $\boldsymbol{v}$, and the boundary condition for $\boldsymbol{v}^*$ at solid walls is the same as that for $\boldsymbol{v}$. The form of $\boldsymbol{v}^*$ suggests that we should define $\rho/(1 - b^2/v^2) = \rho^*$. Then

$$\text{div } \rho^* \boldsymbol{v}^* = 0 \qquad [8]$$

Equation [5] can also be written

$$(\rho \boldsymbol{v} \cdot \nabla)\boldsymbol{v} + \nabla\left(p + \frac{B^2}{2\mu}\right) = (\boldsymbol{B} \cdot \nabla)\frac{\boldsymbol{B}}{\mu} = (\rho \boldsymbol{v} \cdot \nabla)\frac{b^2}{v^2}\boldsymbol{v}$$

Defining $p + B^2/2\mu = p^*$, which is the pressure *felt* by a body at its surface, if there is no magnetic field within the body, we obtain

$$(\rho^* \boldsymbol{v}^* \cdot \nabla)\boldsymbol{v}^* + \nabla p^* = 0 \qquad [9]$$

It is evident that the system of equations is now analogous to that governing the dynamics of an appropriate arbitrary nonconducting gas; p^*, by the conditions [3] and suitable equations of state, has a functional relationship with ρ^*.

The speed of propagation of disturbances a^*, in the new system, is given by

$$a^{*2} = \frac{dp^*}{d\rho^*} = v^{*2}\left(\frac{a^2}{v^2} + \frac{b^2}{v^2} - \frac{a^2 b^2}{v^4}\right) \qquad [10]$$

where we have used the conditions [3], and a is the speed of sound in the absence of magnetic fields, $\sqrt{(\partial p/\partial \rho)_s}$. The analogous Mach number squared is

$$M^{*2} = \left(\frac{v^*}{a^*}\right)^2 = \frac{(v/a)^2(v/b)^2}{(v/a)^2 + (v/b)^2 - 1} \qquad [11]$$

Values of M^{*2} are plotted against v/a and v/b in Fig. 1. The lines $M^{*2} = 0$, $M^{*2} = 1$, and $M^{*2} = \pm\infty$ divide the graph into the following five regions:

1 When $v > b$ and $v > a$, $M^{*2} > 1$ and the equations governing a motion are hyperbolic. Mach waves, at an angle $\sin^{-1} 1/M^*$ to the streamlines, correspond to stationary infinitesimal waves of the fast magnetogasdynamic type. As Kogan and Resler have shown, the waves are inclined downstream from a disturbance to the flow. The gasdynamic analog is supersonic flow.

2 When $v > b$ and $v < a$, $M^{*2} < 1$, and the equations are elliptic. The analog is subsonic flow.

3 When $v < b$ and $v > a$, $M^{*2} < 1$ and the equations are again elliptic. The definition of $\boldsymbol{v}^*$ is such that $\boldsymbol{v}^*$ is antiparallel to $\boldsymbol{v}$; ρ^* is a negative quantity. $\boldsymbol{v}^*$, and ρ^* may be redefined so as to be parallel to $\boldsymbol{v}$ and positive, respectively, and the analog is subsonic flow.

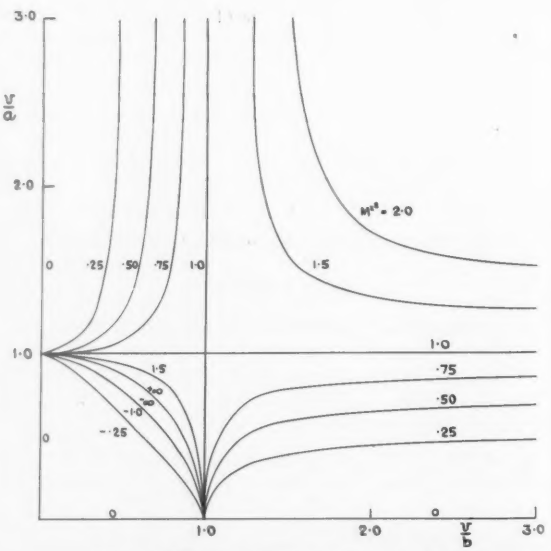

Fig. 1 M^{*2} as a function of v/a and v/b

4 When $v < b, v < a, (v/a)^2 + (v/b)^2 > 1, M^{*2} > 1$ and the equations are hyperbolic. Mach waves correspond to stationary waves of the slow type; Kogan and Resler have shown that the waves are inclined upstream from a disturbance. In some cases, such as linearized flow over bodies, it is convenient to retain the definition of v^* so that, for an ideal flow without a wake, the analog is supersonic flow in the *reverse* direction.

5 When $(v/a)^2 + (v/b)^2 < 1$, M^{*2} is a negative quantity. The equations are elliptic, but there is no analog in gasdynamics.

In the hyperbolic regions, the Prandtl-Meyer function for plane flow is

$$\omega = \int \cot\left(\sin^{-1}\frac{1}{M^*}\right)\frac{dv^*}{v^*} \qquad [12]$$

In terms of v, a and b, Equation [12] gives

$$\omega = \int \frac{\sqrt{((v/a)^2 + (v/b)^2 - 1)((v/a)^2 - 1)((v/b)^2 - 1)}}{(v/b)^2 - 1}\frac{dv}{v} \qquad [13]$$

where the positive square root is taken. Kogan has given characteristic equations for the hodograph plane; if a Prandtl-Meyer function is derived from his results, it has the form of Equation [13]. If $\tau^* = 1/\rho^*$, the steepening, or spreading, of waves depends on the sign of $\tau^{*3}d^2p^*/d\rho^{*2}$ which may be written

$$\tau^{*3}\frac{d^2p^*}{d\rho^{*2}} = \left[1 - \left(\frac{b}{v}\right)^2\right]^3\left\{3b^2\left[1 - \left(\frac{a}{v}\right)^2\right] + \left[1 - \left(\frac{b}{v}\right)^2\right]\tau^3\left(\frac{\partial^2 p}{\partial\tau^2}\right)_s\right\} \qquad [14]$$

The quantity $\tau^3(\partial^2 p/\partial\tau^2)_s$ is positive for all known fluids. From Equation [14] we can deduce that compression waves of region 4 steepen when they are inclined upstream.

When $v = b$, there is a special solution, which is not apparent from the analogy. Chandrasekhar (3) has shown that then v, b and a etc. may be constant throughout the flow; the direction of flow and vorticity are arbitrary, and acceleration of the gas is given by magnetic forces alone. The solution only applies for special boundary conditions.

The analogy is most easily applied to linearized theories of gasdynamics, where a relation between the pressure and density is not required (i.e., provided p^* varies locally with ρ^* in a reasonable manner, the form of the p^*, ρ^* relation does not matter). Aerodynamic forces for bodies, with no internal magnetic field, can be calculated from the distribution of p^*, and p^* can be found from the pressure coefficient of the analogous flow

$$C_p = \frac{p^* - p_\infty{}^*}{(1/2)\rho_\infty{}^* v_\infty{}^{*2}} \qquad [15]$$

In region 4, where the analogous flow is taken in the reverse direction, ρ^* is negative; the p^* variation is of opposite sign to the pressure variation of the analog, and there will be positive wave drag on a body in the magnetogasdynamic flow. Linearized theory of subsonic flow can be extended to cover region 5.

The author wishes to thank Dr. J. A. Shercliff for his help and advice in this work.

Nomenclature

a	=	local speed of sound
b	=	Alfvén wave speed
$\boldsymbol{B}$	=	magnetic field vector (magnitude B)
C_p	=	pressure coefficient
$\boldsymbol{E}$	=	electric field vector
h	=	enthalpy
h_0	=	stagnation enthalpy
$\boldsymbol{j}$	=	current density vector
k	=	a constant of a flow
M	=	Mach number
p	=	pressure
s	=	entropy
$\boldsymbol{v}$	=	gas velocity vector (magnitude v)
μ	=	magnetic permeability
ρ	=	density
τ	=	specific volume
ω	=	Prandtl-Meyer function

Subscripts

*	=	quantity defined to have analogy in gasdynamics
∞	=	free stream conditions
r, θ, z	=	directions in cylindrical polar coordinates

References

1 Sears, W. R., "Magnetohydrodynamic Effects in Aerodynamic Flows," ARS JOURNAL, vol. 29, no. 6, June, 1959, pp. 397–406.
2 Kogan, M. N., "Dynamics of Two-Dimensional and Axisymmetric Flow of Gas Having Infinite Electric Conductivity," *Prikl. Mat. Mekh.*, vol. 23, no. 1, Jan.-Feb. 1959, pp. 70–80.
3 Chandrasekhar, S., "On Cosmic Magnetic Fields," Proc. Nat. Acad. Sci., U.S.A., vol. 43, no. 1, Jan. 1957, pp. 24–27.
4 Resler, E. L., Jr. and McCune, J. E., "Electrodynamic Interaction with Aerodynamic Flow," in "The Magnetodynamics of Conducting Fluids," Bershader, D., Ed., Stanford University Press, 1959, pp. 120–136.

Analog Computer Technique for Plotting Frequency Response

JOHN L. WEBSTER[1] and DAVID N. SCHULTZ[2]

Chrysler Corp., Missile Division, Huntsville, Ala.

This article describes a direct method of obtaining frequency response curves during analog computer studies. The system under study is driven by a constant amplitude, varying frequency sine wave. System output is then rectified and recorded on the *Y* axis of a recorder whose *X* axis is swept at the same rate as that of the driving frequency. A suitable driving function can be generated using analog computer components.

Received Sept. 11, 1959.
[1] Senior Engineer, Systems Analysis and Data Evaluation Group. Member ARS.
[2] Engineer, Systems Analysis Unit.

Driving Function

THE DRIVING function must be sinusoidal and of constant amplitude. The frequency must vary such that equal samples of response data are obtained in all divisions of the frequency range. To comply with these requirements, an exponentially decaying sweep is utilized sweeping through the higher frequencies rapidly and dwelling sufficiently long at the lower frequencies to obtain an equal number of samples.

The driving function is therefore

$$E = a \sin(0.01bBe^{-ct}t) \qquad [1]$$

with the 0.01 resulting from the particular multipliers used. The amplitude is fixed by a and the frequency varies as

$$W = 0.01bBe^{-ct}\ \frac{\text{rad}}{\text{sec}} \quad \text{or} \quad f = \frac{0.01\ bBe^{-ct}}{2\pi}\ \text{cps} \qquad [2]$$

For the X axis to vary at the same rate, the x displacement becomes

$$x = GBe^{-ct} \text{ in.} \quad [3]$$

from which

$$X = GB \text{ in.} \quad [4]$$

Fig. 2 illustrates the computer setup used to generate these functions. A biased diode is utilized as a clamper to stop the exponential decay when

$$W = 0.01bd \frac{\text{rad}}{\text{sec}} \quad \text{or} \quad f = \frac{0.01bd}{2\pi} \text{ cps} \quad [5]$$

This will also stop the X axis sweep of the recorder when

$$x = Gd \quad [6]$$

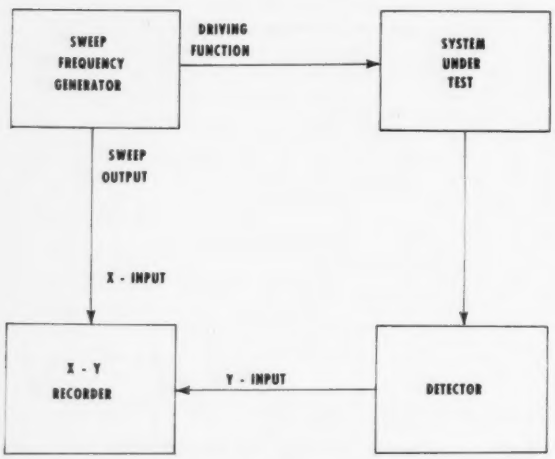

Fig. 1 Block diagram of frequency response measuring technique

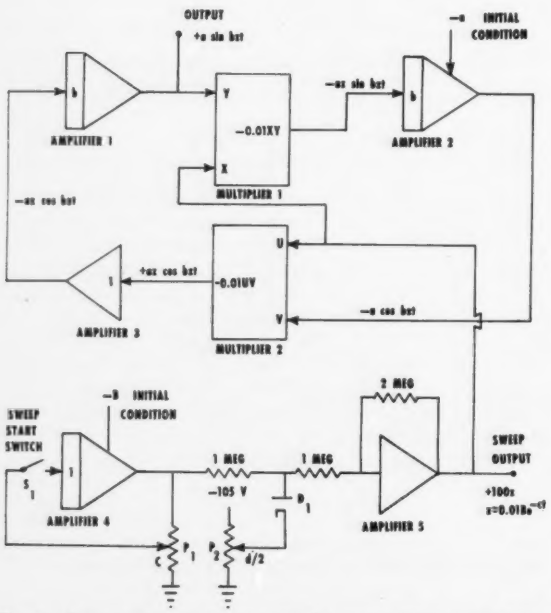

Fig. 2 Computer setup to generate the sweep frequency driving function

Therefore from Equations [4 and 6], the length of the recorded display will be

$$L = G(B - d) \quad \text{or} \quad L = X(1 - d/B) \text{ in.} \quad [7]$$

The maximum and minimum frequencies of the sweep range are fixed by the products bB and bd respectively. The potentiometer c may be used to control computing time and the number of samples recorded per inch of X distance.

From Equations [3 and 4]

$$\left|\frac{dx}{dt}\right| = cXe^{-ct} \frac{\text{in.}}{\text{sec}} \quad [8]$$

Therefore, the samples recorded per inch will be

$$S = \frac{f}{|dx/dt|} = \frac{0.01bB}{2\pi Xc} \frac{\text{samples}}{\text{in.}} \quad [9]$$

From Equations [2 and 5], computing time required to complete the sweep becomes

$$T = \frac{1}{c} \log_e \frac{B}{d} \quad [10]$$

Conclusion

With the computer setup as indicated by Figs. 1 and 2 and adjusted as in the preceding equations, it is possible to plot directly frequency response of any system being studied on the computer.

The system under test should generally be operating in the region of 0.1 to 20.0 rad per sec on the computer, and therefore time scaling may be required in many instances.

To minimize integration errors, the samples per inch and frequency range swept should be selected to keep the computing time less than 2 min.

To avoid transient disturbances associated with the sudden

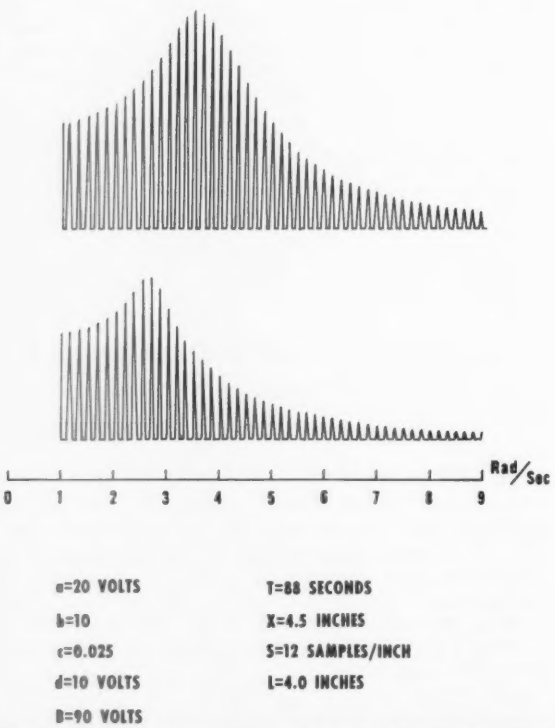

Fig. 3 Two typical response curves obtained by the described technique

application of the driving function, the problem should be computing before the sweep is started.

Fig. 3 illustrates the type of frequency response curves obtained by this technique.

Nomenclature

E = output voltage
a = initial condition voltage of integrator amplifier no. 2
b = gain of integrators 1 and 2
t = time, sec
B = initial condition voltage of integrator amplifier no. 4
c = setting of potentiometer P_1
$d/2$ = voltage set at arm of P_2
W = angular velocity, rad/sec
f = frequency, cps
X = total displacement from zero along X axis
G = X axis gain of recorder
x = instantaneous displacement from zero along X axis
L = length of display, in.
S = samples recorded per inch of display
T = total time required to complete the sweep

Some Characteristics of the Planar Satellite Orbit

JOSEF S. PISTINER[1]

The Martin Co., Denver, Colo.

The classical use of the various anomalies to describe the orbital mechanics of satellites often becomes exceedingly complex. This paper, on the other hand, describes in relatively simple mathematical or graphical form some of the important orbital characteristics of satellites in terms of the true anomaly alone. In addition, the concept of a simple orbital energy diagram is developed and its utility indicated. The approach presented in this paper restricts itself to the planar two-body problem.

Orbit Ellipse

FIG. 1 defines the orbit ellipse with its significant parameters and the center of a spherical celestial body at one of its foci. The orbit is assumed to be planar and in the gravitational (central force) field of the celestial body. A conservative system has been assumed. Therefore, the satellite's total angular momentum and total orbital energy (kinetic plus potential) are both constant. Or

$$\ell = mrv_\theta = \text{total angular momentum} = \text{constant} \quad [1]$$

and from (1)[2]

$$E = \frac{m}{2}(v_\theta^2 + v_r^2) - \frac{\mu m}{r} = \text{total orbital energy} = \text{constant} \quad [2]$$

Equation [2] may be rewritten as

$$\frac{2E}{m} + \left(\frac{\mu m}{\ell}\right)^2 = v_r^2 + \left(v_\theta - \frac{\mu m}{\ell}\right)^2 \quad [3]$$

Using the velocity parameter concept established by Altman (2), let

$$C = \mu m/\ell \quad [4]$$

and

$$R^2 = 2E/m + C^2 \quad [5]$$

By use of the vis-viva integral it can also be shown that

$$E = -(\mu m/2a) \quad [6]$$

Equation [5], therefore, may be rewritten as

$$C^2 - R^2 = -\frac{2E}{m} = \frac{\mu}{a} \quad [7]$$

Note that the parameters R and C are constant for a given orbit and have the dimensions of linear velocity.

Received Sept. 11, 1959.

[1] Design Engineer, Advanced Systems Section Staff, Denver Div.

[2] Numbers in parentheses indicate References at end of paper.

Since the eccentricity of the orbit may be defined (3) by

$$e = \sqrt{1 + \frac{2E}{m}\left(\frac{\ell}{\mu m}\right)^2} \quad [8]$$

it can be easily shown that

$$e = R/C \quad [9]$$

It can further be shown that

$$v_\theta = C + R\cos\varphi \quad [10]$$

and

$$v_r = R\sin\varphi \quad [11]$$

Therefore

$$\tan\theta = \frac{v_r}{v_\theta} = \frac{R\sin\varphi}{C + R\cos\varphi} = \frac{e\sin\varphi}{1 + e\cos\varphi} \quad [12]$$

Orbital Energy Diagram

Equation [7] may be considered to define an orbital energy diagram if R^2 is plotted vs. C^2 (Fig. 2). Note that the dimen-

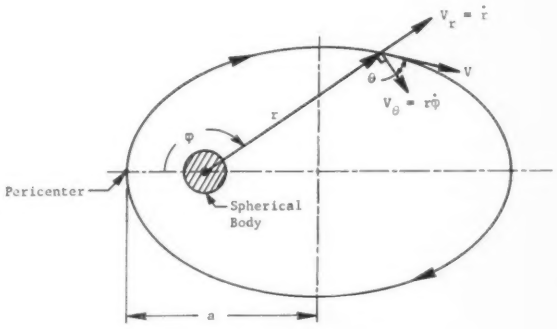

Fig. 1 Elliptic orbit

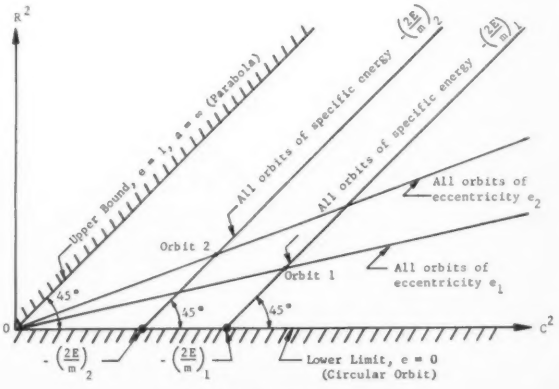

Fig. 2 Orbital energy diagram

sions of R^2 and C^2 are energy per unit mass (or specific energy). Since

$$C^2 - R^2 = -\frac{2E}{m} = \frac{\mu}{a} = \text{constant}$$

any straight line on the orbital energy diagram with a slope of 45 deg represents all orbits of a given specific energy (or given semimajor axis). Also, since $e = R/C$, a straight line (through the origin) with a slope numerically equal to the square of a given eccentricity will represent all orbits with this eccentricity. Hence, the point resulting from the intersection of a line of constant specific energy with a line of constant eccentricity will uniquely define a given elliptic orbit.

Note that the C^2-axis intercept of a line of constant specific energy is numerically equal to the value of this specific energy. Therefore, the theoretical minimum change in specific energy required to transfer, for example, from orbit 1 to orbit 2 (see Fig. 2) is given by the difference in C^2-axis intercepts.

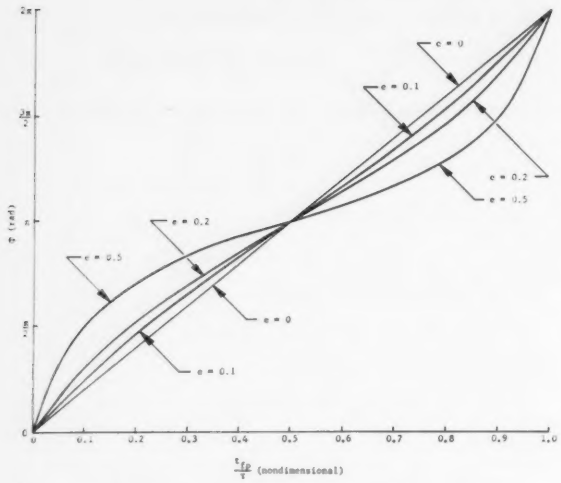

Fig. 3 True anomaly φ vs. time t

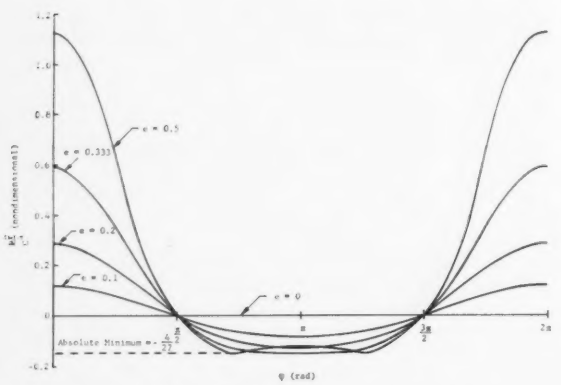

Fig. 4 Radial acceleration $\ddot{r}$ vs. true anomaly φ

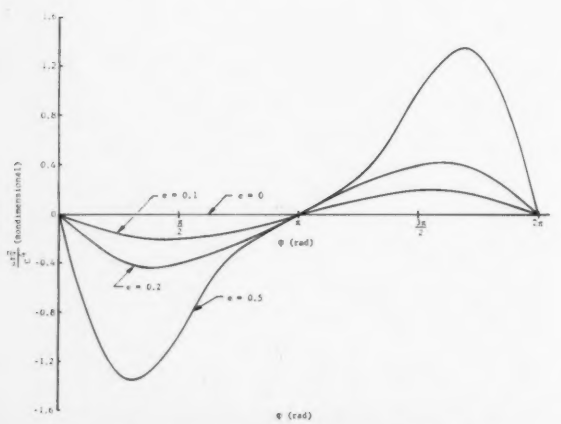

Fig. 5 Normal acceleration $r\ddot{\varphi}$ vs. true anomaly φ

True Anomaly as Function of Time

It can be shown that

$$\dot{\varphi} = \frac{d\varphi}{dt} = \frac{C}{\mu} v_\theta^2 \qquad [13]$$

or, by use of Equation [10]

$$\dot{\varphi} = (C/\mu)(C + R\cos\varphi)^2 \qquad [14]$$

Therefore

$$\int_{\varphi_0}^{\varphi} \frac{d\varphi}{(C + R\cos\varphi)^2} = \int_{t_o}^{t} \frac{C}{\mu}\, dt = \frac{C}{\mu}(t - t_o) \qquad [15]$$

The integration of Equation [15] may be appreciably simplified by letting

$$(t - t_o) = t_{fp} = \text{time from pericenter passage}$$

then

$$\varphi_o = 0$$

With these simplifications, integration and simplification results in

$$\frac{C}{\mu} t_{fp} = -\frac{R\sin\varphi}{(C^2 - R^2)(C + R\cos\varphi)} + \frac{2C}{(C^2 - R^2)^{3/2}} \tan^{-1}\left[\frac{\sqrt{C^2 - R^2}}{C + R}\tan\frac{\varphi}{2}\right] \qquad [16]$$

Since the period of an elliptic orbit is given by

$$\tau = \frac{2\pi a^{3/2}}{\mu^{1/2}} = \frac{2\pi\mu}{(C^2 - R^2)^{3/2}} \qquad [17]$$

Equation [16] finally may be rewritten in terms of τ, e and φ

$$\frac{t_{fp}}{\tau} = \frac{1}{\pi}\left\{\tan^{-1}\left[\sqrt{\frac{1-e}{1+e}}\tan\frac{\varphi}{2}\right] - \frac{\sqrt{1-e^2}}{2}\left(\frac{e\sin\varphi}{1 + e\cos\varphi}\right)\right\} \qquad [18]$$

Fig. 3 is a plot of φ vs. t_{fp}/τ for several values of e.

By use of Equations [9, 14 and 17]

$$\dot{\varphi} = \frac{2\pi}{\tau}\frac{(1 + e\cos\varphi)^2}{(1 - e^2)^{3/2}} \qquad [19]$$

It can also be shown that

$$\ddot{\varphi} = \frac{d^2\varphi}{dt^2} = -2e\dot{\varphi}^2\left(\frac{\sin\varphi}{1 + e\cos\varphi}\right) \qquad [20]$$

or

$$\ddot{\varphi} = -2\dot{\varphi}^2\left(\frac{v_r}{v_\theta}\right) \qquad [21]$$

Path Angle as Function of True Anomaly and Orbit Eccentricity

The path angle is defined as the angle between the total velocity vector of the satellite and the local horizon. The tangent of this angle is given by Equation [12].

It is of interest to note that the maxima and minima of v_r/v_θ ($= \tan\theta$) occur when

$$\cos\varphi + e = 0 \qquad [22]$$

When Equation [22] is satisfied, then

$$\left(\frac{v_r}{v_\theta}\right)_{\max-\min} = \pm\frac{e}{\sqrt{1-e^2}} \qquad [23]$$

Since v_r/v_θ reaches a maximum when

$$\tan\frac{\varphi}{2} = \sqrt{\frac{1+e}{1-e}}$$

or

$$\tan\varphi = \frac{\sqrt{1-e^2}}{-e}$$

it can be shown that the time at which this maximum occurs is given by

$$\frac{t_{fp}}{\tau} = 0.25 - \frac{e}{2\pi} \qquad [24]$$

Note also that for $(v_r/v_\theta)_{\max}$, in an elliptic orbit

$$\frac{t_{fp}}{\tau} > \frac{\pi-2}{4\pi}$$

always.

Radial and Normal Acceleration as Functions of True Anomaly and Eccentricity

A knowledge of the radial and normal accelerations of a satellite in an elliptic orbit is useful in establishing the vehicle's stabilization and attitude control requirements. Note that the magnitude of these accelerations is of the order of a small fraction of one gravity (g).

Radial acceleration

Equation [2] may be written as

$$E = \frac{1}{2}m(\dot{r}^2 + r^2\dot{\varphi}^2) - \frac{\mu m}{r} = \text{constant} \qquad [25]$$

Differentiation of Equation [25], assuming the vehicle mass m to be constant, and simplification results in

$$\ddot{r} = r\dot{\varphi}^2 - \frac{\mu}{r^2} \qquad [26]$$

After further substitution and simplification, Equation [26] may be written in the following nondimensional form

$$\frac{\mu\ddot{r}}{C^4} = e\cos\varphi(1 + e\cos\varphi)^2 \qquad [27]$$

Fig. 4 is a plot of $\mu\ddot{r}/C^4$ vs. φ for several values of eccentricity e. Note that for $\mu\ddot{r}/C^4$ to be an extremum

$$\sin\varphi(1 + e\cos\varphi)(1 + 3e\cos\varphi) = 0$$

Therefore, the following conditions for extrema exist:

(a) $\sin\varphi = 0$ or $\varphi = n\pi$ $(n = 0, 1, 2)$

(b) $\cos\varphi = -1/e$

This condition is nonexistent since $e < 1$ for elliptic orbits.

(c) $\cos\varphi = -1/3e$

This condition exists only for $e \geq \frac{1}{3}$ and results in an absolute minimum of $\mu\ddot{r}/C^4$.

Therefore

$$\left(\frac{\mu\ddot{r}}{C^4}\right)_{\max} = e(1+e)^2 \left\{\begin{matrix}0 \leq e < 1\\ \varphi = 0,\ 2\pi\end{matrix}\right\}$$

and

$$\left(\frac{\mu\ddot{r}}{C^4}\right)_{\min} = -e(1-e)^2 \left\{\begin{matrix}0 \leq e \leq \frac{1}{3}\\ \varphi = \pi\end{matrix}\right\}$$

$$= -\frac{4}{27} \left\{\begin{matrix}\frac{1}{3} \leq e < 1\\ \varphi = \cos^{-1}\left(-\frac{1}{3e}\right)\end{matrix}\right\}$$

Normal acceleration

It can be shown that

$$r\ddot{\varphi}/\ddot{r} = -2\tan\varphi \qquad [28]$$

Substitution of Equation [27] into Equation [28] results in the following nondimensional equation

$$\mu r\ddot{\varphi}/C^4 = -2e\sin\varphi(1 + e\cos\varphi)^2 \qquad [29]$$

Fig. 5 is a plot of $\mu r\ddot{\varphi}/C^4$ vs. φ for several values of e. Note that for $\mu r\ddot{\varphi}/C^4$ to be an extremum

$$\cos\varphi + 3e\cos^2\varphi - 2e = 0$$

or

$$\cos\varphi = \frac{1}{6e}\left[-1 \pm \sqrt{1 + 24e^2}\right] \qquad [30]$$

Obviously, extrema exist only if a solution of Equations [30] results in

$$-1 \leq \cos\varphi \leq +1$$

Nomenclature

- a = length of semimajor axis of orbit ellipse
- e = orbit eccentricity
- ℓ = satellite total angular momentum
- m = satellite mass
- r = radial distance from focus of orbit ellipse to satellite center of mass
- t = time
- t_{fp} = time from pericenter passage
- t_o = reference value of time
- v = total velocity of satellite center of mass
- v_θ = normal velocity component of satellite center of mass
- v_r = radial velocity component of satellite center of mass
- C = velocity parameter
- E = total energy (kinetic plus potential) of satellite center of mass
- R = velocity parameter
- θ = path angle (= angle between total velocity vector of the satellite center of mass and the local horizon)
- μ = gravitational constant ($= 1.41008 \times 10^{16}$ ft^3/sec^2 for terrestrial orbits)
- τ = period of orbit
- φ = true anomaly
- φ_o = reference value of true anomaly

References

1 MacMillan, W. D., "Statics and the Dynamics of a Particle," Dover Publications, N. Y., 1958, p. 277.

2 Altman, S. P., "Orbital Transfer for Satellites," Martin-Denver Rep. no. M-M-MI-59-11, April 1959, p. 12.

3 Goldstein, H., "Classical Mechanics," Addison-Wesley Press, Cambridge, Mass., 1951, p. 78.

Symmetry of the Earth's Figure[1]

J. L. BRENNER[2]

Stanford Research Institute, Menlo Park, Calif.

R. FULTON[3] and N. SHERMAN[4]

University of California, Livermore, Calif.

By means of a special numerical integration carried out for nine hundred revolutions, it is shown that the oblateness of Earth causes long period changes in the shape, size and inclination of the osculating orbit of the Vanguard I satellite (1958 Beta two). Unless many determinations of these parameters are made per revolution, the effect of an Earth with equatorial symmetry can imitate in period, amplitude and phase the effect which might be expected from a "pear-shaped" potential. This result, which has been verified by independent analysis using an appropriate perturbation theory, shows that published evidence does not support the hypothesis that Earth's mass distribution is asymmetric with respect to its equatorial plane.

IF THE only force acting on an Earth satellite were the attraction of Earth itself, and if the mass of Earth were spherically homogeneous, the orbit of a satellite would be an ellipse with the center of Earth at one focus. This is a simple consequence of the fact that such a mass distribution produces a central, inverse-square force on the satellite. The drag of the atmosphere on the Vanguard I satellite is very small, and the perturbations on the orbit due to the sun, moon and tides of Earth are also small. The main perturbing force, due to the equatorial bulge of Earth, is neither central nor inverse square. This force is small enough itself to be considered as a perturbation: The equatorial and polar diameters of Earth differ by less than one half of one per cent.

Although the effects of the equatorial bulge on the Vanguard I satellite are relatively small, some are cumulative. During the several thousand revolutions that the satellite has been observed, these effects have been verified observationally. The magnitude of these effects can be used to confirm (and even to improve) the estimate of the magnitude of the bulge which is obtained from geodesy (2).[5]

During the first revolution, the drag-free orbit of a satellite lies roughly in a plane. The perturbation caused by the equatorial bulge can be described as first, a slow regression of this plane (without changing its inclination to the Equator), and second, a precession in the orbital plane of the perigee (closest point).

If a more accurate description of the orbit is attempted, it is found that the rough term "orbital plane" is not precise enough for practical use. Fig. 1 shows that the osculating inclination varies considerably even during a single revolution. Fig. 2 shows that there is also a relatively large variation of osculating eccentricity during a single revolution. By a special analysis (3), it has been possible to derive expressions for variation of perigee distance, of maximum latitude and of shape.

The results of that analysis have been confirmed by direct numerical integration of the differential equations of motion (1). These equations are (in Cartesian coordinates)

$$\frac{d}{dt}\frac{\partial L}{\partial \dot{x}} = -\frac{\partial V}{\partial x}$$

$$\frac{d}{dt}\frac{\partial L}{\partial \dot{y}} = -\frac{\partial V}{\partial y}$$

$$\frac{d}{dt}\frac{\partial L}{\partial \dot{z}} = -\frac{\partial V}{\partial z}$$

Received Sept. 21, 1959.

[1] This research was supported in part by the U. S. Air Force under Contract no. AF 29(600)-1773, and the U. S. Atomic Energy Commission, monitored by Air Force Missile Development Center, Air Research and Development Command.

[2] Research Mathematician. Member ARS.

[3] Lawrence Radiation Laboratory.

[4] Physicist, Lawrence Radiation Laboratory. Member ARS.

[5] Numbers in parentheses indicate References at end of paper.

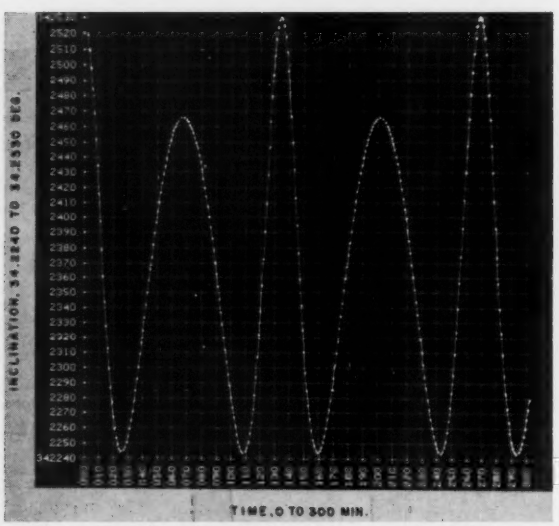

Fig. 1 Variation of inclination during several revolutions

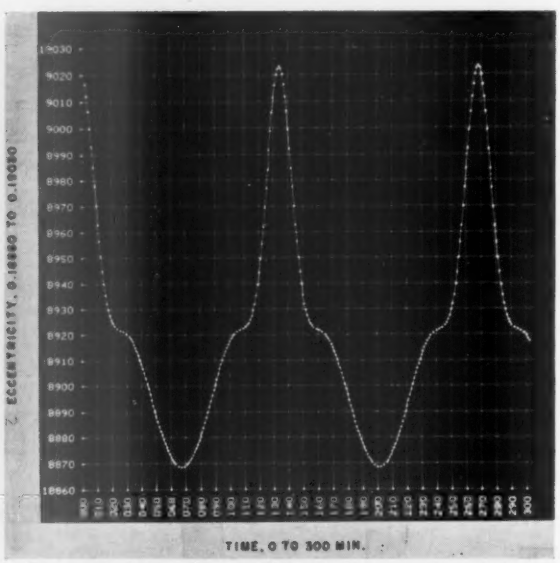

Fig. 2 Variation of eccentricity during several revolutions

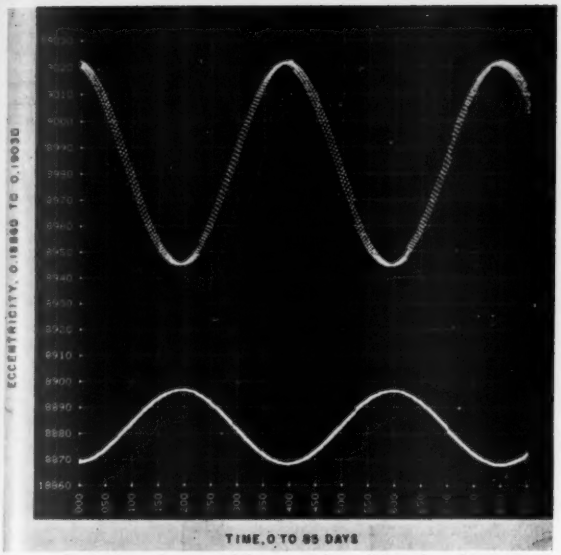

Fig. 3 Variation of eccentricity at perigee (above) and at apogee (below) during an 80-day period

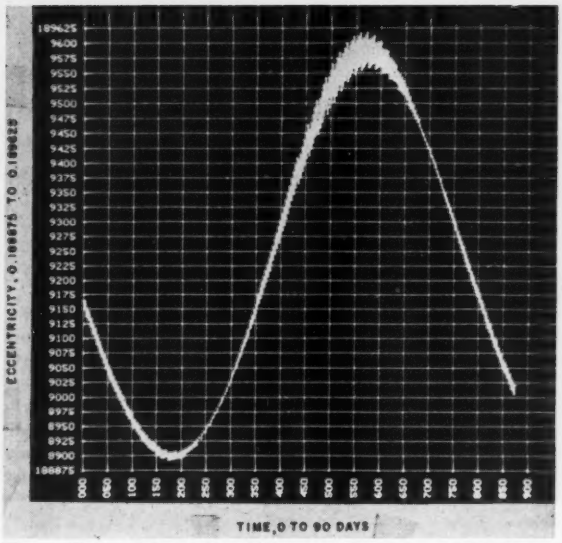

Fig. 4 Eccentricity at ascending crossing of $\delta = +30$ deg vs. time in days

where

$$L = T - V$$

$$T = (1/2)(\dot{x}^2 + \dot{y}^2 + \dot{z}^2)$$

$$V = -\frac{gR^2}{r}\left[1 + J\,\frac{R^2}{r^2}\left(\frac{1}{3} - \frac{z^2}{r^2}\right)\right]$$

$$r = (x^2 + y^2 + z^2)^{1/2}$$

assuming that only the "second harmonic" of the gravitational potential field has nonzero coefficient. Here, R is the equatorial radius of Earth, and $g(1 + J)$ is the algebraic sum of the observed acceleration of gravity at the Equator and the "centrifugal" force there.

Fig. 3 shows the variation of osculating eccentricity at apogee and at perigee during some nine hundred revolutions. Both quantities have a 40-day period, but have opposite phase. From this figure it is seen that the term "eccentricity" not further specified can be expected to vary in any manner provided it stays within the extreme limits shown in the figure. To emphasize this possibility, we computed the osculating eccentricity at successive northward crossings of declination +30 deg. The result, shown in Fig. 4, shows the same period, amplitude and phase as has been used (4) to "prove" that Earth's gravitational field has a nonzero third harmonic. This conclusion is therefore open to question and, in our minds, is not established.

Our results and methods have successfully passed several decisive checks.

We have been able to obtain spurious variations not only in this osculating eccentricity, but also in the osculating inclination, rate of change of longitude of node, and rate of change of argument of perigee. Hence none of these quantities, nor all of them together, give evidence concerning the existence of the third harmonic in Earth's gravitational potential field. The magnitude of the coefficient of this harmonic (if its existence can be proved) is in our minds as likely to be 10^{-8} as $2 \cdot 10^{-6}$, the value derived in (4).

Acknowledgment

It is a pleasure to thank the scientific staff of Air Force Missile Development Center, Holloman Air Force Base, N. Mex., and of University of California Lawrence Radiation Laboratory, Livermore, for encouragement and for detailed help. Dr. James A. Ward of AFMDC had technical cognizance of the work. Professor L. E. Cunningham of University of California gave us valuable suggestions.

References

1 Smith, V. C., Bruijnes, H. R. and Sherman, N. W., "The Satellite Code," Lawrence Radiation Laboratory Rep. U.C.R.L.-5462, June 1959.

2 King-Hele, D. G. and Merson, R. H., "A New Value for the Earth's Flattening Derived from Measurements of Satellite Orbits," *Nature*, vol. 183, March 28, 1959, pp. 881–882.

3 Brenner, J. L., Latta, G. E. and Weisfield, M., "A New Coordinate System for Satellite Orbit Theory," Interim Technical Rep. no. 2, Stanford Research Institute, June 15, 1959.

4 O'Keefe, J. A., Eckels, A. and Squires, R. K., "Vanguard Measurements Give Pear-Shaped Component of Earth's Figure," *Science*, vol. 129, 1959, pp. 565–566.

Thermal Decomposition of Liquid Phase n-Propyl Nitrate and Its Compatibility With Various Metals and Other Additives

ADOLPH B. AMSTER[1] and JOSEPH B. LEVY[2]

U. S. Naval Ordnance Laboratory, Silver Spring, Md.

Pure normal propyl nitrate has been found to undergo negligible decomposition at normal temperatures and only slight decomposition at its normal boiling point. The rate is accelerated by impurities, such as nitrogen dioxide, acetaldehyde, water and acetic acid. The experimental results also predict safe storage for at least a year at temperatures up to 160 F in containers of hard copper, ST aluminum alloy, 2S soft aluminum, K Monel, 303 stainless steel and 1020 cold rolled steel.

IN EVALUATING the hazards associated with the handling of n-propyl nitrate (NPN) it is appropriate to investigate its stability. The thermal decomposition of gaseous NPN has already been examined (1),[3] yet it is well known (2) that in many cases the reaction mechanism changes in going from the gas phase to the liquid phase. The possibility that this might occur with NPN, coupled with the possibility that small amounts of impurities might affect such reactions, led to the studies described herein.

Experimental Procedures

The NPN used in these experiments was obtained by fractional distillation of material supplied by the Ethyl Corp. The commercial product was light amber in color, but the distillate was colorless. Two separate distillations were conducted in a column of about 20 theoretical plates. Material was collected at 53.6–53.9 C at 100 mm Hg pressure and at 65.8 C at 168 mm Hg pressure. In each case, several fractions were taken and their infrared spectra compared with that of the commercial material. No differences were observed. All of the spectroscopic work reported herein was performed with a Perkin-Elmer model 21 double beam spectrophotometer using NaCl optics and cell faces.

Table 1 Analysis of impurities in NPN using infrared spectroscopy

Compound	Frequencies useful for analysis, μ	Minimum detectable concentration, per cent
n-propyl nitrite	12.70	0.3
	8.70	...
	9.45	...
nitroethane	6.50	1.0
ethanol	9.50	1.0
n-propanol	9.9	1.0
acetaldehyde	5.83	0.6
propionaldehyde	5.85	0.2
acetic acid	5.87	0.1

Table 2 Effect of heat on n-propyl nitrate

Run	Temp.	Time	Decomposition
1	50 C	up to one week	no perceptible amount
2	85 C	up to 17 days	no perceptible amount
3	B.Pt (111 C)	7 days	no perceptible amount
4	B. Pt. (110 C)	12 days	slight decomposition

Small quantities of potential reaction or decomposition products were added to pure NPN to determine the extent to which they were detectable. The results, including the substances added, the frequencies useful for analysis and the minimum detectable concentration are given in Table 1.

Simultaneously, samples of NPN were heated in containers open to the dry atmosphere, and spectra of the resulting liquids were compared with that of the original sample.

The effect of increasingly vigorous heat treatment is indicated in Table 2 where it is seen that only in the most vigorously treated sample was there any detectable difference. Examination of the resultant spectra indicated that the potential impurities might include acetaldehyde, propionaldehyde, acetic acid or a combination of these. The mechanism proposed for the gas phase reaction predicts acetaldehyde and n-propyl nitrite (1). Decomposition of the latter would yield propionaldehyde whereas oxidation of acetaldehyde by nitrogen dioxide or air could give acetic acid. Quantitative analysis indicated that an insignificant quantity of the NPN had decomposed. Thus, even the relatively vigorous treatment of refluxing at atmospheric pressure for prolonged periods causes no major decomposition.

Thermal Stability of NPN in the Presence of Various Additives

The compatibility of NPN with each of a number of different metals and other additives has been examined. In each case, 1 ml of commercial grade NPN was placed in a Pyrex glass vial with the addendum. The metal samples used were in the form of smooth round pellets $\frac{1}{4}$ in. in diameter and $\frac{1}{8}$ in. in thickness, and were weighed before and after treatment. The sample vials were of proper size so that the pellets were completely covered by liquid. The contents were frozen and the vials evacuated and sealed. Each sample was then placed for a specified period in a bath maintained at 100 C. At the conclusion of the heating period the remaining liquid was dissolved in iso-octane for quantitative spectroscopic analysis to determine whether any NPN had decomposed. The experimental results are shown in Table 3. These analyses were performed using a pair of matched cells at a wave length of 11.600μ and a slit width of 399μ. Study of the spectra of pure NPN and of NPN mixed with possible reaction products indicated that this wave length is that most suitable.

The relation between optical density and concentration had been determined. It follows Beer's law, i.e., is linear, at concentrations corresponding to less than 100 per cent of the original NPN present in the solvent, but at higher levels the

Received Sept. 11, 1959.

[1] Supervisory Chemist, Physical Chemistry Division. Member ARS.

[2] Present address: Atlantic Research Corp., Alexandria, Va.

[3] Numbers in parentheses indicate References at end of paper.

optical density becomes quite insensitive to the concentration. Therefore since there is no mechanism here for NPN production, all analyses over 100 per cent are reported as 100 per cent with the actual results given in parentheses. Results indicating decomposition, i.e., less than 100 per cent NPN, are deemed reliable.

Discussion

The conditions indicated in Table 3 are quite rigorous. Taking the activation energy for NPN as 36.9 kcal/mole (3), 6 days at 100 C, for example, correspond to about a year at 70 C (160 F). Of the runs 4–10 of Table 3 in which metal additives were used, none gave evidence of significant destruction of NPN, the variations in the NPN analyses being within the error of the measurement. Run 9 with cold rolled steel gave some evidence of reaction in that the sample showed a gain in weight of 1–2 per cent.

Runs 11–14, in which chemicals which might be formed in NPN by its decomposition were the additives, showed striking results especially with nitrogen dioxide and acetaldehyde. Water and acetic acid likewise show a deleterious, though much less marked, effect. It is interesting to point out that although nitrogen dioxide inhibits the gas phase decomposition of NPN (1) it accelerates that in the liquid phase; thus the difference in phase does affect the mechanism of the reaction.

Conclusions and Recommendations

After a careful review of the data obtained during the course of this investigation some conclusions may be drawn.

1 The following materials are compatible with NPN and can be used as containers:

Hard copper
ST aluminum alloy
2S soft aluminum } excellent
K Monel
303 stainless steel
1020 cold rolled steel (for periods not to exceed one year)

2 In containers of the above materials the experimental results predict a storage life for NPN, in these containers, of at least a year at 160 F.

Detailed discussions of the investigations reported herein including the spectra referred to may be found in (4,5).

References

1 Levy, J. B. and Adrian, F. J., "The Thermal Decomposition of Nitrate Esters III. N-Propyl Nitrate," *J. Amer. Chem. Soc.*, vol. 77, 1955, p. 2015.

2 Frost, A. A. and Pearson, R. G., "Kinetics and Mechanisms," John Wiley and Sons, N. Y., 1953, chap. 7.

3 Phillips, L., "Thermal Decomposition of Organic Nitrates," *Nature*, vol. 160, 1947, p. 753; *see also* Levy, J. B., "The Thermal Decomposition of Nitrate Esters II. The Effect of Additives on the Thermal Decomposition of Ethyl Nitrate," *J. Amer. Chem. Soc.*, vol. 76, 1954, p. 3790.

4 Amster, A. B., Edwards, G. D., Hogge, E. A. and Levy, J. B., "Research on the Safety Characteristics of Normal Propyl Nitrate," NavOrd Rep. 4309, June 5, 1956.

5 Amster, A. B., Edwards, G. D. and Levy, J. B., "Research on the Safety Characteristics of Normal Propyl Nitrate. II. Terminal Report," NavOrd Rep. 4493, March 13, 1957.

Table 3 Thermal stability of NPN in the presence of various additives

Run	Material	Heating period, days 100 C	Pellet weight, gm Before	After	Per cent NPN remaining	Compatibility	Remarks
1	pure NPN	6	...	...	100	...	control
2	pure NPN	13	...	...	96	...	control
3	pure NPN	13	...	...	~100 (>110)	...	...
4	hard copper	6	0.8935	0.8935	96	excellent	...
5	ST Al alloy	6	0.2720	0.2719	98	excellent	...
6	2S soft Al	13	0.2706	0.2704	~100 (>110)	excellent	...
7	K Monel	13	0.9082	0.9083	~100 (>110)	excellent	...
8	303 stainless steel	6	0.7775	0.7776	95	excellent	...
9	1020 cold rolled steel	6	0.7800	0.7911	96	poor	...
10	Armco cast iron	13	0.7823	0.7822	~100 (100)	good[a]	...
11	saturated with NO_2	6	...	...	22	...	1 ml saturated liquid used
12	trace CH_3CHO	6	...	...	20	...	CH_3CHO added to 1 ml NPN
13	saturated with water	6	...	...	81	...	1 ml saturated liquid used
14	0.1 ml acetic acid	6	...	...	91	...	...

[a] Pellet showed rust colored discoloration.

Refraction Correction Techniques in Earth Satellite Optical Tracking for Precision Prediction[1]

ALBERT D. WASEL[2]

Lockheed Aircraft Corp., Missiles and Space Division, Sunnyvale, Calif.

An analysis to account for atmospheric refraction in photographic satellite tracking has been made. Assuming star background satellite photographs, yielding right ascension and declination of occulted bodies, a definite integral formula is developed for determining "central zenith distances" of a satellite orbiting a body having appreciable atmosphere (comparable to that of Earth). A first approximation for evaluation of the formula is detailed. Next, a method for constructing a refraction table using culmination techniques is outlined. Finally, a possible high precision combination optical-radar tracking and prediction system is suggested, and some of the problems caused by an assumption that Earth is ellipsoidal are indicated.

FROM the beginning of Earth satellite programs, opening with the IGY satellites, designers and systems engineers have favored electronic over optical tracking. At the same time, however, greater and greater accuracy in determining position and motion for acquisition and especially for ephemerides construction, has been demanded. When the major problem in optical systems, that of processing time-lag, is alleviated, and the ultimate system selection is made, it is certain that atmospheric light refraction will be accounted for in the optical systems. It is the aim of this paper to present a first solution to the refraction problem.

Determination and Incorporation of Central Zenith Distance Into a Prediction Program

It is assumed that a number of satellite intercepts providing the right ascension *r.a.* of the occulted star and its declination δ along with time t are available, say from star background photograph readings. (See Fig. 1 for these as well as other relevant quantities.) The polar angle θ_s of the satellite, relative to the zenith direction as polar direction, will be called the "central zenith distance" of the satellite in the remainder of this paper. The tracking station is located at T. Apparent right ascension and declination $r.a._A$ and δ_A are shown for the convenience of the reader.

The following paragraphs outline a procedure for determining the true direction of the satellite after correcting for refraction. Range, or more directly, vectorial radius distance, is determined simultaneously.

The first step is to transform the *r.a.* and δ values into corresponding values of azimuth A_* and elevation angle α_*. This might be done by computing inertial direction numbers, "rotating" to Earth oriented direction numbers with the aid of the Greenwich hour angles of the inertial reference point, and then "rotating" to spherical Earth tracking station horizon orientation. A suitable reference point is "the first point of Aries." Tables of hour-angle values of this quantity are available (1).[3] Corrections for Earth oblateness could be made; but to avoid complexity a spherical Earth is assumed here.

The second step is to compute ζ_0, the apparent zenith distance of the satellite (or the occulted star). This can be done by solving iteratively

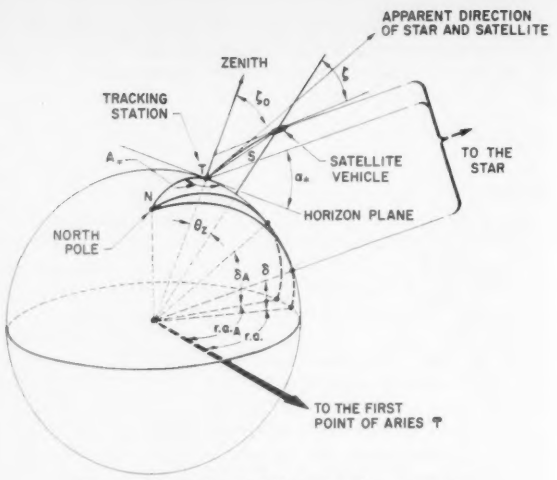

Fig. 1 Atmospheric light refraction geometry

$$\zeta_0 = \frac{\pi}{2} - [\alpha_* + R(\zeta_0)] \qquad [1]$$

where $R(\zeta_0)$ is given (2) as

$$R(\zeta_0) = 58.294'' \tan \zeta_0 - 0.0668'' \tan^3 \zeta_0 \qquad [2]$$

an empirical formula whose coefficients were derived from observations of stars.

Under the assumption of a spherical Earth, it can be shown (2) that

$$\mu r \sin \zeta = \text{constant} \qquad [3]$$

where μ is the index of atmospheric refraction of light and is a function only of the radius vector distance to the satellite, and ζ is the angle between the radius vector and the tangent. Now, by definition

$$\mu = v_\infty / v \qquad [4]$$

Here v is the speed of light and v_∞ is the speed of light in a vacuum. Thus

$$(r \sin \zeta)/v = C \qquad [5]$$

By substituting values of the variables at Earth's surface (denoted by zero subscripts) into Equation [5], the value of C is found to be $R \sin \zeta_0 / v_0$, where R denotes the radius of Earth. Values of these quantities are given in recent publications (3). From polar coordinate representation

$$\tan \zeta = r/(dr/d\theta_s) \qquad [6]$$

yielding

$$\sin \zeta = (r\, d\theta_s)/\sqrt{(dr)^2 + (r d\theta_s)^2} \qquad [7]$$

Combination of Equations [5 and 7] and simplification, yield

$$\frac{d\theta_s}{dr} = \frac{Cv}{r\sqrt{r^2 - C^2v^2}} \qquad [8]$$

and in turn

$$\theta_s = C \int_R^r \frac{v\, dr}{r\sqrt{r^2 - C^2v^2}} \qquad [9]$$

From (3)

$$v = \frac{v_0}{\{1 + [(\bar{\mu} - 1)/T]273.16\}} \left(\frac{\rho}{\rho_0}\right)\left(\frac{T}{273.16}\right) \qquad [10]$$

Received Aug. 27, 1959.

[1] The research described in this report was performed under Contract AF 18(600)-1847. The work was conducted under the cognizance of the Air Research and Development Command.

[2] Staff scientist. Member ARS.

[3] Numbers in parentheses indicate References at end of paper.

where T is the temperature in deg K and the bars indicate values at zero deg C and 760 mm of mercury. A recent representation of the atmospheric density ρ is given in (4) as

$$\rho = \text{constant} \times \{[aR(r - R)/r] - b\}^{-c} \qquad [11]$$

where a, b and c are constants. Thus, the integrand in Equation [9] is now expressed as a function of r and the determination of θ_z depends on the evaluation of a definite integral. This evaluation can surely be done satisfactorily on the computing machines in conjunction with a prediction program. Several approximation techniques, however, will be given in later sections.

Assuming θ_z has now been calculated for the predicted values of r at the times of the intercepts under consideration, the elevation angles α can be determined from

$$\tan \alpha = (r \cos \theta_z - R)/(r \sin \theta_z) \qquad [12]$$

Then, from a number of pairs of values of A_* and α, corresponding values of slant range S can be found by triangulation (in the cases of simultaneous intercepts from two different tracking stations); by direction only methods (5); by direction plus Doppler shift data methods (5,6) when supplemental Doppler data are available; or by two-station minimum distance methods (7). Then improved values of r can be determined from

$$r = [(R + S \sin \alpha)^2 + S^2 \cos^2 \alpha]^{1/2} \qquad [13]$$

At this point an iteration should be performed by repeatedly substituting the value of r computed in Equation [13] into Equation [9] to obtain a new θ_z, and then substituting into Equation [12], calculating S by one of the processes called out previously and determining new values of r by Equation [13]. The limiting values of α and S, along with corresponding values of A_*, would then be available for insertion into a basic prediction program.

First Approximation to the Central Zenith Distance

Substitution of the value of C into Equation [9], using the definition of index of refraction given by Equation [4], and simplification yield

$$\theta_z = R \sin \zeta_0 \int_R^r \frac{dr}{r[(\mu/\mu_0)^2 r^2 - R^2 \sin^2 \zeta_0]^{1/2}} \qquad [14]$$

For terrestrial space it is reasonable to replace (μ/μ_0) by $1 + \xi$, where ξ is a small positive number, since μ and μ_0 are nearly equal in that case. Then Equation [14] can be written approximately as

$$\theta_z = R \sin \zeta_0 \left[\int_R^r \frac{dr}{r(r^2 - R^2 \sin^2 \zeta_0)^{1/2}} - \int_R^r \frac{\xi r \, dr}{(r^2 - R^2 \sin^2 \zeta_0)^{3/2}} \right] \qquad [15]$$

neglecting powers of ξ that are higher than 1. Following Smart (2), Equation [15] can be further reduced to

$$\theta_z = \zeta_0 - \text{arc sin} \frac{R \sin \zeta_0}{r} - \frac{\sin \zeta_0}{R \cos^2 \zeta_0} \int_R^r \xi \, dr \qquad [16]$$

If the function consisting of the first two terms of $r.m.$ of Equation [16] is expanded about $\eta = 0$, where $R/r = 1 - \eta$ (with η a small positive number, and the second and higher powers of η neglected) and ξ is replaced by $[(\mu/\mu_0) - 1]$, then Equation [16] becomes

$$\theta_z = \left(1 - \frac{R}{r}\right) \tan \zeta_0 - \frac{\sin \zeta_0}{R \cos^2 \zeta_0} \int_R^r \left(\frac{\mu}{\mu_0} - 1\right) dr \qquad [17]$$

If μ is replaced in Equation [17] by $1 + k\rho$, following the "Law of Gladstone and Dale," Equation [17] becomes

$$\theta_z = \left(1 - \frac{R}{r}\right) \tan \zeta_0 - \tan \zeta_0 (1 + \tan^2 \zeta_0) \times \left[\left(\frac{1 - \mu_0}{\mu_0}\right) \left(\frac{r - R}{R}\right) + \frac{1}{R} \int_R^r k\rho dr \right] \qquad [18]$$

which has the form

$$\theta_z = A(r) \tan \zeta_0 + B(r) \tan^3 \zeta_0 \qquad [19]$$

The integral $\int_R^r \rho \, dr$ appearing in $B(r)$ can be written in closed form in the following expression for ρ

$$\rho = K(a + b/r)^{-\lambda^2} \qquad [20]$$

where a, b and λ are constants (4). The integral in question can be integrated by first making the transformation $r = 1/\nu$ and then using a reduction formula twice to get the power form

$$\int_{1/R}^{1/r} (a + b\nu)^{-\lambda^2} d\nu \qquad [21]$$

Thus, Equation [19] represents a closed form first approximation for the central zenith distance as a function of radial distance and apparent zenith distance.

Culmination Method of Central Zenith Distance Table Construction

For situations where table look-up is favored over real-time calculation, or for checks on calculations made by the method just discussed, it might be desirable to have at one's disposal a table of values of θ_z against r and ζ_0. This could be done in the following way. For an existing, well-known satellite with nearly circular orbit, determine the latitudes θ and θ' and zenith distances ζ_0 and ζ_0' of two culminations (crossings of the local hour circle) of a selected tracking station, say one north and one south. Substitute these values into the following equations

$$\theta_z \equiv L - \theta = A(r) \tan \zeta_0 + B(r) \tan^3 \zeta_0$$
$$\theta_z' \equiv L - \theta' = A(r) \tan \zeta_0' + B(r) \tan^3 \zeta_0' \qquad [22]$$

To derive these equations, see Fig. 2. The latitude of the tracking station at T is denoted by L.

Simultaneous solution of Equations [22], using the appropriate tracking station latitude, will yield $A(r)$ and $B(r)$ for the measured ζ_0, and r, θ, θ', assumed to be known accurately. Thus, a table of central zenith distances can be

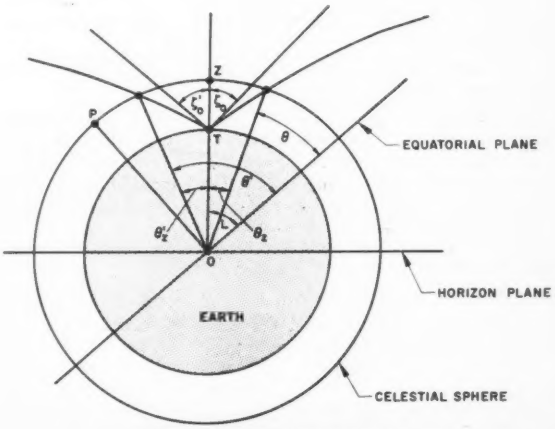

Fig. 2 Culmination geometry

constructed for various values of ζ_0, obtained from different sightings, for a particular radius vector r. Repetition of this procedure for a range of values of r would produce a complete table.

Discussion

If a tracking system provides accurate range values S, say from radar equipment, as well as accurate values of $r.a.$ and δ of an occulted celestial body, then there is an alternate to the procedure explained previously. As before, compute θ_z from Equation [9] using the *predicted* value of r. Then use S and

$$r^2 - 2Rr\cos\theta_z + R^2 - S^2 = 0 \qquad [23]$$

to determine a new r, and iterate. It might be that a tracking system approaching the ultimate in precision would use radar range and optical directional values in this manner as its basic input quantities.

Note further that the iterative process using Equation [1] for determining ζ_0 is precluded if a theodolite is used in conjunction with the camera in obtaining the star background photographs. The zenith distance ζ_0 is measured directly by the theodolite in this case.

Since Earth is nearly ellipsoidal, further accuracy might be obtained if the fundamental relation expressed by Equation [3] were to be replaced by a similar relation valid under the ellipsoidal assumption. This would require that the inertial direction numbers be transformed to ellipsoidal Earth-tracking station orientation, and that Equations [12 and 13] be replaced by equations accounting for oblateness in the geometry.

Finally it should be pointed out that, although the analysis for determining central zenith distance was done for application to refraction of light through the atmosphere, it should be equally satisfactory for refraction of any electromagnetic energy transmission through a medium homogeneous in spherical shell lamina.

References

1 "The American Ephemeris and Nautical Almanac," U. S. Gov. Printing Office, Washington, D. C., 1959.

2 Smart, W. M., "Text-book on Spherical Astronomy," Cambridge Univ. Press, N. Y., 1956, 4th ed., pp. 63, 67, 68.

3 Gray, D. E., "American Institute of Physics Handbook," McGraw-Hill Book Co., Inc., N. Y., 1957.

4 Smithsonian Institute Astrophysical Observatory, "Research in Space Science," Special Rep. no. 7, Dec. 1957, Cambridge, Mass.

5 Harris, A., Patterson, P. and Wasel, A. D., "Earth Satellite Range Determination Using Direction Plus Doppler Frequency and Direction Only Techniques," LMSD-5082, Lockheed Missiles and Space Division, Sunnyvale, Calif., 1958.

6 Wasel, A. D., "A Direct Direction-Doppler Slant-Range Determination Technique for Orbiting Space Vehicles," LMSD-48414, Lockheed Missiles and Space Division, Sunnyvale, Calif., 1959.

7 Wasel, A. D., "Orbital Elements, Trajectory Simulation, and Prediction for Earth Satellites," *J. Brit. Interplanet. Soc.* (to be published).

Iterative Solution of the *N*-Body Problem for Real Time

L. M. RAUCH[1]

General Dynamics Corp., San Diego, Calif.

THIS paper deals formally with the iterative process in the solution of the noncolliding N-body problem. The independent parameter is no longer the potent pseudo-time (3)[2] but the real time.

The process makes use of the Steffensen (4,5) coefficients. These coefficients were introduced by Steffensen for the three-body problem and extended by Cheney (1) to N bodies.

The iterative process, as formulated in the paper, has a number of features worth noting:

1 It is an alternative process in the solution of the N-body problem.

2 The sequence of iterative solutions converges rapidly to the limiting solution of the system of differential equations.

3 The process, as such, is nonrecursive, so that any successive approximation is independent of any of the preceding determinations.

4 A large digital computer (say, the IBM 704) is not necessary in the numeric determinations.

The paper is divided into three parts. The first part formulates the iterative process as applied to the system of equations of motion for the N bodies. This is followed by deductions of the explicit solutions. The concluding part gives a summary of the inputs and equations in numerization of the N-body problem.

Iterative Process

This part deals with the equations of motion of N bodies in a Newtonian potential field (6) and the transformation of these equations into iterative form.

Received Sept. 11, 1959.

[1] Senior Research Engineer, Convair (Astronautics Div.).

[2] Numbers in parentheses indicate References at end of paper.

Equations of motion

The n given quantities (M_i) are assumed to be point masses. Their position vectors x^i are given by the components x^{ih} in an inertial space. It is specified that the range for the super or subscripts is given as

$$i,j = 1,2,\ldots,n \qquad h = 1,2,3 \qquad k = 0,1,2,\ldots \qquad i \neq j \qquad [1]$$

The magnitude F_{ij} of the attractive force exerted by the mass M_j on M_i is given by

$$F_{ij} = GM_iM_j/r^{ij}$$

where r^{ij}, the square of the magnitude of the position vector between the i and j particles, is given by

$$r^{ij} = \sum_h (x^{ih} - x^{jh})^2 \qquad S^{ij} = (r^{ij})^{-3/2} \qquad [2]$$

The direction of the force vector is along the unit vector $(r^{ij})^{-1/2}(x^j - x^i)$. Thus, the total attractive force on the mass M_i is

$$\sum_j GM_iM_j(x^j - x^i)S^{ij}$$

The application of the second law of motion leads to

$$\ddot{x}^i = \sum_j GM_jS^{ij}(x^j - x^i) \qquad [3]$$

which is a set of $3n$ differential equations of the second order.

Iterative system of differential equations

To specify an iterative system of Equation [3], the following operations are performed: Express the quantities in Equation [2] and the solution x^{ih} of Equation [3] in power series

$$\dot{x}^{ih} = \sum_{k=0}^{\infty} \xi_k{}^{ih}t^k \qquad r^{ij} = \sum_{k=0}^{\infty} \rho_k{}^{ij}t^k \qquad S^{ij} = \sum_{k=0}^{\infty} \sigma_k{}^{ij}t^k \qquad [4]$$

Next, form the finite sums

$$x_\alpha{}^{ih} = \sum_{k=0}^{\alpha+\beta} \xi_k{}^{ih}t^k \qquad r^{ij}\sum_{k=0}^{\alpha+\beta} \xi_k{}^{ij}t^k \qquad S_\alpha{}^{ij} = \sum_{k=0}^{\alpha+\beta} \sigma_k{}^{ij}t^k \qquad [5]$$

where β is an arbitrary fixed integer > 0, $\alpha = 1,2,3,\ldots$.

Finally, write the approximate system of Equation [3], namely

$$\ddot{x}_\alpha{}^{ih} = \sum_j GM_jS_\alpha{}^{ij}(x_\alpha{}^{jh} - x_\alpha{}^{ih}) \qquad \alpha = 1,2,3, \ldots \quad [6]$$

The system [6] differs from [3] in the sense that the solutions x^{ih} of [3] are given by the solutions $x_\alpha{}^{ih}$ by means of a limit, namely

$$\lim_{\alpha \to \infty} x_\alpha{}^{ih} = x^{ih} \qquad [7]$$

for any i,h; $\alpha = 1,2,3, \ldots$.

The approximate system turns into an iterative one by a substitution of $(\alpha - 1)$ for α in the right member [6]. Thus, the iterative system of differential equations is defined as

$$\ddot{\bar{x}}_\alpha{}^{ih} = \sum_j GM_jS_{\alpha-1}{}^{ij}(x_{\alpha-1}{}^{jh} - x_{\alpha-1}{}^{ih}) \qquad [8]$$

where

$$\ddot{\bar{x}}_\alpha{}^{ih} = \ddot{x}_\alpha{}^{ih} + \epsilon_\alpha{}^{ih} \qquad [9]$$

The function $\epsilon_\alpha{}^{ih}$ is defined by Equation [9]. However, in (3) it is shown that

$$\lim_{\alpha \to \infty} \epsilon_\alpha{}^{ih}(t) = 0 \qquad [10]$$

for any i,h and t in a defined interval. It will be assumed in this paper that Equation [10] is valid.

Equate the right members of the two types of systems [6,8], so that

$$\sum_j M_jS_\alpha{}^{ij}(x_\alpha{}^{jh} - x_\alpha{}^{ih}) = \sum_j M_jS_{\alpha-1}{}^{ij}(x_{\alpha-1}{}^{jh} - x_{\alpha-1}{}^{ih}) + (\epsilon_\alpha{}^{ih}/G) \qquad [11]$$

The formal solution $x_\alpha{}^{ih}$ of the approximate system is found by solving Equation [11], namely

$$x_\alpha{}^{ih} = \frac{\bar{x}_{\alpha-1}{}^{ih}\sum_j M_jS_{\alpha-1}{}^{ij} + \sum_j M_j(S_\alpha{}^{ij}x_\alpha{}^{jh} - S_{\alpha-1}{}^{ij}x_{\alpha-1}{}^{jh})}{\sum_j M_jS_\alpha{}^{ij}} - \frac{\epsilon_\alpha{}^{ih}}{\sum_j GM_jS_\alpha{}^{ij}} \qquad [12]$$

Nonrecursive form of the iterative solution

We now reduce the formula [12] to a nonrecursive form. Define the following symbols

$$A_\alpha{}^i = \sum_j M_jS_\alpha{}^{ij}$$
$$C_\alpha{}^{ih} = \sum_j M_j(S_\alpha{}^{ij}x_\alpha{}^{jh} - S_{\alpha-1}{}^{ij}x_{\alpha-1}{}^{jh}) \qquad [13]$$

The symbolic form of Equation [12] is given as

$$x_\alpha{}^{ih} = \frac{\bar{x}_{\alpha-1}{}^{ih}A_{\alpha-1}{}^i + C_\alpha{}^{ih}}{A_\alpha{}^i} - \sigma_\alpha{}^{ih} \qquad [14]$$

where

$$\sigma_\alpha{}^{ih} = \epsilon_\alpha{}^{ih}/A_\alpha{}^i \qquad [15]$$

It may be shown by mathematical induction that the recursive formulas [14 and 15] may be reduced to a nonrecursive form. It is given as

$$x_\alpha{}^{ih} = \frac{A_0{}^i}{A_\alpha{}^i}x_0{}^{ih} - \frac{\sum_{q=0}^{\alpha-1}\left[C_{\alpha-q}{}^{ih}\prod_{a=1}^{\alpha-1}A_{\alpha-a}{}^i\right]}{\prod_{a=0}^{\alpha-1}A_{\alpha-a}{}^i} - \sigma_\alpha{}^{ih} \qquad \alpha = 1,2, \ldots \quad [16]$$

which may be reduced to

$$x_\alpha{}^{ih} = \frac{A_0{}^i}{A_\alpha{}^i}x_0{}^{ih} + \frac{\sum_{q=0}^{\alpha-1}C_{\alpha-q}{}^{ih}}{A_\alpha{}^i} - \sigma_\alpha{}^{ih} \qquad \sigma_\alpha{}^{ih} = \frac{\sum_{q=0}^{\alpha-1}\epsilon_{\alpha-q}{}^{ih}}{A_\alpha{}^i} \qquad [17]$$

Equation [17] is a linear relation between $x_\alpha{}^{ih}$ and $x_0{}^{ih}$ for any i,h. The quantity $\sigma_\alpha{}^{ih}$ is given in (3) as

$$\lim_{\alpha \to \infty} \sigma_\alpha{}^{ih}(t) = 0 \qquad [18]$$

for any i,h and t in a defined interval. Equation [17] is an iterative, nonrecursive approximation of the system of the equations of motion [6] provided a meaning may be attached to the initial iterative function $x_0{}^{ih}$ and if the quantities A and C are known functions. The part that follows will establish a meaning to the above mentioned quantities (x_0,A,C).

Explicit Formulation of the Iterative Solution

To explicitly formulate the iterative solution given by Equation [17], a meaning must be attached to the initial iterative function $x_0{}^{ih}$ and the functional quantities $A_\alpha{}^i$, $C_\alpha{}^{ih}$. We do so by first expressing these quantities in terms of the definitions [5] and then evaluating the coefficients in these definitions.

Expressions for the quantities in the iterative formula

By means of the first definition in Equations [5 and 13], the quantity $A_\alpha{}^i$ becomes

$$A_\alpha{}^i = \sum_j M_jS_\alpha{}^{ij} = \sum_j M_j\sum_{k=0}^{\alpha+\beta}\sigma_k{}^{ij}t^k \qquad [19]$$

The symbol $C_\alpha{}^{ih}$, because of Equations [5 and 13], becomes

$$C_\alpha{}^{ih} = \sum_j M_j[S_\alpha{}^{ij}x_\alpha{}^{jh} - S_{\alpha-1}{}^{ij}x_{\alpha-1}{}^{jh}] = \sum_j M_j\left[\sum_{k=0}^{\alpha+\beta}\sigma_k{}^{ij}t^k\sum_{l=0}^{\alpha+\beta}\xi^{jh}{}_lt^l - \sum_{k=0}^{\alpha+\beta-1}\sigma_k{}^{ij}t^k\sum_{l=0}^{\alpha+\beta-1}\xi^{jh}{}_lt^l\right]$$

$$= \sum_j M_j\left[\sigma_{\alpha+\beta}{}^{ij}t^{\alpha+\beta}\sum_{l=0}^{\alpha+\beta}(\xi^{jh}{}_lt^l + \xi_{\alpha+\beta}{}^{ih}t^{\alpha+\beta}\sum_{k=0}^{\alpha+\beta-1}\sigma_k{}^{ij}t^k + \sum_{k=0}^{\alpha+\beta-1}\sigma_k{}^{ij}t^k\sum_{l=0}^{\alpha+\beta-1}\xi_l{}^{jh}t^l - \sum_{k=0}^{\alpha+\beta-1}\sigma_k{}^{ij}t^k\sum_{l=0}^{\alpha+\beta-1}\xi_l{}^{jh}t^l\right]$$

so that

$$C_\alpha{}^{ih} = t^{\alpha+\beta}\sum_j M_j\left[\sigma_{\alpha+\beta}{}^{ij}\sum_{k=0}^{\alpha+\beta}\xi_k{}^{jh}t^k + \xi_{\alpha+\beta}{}^{ih}\sum_{k=0}^{\alpha+\beta-1}\sigma_k{}^{ij}t^k\right] \qquad [20]$$

We define the function $x_0{}^{ih}$ by the assumption that the quantity $x_\alpha{}^{ih}$ in Equation [5] is to be valid for $\alpha = 0$. Thus

$$x_0{}^{ih} = \sum_{k=0}^{\beta}\xi_k{}^{ih}t^k \qquad [21]$$

Explicit formulation of the functions A, C and x_0

To formulate the iterative expression [17], the functions of time $A_\alpha{}^i(t)$, $C_\alpha{}^{ih}(t)$ and $x_0{}^i(t)$ of Equations [19–21] must be well-defined. This implies a knowledge of the coefficients ξ, σ (and ρ) of the series [4]. Fortunately, the investigations by Steffensen (4,5) and Cheney (1) allow an immediate determination. The paper by Cheney gives the following recursion formulas

$$\rho_k{}^{ij} = \sum_h \sum_{v=0}^{k} (\xi_v{}^{ih}\xi_{k-v}^{ih} - 2\xi_v{}^{ih}\xi_{k-v}^{jh} + \xi_v{}^{jh}\xi_{k-v}^{jh}) \qquad k = 0,1,2,\ldots \quad [22]$$

$$\sigma_k{}^{ij} = -(2k\rho_0{}^{ij})^{-1}\left[\sum_{v=0}^{k-2} 2(v+1)\rho_{k-v-1}^{ij}\,\sigma_{v-1}^{ij} + \sum_{v=0}^{k-1} 3(v+1)\,\sigma_{k-v-1}^{ij}\rho_{v+1}^{ij}\right]$$

$$\sum_{v=0}^{k-2}(\ ) = 0 \qquad k = 1$$

.....[23]

$$\xi_{k+1}^{ih} = (k^2+k)^{-1}\sum_{v=0}^{k-1} GM_j\sigma_{k-v-1}^{ij}(\xi_v{}^{jh} - \xi_v{}^{ih}) \quad [24]$$

These may be reduced to the following forms

$$\rho_k{}^{ij} = \sum_h \sum_{v=0}^{k} [\xi_v{}^{ih}(\xi_{k-v}^{ih} - \xi_{k-v}^{jh}) + \xi_{k-v}^{jh}(\xi_v{}^{jh} - \xi_v{}^{ih})]$$

$$= \sum_k \sum_{v=0}^{k} [\xi_v{}^{ih}(\xi_{k-v}^{ih} - \xi_{k-v}^{jh}) + \xi_{k-v}^{jh}(\xi_v{}^{jh} - \xi_v{}^{ih})]$$

so that

$$\rho_k{}^{ij} = \sum_k \sum_{v=0}^{k} (\xi_v{}^{ih} - \xi_v{}^{jh})(\xi_{k-v}^{ih} - \xi_{k-v}^{jh})$$

$$\sigma_k{}^{ij} = -(2k\rho_0{}^{ij})^{-1}\left[\sum_{v=0}^{k-2} 2(k-v-1)\sigma_{k-v-1}^{ij}\rho_{v-1}^{ij} + \sum_{v=0}^{k-2} 3(v+1)\sigma_{k-v-1}^{ij}\rho_{v+1}^{ij} + 3k\,\sigma_0{}^{ij}\rho_k{}^{ij}\right]$$

.....[25]

so that

$$\sigma_k{}^{ij} = -(2k\rho_0{}^{ij})^{-1}\left[\sum_{v=0}^{k-2}(2k+v+1)\sigma_{k-v-1}^{ij}\rho_{v+1}^{ij} + 3k\sigma_0{}^{ij}\rho_k{}^{ij}\right]$$

$$\sum_{v=0}^{k-2}(\ ) = 0 \qquad k = 1$$

.....[26]

$$\xi_{k+1}^{ih} = (k^2+k)^{-1}\sum_{v=0}^{k-1} GM_j\sigma_{k-v-1}^{ij}(\xi_v{}^{jh} - \xi_v{}^{ih}) \quad [27]$$

Slight consideration of the above three recursion formulas indicates that the evaluation of ρ and σ and so ξ depends on a priori knowledge of $\xi_0{}^{ih}$ and $\xi_1{}^{ih}$. But these 6 n quantities specify the initial position and velocity of each of the n masses.

With this information given ($\xi_0{}^{ih}$, $\xi_1{}^{ih}$), the value of $\rho_0{}^{ij}$ is computed from Equation [25], namely

$$\rho_0{}^{ij} = \sum_h (\xi_0{}^{ih} - \xi_0{}^{jh})^2 \quad [28]$$

The quantity

$$\sigma_0{}^{ij} = (\rho_0{}^{ij})^{-3/2} \quad [29]$$

is found from Equations [2 and 4] for $t = 0$. Subsequently the formulas [25–27] are used cyclically with $k = 1,2,\ldots,$ consecutively, to determine the three sets of quantities $(\rho_k{}^{ij}, \sigma_k{}^{ij}, \xi_{k+1}^{ih})$.

Summary of the Method

The existence theorem for the iterative solution [17] of the system of Equations [3] is given in (3). We restate it in the following form:

Theorem: The equality

$$\lim_{\alpha\to\infty} x_\alpha{}^{ih}(t) = x^{ih}(t)$$

holds for any i,h and t in a defined region R where

$x_\alpha{}^{ih}$ = iterative solution for any $\alpha = 1, 2, \ldots$ and given by Equation [17]

$\lim_{\alpha\to\infty} \sigma_\alpha{}^{ih} = 0$

$x^{ih}(t)$ = set of solutions for the given system

The region R (or interval for real t) is defined, briefly, as the open circular subregion in the t plane, whose boundary includes that singularity whose modulus has the least value of every singular point (2) given in the right-hand member of Equation [3].

The procedure in the determination of any one set of iterative solutions is then as follows:

1 Choose any reasonable value in the sequence $\alpha = 1,2,3,\ldots$ for formula [17].

2 Choose any value for $\beta > 0$. A too large value for β would imply the determination of more coefficients from the formulas [25–27], since the initial function $x_0{}^{ih}$ is specified by

$$x_0{}^{ih}(t) = \sum_{k=0}^{\beta} \xi_k{}^{ih}t^k$$

3 Find the values for the sets $(\rho_1{}^{ij}, \sigma_1{}^{ij}, \xi_2{}^{ih}), \ldots, (\rho_{\alpha+\beta-1}^{ij}, \sigma_{\alpha+\beta-1}^{ij}, \xi_{\alpha+\beta})$ from the recursion formulas [25–27].

4 The quantities $\xi_0{}^{ih}$, $\xi_1{}^{ih}$ (which determine all subsequent coefficients) are the arbitrary constants determined by the initial conditions $x^{ih}(0)$, $\dot{x}^{ih}(0)$ and found by the equalities

$$x^{ih}(t) = \sum_{k=0}^{\infty} \xi_k{}^{ih}t^k \qquad \dot{x}^{ih}(t) = \sum_{k=1}^{\infty} k\xi_k{}^{ih}t^{k-1}$$

for $t = 0$, namely

$$\xi_0{}^{ih} = x^{ih}(0) \qquad \xi_1{}^{ih} = \dot{x}^{ih}(0)$$

5 Substitute the coefficients computed in step 3 into the formulas [19–21].

6 The values thus found are then incorporated into Equation [17] with the understanding that $\sigma_\alpha{}^{ih}(t) \to 0$, $\alpha \to \infty$.

References

1 Cheney, W., "Power Series for the N-Body Problem," Mathematical Pre-Prints, no. 16, Nov. 1958, Convair-Astronautics, San Diego, Calif.

2 Knopp, K., "Theory of Functions," Part I, Dover Publications, N. Y., 1945.

3 Rauch, L. M. and Riddell, W. C., "The Iterative Solution of the Analytic N-Body Problem," Applied Math. Series, no. 20, May 1959, Convair-Astronautics, San Diego, Calif.

4 Steffensen, J. F., "On the Restricted Problem of Three Bodies," *Mat. Fys. Medd. Dan. Vid. Selks.*, vol. 30, no. 18, 1956.

5 Steffensen, J. F., "On the Problem of Three Bodies in the Plane," *Mat. Fys. Medd. Dan. Vid. Selks.*, vol. 31, no. 3, 1957.

6 Whittaker, E. T., "Analytical Dynamics," Cambridge University Press, N. Y., 1927.

Mass Considerations in Ring Supported Solar Sails

W. E. JAHSMAN[1]

Lockheed Aircraft Corp., Palo Alto, Calif.

IN A RECENT article (1),[2] Tsu has described how a solar sail may be used for interplanetary travel. He has discussed the several advantages of this device: Mass ratio of unity; no fuel, propellant or propulsive powerplant required; and no waste-heat disposal problem. He has also mentioned certain problem areas in solar sail design: Need for a sail material with low mass per unit area and high reflectivity; fabrication, handling and packaging techniques for the sail; and in-flight maneuvering and control. The purpose of this note is to point out another equally important problem when a ring is used to support the sail: The contribution of the ring mass to the overall system mass.

The necessity of a supporting ring is obvious; without one, the sail becomes a parachute, and the requirement of low sail mass per unit area (for a given thrust) is not satisfied. Maneuvering and control problems also become much more serious. On the other hand, the ring dimensions must be chosen so that strength and/or stability limitations are not exceeded. The following equations of motion for the sail oriented normal to the sun's rays are formulated with these considerations in mind. (Tsu's nomenclature is used wherever possible.)

$$p_0 \pi a^2 f(\gamma) - 2\pi a P \sin\gamma = m_s \alpha \qquad [1]$$

$$2\pi a P \sin\gamma - nT\cos\delta = m_r \alpha \qquad [2]$$

$$nT\cos\delta = m_p \alpha \qquad [3]$$

$$m_s = \rho_s \pi a^2 t_s g(\gamma) \qquad [4]$$

$$m_r = \rho_r 2\pi a h^2 \qquad [5a]$$

$$P\cos\gamma + \frac{nT\sin\delta}{2\pi a} \leqq \begin{cases} \dfrac{E_r h}{4}\left(\dfrac{h}{a}\right)^3 \text{ [stability limit, see (2)]} \\ \sigma_{\text{all},r}\, h\left(\dfrac{h}{a}\right) \text{ (strength limit)} \end{cases} \qquad [6a]$$

$$P \leqq \sigma_{\text{all},s}\, t_s \qquad [7]$$

The reader is referred to Fig. 1 and the Nomenclature for a description of the symbols.

If one is interested in optimization of one of the variables, say α, expressions [1 to 7] may be combined to a single relation between α and a, δ and γ. (The payload mass m_p and the physical and material properties ρ, E and σ_{all} are taken to be fixed parameters.) Maximum acceleration within specified ranges of a, δ and γ may then be found. Here, however, it will be sufficient to consider an example given by Tsu to demonstrate the effect of the ring. First it should be noted that to obtain a lower bound on the ring mass, only expressions [2, 3, 6a and 5a] need be studied. Adding Equations [2 and 3] gives

$$P = \frac{(m_r + m_p)\alpha}{2\pi a \sin\gamma} \qquad [8]$$

If δ is sufficiently small, the second term on the left-hand side of expression [6a] may be neglected with respect to the first. This restriction is equivalent to lengthening the shroud lines, which is permissible as long as the assumption of massless shroud lines can be satisfied. Then, by substituting for P in expression [6a] from Equation [8], one obtains a relation for the ring depth[3] h

$$h^4 > \frac{2a^2(m_r + m_p)\alpha\cot\gamma}{\pi E_r} \qquad [9]$$

Finally, an expression for m_r the ring mass is found by substituting for h in Equation [5a] from expression [9]

$$m_r > 2\pi\rho_r a^2 \sqrt{\frac{2(m_r + m_p)\alpha\cot\gamma}{\pi E_r}} \qquad [10a]$$

Expression [10a] shows that high modulus, low density ring material will reduce the ring mass requirements; hence, beryllium ($E_r = 45 \times 10^6$ psi $= 3.1 \times 10^{12}$ dynes/cm^2 and $\rho = 1.85$ gm/cm^3) is chosen in this example. Also, since γ should be kept small from sail mass considerations, cot γ is taken as 10 ($\gamma \simeq 5.8$ deg). Other data supplied by Tsu are[4]

$$\begin{aligned} \rho_s &= 1.18 \text{ gm/cm}^3 \\ a &= 2.5 \times 10^4 \text{ cm} \\ \alpha &= 0.2 \text{ cm/sec}^2 \\ t_s &= 1.72 \times 10^{-4} \text{ cm} \\ m_s &= 4 \times 10^5 \text{ gm} \\ m_r + m_p &= 5 \times 10^5 \text{ gm} \end{aligned}$$

Substituting the appropriate values into expression [10a] gives $m_r > 33.5 \times 10^5$ gm, an impossible result since $m_r < m_r + m_p = 5 \times 10^5$ gm. Referring to expression [10a], we see that in order to get a physically meaningful answer, we must relax the requirement on γ (allowing the sail to become more

Received Oct. 26, 1959.

[1] Research Scientist, Missiles and Space Division.

[2] Numbers in parentheses indicate References at end of paper.

[3] The stability limitation will undoubtedly govern in most structures of this type. Dimensions and loads which are obtained using this criterion may subsequently be substituted into the latter of expressions [6a] for the ring and expression [7] for the sail, to check that strength limitations are not exceeded.

[4] It should be pointed out that depositing a "few microns" ($1\mu = 10^{-4}$ cm) of aluminum on a plastic base to achieve high reflectivity more than doubles the sail thickness (hence, mass) in this example. Development of a highly reflective plastic is clearly desirable.

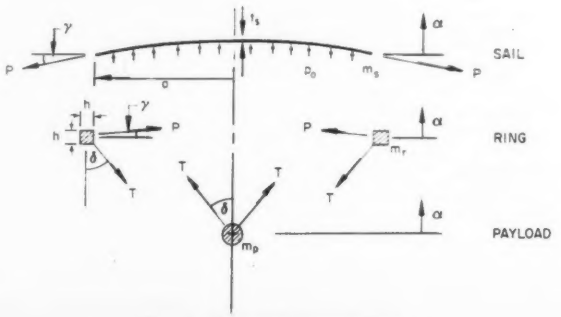

Fig. 1 Solar sail components

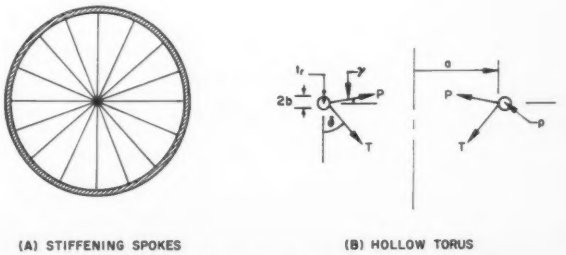

Fig. 2 Methods for reducing supporting ring mass

parachute shaped and thereby increasing the sail mass), or reduce α (thereby accepting a considerably smaller acceleration).

Two methods of reducing the ring mass come immediately to mind—adding spokes and replacing the solid ring by a hollow torus. These two methods are illustrated in Fig. 2.

The effect of the number of equally spaced spokes i is to introduce a factor of $(i^2 - 1)/3$ to the denominator of expression [10a]. For the ring illustrated in Fig. 2, i is 16 and m_r is greater than 3.6×10^5 gm. Thus the use of spokes will certainly aid in reducing the ring mass; however, as i becomes large, the spoke mass will become significant.

A much greater reduction of ring mass can be achieved by replacing the ring with a solid cross section by a hollow torus. If the torus wall is sufficiently thin, pressurization may be necessary to maintain circularity of the cross section. Then the ring mass is given by

$$m_r' = 4\pi^2\rho_r' abt_r + 2\pi^2\rho_g ab^2 \qquad [5b]$$

(see Fig. 2b). Furthermore, by assuming that torus strength is determined either by stability or by noncompressive wall stress conditions, we can replace expression [6a] by

$$P\cos\gamma + \frac{nT\sin\delta}{2\pi a} \leqq \begin{cases} 3\pi E_r' t_r \left(\dfrac{b}{a}\right)^3 \\ \dfrac{\pi p b^2}{a} \end{cases} \qquad [6b]$$

Combining [2, 3, 5b and 6b] as before provides an expression for m_r'

$$m_r' > 4\pi^2\rho_r' a t_r \left[\frac{a^2(m_r' + m_p)\alpha\cot\gamma}{6\pi^2 E_r' t_r}\right]^{1/3} + 2\pi^2\rho_g a\left[\frac{a^2(m_r' + m_p)\alpha\cot\gamma}{6\pi^2 E_r' t_r}\right]^{2/3} \qquad [10b]$$

In this calculation, the torus is assumed to be fabricated from plastic film. From a practical standpoint, this design has the advantages that it may be packaged during ferrying and easily erected by inflation in orbit. In addition subsequent calculations will show that there is relatively little improvement in mass reduction by using beryllium. Hence, when the ring material and thickness are the same as those of the sail, it is found that $m_r' > 5 \times 10^3$ gm when $E_r' = 5 \times 10^6$ psi $= 3.45 \times 10^{10}$ dynes/cm^2. The mass of gas and ring material (first and second terms on the right-hand side of expression [10b]) are about equal because of the large gas volume. The density of the gas (air) was found using the perfect gas law with a temperature of 100 F and a pressure governed by $\sigma'_{all,r}$, the allowable stress in the torus wall

$$pb/t_r \leqq \sigma'_{all,r} \qquad [11]$$

In this example, $\sigma'_{all,r}$ was taken to be 2500 psi $= 1.72 \times 10^8$ dynes/cm^2.

The value 5×10^3 gm is only 1 per cent of the ring and payload mass. If beryllium is used, this figure is reduced to about 0.33 per cent. Thus, the ring mass can be made a very small fraction of the solar sail system mass if a hollow, pressurized torus design is used. On the other hand, the problem of micrometeorite puncture and subsequent loss of stiffness cannot be accurately solved until more precise data on distribution of matter in space is obtained. Furthermore, the exact theory of pressurized membranes has not yet been developed; expression [6b], which is a rough approximation at best, may be superseded later on by more exact formulas. Hence, there is still considerable work to be done in the design of solar sails before they can ever be considered as a feasible means of interplanetary travel.

Nomenclature

E	=	Young's modulus
P	=	stress resultant at the edge of the sail
T	=	tension in the shroud lines
a	=	radius of the sail (and ring)
b	=	radius of the torus cross section
$f(\gamma)$	=	function representing dependence on γ of total thrust due to radiation
$g(\gamma)$	=	function representing dependence of sail mass on γ
h	=	width and depth of ring cross section
i	=	number of stiffening spokes
m	=	mass
n	=	number of shroud lines
p	=	internal pressure in torus
p_0	=	radiation pressure
t	=	ring or torus wall thickness
α	=	acceleration of solar sail system
δ	=	shroud line angle
γ	=	sail edge angle
ν	=	Poisson's ratio
ρ	=	mass density
σ_{all}	=	allowable stress

Subscripts

p	=	payload
r	=	ring (or torus)
s	=	sail
$'$	=	refers to torus

References

1 Tsu, T. C., "Interplanetary Travel by Solar Sail," ARS JOURNAL, vol. 29, no. 6, June 1959, pp. 422–427.

2 Timoshenko, S., "Strength of Materials, Vol. 2," Van Nostrand Co., Inc., N. Y., 2nd ed., p. 216.

Prandtl-Meyer Expansion in Equilibrium Air[1]

HAIM KENNET[2]

Massachusetts Institute of Technology, Cambridge, Mass.

PRANDTL-MEYER flow for air in dissociative equilibrium is encountered in both external and internal fluid dynamics, particularly in hypersonic flow and rocket engine nozzle flow. The problem has been considered by many authors, e.g., Feldman (1),[3] Heims (2), Hayes and Probstein (3), and the solution usually advocated is a numerical integration of the appropriate relations along an isentrope. It is intended to show here that by making use of some simple approximations, which are valid for equilibrium air in hypersonic flow, a closed form expression can be obtained relating the pressure p to the angle of turn θ.

The basic equation for Prandtl-Meyer flow can be obtained by combining the momentum and global continuity equations which, for an inviscid gas, do not show explicitly that the gas is in a dissociated state. Hence, the well-known relation

$$\frac{dq}{q} = -\frac{d\theta}{\sqrt{M^2 - 1}} \qquad [1]$$

is still valid. Making use of the energy equation, which relates the velocity q to the enthalpy h of the gas, namely

$$\frac{q^2}{2} + h = \frac{U_\infty^2}{2} + h_\infty = h_t \qquad [2]$$

Received Oct. 26, 1959.

[1] This investigation was supported by the Office of Scientific Research, USAF, under Contract AF49(638)-160.

[2] Research Assistant, Department of Aeronautics and Astronautics.

[3] Numbers in parentheses indicate References at end of paper.

where h_t is the stagnation enthalpy, and the hypersonic approximation, valid for large Mach number M

$$\sqrt{M^2 - 1} \cong M = q/a \qquad [3]$$

an expression relating the angle of turn to the enthalpy of the gas and its speed of sound a is found

$$\int_{\theta_1=0}^{\theta} d\theta = 0.8454 \int_{h_1^*}^{h^*} \frac{dh^*}{a^* \sqrt{2(h_t^* - h^*)}} \qquad [4]$$

Dimensionless flow variables are introduced at this point to conform to Feldman's Mollier chart notation. These dimensionless quantities

$$h^* = \frac{h}{h_0} \qquad a^* = \frac{a}{a_0} \qquad p^* = \frac{p}{p_0} \qquad s^* = \frac{s}{s_0} \qquad [5]$$

are given in terms of the following reference quantities

$$\begin{aligned} h_0 &= RT_0 = 84.75 \times 10^4 \text{ ft}^2/\text{sec}^2 \\ a_0 &= 1089 \text{ fps} \\ p_0 &= 1 \text{ atm} \\ s_0 &= R = 6.886 \times 10^{-2} \text{ Btu/lb R} \end{aligned}$$

The constant in front of the integral sign in Equation [4] is merely the result of this particular choice of the reference quantities

$$\sqrt{RT_0}/a_0 = 0.8454 \qquad [6]$$

For constant entropy $s^* = s/R$ the Mollier chart shows that h^* and a^* vary linearly with $\log_{10} p^*$, provided p^* does not vary by more than one order of magnitude. For larger variations in p^*, the relation between a^*, h^* and $\log_{10} p^*$ is piecewise linear. The following analysis is nevertheless applicable. Consequently

$$\begin{aligned} h^* &= a_1 + a_2 \log_{10} p^* \\ a^* &= b_1 + b_2 \log_{10} p^* \end{aligned} \qquad [7]$$

where a_1, a_2, b_1, b_2 are entropy dependent constants to be determined from the Mollier chart. When Equations [7] are substituted into Equation [4], integration and further manipulations yield

$$p^* = Ae^{-B \cdot \tanh^2(C + D\theta)} \qquad [8]$$

Here

$$\begin{aligned} A &= 10^{(h_t^* - a_1)/a_2} \\ B &= \left[\left(\frac{b_1}{b_2}\right) - \left(\frac{h_t^* - a_1}{a_2}\right)\right] \ln 10 \\ C &= \tanh^{-1} \sqrt{\left(\frac{1}{1 + \frac{b_1}{b^2}\left(\frac{h_t^* - a_1}{a_2}\right)}\right) - \left(\frac{\log_{10} p^*}{\frac{h_t^* - a_1}{a_2} + \frac{b_1}{b_2}}\right)} \\ D &= \frac{b_2}{1.6908 a_2} \sqrt{h_t^* - 2a_1 + 2a_2(b_1/b_2)} \end{aligned} \qquad [9]$$

To demonstrate the effects of large amounts of dissociation, an expansion along a geodesic on the surface of a nonlifting circular ogive, with a cone angle $\theta_v = 37$ deg, flying at $M_\infty = 20$ at an altitude of 130,000 ft has been calculated with and without dissociation. At 130,000 ft

$$\begin{aligned} p_\infty &= 3.5 \times 10^{-3} \text{ atm} \\ a_\infty &= 1.1 \times 10^3 \text{ fps} \\ h_\infty/RT_0 &= 3.5 \\ T_\infty &= 273.16\text{K} \end{aligned}$$

The conical shock relations for inviscid flow were taken from (4), whereas those for dissociated air were taken from Romig (5). For this particular case the entropy behind the shock for the dissociated stream is $s_2^* = 39$. Hence, from the Mollier chart

$$\begin{aligned} a_1 &= 123.707 \\ a_2 &= 43.103 \\ b_1 &= 4.282 \\ b_2 &= 0.877 \end{aligned}$$

For an expansion of $\theta_2 = -10$ deg, the result for the pressure is: With dissociation, $p_2 = 0.193$ atm, without dissociation, $p_2 = 0.371$ atm.

References

1 Feldman, S., "Hypersonic Gas Dynamic Charts for Equilibrium Air," Avco Research Laboratory, Everett, Mass., Jan. 1957.

2 Heims, S. P., "Prandtl-Meyer Expansion of Chemically Reacting Gases in Local Chemical and Thermodynamic Equilibrium," NACA TN 4230, March 1958.

3 Hayes, W. D. and Probstein, R. F., "Hypersonic Flow Theory," Academic Press, N. Y., 1959.

4 Ames Research Staff, "Equations Tables and Charts for Compressible Flow," NACA TR 1135.

5 Romig, M. F., "Conical Flow Parameters for Air in Dissociation Equilibrium: Final Results," Convair Scientific Research Laboratory Research Note 14, San Diego, Calif., Jan. 1958.

Convection in a Fluid at Supercritical Pressures

J. D. GRIFFITH[1] and R. H. SABERSKY[2]

California Institute of Technology, Pasadena, Calif.

HEAT transfer to fluids near their critical point is becoming increasingly important in connection with such applications as the cooling of rocket motors with hydrocarbon fuels or the heating of water in high pressure boilers. Several theoretical and experimental papers have been published on this subject, e.g. (1–4).[3] The principal characteristic of a fluid near its critical point is the strong effect of temperature and pressure on the density, specific heat and viscosity. By taking this variation in properties into account, the heat transfer rates for several fluids and in a fairly wide range near the critical point have been predicted successfully. For some fluids, however, very large increases in heat transfer coefficient have been observed which cannot be explained on the basis of property variations (2). It has been suggested that these increases might be caused by the formation and collapse of low density, bubble-like aggregates near the heating surface (2,4). These aggregates, although consisting of the same phase as the surrounding fluid, are believed to behave in a manner very similar to vapor bubbles. The improvement in convection is therefore attributed to the agitation caused by the motion of the aggregates.

The purpose of the present set of experiments was to visually observe the fluid motion in the neighborhood of the heating

Received Oct. 20, 1959.

[1] Graduate Student.

[2] Associate Professor of Mechanical Engineering. Member ARS.

[3] Numbers in parentheses indicate References at end of paper.

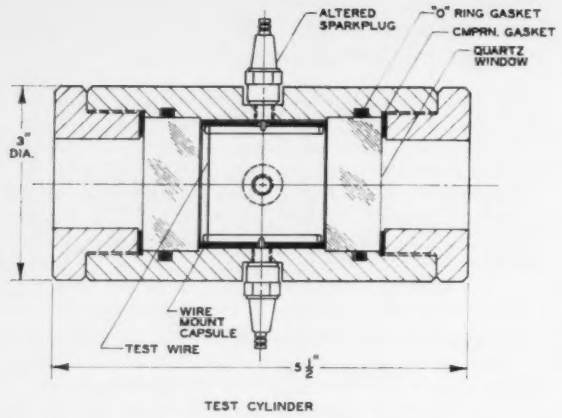

Fig. 1 Sketch of test cylinder

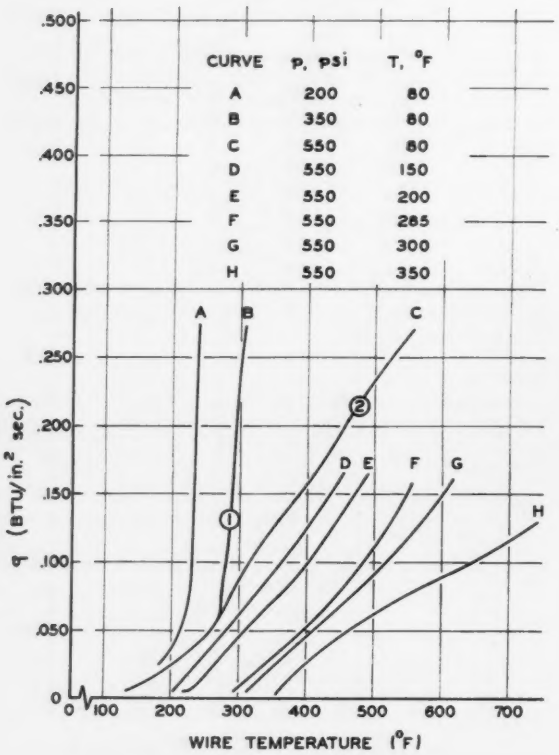

Fig. 2 Heat transfer rate vs. wire temperature for various fluid pressures and bulk temperatures

surface, to determine if any bubble-like motion can be detected, and if so, to relate this motion to any sharp increases in the heat transfer rate.

Test Equipment

An electrically heated wire was selected as the heating surface. The wire was made part of a Wheatstone bridge. Changes in resistance of the wire were measured by the unbalance of the bridge. From this unbalance the wire temperature was then computed. The test wire was enclosed in a heavy steel cylinder, the ends of which were provided with thick quartz windows. A schematic sketch of the cylinder is shown in Fig. 1. The cylinder was filled with the test fluid and the fluid was pressurized by means of a high pressure nitrogen system. The wire and surrounding region were illuminated by a Schlieren system. The motion of the fluid could be observed on the ground glass of a camera and photographs of the flow picture could be taken.

Experimental Results

For the present experiments Freon 114A was used as a test fluid. It was selected mainly because of its relatively low critical pressure ($p_{cr} \approx 478$ psia) and temperature ($T_{cr} \approx 294$ F). The wire temperature was then measured as a function of the heat transfer rate for several values of pressure, both below and above the critical pressure. Photographs were taken at most of the points at which measurements were made.

The results are summarized in a graph (Fig. 2), showing the heat transfer rate as a function of the wire temperature for various fluid pressures. The first two curves, labeled A and B, were taken at pressures below the critical. These curves show the characteristic rapid rise in heat transfer rate with wall temperature, which coincides with the onset of nucleate boiling. The corresponding photographs clearly show bubbles. One of these, which was taken at the point marked "1" in Fig. 2, is shown in Fig. 3. The data for curves C through H were taken at supercritical pressure. An examination of the photographs corresponding to these curves as well as visual observation in this region, did show bubble-like activity in some instances, as had been hypothesized. This phenomenon was observed principally at relatively high temperature differences, the conditions indicated by point 2 in Fig. 2 being typical. A photograph taken at this point is reproduced in

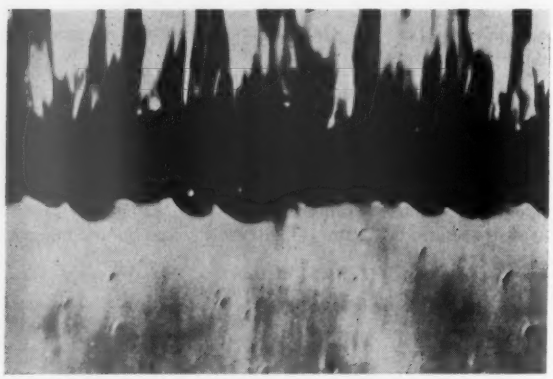

Fig. 3 Bubble formation in the nucleate boiling range at a pressure of 350 psi and a bulk temperature of 80F

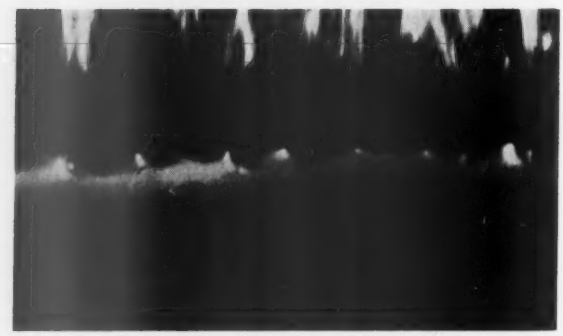

Fig. 4 Bubble formation in the supercritical range at a pressure of 550 psi and a bulk temperature of 80F

Fig. 4. However, the bubble-like activity that was observed did not result in any observable change in the slope of the heat transfer curve. The activity was apparently not sufficiently large to overshadow the effects of the normal convection. Nevertheless the observations do support the view that bubble-like activity might exist at supercritical pressures.

Conclusion

In the foregoing a simple experiment has been described for the study of free convective flow patterns in a fluid at pressures beyond the critical. The visual results give some indication that bubble-like aggregates may form under these conditions. For the particular fluid and under the prevailing test conditions, the bubble-like motion did not lead to any abrupt increase in the heat transfer rate as is observed in nucleate boiling. However, this result should not be interpreted to mean that such activity may not significantly contribute to heat convection in a different fluid or under different conditions of test.

It is planned to continue the experiments and to include several other test fluids.

References

1 Doughty, D. L. and Drake, R. M., "Free Convection Heat Transfer from a Horizontal Right Circular Cylinder to Freon 12 Near the Critical State," Trans., ASME, vol. 78, 1956, p. 1843.

2 Dickinson, N. L. and Welch, C. P., "Heat Transfer to Supercritical Water," Trans., ASME, vol. 80, April 1958, p. 746.

3 Bringer, R. P. and Smith, J. M., "Heat Transfer in the Critical Region," *J. AIChE*, vol. 3,1957, p. 148.

4 Goldmann, K., "Heat Transfer to Supercritical Water and Other Fluids with Temperature Dependent Properties," AIChE-Chem. Eng. Progress Symposium Series, no. 11, 1954.

New Patents

George F. McLaughlin, *Contributor*

Auxiliary carriage for a missile (2,899,898). W. H. Goss, Silver Spring, Md., assignor to the U. S. Navy.

Carriage comprising a number of auxiliary rockets secured to each other at their forward ends. A thrust plate secures them at their rear ends and orbits the rear end of the missile.

Stiffener and stabilizer for supersonic vehicles (2,899,899). J. Hirsch, Pacific Palisades, Calif.

First and second fins mounted on one of the two missile elements affixed together. A third fin mounted on the other element is disposed midway between the first and second fins. Shock waves of equal magnitude are produced between the first and second fins when the spaces between fins are identical, and of unequal magnitude when they are not identical; in this case a restoring force to equalize the spaces is provided.

Roll control (2,911,912). A. E. Wetherbee Jr., Newington, Conn., assignor to the United Aircraft Corp.

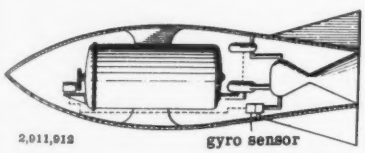

Paddle-like member with flat surfaces immersed in liquid fuel in a flight vehicle. Power means moves the paddles and opposes rolling motion about the longitudinal axis.

Duct appendix balloon (2,900,147). W. F. Huch, E. P. Ney and J. R. Winckler, St. Paul, Minn., assignors to the U. S. Navy.

Free high altitude plastic balloon with an opening on top. An outside duct extends throughout the length of the envelope. In flight, gas will escape from the duct bottom when gas in the envelope tends to be superpressured at a level below that of the duct bottom. The distance of the lower end of the duct from the bottom of the envelope is predetermined to thereby predetermine the desired ceiling altitude of the balloon.

Combined ramjet and rocket engine (2,912,820). Q. R. Whitmore, Wayne, Nebr., assignor to the U. S. Navy.

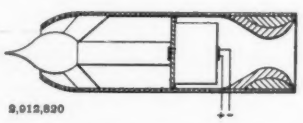

Engine casing with rocket fuel burning means upstream of the discharge nozzle. A partition separating the chamber into two parts is destructible by the heat generated by the burning of the rocket fuel, thereby connecting the chambers. The engine then functions as a ramjet.

Ejection seat catapult (2,900,150). G. E. Hirt and E. A. Martino, East Haven, Conn., assignors to Talco Engineering Co., Inc.

Emergency escape rocket device attached to the seat of an aircraft. Upon initiating a charge into the chamber, the rocket releases a propulsive charge, ejecting the seat and occupant from the aircraft.

Rocket fuel and fuel additive (2,900,788). R. S. Felberg and J. R. Gould (Member ARS), Morristown, N. J., assignors to Thiokol Chemical Corp.

Hypergolic propellant formed by mixing methylamino, butadiene and nonhypergolic jet-type hydrocarbon fuel, contacting the propellant with an equal volume of fuming nitric acid.

Rocket launcher (2,900,874). W. W. Tjossem, Burbank, Calif., assignor to Lockheed Aircraft Corp.

Cylindrical turrets containing rocket tubes. Under sides of cylinders are flattened to correspond with the contour of the aircraft body in which the turrets are mounted. Rotating the turrets successively projects the rockets beyond the aircraft surface.

Bridge circuit for position measuring device (2,902,765). W. T. Chater, El Segundo, Calif., assignor to Hughes Aircraft Co.

Incremental displacement detecting system including a grooved scale of magnetic material, an electromagnetic detector head, and a T-Bridge impedance network controlling a circuit. A detector head core is disposed in flux linkage with the scale, forming a variable reluctance magnetic circuit with the scale.

Container for separate storage of liquid propellants (2,902,822). J. D. McKiernan (Member ARS), Brooklyn, N. Y., assignor to the U. S. Navy.

Bipropellant rocket with a partition having gas ports covered by burst disks adjacent the gas producing means. The partition and casing form a propellant storage space, and a tubular member forms a second storage chamber for a different propellant.

Solar tracking system (2,913,583). N. J. Regnier and M. R. Shaffer, N. Hollywood, Calif., assignors to Hoffman Electronics Corp.

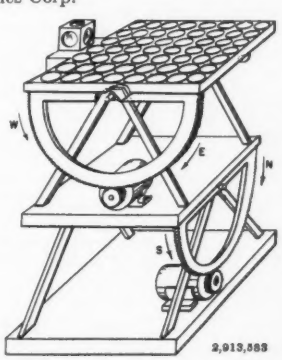

Electrically intercoupled solar cells mounted on a support permitting the cells to be tilted. Cells are coupled across relay windings controlling batteries powering motors geared to tilt the support.

EDITOR'S NOTE: Patents listed above were selected from the Official Gazette of the U. S. Patent Office. Printed copies of patents may be obtained from the Commissioner of Patents, Washington 25, D. C., at a cost of 25 cents each; design patents, 10 cents.

Electronic monitors for thrust chamber pressure (2,902,824). W. A. Sponzilli, Cincinnati, Ohio, assignor to the U. S. Air Force.

Apparatus for monitoring transient pressure in a reaction motor. Means responsive to pressure consisting of upper and lower limit electrical bridge circuits containing variable resistances responsive to chamber pressure. Motor controls connected to the bridge balance detecting means actuate when either circuit is in balance.

Pulse jet (2,903,850). T. G. Lang, Los Angeles, Calif.

Underwater propulsion device consisting of a variable volume chamber adapted to intermittently receive ambient water. Gas flows from a gas chamber into the water, forcing the water out from the chamber.

Jet deflector (2,903,851). W. A. Fiedler, Woodland Hills, Calif., assignor to the U. S. Navy.

Thrust deflector for a supersonic flow nozzle having the inner portion of a wedge within the nozzle terminating in a sharp leading edge, to produce an attached shock wave.

Sighting instrument (2,903,940). J. P. Hadjilias, Athens, Greece.

Prism assembly with two optical prisms, each adapted to reflect rays inwardly. Rays are directed toward an indicator line along which spaced images of an object, sighted through the prisms, appear. Means for determining the angular position of the prism relatively to a reference system.

Means for prolonging balloon flight (2,904,285). W. F. Huch, St. Paul, Minn., assignor to U. S. Navy.

High altitude balloon system having a predetermined ceiling altitude. The inextensible film envelope has slight permeability and loss of lift at a predetermined rate. The envelope carries a container of nongaseous highly evaporative substance which compensates for the normal loss of lift.

Radiant energy converter (2,904,612). N. J. Regnier, Los Angeles, Calif., assignor to Hoffman Electronics Corp.

Converter cells disposed across one face of a planar base in a uniform pattern, having active faces parallel to the base, and directed away from the base in a common direction. Annular reflectors encircle each cell to reflect radiation onto active parts of cells.

Large area solar energy converter (2,904,613). M. E. Paradise, Highland Park, Ill., assignor to Hoffman Electronics Corp.

Semiconductor particles electrically insulated from each other, each having two regions, one having one direction, and the other a second direction. A conductive plate is located between the first regions, and electrical connections are made between the second regions.

Fuel and rapid ignition apparatus for ramjets and rockets (2,906,094). G. H. Damon and J. Ribovich, McKeesport, Pa.

Combustion unit containing a fuel mass with side walls conforming to the casing interior, a coating of heat producing materials on an igniter duct, and a device initiating ignition of the coating.

Jet propelled aircraft with tiltable combustion chambers (2,912,188). D. E. Singelmann and J. R. Hall, Kenmore, N. Y., assignors to Bell Aircraft Corp.

Primary and auxiliary combustion chambers terminating in thrust nozzles. The primary chamber located slightly forward of the pitch axis and the auxiliary chamber at the aft end of the body. Chambers are mounted on pivots to vector between horizontal and vertical directions.

Jet propelled aircraft with jet flaps (2,912,189). R. Pouit, Asnieres, France.

Pair of jet engines mounted on a wing. Trailing edge nozzles are located along a substantial portion of the trailing edge. A conduit leads from one engine to the other to feed compressed air to a jet nozzle on the opposite side of the aircraft if one powerplant fails.

Ear protector (2,910,980). R. D. Stewart, Midland, Mich., assignor to the Dow Chemical Co.

Organopolysiloxane rubber protector conforming precisely to the surface of the outer ear and covering the mouth of the auditory canal.

Book Reviews

Ali Bulent Cambel, Northwestern University, *Associate Editor*

Vistas in Astronautics, Vol. II, by Morton Alperin and H. F. Gregory, Pergamon Press, New York, 1959, x + 318 pp. $15.00.

Reviewed by RAYMOND L. CHUAN
University of Southern California

The proceedings of the Second Annual Astronautics Symposium are presented in this volume. The scope is necessarily very wide; it ranges from observational astronomy to design studies in plasma propulsion, from measured data on micrometeorite impacts on an artificial satellite to philosophizing on the justification for it all. From the mundane to the exotic, from science to fiction, the preliminary and uncoordinated efforts made by this country in the second year of the Space Era are reported in five parts: Space Environment and Vacuum Research; Control and Propulsion of Vehicles Outside the Atmosphere; Panel Discussion (*on utilization of space vehicles*); Departure, Space Navigation and Re-Entry Problems; The Earth's Moon. The rejuvenation of old established subjects, which the scientific community had laid aside until recently, for application to new engineering problems is abundantly evident in most of the 25 papers presented. Since it presents nothing that is essentially new or original, the volume will mainly be of historic interest in a fast developing field in which hardware construction will, at least for some years to come, outdistance basic understanding in the relevant sciences.

Missile Engineering Handbook (Vol. IV of Principles of Guided Missile Design Series) by C. W. Besserer, Van Nostrand Co., Princeton, N. J., xi + 600 pp. $14.50.

Reviewed by ALLEN E. FUHS
Space Technology Laboratories

Perhaps one of your first thoughts concerning a missile engineering handbook is this: How can material be selected which won't soon be obsolete and yet will be useful? The design of a guided missile requires, in addition to the "hot off the launch pad" data, much information of a permanent nature which has accumulated in scattered scientific areas. For example, the demands of reliability have placed a new emphasis on statistics and probability. With the advent of spaceflight, accurate values of the gravitational "constant" as a function of altitude take on new significance. There are many facts which are of lasting importance to the engineer-missileman. Besserer's handbook collects these facts, plus some of a more transient character, from many sources.

Engineers who use handbooks may not realize it but they acquire certain "tastes in tables." These preferences arise from the fact that there are numerous ways to present the same information; e.g., conversion factors can be in tabular form like a mileage table on a road map. In this handbook conversion factors are given in the columnar form; with this presentation, errors in the use of the table are minimized. In a similar manner, the other tables and figures are laid out in easily assimilated form.

Of course, the real value of a handbook is the completeness and accuracy of the information. These are attributes more difficult to evaluate. To give an indication of the completeness, there are sections on general data, such as conversion

Multi-Use Automated Maintenance

MPTE

The recent demonstration of multi-purpose test equipment (MPTE), developed by RCA under a series of Army Ordnance contracts, highlights *a new dimension in automated multi-use systems support* and culminates a long-term RCA effort in this field. This General Evaluation Equipment is an automated, transistorized, dynamic checkout system. It contains a completely modularized array of electronic and mechanical evaluation equipment, capable of checking a variety of electromechanical devices, ranging from radar subassemblies to missile guidance computers. MPTE provides the stimuli, programming, control, measurement and test functions for the NIKE AJAX, NIKE HERCULES, LACROSSE, HAWK and CORPORAL missile systems and has been extended to other weapons systems related to our defense efforts.

RADIO CORPORATION of AMERICA

DEFENSE ELECTRONIC PRODUCTS

CAMDEN, NEW JERSEY

Tmk(s)®

factors and physical constants, properties of the atmosphere, environmental data and reliability, properties of materials and structures, aerodynamics, avionics, propulsion, spaceflight data, miscellaneous data, such as selected military specifications, design analyses and check lists, and finally a glossary of missile terms and abbreviations. The glossary is an excellent feature of the book; about one third of the book is devoted to the glossary and abbreviations. It goes from Angstrom unit through diergolic propellants, loxodromic curves, SSIP (subsystem integration plan), and ZIP fuels. With the aid of this glossary anyone can converse with the most starry-eyed missileman and the many specialists who support him. The author has wisely excluded information which is readily available in other engineering handbooks.

Before discussing the book's accuracy, here is a brief story about two engineers who decided to write a book. At the start the writers agreed to produce a book entirely free from errors. After checking the galley proofs, these authors concluded that their book would have fewer errors than any other book in the field. As the book went to press the first engineer told the second engineer that succeeding editions would certainly achieve their goal of perfection. The "Missile Engineering Handbook" reflects the attention to detail which produces a relatively error-free book. In addition, most sources of data are listed so that the reader may verify the accuracy.

The "Missile Engineering Handbook" is the fourth volume in a series which provides a basis for formal instruction or self-study in guided missiles and spaceflight. The other volumes of the series present the physical descriptions and mathematical derivations. This handbook is a collection of data useful for the preliminary analysis and initial design studies of future missiles. Much of the design engineer's time is consumed searching through scientific journals, books and reports to find pertinent data; this handbook should help to reduce time spent in search.

Fundamentals of Advanced Missiles, by Richard B. Dow, John Wiley and Sons, Inc., New York, 1958. xvi + 567 pp. $11.75.

Reviewed by JOHN GUSTAVSON
Grand Central Rocket Co.

This volume presents an example of the difficulties an author must face when writing a book on a vehicle system. He is squeezed between the danger of omitting important parts and the equally serious risk of spreading his treatment thin.

The present volume discusses exterior ballistics, fluid mechanics, aerodynamics propulsion, statistical analysis, microwaves, infrared radiation, radar, guidance and missile systems, in that order. Admittedly, most of these subjects form the fundamentals of advanced missiles, but this reviewer would have liked to have seen them treated in a different fashion. I would take a missile, break it apart, indicate the function of each subsystem, such as guidance, propulsion and control surfaces. Then treat each underlying science in a cursory manner, making certain that there is a solid red line throughout the volume, and making sure that no major subsystem is left out. In this book, I missed sections on structures, warheads and rocket control of large missiles.

The author has included references on each page in the form of footnotes, but unfortunately, they are not brought up to the date of publication. The book would have benefited by the inclusion of a literature list at the end of each chapter.

The treatment in the many different sections of the book varies from good and basic to light and outdated.

I suggest that the reader consider this book as a conglomerate of separate treatises on some of the topics related to our missile age. The book may serve as an introduction to these separate topics, but unfortunately, not to the subject of advanced missiles.

Introduction to the Theory of Compressible Flow, by Shih-I Pai, Van Nostrand Co., Princeton, N. J., 1959, xiii + 385 pp. $9.75.

Reviewed by JAMES J. KAUZLARICH
Worcester Polytechnic Institute

The opening sections of the text will alert the reader to the fact that Dr. Pai intends to make as much use of modern mathematical notation as possible. For instance, the topics of fundamental equations, material differentiation, and boundary and initial conditions make up most of Chapter I. Chapter II is made up of a few pages on thermodynamics, and Chapter III opens the essential subject matter of the text, one-dimensional flow of an inviscid compressible fluid. The following chapter, on shock waves, completes the part of the text that deals only with one-dimensional motion.

By Chapter IV another characteristic of this book becomes evident; the author presents the material at a level that presupposes a firm grasp of physical concepts. Here along with additional concepts and definitions, stagnation enthalpy is introduced as a definition, considerations of constant cross-sectional area nozzles are taken up, and the idea that "many practical flow problems may be approximated by isentropic flow" is mentioned. It appears that the title of the book would be more appropriate if the word introduction were deleted.

The text is based on the author's lecture notes, and is intended to give essential results and useful techniques in the theoretical analysis of compressible flow. In carrying this out, the text covers the subject from the point of view of applied mathematics.

At Chapter V, fundamental equations of the aerodynamics of a compressible inviscid and non-heat-conducting fluid, the author gives what can be considered the usual coverage in an introductory gasdynamics course, and in the following 310 pages investigates many and varied topics in compressible fluid mechanics. Chapter V sets the stage for many chapters on methods of solution of the fundamental equations, i.e., VI on method of small perturbation, VII on two-dimensional subsonic steady potential flow, VIII on hodograph method, IX on exact solutions of two-dimensional isentropic steady flow equations, X on two-dimensional steady transonic and hypersonic flows, XI on method of characteristics and XII on linearized theory of three-dimensional potential flow.

In Chapter XIII on nonlinear theory of three-dimensional compressible flow, topics of considerable interest are treated. The problem of supersonic flow over a cone at zero angle of attack is taken up along with a study of transonic, hypersonic and supersonic similarity laws as well as nonsteady compressible flow. Chapter XIV is concerned with anisentropic (rotational) flow of inviscid compressible fluid, and especially, flow conditions behind a curved shock.

In Chapter XV, the author extends his treatment of compressible fluid flow to include viscous flow effects. This chapter is mainly concerned with the development of the Navier-Stokes equation and the energy equation. With these developments completed, it is now possible to take up a study of shock wave structure.

Chapter XVI on boundary layer flow, and XVII on magnetogasdynamics, constitute the remainder of the text. In both the author has presented the subject material in concise form. Actually only enough space is taken to present a few of the more important topics from the extensive literature on these subjects.

This book covers a large range of material in as digestible a form as may be possible considering the outline assumed. The text omits much of the physical description of typical problems, but this is not a handicap if one is familiar with the applications. For further study, the most important references are listed at the end of each chapter.

Astronomy, by Theodore G. Mehlin, John Wiley and Sons, Inc., New York, 392 pp. $7.95.

Reviewed by S. F. SINGER
University of Maryland

This volume is a very elementary treatment of astronomy written in a simple and understandable way. It is well illustrated, uses a minimum of mathematics and also includes fairly simple problems. It is to be viewed more as a cultural, historical and phenomenological introduction to astronomy, and will be appreciated by those who wish to become acquainted with the subject because of its cultural implications and to learn the significance of space research. It will be a disappointment to anyone who wishes to explore the subject in a more technical manner and become informed on astrophysics or celestial mechanics. The book is obviously intended for a course for liberal arts students and can be recommended for this purpose.

from **PLENUM PRESS...**

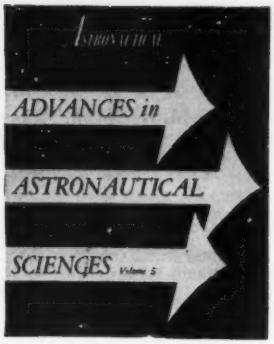

ADVANCES IN THE ASTRONAUTICAL SCIENCES, Vol. 5

This latest volume in the series is the proceedings of the Western National Meeting of the American Astronautical Society which was held in August, 1959. The volume includes the opening address by Dr. Wernher von Braun, and 26 reports which represent original technical research both from theoretical and experimental aspects. Topics under discussion include Space Mechanics, Control and Guidance; Advanced Propulsion and Power; Astronautical Systems and Space Vehicle Design; Space Communication and Instrumentation; Lunar and Planetary Environment. This detailed picture of the scope of current astronautical research will prove invaluable to the scientist, as well as form an excellent guide for the informed layman who desires an insight into the current problems of astronautics.

cloth profusely illustrated $8.00
Also available: Vols. 1-4, $8.00 each. (Price for complete 4-volume set: $28.00)
Detailed tables of contents upon request.

EXPLODING WIRES

Edited by William G. Chace and Howard K. Moore

The increasing contemporary importance of this scientific phenomenon was dramatically indicated by the unexpectedly large attendance at the 1959 Conference on Exploding Wires. This volume, a complete record of the conference, includes reports of theoretical research in the field and new developments and applications. In this book–the first ever published on the subject *in any language*–scientists, students, and technologists will find a wealth of incisive material dealing with high-speed photographic techniques, shock waves, and the physics of fluids.

cloth 374 pages profusely illustrated $9.50

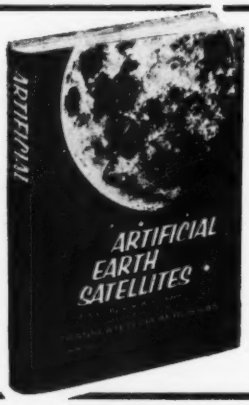

ARTIFICIAL EARTH SATELLITES Volumes 1 and 2

Edited by L. V. Kurnosova **Translated from Russian**

The publication of this double-volume book marks the appearance of the first translation of the revised texts of the reports read at the Fifth Assembly of the Special IGY Committee, which took place at Moscow in August, 1958. Volume 1 explores data obtained by the first two satellites and includes discussions on the ionosphere, cosmic radiation, and space biology. (Data collected on *the first astronaut*–the dog Laika –are presented.) Volume 2 documents work carried out with the third satellite (which contained a complete space laboratory), as well as with rockets.

cloth 236 pages illustrated $9.50

ADVANCES IN CRYOGENIC ENGINEERING, Volumes 1-5

Edited by K. D. Timmerhaus

These five volumes are the proceedings of the Cryogenic Engineering Conferences held in 1954, 1956-1959. (There was no meeting in 1955.) Subjects under discussion include: Cryogenic Tankage for Space Flight Applications; A Study of Condensing-Vacuum Insulation; Multiple-Layer Insulation; Nucleate- and Film-Boiling Studies with Liquid Hydrogen; The Liquefaction of Natural Gas; Some Mechanical Properties of Magnesium Alloys at Low Temperatures; An Experimental Study Concerning the Pressurization and Stratification of Liquid Hydrogen; Maximum-Rate Theory of Impact Sensitivity.

cloth over 250 pages in each volume $13.50 per volume
(Price for complete set of 4 back volumes: $35.00)

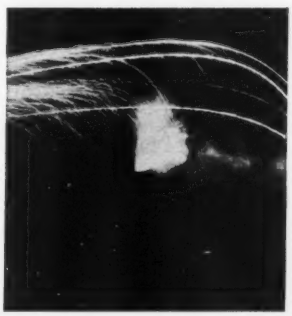

Ignition of cold hydrogen gas by Very pistol

PLENUM PRESS 227 West 17th St., New York 11, N. Y.

Technical Literature Digest

M. H. Smith, *Associate Editor*
The James Forrestal Research Center, Princeton University

Propulsion and Power (Combustion Systems)

Spacecraft Power from Open-cycle Chemical Turbines, by Antonio Orsini, ASTRONAUTICS, vol. 4, Dec. 1959, p. 36.

Water Rockets, by Denis J. Zigrang, ASTRONAUTICS, vol. 4, Dec. 1959, p. 42.

Solid-fuel Ramjet, by H. Powell Jenkins Jr., ASTRONAUTICS, vol. 4, Dec. 1959, p. 44.

Control of Combustion-chamber Pressure and Oxidant-fuel Ratio for a Regeneratively Cooled Hydrogen-fluorine Rocket Engine, by Edward W. Otto and Richard A. Flage, *NASA TN* D-82, Nov. 1959, 61 pp.

Trends in the Development of Liquid Propellant Rocket Engines, by E. G. D. Andrews and A. W. T. Mottram, *Aeron. Quart.*, vol. 10, Aug. 1959, pp. 199–210.

Recent Advances in Ramjet Combustion, by Gordon L. Dugger, ARS JOURNAL, vol. 29, Nov. 1959, pp. 819–827.

Vaporization of Propellants in Rocket Engines, by Richard J. Priem and Marcus F. Heidmann, ARS JOURNAL, vol. 29, Nov. 1959, pp. 828–835.

Unit Converts Waste Rocket Heat to Power, by Michael Yaffee, *Aviation Week*, vol. 71, Nov. 23, 1959, pp. 92–93, 97, 99, 100.

A Detonation Wave Hypersonic Ramjet, by W. H. Sargent and R. A. Gross, *Fairchild Engine & Airplane Corp., Fairchild Engine Div.*, June 1959, 40 pp.

A Three-stage Solid-fuel Sounding Rocket System Suitable for Research at Altitudes Near 200 Nautical Miles, by Waldo L. Dickens and Earl C. Hastings Jr., *NASA TN* D-219, Dec. 1959, 25 pp.

Analysis of the Transient Radiation Heat Transfer of an Uncooled Rocket Engine Operating Outside Earth's Atmosphere, by William H. Robbins, *NASA TN* D-62, Dec. 1959, 25 pp.

Development of TE-60 Plastic Parts Assembly, *Thiokol Chem. Corp., Elkton Div., Final Rep.*, Aug. 29, 1955–March 31, 1959, *Rep.* E120-59, Dec. 1959, 60 pp.

Performance Investigation of a Nonpumping Rocket-ejector System for Altitude Simulation, by Anthony Fortini, *NASA TN* D-257, Dec. 1959, 33 pp.

The Hydrogen-peroxide Rocket Reaction-control System for the X-1B Research Airplane, by James E. Love and Wendell H. Stillwell, *NASA TN* D-185, Dec. 1959, 28 pp.

Rocket Morphology and Nomenclature, by Henry Burlage Jr., ASTRONAUTICS, vol. 5, Jan. 1960, p. 42–43, 75.

Radial Equilibrium in Supersonic Compressors, by A. G. Hammitt and S. M. Bogdonoff, *J. Basic Engng.*, vol. 81D, Dec. 1959 (*Trans., ASME*), pp. 549–558.

Resumé of the Supersonic-compressor Research at NACA Lewis Laboratory, by W. W. Wilcox, E. R. Rysl and M. J. Hartmann, *J. Basic Engng.*, vol. 81D, Dec. 1959 (*Trans., ASME*), pp. 559–568.

Chemical Propulsion: State of the Art, by Kurt R. Stehling, *Space/Aeron.*, vol. 32, no. 6, Dec. 1959, pp. 42–46.

The Rocket: A Past and Future History by Norman P. Gentieu and Meyer M. Markiwotz, *Indl. Res.*, vol. 1, Nov.-Dec. 1959, pp. 70–78.

Investigation of Thrust and Drag Characteristics of a Plug-type Exhaust Nozzle, by Donald P. Hearth and Gerald C. Gorton, *NACA RM* E53L16, Feb. 1954, 39 pp. (Declassified from Confidential by authority of *NASA Pub. Ann.* 4, p. 19, 3/16/59.)

Comparison of Two Methods of Modulating the Throat Area of Convergent Plug Nozzles, by H. George Krull and William T. Beale, *NACA RM* E54L08, May 1955, 20 pp. (Declassified from Confidential by authority of *NASA Pub. Ann.* 4, p. 20, 3/16/59.)

Thrust Characteristics of a Series ot Convergent-divergent Exhaust Nozzles af Subsonic and Supersonic Flight Speeds, by Evan A. Fradenburgh, Gerald C. Gorton and Andrew Beke, *NACA RM* E53L23, March 1954, 24 pp. (Declassified from Confidential by authority of *NASA Pub. Ann.* 4, p. 19, 3/16/59.)

Effects of Several Geometric Variables on Internal Performance of Short Convergent-divergent Exhaust Nozzles, by Fred W. Steffen, H. George Krull and Ralph F. Schmiedlin, *NACA RM* E54L09, Feb. 1955, 24 pp. (Declassified from Confidential by authority of *NASA Pub. Ann.* 4, p. 20, 3/16/59.)

Thrust and Drag Characteristics of a Convergent-divergent Nozzle with Various Exhaust Jet Temperatures, by Donald P. Hearth and Fred A. Wilcox, *NACA RM* E53L23b, March 1954, 20 pp. (Declassified from Confidential by authority of *NASA Pub. Ann.* 4, p. 19, 3/16/59.)

Propulsion and Power (Non-Combustion)

Hearing . . . on the Aircraft Nuclear Propulsion Program, *U. S. Congress, 86th, 1st Session, Joint Committee on Atomic Energy*, July 23, 1959, 418 pp.

Design Considerations of Steady DC Magnetohydrodynamic Electrical Power Generator, by George W. Sutton, *General Electric Co., Missile & Space Vehicle Dept.*, TIS R59SD432, Sept. 1959, 38 pp.

Dynamic Analysis of a Nuclear Rocket Engine System, by Bernard R. Felix and Richard J. Bohl, ARS JOURNAL, vol. 29, Nov. 1959, pp. 853–862.

New Ion Source for Propulsion of Space Vehicles, by C. D. Moak, H. E. Banta, J. W. Johnson and R. F. King, ARS JOURNAL, vol. 29, Nov. 1959, pp. 868–869.

Nuclear Auxiliary Space System May Be Operational Within Year, by Craig Lewis, *Aviation Week*, vol. 71, Nov. 23, 1959, p. 35.

Thermoelectron Engines: Future Power Sources? by G. N. Hatsopoulos, J. Welsh and E. Langberg, *Electronics*, vol. 32, Nov. 13, 1959, pp. 69–72.

Thermomagnetic Generator, by J. F. Elliott, *J. Appl. Phys.*, vol. 30, Nov. 1959, pp. 1774–1777.

Ionic Propulsion, by Robert H. Fox, *Rev. Astron. Sci.*, vol. 1, no. 3, July–Sept. 1959, pp. 7–12.

Competition Rises in Ion, Plasma Fields, by Philip J. Klass, *Aviation Week*, vol. 71, Dec. 7, 1959, pp. 83, 87, 89–90.

New Ideas for Nuclear Reactors, by Eugene P. Wigner, *Nuclear Sci. & Engng.*, vol. 6, no. 5, Nov. 1959, pp. 420–440.

Controlling an Airborne Nuclear Reactor, by Harry L. Loates, *Space/Aeron. Res. & Dev. Handbook*, 1959–1960, pp. F-6–9.

Advanced Airborne APUs (table), *Space/Aeron. Res. & Dev. Handbook*, 1959–1960, pp. F-12–15.

Power from Radioisotopes (nomograph), *Space/Aeron. Res. & Dev. Handbook*, 1959–1960, pp. G-16–17.

Finding the Optimum Load for Solar Cells, by A. J. Heager and T. R. Nisbet, *Space/Aeron.*, vol. 32, no. 6, Dec. 1959, pp. 153–154, 158, 160, 166, 168, 172, 174.

Magnetohydrodynamic Acceleration of Slightly Ionized Viscously Contained Gases, by G. Janes and James A. Fay, *Avco Corp., Avco-Everett Res. Lab.*, Oct. 1959, 18 pp. (2nd Symposium on Advanced Propulsion Concepts, Oct. 1959.)

Pulsed Plasma Accelerator, by Thomas L. Thourson, *Borg-Warner Corp.*, 1959, 21 pp. (2nd Symposium on Advanced Propulsion Concepts, Oct. 1959.)

Flight Magnetohydrodynamics, by Arthur Kantrowitz, *Avco-Everett Res. Lab., Res. Rep.* 51, March 1959, 18 pp.

A Comparison of the Specific Thrust of Ion and Plasma Drive Accelerators, by S. W. Hash, *Lockheed Aircraft Corp., Missile & Space Div.*, Oct. 1959, 15 pp.

The Arc Jet, by Gabriel M. Giannini, *Plasmadyne Corp.*, M-11, 1959, 23 pp.

A Critical Evaluation of the Ion Rocket, by T. M. Littman, *North American Aviation, Inc., Rocketdyne*, 29 pp. (2nd Symposium on Advanced Propulsion Concepts, Oct. 1959.)

The Colloid Rocket: Progress Toward a Charged-liquid-colloid Propulsion System, by Robert D. Schultz and Lane K. Branson, *Aerojet-General Corp., Space Tech. Div.* (AEC NYO-7309), 1959, 20 pp.

Aircraft Nuclear Propulsion Program, (*U. S. Congress, 86th, 1st Session, Joint Comm. on Atomic Energy*), Sept. 1959, 25 pp.

Space Propulsion (*U. S. Congress, 86th, 1st Session, H.R., Committee on Sci. &*

EDITOR'S NOTE: Contributions from Professors E. R. G. Eckert, J. P. Hartnett, T. F. Irvine Jr. and P. J. Schneider of the Heat Transfer Laboratory, University of Minnesota, are gratefully acknowledged.

Astron., House Rep. no. 1087), Aug. 1959, 15 pp.

Space Propulsion (*U. S. Congress, 86th, 1st Session*) *Hearings before the Comm. on Sci. & Astron.*, March 16–20, 23, 1959, no. 16, 1959, 307 pp.

Annual Review of Nuclear Science, vol. 9, Palo Alto, Calif., Annual Rev., Inc., 1959, 625 pp.

Nuclear Fission, by I. Halpern, pp. 245–342, 197 ref.

High-temperature Plasma Research and Controlled Fusion, by R. F. Post, pp. 367–436, 66 ref.

Manned Nuclear Space Systems, Part I: High-thrust Nuclear Systems, by E. B. Konecci, R. F. Trapp and M. M. Hunter, *Aero/Space Engng.*, vol. 19, Jan. 1960, pp. 34–41.

Neon and Oxygen Thermonuclear Reactions, by A. G. W. Cameron, *Astrophys. J.*, vol. 130, Nov. 1959, pp. 895–915.

Propellants and Combustion

Viscosity of Fluids at High Pressures; a Rotating Cylinder Viscometer and the Viscosity of N-pentane, by H. H. Reamer, G. Cokelet and B. H. Sage, *Project Squid Tech. Rep.* CIT-4-P (*ASTIA AD* 208670), Jan. 1959, 33 pp. (Available only on microcards.)

Preliminary Study of a Piston Pump for Cryogenic Fluids, by Arnold E. Biermann and Robert C. Kohl, *NASA Memo* 3-6-59E, March 1959, 27 pp.

Effects of Gas Motion on Heterogeneous Combustion; Natural Convection, Steady Forced Convection, Standing Acoustic Waves, and Shock Waves, Final Summary Report, by William T. Webber, *Wright Air Dev. Center, Tech. Rep.* no. 59-50, April 1959, 88 pp.

Kinetic Studies of Nitric Oxide, by Kurt L. Wray and J. Derek Teare, *Avco-Everett Res. Lab., Res. Note* no. 134, June 1959, 13 pp.

Symposium on Thermal Properties, Purdue University, 1959. Thermodynamic and Transport Properties of Gases, Liquids and Solids, Papers Presented, New York, *Trans., ASME*; McGraw-Hill Book Co., 1959, 472 pp.

Thermochemistry and Thermodynamic Functions of Some Boron Compounds, by W. H. Evans, E. J. Prosen and D. D. Wagman, pp. 226–235.

The Combustion of Boron Hydrides, by W. G. Berl and W. Renich, pp. 236–250.

A Generalized Data-fitting Routine for the LGP-30 Computer: Application to Real-gas Properties of Diborane, by H. J. Galbraith and J. F. Masi, pp. 251–274.

The Low Temperature Thermal and Chemical Thermodynamic Properties of Boron Compounds, by E. F. Westrum, pp. 275–283.

Thermal Conductivity of Liquid Ozone, by T. E. Waterman, pp. 301–303.

The Internal Ballistics of a Supergun, by J. N. Kapur, *Appl. Sci. Res.*, Sect. A, vol. 8, no. 6, 1959, pp. 393–402.

Synthesis of Storable Rocket Fuel During Space Missions, by Eugene L. Colichman, ASTRONAUTICS, vol. 4, Dec. 1959, p. 32.

Dependence of Damage Effects upon Detonation Parameters of Organic High Explosives, by Donna Price, *Chem. Revs.*, vol. 59, Oct. 1959, pp. 801–826.

Consumption of Oxygen Molecules in Hydrocarbon Flames Chiefly by Reaction with Hydrogen Atoms, by C. P. Fenimore and G. W. Jones, *J. Phys. Chem.*, vol. 63, Nov. 1959, pp. 1834–1838.

Detonation Induction Distances in Combustible Gaseous Mixtures at Atmospheric and Elevated Initial Pressures, I Methane-Oxygen, II Carbon Monoxide-Oxygen, III Hydrogen-Oxygen, by Loren E. Bollinger and Rudolph Edse, *Wright Air Dev. Center, Tech. Rep.*, 58-591, March 1959, 88 pp.

Adiabatic Flame Temperatures, Combustion Gas Compositions, and Expansion Ratios of Combustible Gas Mixtures at Various Pressures, by William A. Strauss and Rudolph Edse, *Wright Air Dev. Center, TN* 59–40, July 1959, 43 pp.

Study of Additive Effects in Solid Propellant Burning, by Herman Burwasser, *Aero. Chem. Res. Labs., Inc., Second Quart. Progr. Rep.* TM-17, Oct. 1959, 8 pp.

Total Radiation from Burning Solid Propellant Strands, by David W. Blair and Kimball P. Hall, *Princeton Univ., Aeron. Engng. Dept., Semi-annual Progr. Rep.* for the period 1 April 1959–30 Sept. 1959, Oct. 1959, 8 pp.

Joint Army-Navy-Air Force Ignitability Panel, Proceedings of the Third Meeting held at Applied Physics Laboratory, Silver Spring, Md., *Solid Propellant Info. Agency*, June 1959, 69 pp.

Quarterly Progress Report on Engineering Research (U), *Rohm & Haas Co., Redstone Arsenal Res. Div., Rep.* P-59-17, June 15–Sept. 15, 1959, 17 pp.

Spectrometric Determination of Chlorate Impurities in Ammonium Perchlorate, by Eugene A. Burns, *Calif. Inst. Tech., Jet Prop. Lab. Progr. Rep.* 30-12, May 1959, 8 pp.

Theoretical Performance of Ammonium Nitrite—Water Solutions, by John S. Gordon, *Wright Air Dev. Center, Tech. Rep.* 59-248, March 1959, 7 pp.

Heterogeneous Combustion of Multicomponent Fuels, by Bernard J. Wood, Henry Wise and S. Henry Inami, *NASA TN* D-206, Nov. 1959, 32 pp.

Production and Measurement of Single Drops, Sprays, and Solid Suspensions, by James A. Browning, Reprinted from *Advances in Chemistry*, Series 20 (Amer. Chem. Soc.), Washington, D. C., 1958, pp. 136–154.

The Chemistry of Boron Hydrides and Related Hydrides, by R. M. Parry, R. C. Taylor, C. E. Nordman, G. Kodama and S. G. Shore, *Wright Air Dev. Center, Tech. Rep.* 59-207, May 1959, 178 pp., 141 refs.

Theory of Particle Combustion at High Pressures, by D. B. Spalding, ARS JOURNAL, vol. 29, Nov. 1959, pp. 828–835.

Solubility of Air, N_2 and O_2 in n-Propyl Nitrate, by Adolph B. Amster and Joseph B. Levy, ARS JOURNAL, vol. 29, Nov. 1959, pp. 870–871.

Solids Make Bid for Space Booster Role, by Michael Yaffe, *Aviation Week*, vol. 71, Nov. 23, 1959, pp. 32–34.

Rocketdyne Studies Pumps, Future Liquid Propellants, by Russel Hawkes, *Aviation Week*, vol. 71, Nov. 23, 1959, pp. 57, 59, 61, 65, 67, 69, 73.

Thermal Decomposition of Nitrous Oxide, by B. G. Reuben and J. W. Linnett, *Trans., Faraday Soc.*, vol. 55, Sept. 1959, pp. 1543–1553.

Condensed Systems at High Pressures, by R. H. Wentorf Jr., *J. Phys. Chem.*, vol. 63, Nov. 1959, pp. 1934–1939.

Dielectric Constant of Liquid Ozone and Liquid Ozone-Oxygen Mixtures, by Charles K. Hersh, Gerald M. Platz and Raymond J. Swehla, *J. Phys. Chem.*, vol. 63, Nov. 1959, pp. 1968–1969.

Chemical Reactions of Active Nitrogen, by Harold A. Dewhurst, *J. Phys. Chem.*, vol. 63, Nov. 1959, pp. 1976–1977.

Electric and Magnetic Properties of the Hydrogen Molecule, by T. P. Das and R. Bersohn, *Phys. Rev.*, vol. 115, no. 4, Aug. 15, 1959, pp. 897–910.

On the Existence of the Negative Nitrogen Ion, by Ya. M. Fogel', V. F. Kozlov and A. A. Kalmykov, *Soviet Phys.-JETP*, vol. 36(9), no. 5, Nov. 1959, pp. 963–964.

Blowoff of Propane and Hydrogen Diffusion Flames at High Mach Number, Ramjet Conditions, by R. J. Bacigalupi and E. A. Lezberg, *NASA TN* D-67, Dec. 1959, 24 pp.

Investigation of the Products from Explosions of Diborane-Air Mixtures, by Robert Brown, *Johns Hopkins Univ., Appl. Phys. Lab.*, CF-2844, Sept. 1959, 6 pp.

Studies on Deflagration to Detonation in Propellants and Explosives, *U. S. Bur. Mines, Explosives Res. Lab., Quart. Rep.*, July 1–Sept. 30, 1959, 10 pp.

Combustion Instability in Liquid Propellant Rocket Motors (29th Quarterly Progress for the period 1 May 1959 to 31 July 1959), *Princeton Univ. Aeron. Engng. Dept., Rep.* 216-CC, Sept. 1959, 19 pp.

A One-dimensional Theory of Liquid-fuel Rocket Combustion, by D. B. Spalding, *Gt. Brit., Aeron. Res. Council, Current Paper* 445, May 1958, 18 pp.

Chemical Sampling Downstream of Lean, Flat Hydrogen and Propane Flames, by Burton D. Fine, *NASA TN* D-198, Dec. 1959, 25 pp.

Investigation of Liquid Nitric Oxide as a Rocket Oxidizer, by Loren E. Bollinger and Rudolph Edse, *Wright Air Dev. Center, Tech. Rep.* 59-12, May 1959, 22 pp.

The Preparation of 3,3,3-tris(Nitratomethyl)-Propene-1 and 3,3-bis(Nitratemethyl)-Butene-1, by Lester P. Kuhn and Alan C. Duckworth, *Aberdeen Proving Ground, Ball. Res. Lab., Mem. Rep.* 1230, Aug. 1959, 24 pp.

Binary Nitrogen Compounds of the Elements: A Literature Survey, by Rosemary G. Ehl, Rodney J. Sime and John L. Margrave, *Wright Air Dev. Center, TN* 59–115, June 1959, 75 pp.

Calculation of Shock Hugoniots and Related Quantities for Nitrogen and Oxygen, by R. A. Alpher and H. D. Greber, *General Electric Co., Res. Lab., Schenectady, NY, Rep.* 58-RL-1915, April 1958, 25 pp.

The Mechanism of Polytetrafluoroethylene Pyrolysis, by Henry L. Friedman, *General Electric Co., Missile & Space Vehicle Dept., TIS* R59SD385, June 1959, 26 pp.

Kinetics of the Decomposition of N_2O at High Temperature, by Wendell M. Graven, *J. Amer. Chem. Soc.*, vol. 81, Dec. 5, 1959, pp. 6190–6192.

Vapor Pressure of Diborane, by Leo J. Paridon and George E. MacWood, *J. Phys. Chem.*, vol. 63, Dec. 1959, p. 1997.

The Heat of Vaporization of Diborane, by Leo J. Paridon, George E. MacWood and Jih-Heng Hu, *J. Phys. Chem.*, vol. 63, Dec. 1959, pp. 1998–1999.

Flame Spectra: The Effect of Deuteration on the Hydrocarbon Flame Bands, by G. N. Spokes and A. G. Gaydon, *Proc., Phys. Soc., London*, vol. 74, Nov. 1, 1959, pp. 639–642.

LCAO Wave Functions for Hydrogen Fluoride with Hartee-Fock Atomic Orbitals, by Arnold M. Karo and Leland C. Allen, *J. Chem. Phys.*, vol. 31, Oct. 1959, pp. 968–977.

Metal Combustion Processes, by Irvin Glassman, *Princeton Univ., Aeron. Engng. Dept., Rep.* 473, Aug. 1959, 37 pp.

A One-dimensional Theory of Liquid-fuel Rocket Combustion, by J. Adler, *Gt. Brit., Aeron. Res. Council, Current Paper* 446, May 1958, 7 pp.

Chemical Nonequilibrium Effects on Hydrogen Rocket Impulse at Low Pressures, by J. Gordon Hall, A. Q. Eschenroeder and J. J. Klein, *Cornell Aeron. Lab., Rep.* AD-1118-A-8, Nov. 1959, 10 pp.

Ignition of Solid Propellants by Compression of Gases Entrapped on an Internal Cavity, by C. H. Parr, *Rohm & Haas Co., Quart. Progr. Rep. on Engng. Res., Rep.* P-59-11, March 15–June 15, 1959, pp. 1–17.

The Controlled Thermal Decomposition of Cellulose Nitrate, VII: Carbonyl Compounds, by M. L. Wolfrom and G. P. Arsenault, *Ohio State Univ., Res. Found., Tech. Rep.* 675-14, Oct. 1959, 21 pp.

Mollier Diagrams for the Hydrogen-Oxygen System and Experimental Results of Test on a Rocket Motor of 500-pound Thrust, by Dwight I. Baker, *Calif. Inst. Techn., Jet Prop. Lab., Rep.* 20-127, May 1959, 109 pp.

Theory of the Burning of Mono-propellant Droplets, by D. B. Spalding and V. K. Jain, *Gt. Brit., Aeron. Res. Council, Current Paper* 447, May 1958, 9 pp., 4 figs.

Analytical Solution of a Flame with Cylindrical Symmetry, by J. Menkes, *Calif. Inst. Techn., Jet Prop. Lab., Progr. Rep.* 30-17, Oct. 1959, 8 pp.

Temperature Distribution in Sooty Flames, by F. Rössler, *Annalen der Physik,* vol. 4, nos. 6–8, Oct. 13, 1959, pp. 396–422. (In German.)

A Study of the Interior Ballistic Equations, by R. A. Struble, *Arch. for Rational Mech. & Anal.,* vol. 3, no. 5, Sept. 30, 1959, pp. 397–421.

Theory of Particle Combustion at High Pressures, by D. B. Spalding, ARS JOURNAL, vol. 29, Nov. 1959, pp. 828–835.

Vaporization of Propellants in Rocket Engines, by Richard J. Priem and Marcus F. Heidmann, ARS JOURNAL, vol. 29, Nov. 1959, pp. 836–842.

Solubility of Air, N_2 and O_2 in n-Propyl Nitrate, by Adolph B. Amster and Joseph B. Levy, ARS JOURNAL, vol. 29, Nov. 1959, pp. 870–871.

Esso Accelerates Solid Propellant Search, by Michael Yaffee, *Aviation Week,* vol. 71, Dec. 14, 1959, pp. 68–69, 71, 75, 77–78.

Effect of Argon and Helium on the Thermal Conductivity of the $N_2O_4 \rightleftarrows 2NO_2$ System, by Kenneth P. Coffin, *J. Chem. Phys.,* vol. 31, Nov. 1959, pp. 1290–1297.

Participation of Vibration in Exchange Reactions, by Felix T. Smith, *J. Chem. Phys.,* vol. 31, Nov. 1959, pp. 1352–1359.

A Calculation of the Rates of the Ortho-para Conversions and Isotope Exchanges in Hydrogen, by Isaiah Shavitt, *J. Chem. Phys.,* vol. 31, Nov. 1959, pp. 1359–1367.

Comparison of Hot and Thermal Reactions, by J. L. Magee and W. H. Hamill, *J. Chem. Phys.,* vol. 31, Nov. 1959, pp. 1380–1386.

Mean-first-passage Times and the Collision Theory of Bimolecular Reactions, by B. Widom, *J. Chem. Phys.,* vol. 31, Nov. 1959, pp. 1387–1394.

Reaction of Acetylene with Methyl Radicals, by Charles M. Drew and Alvin S. Gordon, *J. Chem. Phys.,* vol. 31, Nov. 1959, pp. 1416–1417.

NMR Spectra of Normal and Deuterated Methylacetylenes, by Wyman R. Vaughan and Robert C. Taylor, *J. Chem. Phys.,* vol. 31, Nov. 1959, pp. 1425–1426.

Basic Principles of Combustion-model Research, by A. A. Putnam and E. W. Ungar, *J. Engng. for Power (Trans., ASME),* vol. A 81, Oct. 1959, pp. 383–388

The Effect of Fuel Types and Admission Method upon Combustion Efficiency, by H. N. McManus Jr., W. E. Ibele and T. E. Murphy, *J. Engng. for Power (Trans., ASME),* vol. A 81, Oct. 1959, pp. 423–427.

Pressure and Velocity Measurements on Detonation Waves in Hydrogen-Oxygen Mixtures, by D. H. Edwards, G. T. Williams and J. C. Breeze, *J. Fluid. Mech.,* vol. 6, Nov. 1959, pp. 497–517.

Temple Studies High Temperature Flames, by William L. Doyle, *Missiles & Rockets,* vol. 5, Dec. 14, 1959, pp. 17–18.

Fluorine Compounds Point to Many New Propellant Possibilities, by John F. Gall, *Space/Aeron. Res. & Dev. Handbook,* 1959–1960, pp. C-5–9.

Handling and Storage of High Energy Oxidizers, by J. M. Siegmund and H. R. Neumark, *Space/Aeron. Res. & Dev. Handbook,* 1959–1960, pp. L-9–14.

Materials and Structures

Some Contributions to the Heat Conduction and Thermal Stresses Analysis in Aircraft and Missile Structures, by L. Broglio, *Aerotechnica,* vol. 39, no. 2, April 1959, pp. 53–65. (In Italian.)

Materials for Rockets and Reactors, by J. A. Ternisien, *Fusées et Recherche Aéron.,* no. 13, Aug. 1959, pp. 74–84. (In French.)

Fatigue Damage During Complex Stress Histories, by H. W. Liu and H. T. Corten, *NASA TN* D-256, Nov. 1959, 56 pp.

Tensile Properties of 6A-14V Titanium-alloy Sheet under Rapid-heating and Constant-temperature Conditions, by Howard L. Price, *NASA TN* D-121, Nov. 1959, 26 pp.

High Temperature Behavior of Teflon, by Tunis Wentink Jr., *Avco-Everett Res. Lab., Res. Rep.* no. 55, July 1959, 13 pp.

Ceramic Fabrication Processes, W. D. Kingery, Ed., John Wiley & Sons, N. Y., 1958, 235 pp.

Effect of Microstructure on the Electrical and Magnetic Properties of Ceramics, by George Economos, pp. 201–213.

Effect of Microstructure on the Mechanical Properties of Ceramic Materials, by R. L. Coble, pp. 213–228, 46 refs.

Beryllium Applications in Structural Design, by L. A. Riedinger and R. E. Foster, *Rev. Astron. Sci.,* vol. 1, no. 3, July–Sept. 1959, pp. 13–18.

Stabilization Effects of Internal Pressure on the Buckling Behavior of Thin-wall Rocket Motor Cases, by William D. Jordan, *Rohm & Haas Co., Quart. Progr. Rep. on Engng. Res., Rep.* P-51-11, March 15–June 15, 1959, pp. 18–36.

Paint Gives Missiles Thermal Protection, by Michael Yaffee, *Aviation Week,* vol. 71, Dec. 7, 1959, pp. 102–103, 105.

Materials for Environmental Extremes, by G. Sideris, *Electronics,* vol. 32, Dec. 4, 1959, pp. 81–96.

Thermal Degradation of Polymers at High Temperatures, by Samuel L. Madorsky and Sidney Straus, *J. Res., Natl. Bur. Standards, A: Phys. & Chem.,* vol. 63A, no. 3, Nov.–Dec., 1959, pp. 261–264.

New Shielding Materials for High-temperature Application, by H. E. Hungerford, R. F. Mantey and L. P. Van Maele, *Nuclear Sci. & Engng.,* vol. 6, no. 5, Nov. 1959, pp. 396–408.

Titanium Provides Notch-ductile Rocket Cases, by A. N. Eshman, *Space/Aeron.,* vol. 32, no. 6, Dec. 1959, pp. 73–74, 76, 78.

Shock and Vibration in Electronic Mounting (nomographs), by H. C. Lawrence, *Space/Aeron. Res. and Dev. Handbook,* 1959–1960, pp. D-13–14, 15–16.

Extreme Temperature Lubricants and Hydraulic Fluids, *Space/Aeron. Res. & Dev. Handbook,* 1959–1960, pp. G-9–12.

Improved Plastics Meet Needs of High Performance Vehicles, by I. J. Gruntfest, *Space/Aeron. Res. & Dev. Handbook,* 1959–1960, pp. H-6–9.

Mechanical Properties of High Performance Materials (table), by Alan V. Levy, *Space/Aeron. Res. & Dev. Handbook,* 1959–1960, pp. H-10–11.

Properties of Honeycomb Core (table), by D. C. Wilson, *Space/Aeron. Res. & Dev. Handbook,* 1959–1960, pp. H-12–13.

Properties of Refractory Hard Metals and Ceramic Raw Materials (table), by Harry B. Porter, *Space/Aeron. Res. & Dev. Handbook,* 1959–1960, p. H-13.

Stress Rupture Properties of Nickel and Cobalt Alloys (table), by Michel Urbain, *Space/Aeron. Res. & Dev. Handbook,* 1959–1960, p. H-14.

Fluid Dynamics, Heat Transfer and MHD

An Investigation of Steady and Unsteady Heat Transfer in Rocket Motors, by Andre G. Condomines (Thesis, M.S.), *Princeton Univ., Aeron. Engng. Dept.,* 1959, 36 pp., 15 figs.

Heat Transfer and Fluid Flow: A Bibliography of Selected Report Literature, by *U. S. Atomic Energy Comm., Tech. Info. Serv.,* TID-3305 (Supplement 1), June 1958, 432 pp.

Comparison between Molecular and Turbulent Diffusion Processes, by F. N. Frenkiel, *David Taylor Model Basin, Rep.* no. 1320, July 1959, pp. 204–216. (Reprinted from *Int. Conf. Transport Prop. Statistical Mech.,* Brussels, 1956.)

Survey of Thermal, Radiation, and Viscous Damping of Pulsating Air Bubbles in Water, by Charles Devin Jr., *David Taylor Model Basin, Rep.* 1329, Aug. 1959, 37 pp.

Flexure of a Two-dimensional Arc under Forced Convection, by Paul G. Thiene, *Plasmadyne Corp., Rep.* no. T2 TN-089-334, Aug. 23, 1959, 80 pp.

An Arc Tunnel for Magnetohydrodynamic Studies, by Richard J. Rosa, *Avco-Everett Res. Lab., Res. Note* no. 132, June 1959, 11 pp.

End Effects in Magnetohydrodynamic Channel Flow, by Frank Fishman, *Avco-Everett Res. Lab., Res. Note* no. 135, June 1959, 14 pp.

Transport Property Equations for Partially Ionized Gases, by C. W. Baulknight, *General Electric, Missile & Space Vehicle Dept., TIS* R59SD428, Sept. 1959, 12 pp.

Shock Front Thickness and Bulk Viscosity in Polyatomic Gases, by W. H. Andresen and D. F. Hornig, *Brown Univ., Metcalf Res. Lab., Tech. Rep.* 6, July 1955, 13 pp.

Use of a Theoretical Flow Model to Correlate Data for Film Cooling or Heating an Adiabatic Wall by Tangential

Injection of Gases of Different Fluid Properties, by James E. Hatch and S. Stephen Papell, *NASA TN* D-130, Nov. 1959, 43 pp.

On Ablating Heat Shields for Satellite Recovery, by Steven Georgiev, Henry Hidalgo and Mac C. Adams, *Avco-Everett Res. Lab., Res. Rep.* 65, July 1959, 28 pp.

A Theory of Ablation of Glassy Materials for Laminar and Turbulent Heating, by Henry Hidalgo, *Avco-Everett Res. Lab., Res. Rep.* 62, June 1959, 27 pp.

Heat and Mass Transfer Bibliography with Selected Abstracts, by W. L. Christian and T. H. Schiffman, *Wright Air Dev. Center, Tech. Rep.* 58-186, May 1958, 167 pp.

The Effects of Electrode Contamination on the Properties of Air-arc Plasmas, by Harold Y. Washman, Milton Linevsky and John H. McGinn, *General Electric Co., Missile & Space Vehicle Dept.,* TIS R59SD427, Sept. 1959, 16 pp.

The Tailored-interface Hypersonic Shock Tunnel, by Charles E. Wittliff, Merle R. Wilson and Abraham Hertzberg, *Cornell Aeron. Lab., Inc.,* March 12–20, 1958, 26 pp., 18 diagrs.

Electrical and Pressure Losses in a Magnetohydrodynamic Channel Due to End Current Loops, by George W. Sutton, *General Electric Co., Missile and Space Vehicle Dept.,* TIS R59SD431, July 1959, 37 pp. + diagrs.

Effects of Air Dissociation and Ionization at Hypersonic Speed, by Gianni Jarre, *Torino, Lab. Mec. Appl. del Politec., TN* 14, July 1959, 29 pp.

Non-equilibrium Theory of an Ideal-dissociating Gas Through a Conical Nozzle, by N. C. Freeman, *Gt. Brit., Aeron. Res. Council, Current Paper* 438, Aug. 1958, 10 pp.

Mach Waves in Shock Wave Systems from a Detonating Solid Explosive, by D. N. Woodhead and R. Wilson, *Gt. Brit. Min. Power, Safety in Mines Res. Estab., Res. Rep.* 155, May 1959, 48 pp.

Stability of a Horizontal Fluid Layer with Unsteady Heating from Below and Time-dependent Body Force, by Arthur W. Goldstein, *NASA Tech. Rep.* R-4, 1959, 15 pp.

Variational Theory of Chemical Reaction Rates Applied to Three-body Recombination, by James C. Keck, *Avco-Everett Res. Lab., Res. Rep.* 66, Sept. 1959, 62 pp.

Compressible Flow Tables for Gases with Specific Heat Ratios from 1.10 to 1.28, by K. E. Tempelmeyer and G. H. Sheraden, *Arnold Engng. Dev. Center, TN* 58–9, March 1958, 173 pp.

Spreading of Rocket Exhaust Jets at High Altitudes, by E. K. Latvala, *Arnold Engng. Dev. Center, Tech. Rep.* 59-11. June 1959, 37 pp.

Experimental Studies of Shock Waves in Nitrogen, by John C. Camm and James C. Keck, *Avco-Everett Res. Lab., Rep.* 67, June 1959, 18 pp.

Similarity of Far Noise Fields of Jets, by Walton L. Howes, *NASA Tech. Rep.* R-52, 1959, 90 pp., 26 figs.

On Axisymmetrical Jets, with Application to Rocket Jet Flow Fields at High Altitudes, by W. T. Lord, *Gt. Brit. Royal Aircr. Estab., Rep. Aero* 2626. July 1959, 37 pp.

Laminar Mixing of Streams of Different Gases, by Luigi G. Napolitano and A. Pozzi. *Univ. Naples, Inst. Aeron., TN* 1959, 60 pp.

Magnetogasdynamic Flow Regimes, by Ching-Shi Liu and Ali Bulent Cambel, ARS JOURNAL, vol. 29, Nov. 1959, pp. 871–873.

Streamlined Conical Bodies under the Movements of Gases at Hypersonic Speeds, by A. L. Gonor, *Akademiia Nauk SSSR, Izvestiia, Otdelenie Tekhnicheskikh Nauk, Mekhanika i Mashinostroenie,* 1, 1959, pp. 34–40. (In Russian.)

Design of Axisymmetric Jet Nozzles of Minimum Weight, by L. E. Sternin, *Akademiia Nauk SSSR, Izvestiia, Otdelenie Tekhnicheskikh Nauk, Mekhanika i Mashinostroenie,* 1, 1959, pp. 41–45. (In Russian.)

Motion of a Thin Solid Body under the Action of a Strong Shock Wave, by S. S. Grigorian, *Akademiia Nauk SSSR, Izvestiia, Otdelenie Tekhnicheskikh Nauk, Mekhanika i Mashinostroenie,* 1, 1959, pp. 165–166. (In Russian.)

Useful Interference of Wings and Fuselage at Hypersonic Speeds, by G. L. Grodzovskii, *Akademiia Nauk SSSR, Izvestiia, Otdelenie Tekhnicheskikh Nauk, Mekhanika i Mashinostroenie,* 1, 1959, pp. 170–173. (In Russian.)

Hypersonic Flow of an Imperfect Gas Around a Body, by G. A. Liubimov, *Akademiia Nauk SSSR, Izvestiia, Otdelenie Tekhnicheskikh Nauk, Mekhanika i Mashinostroenie,* 1, 1959, pp. 173–176. (In Russian.)

Electromotive Force in a Highly Ionized Plasma Moving Across a Magnetic Field, by M. Sakuntala, B. E. Clotfelter, W. B. Edwards and R. G. Fowler, *J. Appl. Phys.,* vol. 30, Nov. 1959, pp. 1669–1670.

Nonlinear Heat Transfer Problem, by Paul L. Chambré, *J. Appl. Phys.,* vol. 30, Nov. 1959, pp. 1683–1688.

Thermal Conductivity of Clear Fused Silica at High Temperatures, by Kurt L. Wray and Thomas J. Connolly, *J. Appl. Phys.,* vol. 30, Nov. 1959, pp. 1702–1704.

Investigation of Fast Ionization Processes in the Gas Flow Behind a Shock Wave, by A. A. Brandt and R. Kh. Kurtmulaev, *Instruments and Exptl. Tech.,* 6, Nov.-Dec., 1958, pp. 808–810.

Measurement of Rapidly Varying Pressures in a Gas, by S. G. Zaitsev, *Instruments and Exptl. Tech.,* 6, Nov.-Dec., 1958, pp. 811–813.

Mechanism and Speed of Breakup of Drops, by G. D. Gordon, *J. Appl. Phys.,* vol. 30, Nov. 1959, pp. 1759–1761.

Turbulent Flow in a Circular Tube with Arbitrary Internal Heat Sources and Wall Heat Transfer, by R. Siegel and E. M. Sparrow, *J. Heat Transfer, Trans., ASME,* vol. 81, Nov. 1959, pp. 280–290.

Some General Considerations of the Heating of Satellites, by A. J. Eggers Jr., T. J. Wong and R. E. Slye, *J. Heat Transfer, Trans., ASME,* vol. 81, Nov. 1959, pp. 308–314.

The Penetration of Planetary Atmospheres, by Carl Gazley Jr., *J. Heat Transfer, Trans., ASME,* vol. 81, Nov. 1959, pp. 315–322.

Thermodynamic Properties of Helium at Low Temperatures and High Pressures, by D. B. Mann and R. B. Stewart, *J. Heat Transfer, Trans., ASME,* vol. 81, Nov. 1959, pp. 323–326.

Experiments on Porous-wall Cooling and Flow Separation Control in a Supersonic Nozzle, by Leon Green Jr. and Kenneth L. Nall, *J. Aero/Space Sci.,* vol. 26, Nov. 1959, pp. 689–697.

Hypersonic Viscous Flow over Slender Cones, by L. Talbot, T. Koga and P. M. Sherman, *J. Aero/Space Sci.,* vol. 26, Nov. 1959, pp. 723–730.

Heat Transfer in Separated Flows, by Howard K. Larson, *J. Aero/Space Sci.,* vol. 26, Nov. 1959, pp. 731–738.

On An Exact Solution of Incompressible, Inviscid, Hypersonic, Stagnation-point Flow for a Sphere, by Koon-Sang Wan, *J. Aero/Space Sci.,* vol. 26, Nov. 1959, p. 755.

Review of High-temperature Rotating-plasma Experiments, by John M. Wilcox, *Revs. Modern Phys.,* vol. 31, no. 4, Oct. 1959, pp. 1045–1051.

Collision-free Magnetohydrodynamic Shock Wave, by A. Kantrowitz, R. M. Patrick and H. E. Petschek, *Avco-Everett Res. Lab., Res. Rep.* no. 63, Aug. 1959, 12 pp.

Numerical Calculation of Absolute Bremsstrahlung Intensity for a Fully Ionized Fully Dissociated Hydrogenic Gas, by G. Sargent Janes and Harold E Koritz, *Avco-Everett Res. Lab., Res. Rep.* no. 70, Sept. 1959, 13 pp.

The Production and Study of High Speed Shock Waves in a Magnetic Annular Shock Tube, by Richard M. Patrick, *Avco-Everett Res. Lab., Res. Rep.* no. 59, July 1959, 36 pp.

Theory of Shock Front, II: High Temperature Reaction Rates, by J. Derek Teare, Peter Hammerling and Bennett Kivel, *Avco-Everett Res. Lab., Res. Note* no. 133, June 1959, 13 pp.

Variational Theory of Chemical Reaction Rates Applied to Three-body Recombination, by James C. Keck, *Avco-Everett Res. Lab., Res. Rep.* no. 66, Sept. 1959, 62 pp.

Experimental Studies of Shock Waves in Nitrogen, by John C. Camm and James C. Keck, *Avco-Everett Res. Lab., Res. Note* no. 140, June 1959, 18 pp.

Analysis of Temperature Distribution and Radiant Heat Transfer Along a Rectangular Fin of Constant Thickness, by Seymour Lieblein, *NASA TN* D-196, Nov. 1959, 60 pp.

A Method for the Rapid Numerical Solution of the Heat Conduction Equation for Composite Slabs, by Julius W. Enig, *Naval Ord. Lab., NAVORD Rep.* no. 6666, Aug. 20, 1959, 19 pp.

A Study of the Interaction between Carbon and Dissociated Gases, by W. G. Zinman, *General Electric Co., Missile and Space Vehicle Dept., Rep.* R59SD457, Nov. 5, 1959, 14 pp.

Rapid Chemical Reaction in a Laminar Boundary Layer, by S. K. Friedlander and Mitchell Litt, *Appl. Sci. Res.,* Sect. A, vol. 8, no. 6, 1959, pp. 403–412.

Heat Transfer and Friction in Turbulent Vortex Flow, by Frank Kreith and David Margolis, *Appl. Sci. Res.,* Sect. A, vol. 8, no. 6, 1959, pp. 457–473.

Symposium on Thermal Properties, Purdue University, 1959. **Thermodynamic and Transport Properties of Gases, Liquids and Solids, Papers Presented,** New York, *Trans., ASME,* McGraw-Hill Book Co., 1959, 472 pp.

Relations between Molecular Gas Absorptivities and Emissivities, by S. S. Penner, D. Olfe and A. Thomson. pp. 2–13.

Theories of Gas Transport Phenomena, J. S. Dahlher, pp. 14–24.

Review of Modern Theory of the Thermal Conductivity of Metals, by D. J. Schleef. p. 25.

Survey of Recent Work on the Viscosity, Thermal Conductivity and Diffusion of Gases and Gas Mixtures, by P. E. Liley, pp. 40–69.

Review of Available Experimental Data on the Viscosity of Steam, by J. Kestin, pp. 70–77.

Systems and Procedures Developed

for the Search, Coding and Mechanized Processing of Bibliographic Information on Thermophysical Properties, by Y. S. Touloukian, C. H. Stevens, R. H. Rodin, T. Wing and D. W. Smith, pp. 78–91.

Transport Properties of Multicomponent Gas Mixtures at High Temperatures, by C. W. Baulknight, pp. 92–101.

Thermodynamic Properties of Methane-Nitrogen Mixtures, by R. T. Ellington, O. T. Bloomer, B. E. Eskin and D. C. Gami, pp. 102–109.

Correlations and Equations Used in Calculating the Thermodynamic Properties of Freon Refrigerants, by J. J. Martin, pp. 110–122.

The Unmixing of Metal Solutions by a Temperature Gradient, by R. A. Oriani, pp. 123–129.

Thermodynamic and Electrical Properties of Nitrogen at High Temperatures, by F. Martinek, pp. 130–156.

Isentropic Checking of Vapor Tables at Saturation Boundary Lines and Ways of Improving Them, by U. Issarescu, pp. 157–171.

The Liquid Pressure-volume-temperature Relationships; Dew and Bubble Point Pressures and Densities of a Binary Mixture Containing 75 Wt. % Freon-12 and 25 Wt. % Freon-22, by D. White, E. F. Neilson and J. Farmham, pp. 172–179.

Vapor-liquid Phase Equilibria in the Binary Systems of Methane, Ethane and Nitrogen, by R. T. Ellington, B. E. Eakin, J. D. Parent, D. C. Gami and O. T. Bloomer, pp. 180–194.

Application of the B-E-R Equation to Hydrocarbon-Carbon Dioxide Mixtures, by B. E. Eakin and R. T. Ellington, pp. 195–204.

An Equation for the Critical Isotherm of Gases, by U. Rombush, pp. 205–210.

The Virial Equation Applied to Steam, by P. E. Liley, pp. 211–221.

Characterization of Unusual Gaseous Oxide and Hydroxide Molecules in M-O-H Systems at High Temperatures, by F. T. Greene S. P. Randall and J. L. Margrave, pp. 222–225.

Thermal Conductivity of Some Epoxy Plastics, by J. E. Janssen and R. H. Torborg, pp. 284–294.

Thermal Conductivity of Helium-Air Mixtures, by E. R. G. Eckert, W. E. Ibele and T. F. Irvine Jr., pp. 295–300.

Thermal Diffusivity of Nitrogen as Determined by the Cyclic Heat Transfer Method, by W. B. Harrison, W. C. Boteler and J. M. Spurlock, pp. 304–312.

Experiments in the Molecular Diffusion of Gases at High Temperatures, by A. A. Westenberg and R. E. Wolker, pp. 313–320.

The Effect of Moderate Pressures on the Viscosity of Five Gases, by J. Kestin and W. Leidenfrost, pp. 321–338.

The Viscosity of Steam, by F. A. Thomas Jr. and T. W. Jackson, pp. 339–345.

The Viscosity of Steam-Nitrogen Mixtures at Atmospheric Pressure and Elevated Temperatures, by C. F. Bonilla, S. E. Greer and E. A. Taikoff, pp. 346–349.

Fluid Thermal Conductivity by a Transient Method, by P. H. G. Allen, pp. 350–357.

Thermodynamic and Transport Properties of Gaseous Carbon Dioxide, by L. H. Chen, pp. 358–371.

Thermal Expansion Coefficients of Binary Substitutional Solid Solution Alloys, by W. H. Spurgeon, pp. 372–376.

Thermal Diffusivity of Metals at Elevated Temperatures, by C. P. Butler and E. C. Y. Inn, pp. 377–390.

Thermal Conductivity of Aircraft Structural and Reactor Materials, by I. B. Fieldhouse. pp. 391–399.

The Total Emissivity of Aircraft Construction Materials, by J. C. Morris, B. Schurin and O. H. Olson, pp. 400–404.

Specific Heat of Materials, by J. I. Lang, pp. 405–415.

Mechanized Computation of Thermodynamic Tables at the National Bureau of Standards: The Calculation of the Equilibrium Composition and Thermodynamic Properties of Dissociated and Ionized Gaseous Systems, by J. Hilsenrath, M. Klein and D. Y. Sumida, pp. 416–437.

Equilibria in C + H_2 and C + $2H_2$ in a Temperature Range from 5000K to 50,000K at a Total Pressure of 1 Bar, by H. Kroepelin and K. K. Neumann, pp. 453–464.

Mollier Enthalpy-entropy Charts for High-temperature Plasmas, by F. Bosnjakovic, W. Springe, K. F. Knoche and P. Burgholte, pp. 465–472.

Magnetohydrostatic Equilibrium for Plasma in a Torus Tube, by Taro Kihara, *J. Phys. Soc., Japan,* vol. 14, Oct. 1959, pp. 1397–1399.

Two-dimensional Stokes Flow of an Electrically Conducting Fluid in a Uniform Magnetic Field, by Hirowa Yoshinobu and Tsunehiko Kakatani, *J. Phys. Soc., Japan,* vol. 14, Oct. 1959, pp. 1433–1442.

Some Practical Aspects of Kinetic Heating Calculations, by C. L. Bore, *J. Roy. Aeron. Soc.*, vol. 63, Nov. 1959, pp. 637–645.

Charged Particle Energy Losses Due to Excitation of Plasma Oscillations, by Yu. L. Klimontovich, *Soviet Phys.-JETP*, vol. 36(9), no. 5, Nov. 1959, pp. 999–1007.

Penetration of an Electromagnetic Field into a Plasma, by K. N. Stepanov, *Soviet Phys.-JETP*, vol. 36(9), no. 5, Nov. 1959, pp. 1035–1036.

Structure of a Magnetohydrodynamic Shock Wave in a Partially Ionized Gas, by S. B. Pikel'ner, *Soviet Phys.-JETP*, vol. 36(9), no. 5, Nov. 1959, pp. 1089–1093.

Viscosity in the Hydrodynamic Theory of Multiple Particle Production, by A. A. Emel'yanov, *Soviet Phys.-JETP*, vol. 36(9) no. 5, Nov. 1959, pp. 1100–1102.

A Simple Method of Calculating the Degree of Ionization and Thermodynamic Functions of a Multiple Ionized Ideal Gas, by Yu. P. Raizer, *Soviet Phys.-JETP*, vol. 36(9), no. 5, Nov. 1959, pp. 1124–1125.

Studies of Chemical Nonequilibrium in Hypersonic Nozzle Flows, by J. Gordon Hall and Anthony L. Russo, *Cornell Aeron. Lab., Rep.* AD-1118-A-6, Nov. 1959, 53 pp.

Plasma Dynamics, by Frances H. Clauser, *Johns Hopkins Univ., Dept. Aeron.*, 1959, 75 pp.

A Study of the Structure of the Magnetohydrodynamic Switch-on Shock in Steady Plane Motion, by Z. O. Bleviss, *Douglas Aircr. Co., Rep.* SM-23, 720, Oct. 1959, 23 pp.

The Generalized Ohm's Law for a Partially Ionized Gas, by A. Sherman, *General Electric Co., TIS* DF59FPD-807, Oct. 1959, 22 pp.

Ablation in the Stagnation Region of a Sphere in Potential Flow, by W. S. Short, *General Dynamics Corp., Convair,* ZPh-041, *Phys. Sect.*, July 1959, 18 pp.

Heat Transfer in Rotating Turbulent Pipe Flow, by D. C. Briggs, *Stanford Univ., Mech. Engng. Dept. Tech. Rep.* 45, Sept. 1959, 53 pp.

An Experimental Study of Spark Stabilization by a Gas Vortex, by Christopher Cobb and Vernon H. Blackman, *Plasmadyne Corp.*, T-3TN099-334, Aug. 1959, 31 pp.

Plasma Acceleration by Use of Guided Microwaves, by Robert F. Hess and Karlheinz Thom, *NASA TN* D-46, Dec. 1959, 46 pp.

Thermodynamic and Electrical Properties of Mercury Vapor at Pressures below Atmospheric and High Temperatures, by A. Sherman and F. Martinek. *General Electric Co.*, TIS R59 FDP-771, Oct. 1959, 23 pp.

Magnetogasdynamic Flow Regimes, by Ching-Shi Liu and Ali Bulent Cambel, ARS JOURNAL, vol. 29, Nov. 1959, pp. 871–873.

Use of Paramagnetic-resonance Techniques in the Study of Atomic Oxygen Recombinations, by S. Krongelb and M. W. P. Strandberg, *J. Chem. Phys.*, vol. 31, Nov. 1959, pp. 1196–1210.

Equilibrium Properties of a Multicomponent Ionized Gas, by Gilda Maki Harris, *J. Chem. Phys.*, vol. 31, Nov. 1959, pp. 1211–1220.

Molecular Ions, by Robert N. Varney, *J. Chem. Phys.*, vol. 31, Nov. 1959, pp. 1314–1316.

Theory of Thermal Second-order Decomposition of Molecules, by E. E. Nikitin and N. D. Sokolov, *J. Chem. Phys.*, vol. 31, Nov. 1959, pp. 1371–1374.

Viscous Hypersonic Similitude, by Wallace D. Hayes and Ronald F. Probstein, *J. Aero/Space Sci.*, vol. 26, Dec. 1959, pp. 815–824.

Microwave Investigation on Plasma in Shock Tube, by Mikio Takeyama, Shiro Hamamura and Toshiatsu Oda, *J. Phys. Soc., Japan,* vol. 14, Nov. 1959, pp. 1637–1638.

The Structural Effects of Kinetic Heating, *J. Roy. Aeron. Soc.*, vol. 63, Nov. 1959, pp. 615–658.

Some Factors Affecting the Choice of Materials, by W. G. Heath, pp. 615–619.

Design of Transparencies, by J. S. Przemieniecki, pp. 620–636.

Some Practical Aspects of Kinetic Heating Calculations, by C. L. Bore, pp. 637–645.

Advantages and Limitations of Models, by A. J. Sobey, pp. 646–655.

Summary of the Discussion, by Maureen E. Michael and Joan Bruce, pp. 656–658.

Vibrational Relaxation in Gases, by J. D. Lambert and R. Salter, *Proc., Roy. Soc., London,* vol. A 253, Nov. 24, 1959, pp. 277–288.

An Inviscid Boundary Layer of Magnetohydrodynamics, by William S. Lewellen, *Cornell Univ., Grad. of Aeron. Engng.*, Sept. 1959. 46 pp.

The Noise Field from Designed Nozzles at Different Mach Numbers, by J. G. M. Williams and D. C. Stevenson, *Gt. Brit., Aeron. Res. Council, Current Paper* 448, Aug. 1957, 9 pp.

The Effect of Non-uniform Fields on Internal Flows of Conducting Fluids, by A. Sherman, *Amer. Astron. Soc., Preprint* 60-56, Jan. 1960, 22 pp.

Theoretical Investigation of the Sound

Field Produced Downstream of a Choked Two-dimensional Channel Due to Unsteady Upstream Entropy Fluctuations, by J. P. Appleton and H. J. Davies, *Gt. Brit., Aeron. Res. Council, Current Paper* 461, Oct. 1958, 7 pp.

The Wave Motions of Small Amplitude in a Fully Ionized Plasma, Part I: Without External Magnetic Field, by S. I. Pai, *Maryland Univ., TN* BN-191, Nov. 1959, 25 pp.

Some Further Results on Heating a Supersonic Gas Stream with a Radio Frequency Discharge, by Frederick O. Smetana, *Univ. Southern Calif., Engng. Center, USCEC Rep.* 56-207 Nov. 1959, 15 pp.

Substantiation of Nozzle Admittance Theory by Direct Measurement of the Admittance Parameter (Thesis, M.S.E.), by Rudolfo Monti, *Princeton Univ., Aeron. Engng. Dept.*, Oct. 1958, 50 pp.

Spectrographic Temperature Measurements in a Carbon-arc-powered Air Jet, by David H. Greenshields, *NASA TN* D-169, Dec. 1959, 24 pp.

Methods of Predicting Laminar Heat Rates on Hypersonic Vehicles, by Richard J. Wisniewski, *NASA TN* D-201, Dec. 1959, 36 pp.

Comparison of Parameter Methods for Extrapolating High-temperature Data, by R. M. Goldhoff, *J. Basic Engng.*, vol. 81D, Dec. 1959 (*Trans., ASME*), pp. 629–644.

Initial Pressure Dependence of Thermal Conductivity and Viscosity, by Daniel E. Stogryn and Joseph O. Hirschfelder, *J. Chem. Phys.*, vol. 31, Dec. 1959, pp. 1545–1554.

Sublimation in a Hypersonic Environment, by Sinclaire M. Scala, *J. Aero/Space Sci.*, vol. 27, Jan. 1960, pp. 1–12.

Turbulent Heat Transfer on Blunt-nosed Bodies in Two-dimensional and General Three-dimensional Hypersonic Flow, by Roberto Vaglio-Laurin, *J. Aero/-Space Sci.*, vol. 27, Jan. 1960, pp. 27–36.

Effectiveness of Radiation as a Structural Cooling Technique for Hypersonic Vehicles, by Roger A. Anderson and William A. Brooks Jr., *J. Aero/Space Sci.*, vol. 27, Jan. 1960, pp. 41–48.

Compressible Flat-plate Boundary-layer Flow with an Applied Magnetic Field, by William B. Bush, *J. Aero/Space Sci.*, vol. 27, Jan. 1960, pp. 49–58.

On the Maximum Attainable Temperature in Resonance Tubes, by Ascher H. Shapiro, *J. Aero/Space Sci.*, vol. 27, Jan. 1960, pp. 66–67.

Constant-temperature Magneto-gasdynamic Channel Flow, by Jack L. Kerrebrock and Frank E. Marble, *J. Aero/Space Sci.*, vol. 27, Jan. 1960, p. 78.

Flow of Fluids, by Murray Weintraub, *Ind. Engng. Chem.*, vol. 51, March 1959, part 2, pp. 362–367.

Fluid Dynamics, by A. K. Oppenheim, C. V. Sternling, C. A. Sleicher Jr. and R. A. Stern, *Ind. Engng. Chem.*, vol. 51, March 1959, part 2, pp. 437–451.

Heat Transfer, by E. R. G. Eckert, J. P. Hartnett and T. F. Irvine Jr., *Ind. Engng. Chem.*, vol. 51, March 1959, part 2, pp. 452–465.

Mass Transfer, by C. R. Wilke, J. M. Prausnitz and Andreas Acrivos, *Ind. Engng. Chem.* vol. 51, March 1959, part 2, pp. 466–471.

Turbulent Spreading of Round Hot Air Streams in Moving Air, by W. Szablewski, *Ingenieur-Archiv*, vol. 26, no. 5, 1958, pp. 358–368. (In German.)

Transient Heat Transfer for Flow in

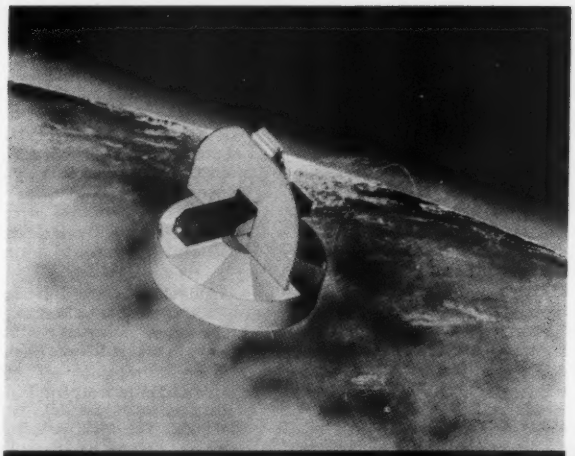

Ball

CONTRACT RESEARCH, DEVELOPMENT, FABRICATION

Specializing in the fields of

- Rocket and Satellite Instrumentation
- Payload Systems
- Solar and Stellar Pointing Systems
- Guidance and Control Systems

WRITE FOR BROCHURE

Ball

Prime Contractors to the NASA, Air Force, Navy

Employment Opportunities Available for Scientists and Engineers with Above Average Abilities

BALL BROTHERS RESEARCH CORP.

INDUSTRIAL PARK BOULDER, COLORADO

Hillcrest 2-2966

Ducts, by Robert Siegel, *J. Appl. Mech. (Trans., ASME)*, vol. 26, Series E., no. 1, March 1959, pp. 140–144.

On the Necessity of Unsteady Flow in Fluid Machines, by R. C. Dean Jr., *J. Basic Engng. (Trans., ASME)*, vol. 81, Series D, March 1959, pp. 24–28.

On Similitude in Rarefied-gas Aerothermodynamics, by F. Marcel Devienne, *J. Aero/Space Sci.*, vol. 26, March 1959, pp. 183–184.

One-dimensional Flow of an Ionized Gas through a Magnetic Field, by R. M. Patrick and T. R. Brogan, *J. Fluid Mech.*, vol. 5, Feb. 1959, pp. 289–309.

Thermodynamic Foundation of the Theory of Plasma, by Taro Kihara, *J. Phys. Soc., Japan*, vol. 14, Feb. 1959, pp. 128–133.

Electron Energy Distributions in Plasmas, I, by R. L. F. Boyd and N. D. Twiddy, *Proc. Roy. Soc.*, Series A, vol. 250, Feb. 24, 1959, pp. 53–69.

Heat Transfer in a Liquid Metal Flowing Turbulently Through a Channel with a Step Function Boundary Temperature, by H. F. Poppendiek, *NASA Memo* 2-5-59W, March 1959, 64 pp.

Heat Transfer Characteristics of Periodically Pulsating Turbulent Pipe Flow, by Wheeler Kay Mueller Jr., *Illinois Univ.*, 1956, 57 pp. (Ph.D. Thesis.)

Effect on the Wall of Two Phase Turbulent Motion, by S. L. Soo and C. L. Tien, *Project Squid, Tech. Rep*, PR-86-P (*ASTIA AD* 209316), Nov. 1958, 37 pp. (Available only on microcards.)

Measurements of Dissociative Recombination and Diffusion in Nitrogen at Low Pressures, by A. C. Faire and K. S. W. Champion, *Phys. Rev.*, vol. 113, Jan. 1, 1959, pp. 1–6.

Significance of Formative Time Lags in Gaseous Breakdown, by Leonard B. Loeb, *Phys. Rev.*, vol. 113, Jan. 1, 1959, pp. 7–12.

Correlation Energy of an Inhomogeneous Electron Gas, by D. A. Kirzhnits, *Soviet Phys.-JETP*, vol. 35 (8), May 1959, pp. 835–845.

Flight Mechanics

Supersonic Flow Past a Family of Blunt Axisymmetric Bodies, by Milton D. Van-Dyke and Helen D. Gordon, *NASA Tech. Rep.* R-1, 1959, 25 pp.

Aerobee-Hi Hypersonic Wind-tunnel Investigation, by R. B. Hulett, *Aerojet-General Corp., Rep.* 965 (Special), June 2, 1955, 7 pp., 40 figs.

Upper Atmosphere Research Report No. XXVII: Aerobee-Hi Report No. 4, the NRL-39, NRL-46, and NRL-50 Firings, by E. C. Pressly and J. W. Townsend Jr., *Naval Res. Lab., NRL Rep.* 4899, March 12, 1957, 31 pp.

Some Thrust and Trajectory Considerations for Lunar Landings, by Richard J. Weber and Werner M. Pauson, *NASA TN* D-134, Nov. 1959, 37 pp.

Remote Controlled Mail and Transport Rockets, by J. Venturini, *Fusées et Recherche Aéron.*, no. 13, Aug. 1959, pp. 63–64. (In French.)

Conception and Selection of Rockets and Missiles, by W. W. Hohenner, *Fusées et Recherche Aéron.*, no. 13, Aug. 1959, pp. 65–73. (In French.)

Why Go to the Moon? by E. Burgess, *Interavia*, vol. 14, Nov. 1959, p. 1387.

Trajectories with Constant Tangential Thrust in Central Gravitational Fields, by W. E. Moeckel, *NASA Tech. Rep.* R-53, 1959, 96 pp.

Departure Trajectories for Interplanetary Vehicles, by W. E. Moeckel, *NASA TN* D-80, Nov. 1959, 35 pp.

The Drag Brake Manned Satellite, by R. W. Detra, A. Kantrowitz, F. R. Riddell and P. H. Rose, *Avco-Everett Res. Lab., Rep.* 64, Aug. 1959, 24 pp.

Composite Trajectories Yielding Maximum Coasting Apogee Velocity, by Stanley Ross, ARS JOURNAL, vol. 29, Nov. 1959, pp. 843–848.

Earth-Period (24-Hr) Satellites, by J. H. Hutcheson, ARS JOURNAL, vol. 29, Nov. 1959, pp. 849–853.

Applicability of Euler's Dynamical Equations to Rocket Motion, by James W. Ellis and Charles W. McArthur, ARS JOURNAL, vol. 29, Nov. 1959, pp. 863–864.

Some Extensions of the Hohmann Transfer Maneuver, by T. N. Edelbaum, ARS JOURNAL, vol. 29, Nov. 1959, pp. 864–865.

Comparison of Minimum Energy Paths and Apogee Designation Paths, by Wayne Tempelman, ARS JOURNAL, vol. 29, Nov. 1959, pp. 865–868.

Escape from a Circular Orbit with Finite Velocity at Infinity, by R. S. Long, *Astron. Acta*, vol. 5, nos. 3–4, 1959, pp. 159–162.

Cold Re-entry of Space Vehicles at Meteor Speeds, by D. H. Robey, *Astron. Acta*, vol. 5, nos. 3–4, 1959, pp. 224–240.

Two Special Lunar Orbits in Space Travel Around the Earth and the Moon, by B. Thüring, *Astron. Acta*, vol. 5, nos. 3–4, 1959, pp. 241–250. (In German.)

An Application of Dynamic Programming to the Determination of Optimal Satellite Trajectories, by Richard Bellman and Stuart Dreyfus, *J. Brit. Interplanet. Soc.*, vol. 17, nos. 3–4, May–Aug. 1959, pp. 78–82.

Orbits of Artificial Satellites, by William T. Thomson, *J. Brit. Interplanet. Soc.*, vol. 17, nos. 3–4, May-Aug. 1959, pp. 83–87.

Range and Accuracy of Long-range Ballistic Missiles, by Irvin G. Henry, *J. Brit. Interplanet. Soc.*, vol. 17, nos. 3–4, May-Aug. 1959, pp. 88–92.

Basic Ballistics, by J. A. H. Bailie, *Flight*, vol. 76, Nov. 6, 1959, pp. 501–506.

Design Parameters and Optimization of Missile Trajectories, by C. A. Traenkle, *Zeitschr. für Flugwissenschaften*, vol. 7, Oct. 1959, pp. 287–293.

Remarks on the Decay of 1958 Zeta, by W. A. Delaney, *Air Force Cambridge Res. Center, Geophys. Res. Directorate, TN* 59-454, May 1959, 9 pp.

An Approximate Analytical Method for Studying Entry into Planetary Atmospheres, by Dean R. Chapman, *NASA Tech. Rep.* R-11, 1959. iii, 44 pp.

United States and Russian Satellites, Lunar Probes and Space Probes, 1957–58–59, *Natl. Aeron. & Space Admin.* 1959, 9 + 14 unnumbered pp.

Photographic Satellite Position Determination, by Mannielou H. Deiter, *Air Force Cambridge Res. Center, TN* 59-215, Feb. 1959, 6 pp.

The Satellite 1959 Gamma (Discoverer II), a Preliminary Analysis, by H. B. Wachernagel, *Air Force Cambridge Res. Center, TN* 59-457, Aug. 1959, 17 pp.

Compilation of Materials on Space and Astronautics, *Special Committee on Space & Astron., 85th U. S. Congress, 2d Session, Senate*, April 1958, 370 pp.

A Catalogue of Positional Data of the Russian Artificial Earth Satellite 1957β, by G. R. Miczaika, W. S. Ripley and E. W. Wahl, *Air Force Cambridge Res. Center, Geophys. Res. Dir., TN* 58-640, Dec. 1958, 306 pp.

Optimum Trajectory Problems, Some Special Cases, by E. W. Graham and B. J. Beane, *Douglas Aircraft Corp., Rep.* SM-23687, Sept. 1959, 51 pp.

Optimum Rocket Trajectories, Part I: Initial Value Variational Solutions, by Daniel O. Dommasch, *Aero/Space Engng.*, vol. 19, Jan. 1960, pp. 46–50.

Lunar Trajectories, by Aubrey B. Mickelwait, ARS JOURNAL, vol. 29, Dec. 1959, pp. 905–914.

Free Flight of a Ballistic Missile, by Albert D. Wheelon, ARS JOURNAL, vol. 29, Dec. 1959, pp. 915–926.

Early Warning Polar Satellites Studied, by Irving Stone, *Aviation Week*, vol. 72, Jan. 4, 1960, pp. 18–20.

Optimal Programming and Control of Satellite Orbits, by C. A. Traenkle, *Zeitschrift für Flugwissenschaften*, vol. 7, Nov. 1959, pp. 305–313.

Advances in Astronautical Sciences, Vol. 2. Proceedings of the 4th Annual Meeting of the American Astronautical Society, Dec. 1957, New York, Plenum Press, 1958.

A Survey of Propulsion and Space Dynamics, by D. B. Cross and Jorgen Jensen, Paper 1, 11 pp.

Optimum Thrust Programming Along Arbitrarily Inclined Rectilinear Paths, by Angelo Miele and Carlos R. Cavoti, Paper 6, 18 pp.

Determination of a Unique Attitude for an Earth Satellite, by William R. Davis, Paper 10, 14 pp.

Minimum Time Interplanetary Orbits, by Dandridge M. Cole, Paper 39, 18 pp.

Advances in Astronautical Sciences, Vol. 3. Proceedings of the Western Regional Meeting of the American Astronautical Society, August 1958, New York, Plenum Press, 1958.

Orbital Mechanics of Satellites, by G. S. Gedeon, Paper 19, 33 pp.

Optimal Transfer Between Coplanar-terminals in a Gravitational Field, by L. G. Vargo, Paper 20, pp 1–9.

Collision Trajectories in the Three-body Problem, by E. T. Benedikt, Paper 21, 23 pp.

Around the Moon in 80 Hours, by Dandridge M. Cole and Donald E. Muir, Paper 27, 30 pp.

Solar and Lunar Perturbations of a Satellite Orbit, by Vjekoslav Gradecak, Paper 28, 8 pp.

Minimum Weight and Optimum Flight Path of Low-acceleration Space Vehicles, by Herman F. Michielsen, Paper 29, 42 pp., 21 refs.

Comparison of Two- and Three-Dimensional Analyses of Earth-Moon Flight, by G. C. Goldbaum and R. J. Gunkel, Paper 31, 15 pp.

The Effect of Aerodynamic Forces on Satellite Attitude, by D. B. DeBra, Paper 32, 20 pp.

Elliptical Orbit Lifetimes, by John Breakwell and Leighton Koehler, Paper 34, 4 pp.

The Effect of Drag on Elliptic Orbits, by Harry E. Williams, Paper 35, 10 pp.

Encke's Method and Variation of Parameters as Applied to Re-entry Trajectories, by Robert M. L. Baker Jr., Paper 35, 10 pp.

Two-dimensional Librations of a Dumbbell-shaped Satellite in a Uniform Gravitational Field, by Trevor A. J. Stoker and Ronaldo F. Vachino, Paper 37, 9 pp.

Advances in Astronautical Sciences, Vol. 4. Proceedings of the Fifth Annual Meeting of the American Astronautical Society, Nov. 1958, New York, Plenum Press, 1959.

Horizon Scanning for Atmospheric Re-entry, by E. G. McCartney, pp. 86–97.

Orbit Decay and Prediction of the Motion of Artificial Satellites, by Herman F. Michielsen, pp. 255–310.

Perturbed Motion of Selenoid Satellites, by E. T. Benedikt and Paul S. Lenin-Cohen, pp. 311–316.

Satellite Rotation, by R. N. Bracewell, pp. 317–328.

Satellite Rendezvous Operation, by Norman V. Petersen, pp. 355–382.

The Effect of Aerodynamic Forces on Satellite Attitude, by D. B. DeBra, *J. Astron. Sci.*, vol. 6, Autumn 1959, pp. 40–45.

Calculation of the Influence of Centrifugal Forces on Surface Pressure for a Body of Arbitrary Shape in Hypersonic Flow, by G. I. Maikapar, *PMM: J. Appl. Math. & Mech. (trans. of Prikladnaya Matematika i Mekhanika)*, vol. 23, no. 1, 1959, pp. 83–91.

Dynamic Analysis of a Simple Reentry Maneuver for a Lifting Satellite, by Frederick C. Grant, *NASA TN* D-47, Sept. 1959, 35 pp.

Piloted Entries into the Earth's Atmosphere, by John M. Eggleston and Donald C. Cheatham, *Inst. Aeron. Sci., Paper* 59-98, June 1959, 40 pp.

Some Aspects of the Design of Hypersonic Boost-glide Aircraft, by Alvin Seiff and H. Julian Allen, *NACA Res. Mem.* A55E26, Aug. 1955, 50 pp. (Declassified from Confidential by authority *NASA TPA* 9, 9/29/59.)

Motion of a Ballistic Missile Angularly Misaligned with the Flight Path Upon Entering the Atmosphere and Its Effect upon Aerodynamic Heating, Aerodynamic Loads, and Miss Distance, by H. Julian Allen, *NACA Res. Mem.* A56F15, Sept. 1956, 66 pp. (Declassified from Confidential by authority *NASA TPA* 9, 9/29/59.)

High-altitude Hypervelocity Flow over Swept Blunt Glider Wings, by Marcus O. Creager, *Inst. Aeron. Sci., Paper* 59-113, June 1959, 13 pp.

Satellite Recovery Techniques for Optimization of Touch-down Accuracy, by Daniel L. Rosamond, *Inst. Aeron. Sci., Paper* 59-92, June 1959, 23 pp.

Analytical and Numerical Studies of Three-dimensional Trajectories to the Moon, by A. B. Mickelwait and R. C. Boonton Jr., *Inst. Aeron. Sci., Paper* 59-90, June 1959, 27 pp.

Vistas in Astronautics, vol. 2 (2nd Annual Astronautics Symposium), N. Y., Pergamon Press, 1959, 318 pp.

Scientific Uses of Cis-lunar Vehicles, by S. F. Singer, pp. 32–38.

Launching of Space Vehicles by Air-breathing Lifting Stages, by A. Ferri, Walter Daskim, Lewis Feldman and Lewis M. Nucci, pp. 163–173.

The Differences between Satellite and Ballistic Missile Re-entry Problems, by F. R. Riddell and G. D. Teare, pp. 174–190.

Comparative Performance of Ballistic and Low-thrust Vehicles for Flight to Mars, by J. H. Irwing and E. K. Blum, pp. 191–217.

Free Flight Missile Trajectories, by Maurice L. Anthony, pp. 219–236.

Flight Mechanics of Low-thrust Space Craft, by Frank M. Perkins, pp. 237–251.

Use of Aerodynamic Lift During Entry Into the Earth's Atmosphere, by Lester Lees, Frederic W. Hartwig and Clarence B. Cohen, ARS JOURNAL, vol. 29, Sept. 1959, pp. 633–641.

Method of Stabilizing an Astronomical Satellite, by Robert F. Newton, ARS JOURNAL, vol. 29, Sept. 1959, pp. 665–666.

Stability Criteria for the Airframe Dynamics of a Liquid-propellant Rocket, by Josef S. Pistiner, *J. Aero/Space Sci.*, vol. 26, Oct. 1959, p. 678.

Importance of the Variation of Drag with Lift in Minimization of Satellite Entry Acceleration, by Frederick C. Grant, *NASA TN* D-120, Oct. 1959, 22 pp.

Water-landing Impact Accelerations for Three Models of Reentry Capsules, by Victor L. Vaught Jr., *NASA TN* D-145, Oct. 1959, 26 pp.

Precision Orbits and Observation Reduction, by Samuel Herrick, *Univ. of Calif. at Los Angeles, Astrodynam. Rep.* 1 (*AFOSR TN* 59 769), June 11, 1959, 21 pp.

Differential Expressions for Low-eccentricity Geocentric Orbits, by Samuel Herrick, Louis G. Walters and C. Geoffrey Hilton, *Univ. of Calif. at Los Angeles, Astrodynam. Rep.* 2 (*AFOSR TN* 59-768), June 11, 1959, 33 pp.

Efficient Precision Orbit Computational Techniques, by Robert M. L. Baker Jr., George B. Westrom, C. Geoffrey Hilton, Jeannine L. Arsenault, Robert H. Gersten and Elsie Browne, *Univ. of Calif. at Los Angeles, Astrodynam. Rep.* 3 (*AFOSR TN* 59-766), June 11, 1959, 69 pp.

Methods and Velocity Requirements for the Rendezvous of Satellites in Circumplanetary Orbits, by William E. Brunk and Richard J. Flaherty, *NASA TN* D-81, Oct. 1959, 42 pp.

Predicted Characteristics of an Inflatable Aluminized-plastic Spherical Earth Satellite with Regard to Temperature, Visibility, Reflection of Radar Waves, and Protection from Ultraviolet Radiation, by George P. Wood and Arlen F. Carter, *NASA TN* D-115, Oct. 1959, 26 pp.

The Stability of Several Missile Nose Configurations in Hypersonic Flow, by E. Brian Pritchard, *Inst. Aeron. Sci., 1959 First Award Papers*, N.Y., Inst. Aeron. Sci., 1959, pp. 120–147.

Measurement of Angular Acceleration in Aircraft and Missiles, by Howard Stern, *Aero/Space Engng.*, vol. 18, Nov. 1959, pp. 48–50.

The Orbital Plane Interpreter, by Harold E. Bamford Jr., *Aero/Space Engng.*, vol. 18, Oct. 1959, pp. 37–39.

Some Economic Aspects of Hypersonic Flight, by Robert Cornog, ARS JOURNAL, vol. 29, Oct. 1959, pp. 706–715.

Effect of the Rotational of a Planetary Atmosphere upon the Orbit of a Close Satellite, by Theodore E. Sterne, ARS JOURNAL, vol. 29, Oct. 1959, pp. 777–782.

Minor Circle Flight for Orbital Launched or Boost-glide Vehicles, by W. H. T. Loh, ARS JOURNAL, vol. 29, Oct. 1959, pp. 789–790.

Controlled Re-entry Techniques Probed, by J. S. Butz Jr., *Aviation Week*, vol. 71, Nov. 2, 1958, pp. 96–103.

Camera Aspect Data, Air Force Aerobee AF-71: Launched: 30 July 1956, 1759 Hours MST, Final Data Report, by Dolores S. Lucero, *New Mexico College of A & MA, Phys. Sci. Lab.*, April 1, 1958, 30 pp.

Optimum Trajectory Problems: Some Special Cases, by E. W. Graham and B. J. Beane, *Douglas Aircr. Co., Santa Monica Div., Rep.* SM-23687, Sept. 1959, 51 pp.

Optimum Exhaust Velocity for Low-thrust Escape, by Lawrence J. Berman, *MIT, Aeron. & Astron. Dept.* (*AFOSR TN* 59-929), Sept. 1959. 13 pp.

Reflection Characteristics of Artificial Satellites Constructed in the Form of Inflated Polyhedrons, by Archibald R. Sinclair, *NASA TN* D-174, Dec. 1959, 9 pp.

Graphical Trajectory Analysis, by Aaron S. Boksenbom, *NASA TN* D-64, Dec. 1959, 46 pp.

Composite Trajectories Yielding Maximum Coasting Apogee Velocity, by Stanley Ross, ARS JOURNAL, vol. 29, Nov. 1959, pp. 843–848.

Earth-Period (24-Hr) Satellites, by J. H. Hutcheson, ARS JOURNAL, vol. 29, Nov. 1959, pp. 849–852.

Applicability of Euler's Dynamical Equations to Rocket Motion, by James W. Ellis and Charles W. McArthur, ARS JOURNAL, vol. 29, Nov. 1959, pp. 863–864.

Some Extensions of the Hohmann Transfer Maneuver, by T. N. Edelbaum, ARS JOURNAL, vol. 29, Nov. 1959, pp. 864–865.

Comparison of Minimum Energy Paths and Apogee Designation Paths, by Wayne Tempelman, ARS JOURNAL, vol. 29, Nov. 1959, pp. 865–868.

Dynamic Problems Associated with Satellite Orbit Control, by B. W. Augenstein, *J. Engng. for Industry (Trans., ASME)*, vol. B81, Nov. 1959, pp. 281–288.

Spinning Ballistic Missiles, by W. H. T. Loh, *J. Aero/Space Sci.*, vol. 26, Dec. 1959, pp. 844–845.

How Plasma Properties Affect Hypersonic Missiles, by J. W. Bond Jr., *Space/Aeronautics Res. and Dev. Handbook*, 1959–1960, pp. B-5–11.

Payload Ratio Optimization for Multistage Rocket Vehicles (nomograph), by C. E. Vandenberg, *Space/Aeronautics Res. & Dev. Handbook*, 1959–1960, pp. B-16–19.

Better Re-entry Test Data with New Shock Tunnel Instruments, by C. J. Harris, E. M. Kaegi and W. R. Warren, *Space/Aeronautics Res. & Dev. Handbook*, 1959–1960, pp. J-6–9.

Gravity Torque on an Orbiting Vehicle, by Brian F. Doolin, *NASA TN* D-70, Sept. 1959, 45 pp.

The Determination of Round-trip Planetary Reconnaissance Trajectories, by Richard B. Battin, *J. Aero/Space Sci.*, vol. 26, Sept. 1959, pp. 545–567.

Design of Missile Bodies for Minimum Drag at Very High Speeds—Thickness Ratio, Lift, and Center of Pressure Given, by T. Strand, *J. Aero/Space Sci.*, vol. 26, Sept. 1959, pp. 568–570.

Similitude of Hypersonic Real-gas Flows over Slender Bodies with Blunted Noses, by Hsien K. Cheng, *J. Aero/Space Sci.*, vol. 26, Sept. 1959, pp. 575–585.

On a Class of Variational Problems in Rocket Flight, by G. Leitmann, *J. Aero/Space Sci.*, vol. 26, Sept. 1959, pp. 586–591.

Lagrange Multipliers and Quasi-steady Flight Mechanics, by Angelo Miele, *J. Aero/Space Sci.*, vol. 26. Sept. 1959, pp. 592–598.

Steady-state Circular Pitching and Yawing Motion of Symmetric Missiles, by Charles H. Murphy, *J. Aero/Space Sci.*, vol. 26, Sept. 1959, p. 600–601.

Aerodynamic Problems of Manned Space Vehicles, by T. R. F. Nonweiler,

J. Roy. Aeron. Sci., vol. 63, Sept. 1959, pp. 521–527.

Satellite Orbits and Atmospheric Densities at Altitudes up to 750km Obtained from the Vanguard Orbit Determination Program, by Joseph W. Siry, *Planetary & Space Sci.*, vol. 1, no. 3. Aug. 1959, pp. 184–192.

Minimum Propulsion for Soft Moon Landing of Instruments, by D. S. Carton, *Cranfield, The College of Aeron., CoA Note* 94, July 1959, 34 pp.

New Methods of Solution for Unretarded Satellite Orbits, by John P. Vinti. *J. Res. Natl. Bur. Standards, V: Math. & Math. Phys.*, vol. 53B, no. 2, Oct.-Dec. 1959, pp. 105–116.

Vehicle Design, Testing and Performance

Ringing in the Future, by John A. Newbauer, ASTRONAUTICS, vol. 4, Dec. 1959, p. 30.

Missiles 1959, *Flight*, vol. 76, Nov. 6, 1959, pp. 507–532.

Air Scooping Vehicle, by Felix Berner and Morton Camac, *Avco-Everett Res. Lab., Res. Rep.* 76, Aug. 1959, 117 pp.

Atlas-Able IV Instrumentation Detailed, *Aviation Week*, vol. 71, Dec. 14, 1959, pp. 53, 55, 57.

U. S. and Soviet Space Firings (table), *Space/Aeron. Res. & Dev. Handbook*, 1959–1960. pp. A-9–10, 12.

U. S. Research and Test Vehicles, *Space/Aeron. Res. & Dev. Handbook*, 1959–1960, pp. A-14, 18, 20, 22, 29.

Boeing Stresses Maneuverability in Bomarc Evolution, by Irwin Stambler, *Space/Aeron.*, vol. 32, no. 6, Dec. 1959, pp. 50–53.

Atlas Reliability Program Yields Improved Components, by C. C. Campbel, *Space/Aeron.*, vol. 32, no. 6, Dec. 1959, pp. 65–66, 68, 71.

The Discus Body and Its Application to V/STOL Aircraft and Space Vehicles, by Martin Gerloff, *Aero/Space Engng.*, vol. 19, Jan. 1960, pp. 51–56.

Unexpected Rocket Problems Boost Test Facility Needs, by J. S. Butz Jr., *Aviation Week*, vol. 72. Jan. 4, 1960, pp. 52–59.

Space Flight in the X-15, by Clayton C. Clark Jr., *Aero/Space Engng.*, vol. 18, April 1959, pp. 43–47.

Guidance and Control

Accuracy Required for a Return from Interplanetary Voyages, by Robert M. L. Baker Jr., *J. Brit. Interplanet. Soc.*, vol. 17, nos. 3–4, May-Aug. 1959, p. 93–98.

An Analysis of the Corridor and Guidance Requirements for Supercircular Entry into Planetary Atmospheres, by Dean R. Chapman, *NASA Tech. Rep.*, R-55, 1959, 76 pp.

Some Notes on Attitude Control of Earth Satellite Vehicles, by Warren Gillespie Jr., Donald G. Eide and Allan B. Churgin, *NASA TN* D-40, Dec. 1959, 80 pp.

Stabilization and Attitude Control of Satellite Vehicles, by William E. Frye and Edward V. B. Stearns, ARS JOURNAL, vol. 29, Dec. 1959, pp. 927–930.

Guidance Techniques for Interplanetary Travel, by Charles D. Bock and Charles J. Mundo, ARS JOURNAL, vol. 29, Dec. 1959, pp. 931–939.

Radio Guidance, by E. King Stodola, ARS JOURNAL, vol. 29, Dec. 1959, pp. 940–945.

Recent Progress in Inertial Guidance, by John Hovorka, John W. Hursh, E. J. Frey, William G. Denhard, Lester R. Grohe, P. J. Gilinson Jr. and W. E. Vander Velde, ARS JOURNAL, vol. 29, Dec. 1959, pp. 945–956.

Doppler Radars for Guidance—Design Techniques and Performance, by Walter R. Fried, ARS JOURNAL, vol. 29, Dec 1959, pp. 957–966.

Principles of Doppler-inertial Guidance, by L. H. Dworetzky and A. Edwards, ARS JOURNAL, vol. 29, Dec. 1959, pp. 967–972.

Infrared Tracking, by R. W. Powell, ARS JOURNAL, vol. 29, Dec. 1959, pp. 973–980.

Celestial Guidance, by R. B. Horsfall, ARS JOURNAL, vol. 29, Dec. 1959, pp. 981–988.

A Parameter Tracking Servo for Adaptive Control Systems, by M. Margolis and C. T. Leondes, *Calif. Univ., Dept. Engng.*, Aug. 1959, 30 pp.

Synthesis of Third Order Contactor Control Systems, by Irmgard Flügge-Lotz, *Stanford Univ., Div. Engng. Mech., Tech. Rep.* 123, Oct. 1959, 30 pp.

A-C Servosystems with Signal Dependent on Error and Its Derivative, by N. P. Vlasov, *Avtomatika i Telemakhanika*, vol. 20, no. 10, 1959, pp. 1357–1365. (In Russian.)

Experimental Determination of Characteristics of Position Power Servosystems, by M. B. Tumarkin. *Avtomatika i Telemekhanika*, vol. 20, no. 10, 1959, pp. 1426–1430. (In Russian.)

High Precision Stellar Navigator for Interplanetary Guidance, by C. D. Bock, *Arma Engng.*, vol. 2, Sept.-Oct. 1959, pp. 12–15.

Short Cut to Setting Accuracies for Missile Guidance, by Benjamin Pernick, *Space/Aeron. Res. & Dev. Handbook*, 1959–1960, pp. D-6–10.

Pressure Feedback Valves: Breakthrough in Hot Gas Servos, by T. S. Honda, *Space/Aeron. Res. & Dev. Handbook*, 1959–1960, pp. G-5–8.

Instrumentation and Communications

Communications-electronics Terminology (Air Force Communications Electronics Doctrine), *Air Force Manual AFM* 100-39, 1959, 857 pp.

Mercury Capsule Communications, by Roger J. Pierce, ASTRONAUTICS, vol. 4, Dec. 1959, p. 24.

Automation Cuts Zeus Transistor Cost, by Philip J. Klass, *Aviation Week*, vol. 71, Nov. 30, 1959, pp. 74–76, 79.

Millimicron Motion Instrumentation, by Jack McElwain, *Instruments and Control Systems*, vol. 32, Nov. 1959, pp. 1688–1691.

Electrodynamic Standards for Vibration Pickups, by R. R. Bouche, *Instruments and Control Systems*, vol. 32, Nov. 1959, pp. 1692–1695.

A Stroboscopic Vibration Analyzer, by S. Edelman, R. Brooks, S. Saito, E. Jones and E. R. Smith, *J. Res., Natl. Bur. Standards*, vol. 63C, no. 2, Oct.-Dec. 1959, pp. 97–104.

Compensation of Non-linear Distortions in Radio Transmitters by Negative Feedback of Signal Envelope, by V. A. Khatskelevitch and L. M. Shur, *Telecommunications (trans. of Elektrosvyaz')*, no. 4, 1958, pp. 357–367.

Frequency Stabilization over a Given Range with the Help of a Generator of Combination Frequencies, by G. M. Utkin, *Telecommunications (trans. of Elektrosvyaz')*, no. 4, 1958, pp. 368–379.

Concerning Measurements of Asymmetry in the Input of Radio Receivers, by A. Z. Fradin and V. A. Olendskii, *Telecommunications (trans. of Elektrosvyaz')*, no. 4, 1958, pp. 390–397.

Matrix Method of Synthesis of Multibeat Relay-contact Circuits of Communications and Control, by M. L. Tsetlin and G. S. Eidus, *Telecommunications (trans. of Elektrosvyaz')*, no. 4, 1958, pp. 407–419.

Literature on Magnetic Elements of Automation, Remote Control and Computing Technique for 1958, *Avtomatika i Telemekhanika*, vol. 20, no. 9. 1959, pp. 1302–1310. (In Russian.)

Radio's Blackout During Re-entry Probed, by Philip J. Klass, *Aviation Week*, vol. 71, Nov. 23, 1959, pp. 28–29.

Triangulation—a Precise Method for Satellite Tracking, by P. G. Kirmser and I. Wakabayashi, *J. Franklin Inst.*, vol. 268, Nov. 1959, pp. 337–351.

The Performance of Thin-film Thermometers in Partially Ionized Shock-tube Flows, by P. V. Marrone and R. A. Hartunian, *Cornell Aeron. Lab. Rep.* AD-1118-A-5, Nov. 1959, 7 pp.

Acoustic Impedance Measurements for Propulsion System Components, by C. L. Dailey, A. C. Brown and J. W. Headley, *Wiancko Engng. Co., Rep.* W2328-F, July 1959, 80 pp.

A Theory of Nearly Linear Systems, by Francis H. Clauser, *Johns Hopkins Univ., Dept. Aeron.*, 1959, 51 pp.

Design and Use of Fine Wire Thermocouples for Research, by Maynard H. Hunt, *U. S. Naval Ord. Test Sta., NAVORD Rep.* 5828, *NOTS TP* 1919, Sept. 1959, 35 pp.

Allegany Ballistics Laboratory Wire Strain Gauges for Measuring Pressure and Thrust in Rockets, by G. H. Moody, *Allegany Ball. Lab.*, B-19, Nov. 1959, 51 pp.

On Increasing Effectivity of Telemetering by N. V. Pozin, *Avtomatika i Telemekhanika*, vol. 20, no. 10, 1959, pp. 1403–1408. (In Russian.)

Data Transcription Laboratory, by R. J. Carr, *Arma Engng.*, vol. 2. Sept.-Oct., 1959, pp. 4–11.

Experimental Observation of Space Vehicles, by Richard Y. Miner, *Arma Engng.*, vol. 2, Sept.-Oct. 1959, pp. 16–21.

Optical Systems Have Space Potential, by Barry Miller. *Aviation Week*, vol. 71, Dec. 14, 1959, pp. 87, 89, 91.

Simulating Space, by Alexander I. Newman and Robert J. Dennis, *Ind. Res.*, vol. 1, Nov.-Dec. 1959, pp. 63–69.

High Intensity, High Speed, Multiflash Apparatus, by G. Dixon-Lewis and E. G. Jackson. *J. Sci. Instr.*, vol. 36, Oct. 1959, pp. 417–418.

Precision Pressure Gauge for the Range 0 to 30 mm of Mercury, by E. H. Hirsch, *J. Sci. Instr.*, vol. 36, Nov. 1959, pp. 477.

Determination of Satellite-orbit Parameters by the Use of the Doppler Effect, by V. A. Kotel'nokiv, V. M. Dubrovin, V. A. Morozov, O. N. Rzhiga and A. M. Shakhovskoi, *Radio Engng. & Electronics (trans. of Radiotekhnika i Elektronika)*, vol. 3, no. 7, 1958, pp. 23–35.

Pulse Amplification of Electric Signals, by P. G. Tager, *Radio Engng. & Electronics (trans. of Radiotekhnika i Elektronika)*, vol. 3. no 7, 1958, pp. 85–97.

Signal Fluctuations from a Multitude of Random Reflectors for a Moving Radar System, by V. B. Shteinshleiger and G. A. Zonnenshtral, *Radio Engng. & Electronics (trans. of Radiotekhnika i Elektronika)*, vol. 3, no. 7, 1958. pp. 98–104.

The Circulation of Pulses in a Strongly Non-linear System with Delayed Dispersive Feedback, by Yu. I. Neimark, Yu. K. Marlakov and L. P. Elkina, *Radio Engng. & Electronics (trans. of Radiotekhnika i Elektronika)*, vol. 3, no. 11, 1958, pp. 37–54.

A System for Protection from Pulse Interference in Apparatus for Recording Meteor Activity, by B. S. Dudnik, B. L. Kascheev, M. F. Lagutin and I. A. Lysenko, *Radio Engng. & Electronics (trans. of Radiotekhnika i Elektronika)*, vol. 3, no. 11, 1958, pp. 79–85.

Aerospace Electromagnetic Spectrum (chart and tables), *Space/Aeron. Res. & Dev. Handbook*, 1959–1960, p. D-14A.

State of the Art: Precision Rotating Components, *Space/Aeron. Res. & Dev. Handbook*, 1959–1960, pp. E-6–11.

Performance of Parametric and Maser Devices (table), by Albert T. Isaacs, *Space/Aeron. Res. & Dev. Handbook*, 1959–1960, pp. E-16–17.

Cameras for Aerospace Vehicle R & D (table), *Space/Aeron. Res. & Dev. Handbook*, 1959–1960, pp. J-12–17.

Research on the Hot-wire and a Momentum-sensitive Device for Transient Water Flow Phase Measurements (MSE Thesis), by Walter S. Davis, *Princeton Univ., Aeron. Engng. Dept., Rep.* 475, Sept. 1959, 71 pp.

Streak Interferometry, by F. D. Bennett, D. D. Shear and H. S. Burden, *Aberdeen Proving Ground, Ball. Res. Labs. Rep.* 1080, Sept. 1959, 26pp.

Research Directed Toward the Attainment and Utilization of High Temperature (Multi-frame High Speed Camera, Exploding Wire Phenomena and Plasma Acceleration), by J. Lloyd Bohn, Francis H. Nadig and Theodore Korneff, *Air Force Cambridge Res. Center, TR* 58–289, March 1958, 66pp.

Description of ADMDC Prototype Camera Station for Satellite Surveillance, by Walter E. Woehl and Richard M. Waetjen, *Air Force Missile Dev. Center, TR* 59–3, March 1959, 41pp.

Reduction of Ballistic Camera Plates, by Charles A. Bodwell and Paul D. Jose, *Air Force Missile Dev. Center, Tech. Rep.* 59–5, Jan. 1959, 63pp.

High Altitude Cloud Photography from Ballistic Missiles, by D. N. Vachon and J. I. F. King, *General Electric Co., Missile & Space Vehicle Dept.*, TIS R598D471, Dec. 1959, 6pp.

Test on Deflection of Flat Oval Bourdon Tubes, by G. Kardos, *J. Basic Engng.*, vol. 81D, Dec. 1959 (*Trans., ASME*), pp. 645–650.

Bending and Stretching of Corrugated Diaphragms, by R. F. Dressler, *J. Basic Engng.*, vol. 81D, Dec. 1959 (*Trans., ASME*), pp. 651–659.

The Electric Spark Method for Quantitative Measurements in Flowing Gases, by H. J. Bomelburg, H. Herzog and J. R. Weske, *Zeitschrift für Flugwissenschaften*, vol. 7, Nov. 1959, pp. 322–239.

Television Telemeter for Missile Test Programs, by Daniel Hochman and Jeremy P. Taylor, *Advances in Astronautics*, vol. 3 (Proc. Western Regional Meeting. Amer, Astron. Soc., Aug. 1958), N. Y., Plenum Press, 1958.

"Light Foot Quantizer" for Highly Precise Time Measurement, by M. A. Alexander and Douglas Epps, *Space/Aeron.*, vol. 32, no 6, Dec. 1959, pp. 101–102, 104, 106.

Designing for Space Communications, by Joseph Vogelman, *Space/Aeron.*, vol. 32, no. 6, Dec. 1959, pp. 126–130.

New Ferrite Phase Shifter Paves Way for Inertialess Scanning Radar, by F. E. Goodwin and T. A. Nussmier, *Space/Aeron.*, vol. 32 no. 6, Dec. 1959, pp. 131–136.

Long Range Radio Communication on Ultra-short Wave, Using Meteor Ionization of the Atmosphere, by M. N. Arone, *Telecommunications (trans. of Elektrosvyaz')*, no. 6, 1958, pp. 630–642.

Oscillations of a System with a Relay of Advancing Characteristics, by I. B. Chelpanov, *J. Appl. Math. Mech. (trans. of Prikladnaya Matematika i Mekhanika)*, vol. 22, no. 1, pp. 67–69.

An Apparatus of a Super-High Pressure with a Simultaneous Achievement of High Temperatures, by S. S. Koksha and G. P. Shakhovskoi, *Instruments and Experimental Techniques (trans. of Pribory i Tekhnika Eksperimenta)*, no. 3, May-June 1958, pp. 415–420.

Atmospheric and Space Physics

Could the Satellites of Mars Be Artificial? by Clyde W. Tombaugh, ASTRONAUTICS, vol. 4, Dec. 1959, p. 38.

A Reply on Mars' Satellites, by Clyde W. Tombaugh. ASTRONAUTICS, vol. 4, Dec. 1959, p. 39.

Nonlinear Effects of Gravitational Radiation, by Asher Peres and Nathan Rosen, *Phys. Rev.*, vol. 115, no. 4, Aug. 15. 1959, pp. 1085–1086.

Small Effects of Solar Flares and the Energy Spectrum of Primary Variation of Cosmic Rays, by E. V. Kolomeets, *Soviet Phys.-JETP*, vol. 36(9), no. 5, Nov. 1959, pp. 960–962.

Calculation of Equivalent Parameters for Non-homogeneous Earth Taking Skin Effect into Account, by P. G. Gorodetskii, *Telecommunications (trans. of Elektrosvyaz')* no. 4, 1958, pp. 434–439.

Structure of the Moon's Surface in Comparison with the Earth; Data and Interpretation, by K. Krejci-Graf, *Astron. Acta*, vol. 5, nos. 3–4, 1959, pp. 163–223. (In German.)

A Gravitational Force Function for the Earth Representing All Deviations from a Spherical Geoid, by Raymond H. Wilson Jr., *J. Franklin Inst.*, vol. 268, Nov. 1959, pp. 378–387.

IGY Results on the Shape of the Earth, by John A. O'Keefe, ARS JOURNAL, vol. 29, Dec. 1959, pp. 902–904.

Decay of Light from a Meteor Train, by G. S. Hawkins and W. E. Howard, *Astrophys. J.*, vol. 130, Nov. 1959, pp. 1003–1007.

Effect of Accommodation on the Transitional Aerodynamic Drag of Meteorites, by Robert M. L. Baker Jr., *Astrophys. J.*, vol. 130, Nov. 1959, pp. 1024–1026.

Derivation and Tabulation of Molecular Integrals, by Roop C. Sahni and James W. Cooley, *NASA TN* D-146, Dec. 1959, 39 pp.

Production of Carbon in the Upper Atmosphere, by K. P. Chopra, *Univ. Southern Calif., Engng. Center, Rep.* 56–208, July 6, 1959, 8 pp.

The Use of Modulated Atomic-beam Techniques for the Study of Space-flight Problems, by G. S. Holister, R. T. Brackmann and W. L. Fite, *General Dynam.*

CHEMICAL PROPULSION SYSTEMS RESEARCH SPECIALIST

ASTRO — The research division of The Marquardt Corporation — is doing applied research on unique propulsion and secondary power techniques. There is particular interest in the direct conversion of chemical reaction into kinetic or electrical energy for the creation of new power systems. In this area there is a need for a chemical propulsion systems research specialist to provide advanced technical leadership. The original nature of the work affords an opportunity for a mature, professionally recognized engineer to make a creative contribution in the areas of:

FUEL CHEMISTRY

CRYOGENICS

CHEMICAL REACTIONS OF COMBUSTION

CHEMICAL KINETICS

PROPULSION SYSTEMS EVALUATION

This is a top technical position requiring a Ph.D. with eight years experience, some of which must be in liquid rocket systems.

Write In Confidence:

FLOYD HARGISS, *Manager Professional Personnel*

THE MARQUARDT CORPORATION

16555 Saticoy Street
Van Nuys, California

American Rocket Society

MEETINGS SCHEDULE 1960

DATE	MEETING	ABSTRACT DEADLINE
March 23–25	**Ground Support Equipment Conference** **Statler-Hilton Hotel** **Detroit, Michigan** SUBJECTS: Classified and unclassified sessions and field trips will explore problems encountered with current equipment, "second generation" GSE, advances in mechanical and electrical GSE and unusual chemical, transportation and legal risks in operation of systems.	**Program printed**
April 6–8	**Structural Design of Space Vehicles Conference** **Santa Barbara Biltmore** **Santa Barbara, California** SUBJECTS: The sessions, to be held in the morning and evening, will cover some problems arising during boost, in orbit and during re-entry and landing. Also, a session on structures/materials aspects of space frames and one on planned and existing vehicles are scheduled.	**Program printed**
May 9–12	**Semi-Annual Meeting and Astronautical Exposition** **Ambassador Hotel** **Los Angeles, California** SUBJECTS: Thirty-one sessions will cover all disciplines of astronautics including all-day session on space observation systems, classified mobile vs. hard base and liquid vs. solid rocket capabilities sessions. Four luncheons, banquet, field trips and ladies program.	**Program printed**
May 23–25	**National Telemetering Conference** **Miramar Hotel** **Santa Monica, California** **Co-Sponsors: ISA, AIEE, ARS, IAS, IRE** SUBJECTS: All fields of telemetry, including space data acquisition systems, biomedical measurements, ground stations, environment measurement and control and space data transmission techniques.	**Passed**
July 18–19	**Propellants, Combustion and Liquid Rockets Conference** **The Ohio State University** **Columbus, Ohio** SUBJECTS: Storable bi-propellants, monopropellants, properties and thermodynamics and liquid rockets.	**March 30**
August 15–20	**XIth International Astronautical Congress** **Stockholm, Sweden** SUBJECTS: Basic sciences, planetary atmosphere environments, interplanetary space, space medicine and biology, trajectories, navigation, guidance and control, space communication, propulsion, vehicles, and economics factors.	**April 15**
September 27–30	**Power Systems Conference** **Miramar Hotel** **Santa Monica, California** SUBJECTS: Power systems and related equipment, will include nuclear display.	**June 24**
December 5–8	**15th Annual Meeting and Astronautical Exposition** **Shoreham Hotel** **Washington, D. C.** SUBJECTS: All areas covered by ARS technical committees.	**August 15**

Corp., General Atomic Div., Rep. G. A.-1024. Oct. 1959, 17 pp.

An Investigation of the Natural Environment of an Artificial Satellite, by M. Downing and R. M. Rhodes, *Convair, General Dynam. Corp., Phys. Sect.*, ZPh-039, Aug. 1959, 29 pp.

CH in the Solar Spectrum, by Charlotte E. Moore and Herbert P. Broida, *J. Res., Natl. Bur. Standards, A. Phys. & Chem.*, vol. 63A, no. 1, July-Aug. 1959, pp. 19–54.

Infrared Studies in the 1- to 15-micron Region to 30,000 Atmospheres, by C. E. Weir, E. R. Lippincott, A. Van Valkenburg and E. N. Bunting, *J. Res., Natl. Bur. Standards, A. Phys. & Chem.*, vol. 63A, no. 1, July-Aug, 1959, pp. 55–62.

OH in the Solar Spectrum, by Charlotte E. Moore and Herbert P. Broida, *J. Res., Natl. Bur. Standards, A. Phys. & Chem.*, vol. 63A, no. 3, Nov.-Dec. 1959, pp. 279–296.

A Method for Measuring Local Density from an Artificial Satellite, by L. R. O. Storey, *J. Res., Natl. Bur. Standards, D. Radio Propagation*, vol. 63 D, no. 3, Nov.-Dec. 1959, pp. 325–340.

Space Vehicle Environment, by Carl Gazley Jr., W. W. Kellogg and E. H. Vestine, *J. Aero/Space Sci.*, vol. 26, Dec. 1959, pp. 770–782.

Human Factors and Bioastronautics

On Man and the Missile, by J. J. Haggerty, *Interavia*, vol. 14, Nov. 1959, pp. 1418–1419.

Evaluation Tests of a Heat Resistant Suit for Personnel Use at High Temperatures in a Supersonic Wind Tunnel, by Lewis R. Carpenter, *Arnold Engng. Dev. Center, TN* 59–123, Oct. 1959, 55 pp.

Mercury Pilots Probe Weightless Flight, by Evert Clark, *Aviation Week*, vol. 72, Jan. 4, 1960, pp. 22–23.

Estimate of the Specific Ionization Caused by Heavy Cosmic Ray Primaries in Tissue or Water, by T. Foelsche, *J. Astron. Sci.*, vol. 6, Winter 1959, pp. 57–62.

Microwave "Hazards" Are Exaggerated, by Charles D. LaFond, *Missiles & Rockets*, vol. 5, Dec. 14, 1959, pp. 20, 23–24.

How to Get the Most Out of Man in Space, by A. M. Mayo, *Space/Aeron. Res. & Dev. Handbook*, 1959–1960, pp. K-5–9.

Exposures and Tolerances for Manned Space Flight, *Space/Aeron. Res. & Dev. Handbook*, 1959–1960, pp. K-10–11.

Parameters of Manned Space Flight (chart), *Space/Aeron. Res. & Dev. Handbook*, 1959–1960, pp. K-12–13.

Some Elementary Considerations Concerning Fringe of Space Environmental Conditions, by Alex J. Moncrieff-Yeates, *Aero/Space Engng.*, vol. 18, Dec. 1959, pp. 32–35.

Law, Sociology and Education

Do We Have a Space Program? by William H. Pickering, ASTRONAUTICS, vol. 5, Jan. 1960, p. 27.

Behind the Luniks, by Y. A. Pobedonostev, ASTRONAUTICS, vol. 5, Jan. 1960, p. 30.

Interview with the Soviet Delegation, by Irwin Hersey and John Newbauer, ASTRONAUTICS, vol. 5, Jan. 1960, p. 34.

SOUTHWEST
"Monoball"®
SELF-ALIGNING BEARINGS

CHARACTERISTICS

	ANALYSIS	RECOMMENDED USE
1	Stainless Steel Ball and Race	For types operating under high temperature (800-1200 degrees F.).
2	Chrome Alloy Steel Ball and Race	For types operating under high radial ultimate loads (3000-893,000 lbs.).
3	Bronze Race and Chrome Steel Ball	For types operating under normal loads with minimum friction requirements.

Thousands in use. Backed by years of service life. Wide variety of Plain Types in bore sizes 3/16" to 6" Dia. Rod end types in similar size range with externally or internally threaded shanks. Our Engineers welcome an opportunity of studying individual requirements and prescribing a type or types which will serve under your demanding conditions. Southwest can design special types to fit individual specifications. As a result of thorough study of different operating conditions, various steel alloys have been used to meet specific needs. Write for Engineering Manual No. 551. Address Dept. ARS-60.

SOUTHWEST PRODUCTS CO.
1705 SO. MOUNTAIN AVE., MONROVIA, CALIFORNIA

New Gateway to Achievement in Astronautics and Aeronautics

Republic Aviation's
New Research & Development Center

Engineers and scientists whose minds are challenged by unsolved problems across the entire spectrum of technologies concerned with space exploration and upper atmosphere flight, are invited to inquire about the exceptional facilities for both theoretical and experimental investigations provided by Republic's new Research and Development Center (scheduled to open Spring 1960).

Senior level openings exist in the following areas:

Space Electronics *(Guidance, Navigation, Communications)* / Hydromagnetics / Advanced Computer Technology / Applied Mathematics / Nuclear Power Packages / Space Environmental Studies *(Life Science)* / Celestial Mechanics / Hypersonics / Electronic Theory / Plasma Physics / Radiation Studies / Re-entry Techniques / Materials Research & Development / Fluid Mechanics

Please forward resumes to: Mr. George R. Hickman
Technical Employment Manager, Dept. 10C

REPUBLIC AVIATION
Farmingdale, Long Island, New York

zeus

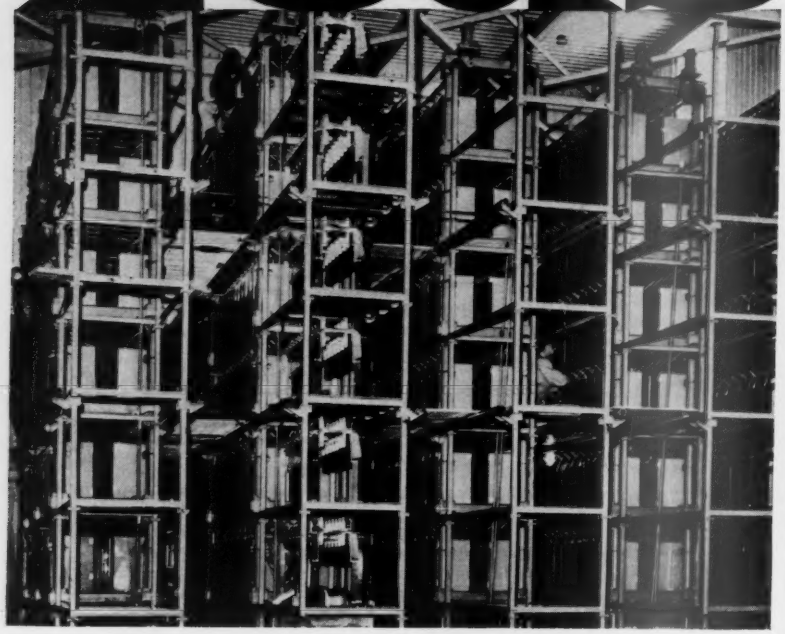

zeus... a giant capacitor bank at Los Alamos has a peak rating of 20 thousand volts, and will deliver 40 million amperes in 10 microseconds. It is a power supply for Project Sherwood investigations in controlled thermonuclear reactions. Los Alamos is one of the nation's leading centers for this and other aspects of plasma physics research.

For employment information write: Director of Personnel
Department 60 - 21

los alamos
scientific laboratory
OF THE UNIVERSITY OF CALIFORNIA
LOS ALAMOS, NEW MEXICO

Index to Advertisers

AEROJET-GENERAL CORP. ..... Back cover
D'Arcy Advertising Co., Los Angeles, Calif.

BALL BROTHERS RESEARCH CORP. 301
Walter L. Schump Advertising, Denver, Colo.

LOCKHEED AIRCRAFT CORP. ... 229
Foote, Cone & Belding, Los Angeles, Calif.

LOS ALAMOS SCIENTIFIC LABORATORY 308
Ward Hicks Advertising, Albuquerque, N. Mex.

THE MARQUARDT CORP. 305
Grant Advertising, Inc., Hollywood, Calif.

THE MARTIN CO., DENVER DIV. ..... 2nd cover
E. M. Halvorson Co., Denver, Colo.

PLENUM PRESS, INC. 295
H. J. Gold Co., New York, N. Y.

RADIO CORP. OF AMERICA 293
Al Paul Lefton Co., Inc., Philadelphia, Pa.

RAMO-WOOLDRIDGE, DIV OF THOMPSON RAMO WOOLDRIDGE INC. 232
The McCarty Co., Los Angeles, Calif.

REPUBLIC AVIATION CORP. ... 307
Deutsch & Shea, Inc., New York, N. Y.

SOUTHWEST PRODUCTS CO. 307
O. K. Fagan Advertising Agency, Los Angeles, Calif.

SPACE TECHNOLOGY LABORATORIES 231
Gaynor & Ducas, Inc., Beverly Hills, Calif.

WYMAN GORDON CO. ..... 3rd cover
The Davis Press, Inc., Worcester, Mass.